Fucosyltransferase IX:
characterization and biological role

Catarina Brito

Dissertation presented to obtain the Doutoramento (Ph.D.) degree in Biochemistry at the Instituto de Tecnologia Química e Biológica, Universidade Nova de Lisboa

Oeiras, 2007

Fucosyltransferase IX: characterization and biological role

Ana Catarina Maurício Brito Ataíde Montes

Dissertation presented to obtain the Doutoramento (Ph.D.) degree in Biochemistry at the Instituto de Tecnologia Química e Biológica, Universidade Nova de Lisboa

Supervisor: Dr. Júlia Costa

Opponents: Dr. Thierry Galli, Dr. Leonor David

Oeiras, October 2007

Supervisor: Dr. Júlia Costa.

President of the Jury: Dr. Claudina Rodrigues-Pousada.

Members of the Jury: Dr. Thierry Galli; Dr. Harald S. Conradt; Dr. Leonor David; Dr. Paula M. Alves; Dr. Ana Luísa Simplício.

Cover: *By author.* Immunofluorescence microscopy of NT2N neurons with labeled low molecular weight neurofilament protein.

Ana Catarina Maurício Brito Ataíde Montes

Ph.D. Thesis

Laboratório de Glicobiologia

Instituto de Tecnologia Química e Biológica, Universidade Nova de Lisboa

Av. da República, Estação Agronómica Nacional

2780-157 Oeiras, Portugal

http://www.itqb.unl.pt

ao Pedro

Acknowledgements

This PhD thesis would not come to print without the help of many people to whom I would like to express my sincere gratitude.

When I finished my final report to obtain the Biochemistry degree, six years ago, I took the resolution that, one day, when writing the PhD thesis, I would not leave the acknowledgements for last. By that time, I felt that I was too much in a hurry, too tired and too emotive to do it adequately. Life runs so fast that only now I realize that the PhD thesis is finished and I was not able to keep up with my resolution. Once again, I feel I am not expressing properly the gratitude to the people whose help and support was so important to me throughout these years. I must apologize for such weak words to describe so strong feelings.

First, I have to thank to my supervisor, Dr. Júlia Costa, for introducing me to the Glycobiology and Membrane Trafficking fields, opening me the doors of the fascinating universe of Science. From the beginning, when she accepted me as an undergraduate student in her Laboratory, her guidance was invaluable. Julia was always available, transmitting knowledge, experience, ideas and also listening, discussing. Her commitment, intelligence and rigor shaped me as an investigator and, over the years, she gave me the freedom to explore my own ideas. I am grateful for the confidence she has placed in me.

I would like to thank Dr. Harald Conradt for his great contribution to this thesis work, namely the clarification of fucosyltransferase IX specificity towards glycoproteins. Most importantly, I thank him for his availability for sharing his vast and deep knowledge in Glycoscience and for transmitting me his profound scientific rigor and critical sense. Our fruitful meetings were always challenging and enlightening.

There are many memorable days in one's life, but some are crucial as they open surprising perspectives and envision unsuspected new paths. I had the *revelation* that "Le^x was in the TI-VAMP compartment" during Dr. Thierry Galli presentation, the first time he came to ITQB. I thank him for his enthusiasm and valuable suggestions, since that first hour, and for welcoming me in his Laboratory and providing me the best working conditions. In Paris, Dr. Lydia Danglot embraced my project with her amazing energy and competence and I am very grateful for that. I also have to thank her for teaching me the tricky business of hippocampal primary cultures and for sharing her knowledge about the hippocampus, the "real" neurons, the mechanisms. Specially, thank you Lydia, for the exchange of experience, for all the discussions, ideas, thoughts, that made my short stay in Paris one of the most challenging periods of my PhD.

I would like to thank Dr. Andrea Streit and Dr. Ten Feizi for the generous gift of the L5 antibody and for the useful and valuable comments. I am especially grateful to Dr. Ten Feizi for the availability to share her profound knowledge about the Lewis^x epitope and for her suggestions.

I would like to thank to Dr. Leonor David and Dr. Celso Reis for providing several anti-Lewis epitopes antibodies and the precious mucins. I also thank to Dr. Celso Reis for all the suggestions, protocols and tips he gave me over the years.

I thank to Dr. Paula Alves for the encouragement and advice. To Cristina Peixoto, reliable colleague and friend, always available for support and wise suggestions. To Telmo Graça, for the HPAEC-PAD, for his commitment with the work, and also for the nice neighborhood. To Vítor Hugo, Luís Maria Fonseca, Ana Barbas, Sandra Viegas, José Andrade, Guida Serra, Isabel Marcelino, Marcos Sousa, Elisabete Nascimento, Sofia Leite and other corridor colleagues, for the help whenever needed, and for creating a friendly environment. To Susana Lopes, for having lightened the last difficult months. To Sofia, for the friendship from early breakfast to late snacks.

A special thanks to all the *Glico* colleagues, the present and the former, for the help and support. To Ricardo Gouveia, who volunteered to be the proofreader of this thesis; to Eda Machado, more than a bench partner, a close companion; to Catarina Gomes and Cristina Escrevente. Thank you all for sharing the work, the worries, the stressful times and also the joys, the fun, the relaxing moments. To Angelina Palma, the ideal friend and co-worker, for her unconditional and absolute companionship, for listening so much, for being with me at all times and for much more this page is too small to contain. To Vítor Sousa, for being a good honest friend, in laugh and annoy, for what he taught me, never oversimplifying things or patronizing me, discussing and making me grow scientifically. To both Angie and Vítor for the unforgettable year. To Vanessa Morais, the challenging lab partner, for all the experimental discussion, for a friendship against all odds. To Nuno Barata, always a patient and pleasant friend, despite I often was not in such good mood.

I thank my friends, the ones who carried me during the last years and the ones that patiently await me without giving up. Thank you Gonçalo, Natacha, Miguel & Luísa, Irina & Alexandre, Ana & Domingos, Ana, Susana & Luís, Vasco, Susana, Patrícia, Jun, Pedro. In the context of this thesis, I thank to Rodrigo Almeida and Nuno Raimundo for the careful readings. Thank you Nuno for the honest criticism that only a true friend is capable.

Agradeço à minha família pelo apoio incondicional, compreensão, carinho e paciência infinda. Mãe, obrigada pelo encorajamento constante, pela fé inabalável em mim, pela ajuda indispensável e insubstituível até à última hora. Pai, obrigada por me teres ensinado a sonhar. Avó, obrigada por cuidares de mim, sempre. Cristina e Nuno, obrigada pela irmandade perfeita, a capacidade de saberem quando mais vos preciso. Glória e Osvaldo, obrigada pelo carinho. Às mães, Círia e Glória, obrigada pela lição de vida de força e resistência.

Por fim, a ti Pedro, a quem dedico esta tese, obrigada pelo *nós*, motor da Vida.

To Fundação para a Ciência e Tecnologia (FCT) and Fundo Social Europeu (FSE) for finantial support (SRFH/BD/9139/2002)

victory is the art of persevering
when others stop trying

Summary

α3/4-Fucosyltransferases (α3/4-FUTs) are glycosyltransferases (GTs) that catalyze the transfer of fucose in an α3/4-linkage onto the *N*-acetylglucosamine residue from acceptors containing the type II or type I (Galβ4/3GlcNAc, respectively) structures, thus synthesizing the fucosylated Lewis (Le) carbohydrate determinants. Fucosyltransferase IX (FUT9), the most recently identified member of the family, presents the higher divergence from the other FUTs and its sequence is the only highly conserved among species. FUT9 synthesizes the Lewis^x (Le^x) epitope (Galβ4(Fucα3)GlcNAc). Recent evidence has suggested that it is the enzyme responsible for the synthesis of Le^x in the mouse brain. Le^x expression has been described in glycoproteins, proteoglycans and glycolipids from the central nervous system (CNS) of diverse species, including rodents and humans.

The major goal of the work presented in this thesis has been to characterize human FUT9 and elucidate the functional role of Le^x in differentiating neurons *in vitro*. In Chapter 2, FUT9 has been cloned from human NT2N neurons and overexpressed in HeLa cells (FUT9wt), where it presented *in vivo* activity with *de novo* synthesis of the Le^x determinant. *In vitro* specificity studies towards small synthetic oligosaccharide acceptors linked to a hydrophobic moiety showed that FUT9wt synthesized preferentially Le^x and Le^y, whereas Le^a was produced with low efficiency, and only in the presence of the activating manganese cation. The corresponding oligosaccharides substituted with α2,3-linked neuraminic acid were not acceptors of FUT9wt. FUT9wt has been found to efficiently fucosylate desialylated *N*-glycans from glycoproteins, such as human asialoerythropoietin, but not native sialylated erythropoietin. Detailed analysis of the modified glycan structures from asialoerythropoietin by HPAEC-PAD and MALDI/TOF-MS showed that FUT9wt predominantly transferred one fucose residue onto the outer antennae of di-, tri- and

tetrantennary structures, containing proximal fucose, with or without repeats, thus synthesizing the corresponding peripherally monofucosylated structures. Difucosylated glycans were also detected, although in minor amounts and only in tetrantennary structures with repeats. These results demonstrated the high specificity of FUT9 for the synthesis of the Le^x determinant in *N*-linked glycans from glycoproteins. Furthermore, FUT9 is an adequate enzyme for *in vitro* synthesis of Le^x-carrier glycoproteins.

FUT9wt was localized in the *trans*-Golgi and *trans*-Golgi network (TGN) of HeLa cells, colocalizing with the *trans*-Golgi and TGN resident enzyme β4-galactosyltransferase and with the TGN marker TGN-46. Deletion of the cytoplasmic tail of FUT9, or just the Ser/Thr cluster contained in it, caused a shift to earlier Golgi sub-compartments, as indicated by higher colocalization with the *cis*-Golgi marker GM130 and redistribution into an endoplasmic reticulum-like pattern after incubation with brefeldin A. These results indicated that the information for intra-Golgi localization is contained in the cytosolic tail of FUT9.

With the purpose of obtaining high amounts of recombinant FUT9, in Chapter 3, a soluble form of the enzyme, sFUT9, was overexpressed in the *Spodoptera frugiperda* Sf9 insect cell line. sFUT9 was efficiently secreted and it presented higher efficiency for fucosylating glycoproteins, both sialylated and non-sialylated, than full-length FUT9wt from HeLa cells. Thus, sFUT9 is suitable for synthetic purposes. Moreover, it can also be used for further functional and structural studies of FUT9, such as the determination of its three-dimensional structure.

In Chapter 4, identification of FUT9 as the enzyme responsible for the synthesis of Le^x in human NT2N neurons cultured *in vitro* was achieved through the detection of *FUT9* transcripts by RT-PCR, detection of FUT9 protein by Western blot, and efficient synthesis of Le^x and Le^y using *in vitro* activity assays. Immunofluorescence confocal microscopy studies showed that the Le^x determinant was present on the plasma membrane and in intracellular vesicles positive for the late endosomal/lysosomal marker lysosomal associated

membrane protein-1 (LAMP-1) and the v-SNARE tetanus neurotoxin-insensitive vesicle-associated membrane protein (TI-VAMP). Furthermore, Le^x was found in the cell bodies and neurites of NT2N neurons. These results associated for the first time the Le^x epitope with the TI-VAMP mediated exocytic pathway, known to be involved in neurite outgrowth. Moreover, antibody incubation assays with an anti-Le^x monoclonal impaired adhesion of NT2N neurons to the surface matrix and inhibited neurite initiation of outgrowth.

The levels of the Le^x epitope during neuronal development in rat primary hippocampal cultures were also studied, as addressed in Chapter 5. Le^x was detected in a subset of GABAergic interneurons, where it was also found to colocalize with the TI-VAMP marker similarly to that found in NT2N human neurons. On the plasma membrane of mature hippocampus GABAergic neurons, Le^x was detected in spine-like protrusions or phillopodia, dendritic domains adjacent to synaptic regions.

In conclusion, the work described in this thesis showed that FUT9 synthesized the Le^x epitope in human NT2N neurons, underlying neuronal adhesion and initiation of neurite outgrowth. Localization of Le^x in the TI-VAMP exocytic pathway in both human and rat neurons suggested common functions for the carbohydrate determinant in the CNS of both organisms. Furthermore, the discovery of efficient synthesis of Le^x on *N*-glycans from glycoproteins by FUT9 indicated that the effectors of those biological functions could be Le^x-glycoprotein carriers.

Sumário

Os α3/4-fucosiltransferases (α3/4-FUTs) são glicosiltransferases (GTs) que catalizam a transferência de fucose, numa ligação α3/4, para resíduos de *N*-acetilglucosamina de aceitadores que contenham estruturas do tipo II ou do tipo I (Galβ4/3GlcNAc, respectivamente), sintetizando assim epítopos fucosilados designados determinantes Lewis (Le). O fucosiltransferase IX (FUT9) foi o último elemento da família a ser identificado, sendo o que apresenta maior divergência em relação aos outros FUTs e o único com elevada homologia entre espécies. O FUT9 sintetiza o epítopo Lewis^x (Le^x) (Galβ4(Fucα3)GlcNAc). Estudos recentes sugeriram que o FUT9 é responsável pela síntese do Le^x no cérebro de murganho. A expressão do Le^x foi descrita em glicoproteínas, proteoglicanos e glicolípidos do sistema nervoso central (SNC) de várias espécies, incluindo roedores e humanos.

O objectivo principal do trabalho apresentado nesta tese foi a caracterização do FUT9 humano e a elucidação da função do Le^x na diferenciação neuronal *in vitro*. No Capítulo 2, o FUT9 humano foi clonado de neurónios NT2N e sobrexpresso em células HeLa (FUT9wt), tendo apresentado actividade *in vivo,* com síntese *de novo* do determinante Le^x. *In vitro*, estudos de especificidade usando aceitadores sintéticos, constituídos por pequenos oligossacáridos ligados a uma porção hidrófoba, revelaram que o FUT9wt sintetizou preferencialmente Le^x e Le^y, enquanto o Le^a foi produzido com baixa eficiência e apenas na presença do catião manganês como activador. Os oligossacáridos correspondentes substituídos com ácido neuramínico, numa ligação α2,3, não foram aceitadores do FUT9wt. Foi observado que o FUT9wt fucosilou eficientemente *N*-glícidos não sialilados de glicoproteínas, como a asialoeritropoietina, mas não a eritropoietina nativa sialilada. A análise por HPAEC-PAD e MALDI/TOF-MS das estruturas glicídicas modificadas revelou que o FUT9wt transferiu predominantemente um resíduo de fucose para as

antenas exteriores de estruturas bi-, tri- e tetrarramificadas contendo fucose próxima, com ou sem repetições, sintetizando as estruturas correspondentes com monofucosilação periférica. Foram ainda detectados glícidos bifucosilados, embora em menores quantidades, e apenas em estruturas tetrarramificadas com repetições. Estes resultados demonstraram a elevada especificidade do FUT9 para sintetizar o determinante Le^x em *N*-glícidos de glicoproteínas. Indicaram ainda que o FUT9 é um enzima adequado para a síntese *in vitro* de glicoproteínas contendo Le^x.

O FUT9wt foi detectado no *trans*-Golgi e no *trans*-Golgi reticular (TGN) de células HeLa, colocalizando com o enzima β4-galactosiltransferase, residente no *trans*-Golgi e no TGN, e com o TGN-46, marcador do TGN. A remoção total da cauda citoplasmática do FUT9, ou apenas do *cluster* de Ser e Thr nela contido, provocou uma deslocalização do enzima para sub-compartimentos anteriores, revelada pela colocalização aumentada com a proteína GM130, marcadora do *cis*-Golgi, e pela redistribuição por compartimentos com uma marcação típica de retículo endoplasmático após incubação com brefeldina A. Estes resultados indicaram que a informação que determina a localização intra-Golgi do FUT9 está contida na cauda citoplasmática do enzima.

Com o objectivo de obter quantidades elevadas de FUT9 recombinante, no Capítulo 3, foi sobrexpressa uma forma solúvel do enzima - sFUT9 - na linha celular de insecto *Spodoptera frugiperda* Sf9. O sFUT9 foi secretado eficientemente e apresentou uma eficácia superior na fucosilação de glicoproteínas, tanto sialiladas como não sialiladas, à apresentada pela forma total do enzima, FUT9wt, expressa em células HeLa. Assim, o sFUT9 é adequado para fins de síntese. Adicionalmente, poderá também ser utilizado em estudos funcionais e estruturais do FUT9, incluindo a determinação da estrutura tridimensional do enzima.

No Capítulo 4, o FUT9 foi identificado como o enzima responsável pela síntese do Le^x em neurónios humanos NT2N em cultura, com base na detecção de transcritos do *FUT9* por RT-PCR, na detecção do enzima FUT9 por *Western*

blot e na síntese eficiente de Le^x e Le^y em ensaios de actividade *in vitro*. Estudos de microscopia confocal de imunofluorescência revelaram que o determinante Le^x se encontrava na membrana plasmática e em vesículas intracelulares positivas para o marcador de endossomas secundários/lisossomas LAMP1 (do inglês *lysosomal-associated membrane protein* 1) e para a v-SNARE TI-VAMP (do inglês *tetanus neurotoxin-insensitive vesicle-associated membrane protein*). Foi ainda observado que o Le^x se encontrava nos corpos celulares e nos prolongamentos neuronais dos neurónios NT2N. Estes resultados relacionaram pela primeira vez o epítopo Le^x com a via de exocitose mediada pela TI-VAMP, que se sabe estar envolvida no crescimento dos prolongamentos neuronais. Para além disso, a incubação com um anticorpo monoclonal anti-Le^x, reduziu a adesão dos neurónios NT2N à superfície da matriz e inibiu a iniciação do crescimento dos prolongamentos neuronais.

Os níveis do epítopo Le^x foram também estudados durante o desenvolvimento de culturas primárias do hipocampo de rato, como descrito no Capítulo 5. O Le^x foi detectado num subgrupo de interneurónios GABAérgicos, tendo-se observado que colocalizava com o marcador TI-VAMP, à semelhança do verificado em neurónios humanos NT2N. Na membrana plasmática de neurónios GABAérgicos maturos, o Le^x foi detectado em protuberâncias semelhantes a espículas ou filopodia, domínios dendríticos adjacentes a regiões sinápticas.

Em conclusão, o trabalho descrito nesta tese mostrou que o FUT9 sintetizou o epítopo Le^x em neurónios humanos NT2N, estando na base dos processos de adesão neuronal e de iniciação do crescimento dos prolongamentos neuronais. A localização do Le^x no compartimento exocítico definido pela TI-VAMP, tanto em neurónios humanos como de rato, sugeriu funções comuns para o determinante glicídico no SNC de ambos os organismos. Ademais, a descoberta de síntese eficiente de Le^x em *N*-glícidos de glicoproteínas pelo FUT9 indicou que os efectores dessas funções biológicas poderão ser glicoproteínas decoradas com Le^x.

Table of contents

Thesis Outline

The work described herein concerns the study of fucosyltransferase IX in the central nervous system. Two lines of research were followed. One of them envisaged the characterization of human fucosyltransferase IX, while the other focused on the investigation of the biosynthetic product of the enzyme in neurons, the Lewis^x determinant, and its biological role during neuronal differentiation.

This dissertation starts with a general introduction to the endomembranous system of mammalian cells, where post-translational modifications, including glycosylation, occur. Particular relevance is given to the Golgi apparatus, as fucosyltransferase IX is a Golgi-resident protein. This is followed by an overview about protein glycosylation, including a summary of current knowledge of localization, structure and mechanism of glycosyltransferases. Fucosylation is focused in detail, specially the α3/4-fucosyltransferase family and the Lewis^x determinant, one of its products. Finally, a brief characterization of the NTera 2 cell line as a model system for human neuronal differentiation is presented.

Chapter 2 describes the cloning, overexpression and characterization of human fucosyltransferase IX. Studies concerning the substrate specificity of the enzyme, in particular towards glycoproteins, and its subcellular localization are presented.

In Chapter 3, the production and characterization of a recombinant soluble form of human fucosyltransferase IX from *Spodoptera frugiperda* Sf9 cells is described.

Chapter 4 is concerned with the levels of Lewis^x determinant during differentiation of human NT2N neurons and with the assignment of fucosyltransferase IX as the enzyme catalyzing its synthesis. The biological role of Lewis^x in human neuritogenesis is addressed.

In Chapter 5, levels of Lewis^x during the development of rat hippocampal neurons in culture are studied and the subpopulation of neurons that express the fucosylated determinant investigated.

Chapter 6 consists of a general discussion, where future perspectives and main conclusions of the work are presented.

List of Figures

List of Tables

Abbreviations

Abbreviation	Full form
A	absorbance
AP	adaptor protein
ApoE	apolipoprotein E
ara-C	cytosine arabinoside
ARF1	ADP ribosylation factor 1
ARFGAP	GTPase activating protein for ARF1
BFA	brefeldin A
BHK	baby hamster kidney
BSA	bovine serum albumin
CCD	conserved oligomeric Golgi complex-dependent
ChABC	chondroitinase ABC
CHO	chinese hamster ovary cells
CHX	cycloheximide
CNS	central nervous system
CNX	calnexin
COG	conserved oligomeric Golgi
COP	coat protein complex
CSPG	chondroitin sulfate proteoglycan
C-type lectin	calcium-dependent type lectin
DC-SIGN	dendritic cell-specific ICAM3 grabbing nonintegrin
dHex	deoxyhexose
DIV	days *in vitro*
DMEM-HG	Dulbecco's modified Eagle's medium- high glucose
DOC	sodium deoxycholate
EC	embryonic carcinoma
ECM	extracellular matrix
EDTA	ethylenediaminetetra-acetic acid
EE	early endosome
EEA-1	early endosome antigen-1
EGF	epidermal growth factor
EndoH	endoglycosidase H
ER	endoplasmic reticulum

Abbreviation	Full form
ERGIC	endoplasmic reticulum-to-Golgi-intermediate compartment
ES	embryonic stem
Fab	antigen binding fragment
FBS	foetal bovine serum
Fuc	fucose
FUT	fucosyltransferase
GA	Golgi apparatus
GABA	γ-aminobutyric acid
GAD	glutamate decarboxylase
GAG	glycosaminoglycan
Gal	galactose
GalNAc	*N*-acetylgalactosamine
GalNAcT	*N*-acetylgalactosaminyltransferase
GalT	galactosyltransferase
GDP	guanoside-5'-diphosphate
GEF	guanine-nucleotide exchange factor
Glc	glucose
GlcA	glucoronic acid
GlcNAc	*N*-acetylglucosamine
GlcNAcT	*N*-acetylglucosaminyltransferase
GP	glycoprotein
GT	glycosyltransferase
GTP	guanoside-5'-triphosphate
HBBS	Hank's balanced salt solution
HeLa	Henrietta Lack's
HEK	human embryonic kidney
HEPES	N-(2-hydroxyethyl)-piperazine-N'-2-ethanesulfonic acid
Hex	hexose
HexNAc	*N*-acetylhexosamine
HNK-1	human natural killer-1 cells epitope
HPAEC-PAD	high pH anion exchange chromatography with pulsed amperometric detection
HRP	horseradish peroxidase
IgG	immunoglobulin G
IgM	immunoglobulin M

Abbreviation	Full form
IL	interleukin
LacNAc	*N*-acetylactosamine
LAMP-1	lysosomal associated membrane protein - 1
LE	late endosome
Le^a	$Lewis^a$
Le^b	$Lewis^b$
Le^x	$Lewis^x$
Le^y	$Lewis^y$
Lyso	lysosome
MALDI/TOF-MS	matrix-assisted laser desorption ionization/time-of-flight mass spectrometry
Man	mannose
Man6P	mannose 6-phosphate group
MAP	microtubule-associated protein
MEM	minimum essential medium
MI	mitosis inhibitors
MOPs	4-morpholinepropanesulfonic acid
MVBs	multivesicular bodies
NCAM	neuronal cell adhesion molecule
NeuAc	*N*-acetylneuraminic acid
NF-L	low molecular weight neurofilament protein
NF-M P-	hypophosphorylated medium molecular weight neurofilament protein
NF-M P+	hyperphosphorylated medium molecular weight neurofilament protein
NP-40	Nonidet-P40
NT2 cell line	NTera2/cl.D1 cell line
$NT2^-$ cells	NTera2/cl.D1 undifferentiated cells
NT2N neurons	post-mitotic neurons derived from $NT2^-$ cells
NT2A astrocytes	astrocytes derived from $NT2^-$ cells
OD	optical density
PAGE	polyacrylamide gel electrophoresis
PBS	phosphate buffered saline
PBSCM	phosphate buffered saline supplemented with $CaCl_2$ and $MgCl_2$
PCR	polymerase chain reaction
PF	paraformaldehyde
PG	proteoglycan

Abbreviation	Full form
PM	plasma membrane
PNGaseF	peptide-*N*-glycosidase F
PO	poly-DL-ornithine
RA	retinoic acid
RE	recycling endosome
RPTPβ	receptor-type protein-tyrosine phosphatase β
RT-PCR	reverse transcription polymerase chain reaction
SCGs	sympathetic cervical ganglia
SD	standard deviation
SDS	sodium dodecyl sulphate
sFUT9	soluble fucosyltransferase IX
SialylT	sialyltransferase
sLacNAc	sialyl-*N*-acetylactosamine
sLe^a	sialyl-Lewis^a
sLe^x	sialyl-Lewis^x
SNAP	synaptosomal associated protein
SNARE	soluble *N*-ethylmaleimide-sensitive factor attachment protein receptor
SSEA-1	stage specific embryonic antigen-1
suc	sucrose
SYT7	synaptotagmin VII
TFA	trifluoracetic acid
TGF-β	transforming growth factor-β
TGN	*trans*-Golgi Network
TI-VAMP	tetanus neurotoxin-insensitive vesicle associated membrane protein
TM	transmembrane domain
Tris	tris(hydroxymethyl)aminomethane
TX-100	Triton X-100
UV	ultra-violet
VTCs	vesicular-tubular clusters
wt	wild-type

Amino Acid nomenclature:

Abbreviations		Amino acid name
Ala	A	Alanine
Arg	R	Arginine
Asn	N	Asparagine
Asp	D	Aspartate (Aspartic Acid)
Cys	C	Cysteine
Gln	Q	Glutamine
Glu	E	Glutamate (Glutamic Acid)
Gly	G	Glycine
His	H	Histidine
Ile	I	Isoleucine
Leu	L	Leucine
Lys	K	Lysine
Met	M	Methionine
Phe	P	Phenylalanine
Pro	P	Proline
Ser	S	Serine
Thr	T	Threonine
Trp	W	Tryptophan
Tyr	Y	Tyrosine
Val	V	Valine

Chapter 1

General introduction

1. General introduction

1.1. Membrane transport in mammalian cells

A hallmark of eukaryotic cells is the presence of an elaborate endomembrane system that is responsible for the exchange of macromolecules between cells and their environment. The secretory pathway delivers newly synthesized proteins, carbohydrates and lipids to the plasma membrane and extracellular matrix, modifying them during the trafficking process (Figure 1, green arrows and membranes), whereas the endocytic pathway takes up macromolecules into the cell (Figure 1, blue arrows and membranes). Transport along these pathways occurs through anterograde or retrograde translocation of material between different membrane-enclosed organelles, via small vesicles and large transport containers. Despite this transfer, each organelle maintains its characteristic set of resident macromolecules via several mechanisms, of which retrieval (Figure 1, red arrows) plays a fundamental role (Bonifacino and Lippincott-Schwartz, 2003).

1.1.1. The secretory pathway

1.1.1.1. The endoplasmic reticulum

The nascent proteins are targeted to the membrane of the endoplasmic reticulum (ER) and translocated into or across the ER via a cotranslational process. Once in the ER, proteins are processed for trafficking through the secretory pathway. One of the initial events in this process is the transfer of a precursor oligosaccharide to specific Asn residues in the polypeptide chain, the first step in *N*-glycosylation (See Section 1.2.1). Folding of the newly synthesized

polypeptides into their correct three-dimensional conformation is also started co-translationally in the ER. The quality control machinery in the lumen of the ER assures that only correctly folded proteins exit this compartment. Misfolded proteins are retained, triggering the unfolded protein response (UPR) pathway, which will regulate a battery of genes involved in ER-associated protein degradation (ERAD) but also in protein translocation, folding, glycosylation, and trafficking (reviewed by Ruddock and Molinari, 2006).

Following ER processing, proteins are concentrated in ER export sites (ERES), specialized domains of the ER membrane, also known as transitional ER (tER), responsible for the export of secretory cargo. In mammalian cells, ERES are distributed throughout the cytoplasm but concentrated in the juxtanuclear region adjacent to the Golgi apparatus (GA) (reviewed by Watson and Stephens, 2005). These sites are characterized by the presence of the coat protein complex II (COPII) (Figure 1), formed by the assembly of a set of soluble proteins, which mediates the biogenesis of transport carriers. The COPII mediates the selection of cargo from within the ER lumen, either directly (transmembrane cargo molecules) or indirectly via specific cargo receptors (soluble cargo and some transmembrane cargo molecules) (reviewed by Tang *et al.*, 2005). After detaching from the membrane of the ER, COPII carriers (vesicles and/or tubules) loose the COPII coat and undergo fusion to form pleiotropic membrane structures termed VTCs (vesicular-tubular clusters), that constitute the ER-to-Golgi-intermediate compartment (ERGIC, Figure 1). VTCs are then delivered to the *cis*-Golgi, fusing with the Golgi membrane and being absorbed into the stack (reviewed by Watson and Stephens, 2005).

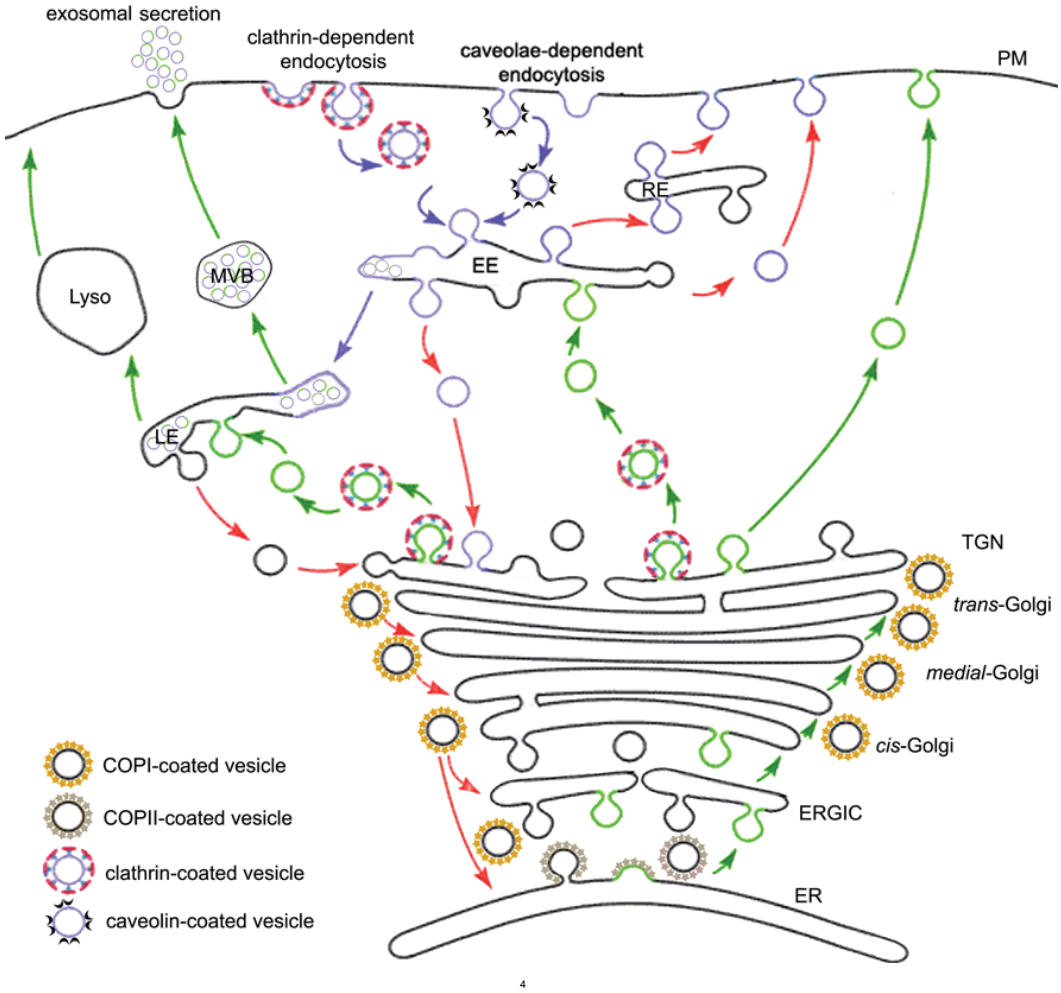

Figure 1: Schematic representation of the secretory and endocytic pathways. In the secretory pathway (green arrows and membranes) newly synthesized proteins are exported from the ER via coat protein complex II (COPII) coated-carriers that fuse into the ER-to-Golgi intermediate compartment (ERGIC) and subsequently the *cis*-Golgi. Material is transported along the Golgi apparatus until the *trans*-Golgi network (TGN), where cargo targeted to endosomal compartments is packed in clathrin-coated vesicles and transported to the early endosome (EE) and to the late endosome (LE), while membrane components and secretory cargo are transported to the plasma membrane (PM). The endocytic pathway (blue arrows and membranes) can occur via clathrin-coated vesicles or caveolae. Molecules are internalized into EE, transported into the LE and subsequently packed into lysosomes (Lyso) for degradation. Lyso can also act as

secretory compartments, fusing with the PM. Multivesicular bodies (MVBs) derived from the LE can fuse with the PM, releasing the internal vesicles as exosomes. Retrieval is observed in the exocytic and endocytic pathways (red arrows): recycling of ER-resident proteins from the GA and intra-Golgi recycling are mediated by COPI-coated vesicles; internalized material can be recycled from the EE back to the PM directly or via recycling endosomes (RE). Adapted from Kartberg *et al.*, 2005; Keller *et al.*, 2006; van der Goot and Gruenberg, 2006; van Niel *et al.*, 2006.

1.1.1.2. The Golgi apparatus

The GA comprises a stack of distinct compartments (cisternae) arranged from *cis* to *trans*. It acts as the central organelle of the secretory pathway, receiving newly synthesized proteins and lipids from the ER in the *cis*-side, covalently modifying them while they move through the stack to the *trans*-side, until the *trans*-Golgi network (TGN), where they are targeted to the final cellular destinations (anterograde transport) (Munro, 2005). Concomitantly, recycling of proteins and lipids to previous compartments (retrograde transport) occurs.

A century after the GA discovery, fundamental molecular mechanisms underlying the maintenance of Golgi's morphological and functional integrity, despite the constant flow of lipids and proteins along the exocytic pathway, remain unclear. These have been extensively addressed in the last decades, although they are still far from being fully understood.

The observation of numerous, small sized (70-90 nm), peri-Golgi vesicles, which bud from the Golgi cisternae in a COPI coat dependent manner (Orci *et al.*, 1986; Malhotra *et al.*, 1989), contributed to the proposal of several models. For many years, the predominant model defended vesicular transport and stable compartments, stating that newly synthesized cargo was transported in the anterograde direction by default. Transport would occur first via COPII vesicles leaving the ER and subsequently via COPI vesicles, budding and fusing

sequentially with Golgi cisternae. On the other hand, Golgi-resident proteins would be confined to the stable cisternae via retention signals excluding them from the trafficking vesicles (reviewed by Rothman and Wieland, 1996).

However, the vesicular transport/stable compartments model could not explain the transport through the GA of molecules like 300 nm procollagen fibers (Bonfanti *et al.*, 1998), far too large to fit in the vesicular transporters. Furthermore, it was observed that glycosyltransferases (GTs) localized in the *cis*-Golgi were processed by late-Golgi acting enzymes (Hoe *et al.*, 1995; Harris and Waters, 1996) and that retrograde COPI vesicles recycled membrane-bound proteins containing the cytoplasmic ER recycling motif K(X)KXX (Cosson and Letourneur, 1994; Letourneur *et al.*, 1994).

Despite some divergent data (Orci *et al.*, 2000; Cosson *et al.*, 2002), *in vitro* and *in situ* studies showed that COPI vesicles were enriched in several Golgi-resident proteins, in a process dependent of GTP hydrolysis by the small GTPase ADP ribosylation factor 1 (ARF1) (Lanoix *et al.*, 1999), and depleted of anterograde cargo that remained in the cisternae (Lanoix *et al.*, 2001; Martinez-Menarguez *et al.*, 2001; Mironov *et al.*, 2001; Malsam *et al.*, 2005). In previous work we have observed that COPI vesicles, formed *in vitro* from Golgi membranes of Baby Hamster Kidney (BHK) cells, were enriched in the *trans*-Golgi and TGN resident enzyme fucosyltransferase III (FUT3), contrary to anterograde cargo, such as transferrin receptor (plasma membrane resident) or ApoE (soluble secretory protein), which were not detected in the same vesicles (Sousa *et al.*, 2003). Lately, evidence suggested trafficking via transient tubular connections that may mediate several processes (reviewed by Mironov *et al.*, 2005), such as the recycling of GA resident enzymes (Kweon *et al.*, 2004).

All this data pointed to cisternal maturation/progression models, which stated that retrograde traffic via COPI transporters and/or tubular connections would be responsible for the constant maturation of Golgi cisternae into later compartments (reviewed by Kartberg *et al.*, 2005).

Although this is still a theme subject to intense debate, the cisternal maturation model collects nowadays more substantial support from experimental evidence. Two very recent studies in yeast have shown that markers of the early Golgi were consistently replaced with late Golgi markers (but never vice versa) (Losev *et al.*, 2006; Matsuura-Tokita *et al.*, 2006), confirming by direct observation the cisternal maturation hypothesis. So, throughout this thesis localization in the GA will be discussed in the context of the cisternal maturation model.

Assuming the cisternal maturation model, Golgi-resident proteins would be concentrated in retrograde COPI transporters and retrieved back to previous compartments. Therefore, Golgi localization would depend on sorting into COPI transporters and targeting to the acceptor membrane.

1.1.1.2.1 COPI transporters

COPI coat formation involves the interaction of the soluble coatomer protein complex to the membrane, via specific motifs present in the cytoplasmic domains of resident proteins (as, for example, the di-Lys K(X)KXX ER-retrieval motif) and via the small GTPase ARF1 in its GTP bound form. The several components polymerize in a lattice on the membrane, inducing sorting, budding and fission. Subsequent disassembly of the coat requires GTP hydrolysis on ARF1 by the membrane-associated GTPase activating protein for ARF1 (ARFGAP) (reviewed by Lippincott-Schwartz and Liu, 2006). A role for ARFGAP in cargo sorting into COPI vesicles has also been suggested (reviewed by Kartberg *et al.*, 2005) in a mechanism that would involve direct interactions with cytoplasmic domains of cargo proteins (Lanoix *et al.*, 2001).

Recently, new insights into the dynamics of COPI coat components, given by live-cell imaging techniques and photobleaching studies, suggested that all components and regulators involved in the process cycle on and off membranes, in a mechanism uncoupled from vesicle formation and independently of vesicle budding. The model hypothesizes that COPI coat has the ability to

self-assemble, acting as a molecular machine that drives membrane sorting and trafficking processes (Lippincott-Schwartz and Liu, 2006).

1.1.1.2.2. Membrane targeting

After COPI vesicle formation, the processes of directioning, targeting, docking and finally fusion will depend on conserved proteins that act in a regulated cascade: SNAREs (soluble *N*-ethylmaleimide-sensitive factor attachment protein receptors) on vesicle and target membranes, tethering factors and regulatory Rab small GTPases (Lupashin and Sztul, 2005).

SNARES are a family of short coiled-coil membrane associated proteins that act in docking and fusion events, via the formation of a *trans*-SNARE complex (or SNAREpin) between one v-SNARE in the vesicle membrane and three t-SNAREs chains associated with the target compartment (reviewed by Hong, 2005). The combinatory use of different SNAREs gives rise to a wide variety of complexes. For example, the SNARE complexes consisting of GS15–Ykt6–GS-28–syntaxin-5 and membrin–Bet1–Sec22b–Syntaxin-5 are both involved in Golgi transport. After fusion, the *trans*-SNARE complex is converted into a *cis*-SNARE complex and then disassembles in a process driven by ATP hydrolysis (reviewed by Hong, 2005).

Direct interactions between SNAREs and COPI coat have been observed (Rein *et al.*, 2002). Formation of *trans*-SNARE complexes involved in intra-Golgi transport has been shown to require tethering factors, like the golgin p115 (Shorter *et al.*, 2002; Puthenveedu and Linstedt, 2004) and the multisubunit conserved oligomeric Golgi (COG) complex (Suvorova *et al.*, 2002). Tethering factors, recruited by small GTPases, act as physical links, maintaining the vesicles and the acceptor membrane in close proximity (reviewed by Lupashin and Sztul, 2005). The number of known compartment-specific tethering factors (Allan *et al.*, 2000; Shorter *et al.*, 2002; Suvorova *et al.*, 2002) is growing and cooperativity between different types of tethers was recently found (Sohda *et al.*,

2007). This suggests a critical role for tethering factors in the fusion process, imposing membrane selectivity to vesicle-docking events.

The identification of different subpopulations of COPI vesicles enriched in distinct cargo molecules, defined by different tethering factors and different SNAREs (Malsam *et al.*, 2005), confirmed the importance of vesicle targeting events in the regulation of intra-Golgi transport. In summary, the concerted action of the large variety of SNAREs and tethering complexes, together with their effectors and regulators, impose membrane selectivity to vesicle-docking events and contributes to the spatial and temporal regulation of COPI transporters fusion with target Golgi membranes.

1.1.1.3. The trans-Golgi network

At the TGN, cargo is sorted into carriers moving to different destinations in the cell, including the endosomal compartments and the plasma membrane. In some cell types there is also regulated secretion from specific storage compartments. Evidence from live-imaging studies suggested that proteins travelling along the exocytic pathway leave the GA predominantly via tubular carriers emerging from specific cargo domains of the TGN (reviewed by Gleeson *et al.*, 2004).

Cargo targeted to the endosomal compartments is incorporated into clathrin-coated vesicles (Figure 1). The machinery needed for the formation of clathrin-coated vesicles is complex and involves the recruitment of clathrin adaptors which simultaneously bind to clathrin and to other machinery components including specific receptors (Owen *et al.*, 2004). Clathrin adaptors, the heterotetrameric adaptor protein (AP) complexes AP-1, AP-2, AP-3, and AP-4 and the monomeric GGA1, GGA2, and GGA3 proteins, associate with the cytosolic domains of the transmembrane proteins via specific sorting signals.

A classical example is the mannose 6-phosphate group (Man6P) present in lysosomal hydrolases. This glycan motif is recognized by the Man6P-receptor that recycles between the TGN and the endosomal compartment (reviewed by Gu *et al.*, 2001). Other sorting signals that mediate endosomal and lysosomal targeting include the Tyr motifs, based on the amino acid sequence YXXØ (where X and Ø represents any amino acid residue and one with a bulky hydrophobic side chain, respectively), and the dileucine-based motifs (D/EXXXLL/I) (reviewed by Traub, 2005).

Recent models propose that sorting continues at post-TGN locations. Evidence accumulated in the last years consolidates the hypothesis that endosomal intermediates are part of the secretory pathway (reviewed by Rodriguez-Boulan and Musch, 2005), as described below in Section 1.2.3.

1.1.2. The endocytic pathway

The endocytic pathway starts with the invagination of specific areas of the plasma membrane and internalization of the resulting vesicles (Figure 1). Endocytosis can occur via three main mechanisms: clathrin-coated vesicles, caveolae or non-caveolar non-clathrin entry pathways.

With the exception of caveolae, whose destination can be regulated, all endocytic routes are thought to converge into endosomes. Endocytosed molecules first appearing in early endosomes (EE, Figure 1) where sorting takes place. Plasma membrane receptors are recycled directly or through recycling endosomes (RE, Figure 1), whereas other molecules are routed towards the TGN (Figure 1). Concomitantly, specific regions of the EE limiting membrane suffer local invaginations, which generate intraluminal vesicles. These contain cytoplasmic material and also membrane proteins with the extracellular domains exposed at the surface. EE regions enriched in intraluminal vesicles detach and fuse with the late endosomes (LE, Figure 1). Also, clathrin-coated vesicles

derived from the TGN fuse with the LE releasing digestive enzymes (Figure 1) (reviewed by van der Goot and Gruenberg, 2006; Perret *et al.*, 2005).

From the LE, some molecules are recycled to the TGN (Figure 1), like the Man6P-receptor, others integrated in intraluminal vesicles by reverse budding. These can be targeted to lysosomes (Lyso, Figure 1) for degradation or be integrated in multivesicular bodies (MVBs, Figure 1) that are targeted to the plasma membrane for exocytosis (Section 1.1.3) (reviewed by Keller *et al.*, 2006; van Niel *et al.*, 2006).

Caveolae-mediated endocytosis (Figure 1) represents a low capacity but highly regulated pathway, restricted to certain cell types, contrary to the ubiquitous clathrin-mediated endocytosis. It occurs via caveolae, first described as smooth-surfaced flask-shaped pits covering the surface of many mammalian cell types (reviewed by Perret *et al.*, 2005). The major protein constituent of calveolae is caveolin-1/caveolin-2 (or caveolin-3 in the muscle), associated with lipid raft domains (reviewed by Kirkham and Parton, 2005). Caveolar budding is induced by specific ligands such as viruses and toxins, like the simian virus 40 and the cholera toxin. From caveolae, molecules can be sorted into EE or be transported to the ER or to the GA. In polarized cells, caveolae are also involved in basolateral-to-apical transcytosis (reviewed by Perret *et al.*, 2005).

Concerning the non-caveolar non-clathrin endocytosis, although its mechanisms and components are not well understood, it has been suggested to be a specialized high capacity pathway for lipids. Lipid-based sorting appears to be an important feature, as shown by sensitivity to cholesterol depleting agents and association of internalized components with lipid rafts (Kirkham and Parton, 2005).

1.1.3. Non-conventional endosomal secretion

Recently, novel findings suggested that endosomal compartments are key players not only in the endocytic pathway but also in the sorting of proteins in the biosynthetic routes, and that non-conventional secretion associated with endosomal compartments can also occur (reviewed by Rodriguez-Boulan and Musch, 2005).

A mechanism of endosomal secretion occurs via MVBs, which can fuse with the plasma membrane and release their cargo into the extracellular space (Figure 1). The released intraluminal vesicles are called exosomes and many cell types secrete them via this mechanism, including haematopoietic cells, B- and T-lymphocytes, dendritic cells, mast cells, platelets, intestinal epithelial cells, astrocytes, tumor cells and neurons (reviewed by Keller *et al.*, 2006; van Niel *et al.*, 2006).

Additionally, lysosomes also function as secretory organelles undergoing Ca^{2+}-triggered exocytosis in non-specialized secretory cells. This pathway is involved in the membrane repair mechanism in several cell types, such as fibroblasts (Rodriguez *et al.*, 1997; Reddy *et al.*, 2001), and is subverted by the trypanosome parasite to invade the host cell (reviewed by Andrews, 2002). Melanosomes are also a form of secretory lysosome in melanocytes that store and release melanin (reviewed by Stinchcombe *et al.*, 2004).

Although the set of proteins required for effective lysosomal secretion varies in each cell type, lysosomal exocytosis involved in membrane repair has been shown to be regulated by the lysosomal Ca^{2+}-sensor synaptotagmin VII (SYT7) (Martinez *et al.*, 2000; Reddy *et al.*, 2001). Membrane fusion is facilitated by the interaction of SYT7 with the plasma membrane t-SNARE, composed of synaptosomal associated protein of 23 kDa (SNAP-23) and syntaxin 4, which form a *trans*-SNARE complex with the lysosomal tetanus neurotoxin–insensitive vesicle associated membrane protein (TI-VAMP) (Rao *et al.*, 2004).

Secretory lysosomes seem to share many of the intricate molecular machinery required for neurite outgrowth: expression of TI-VAMP mutants (Martinez-Arca *et al.*, 2000; Martinez-Arca *et al.*, 2001) and TI-VAMP silencing in neuronal cells (Alberts *et al.*, 2003) impaired neurite outgrowth; TI-VAMP forms *trans*-SNARE complexes with the plasma membrane syntaxin 4 and SNAP-25, the neuronal homologue of SNAP-23 (reviewed by Proux-Gillardeaux *et al.*, 2005). Furthermore, the involvement of SYT7 in neurite outgrowth was recently demonstrated (Arantes and Andrews, 2006), suggesting that Ca^{2+}-regulated exocytosis from TI-VAMP-containing lysosomal compartments are the membrane source for neurite outgrowth.

The non-conventional secretion events associated with endosomal compartments suggest the existence of cross talk between the secretory and endocytic pathways. A new perception of the endomembrane system and intracellular traffic emerges where the classical boundaries separating secretory and endocytic compartments become blurred.

1.2. Protein glycosylation

Glycosylation is the major post-translational modification of lipids and proteins that occurs along the secretory pathway of eukaryotic systems. Most secreted and membrane-bound proteins are glycosylated, from immunoglobulins to proteins of the extracellular matrix such as fibronectin and laminin (reviewed by Jones *et al.*, 2005). The oligosaccharide components of glycoproteins and glycolipids were often thought of as elaborate sugar ornaments, but their importance in cell-cell communication, cell adhesion, cell protection and quality control has begun to be appreciated.

The two most common types of glycosylation are *N*- and *O*-linked glycosylation. The *N*-glycosidic bond occurs via the nitrogen atom of the amide

group of an Asn residue and the *O*-glycosidic bond via the oxygen of any residue containing an hydroxyl group, like Ser or Thr (reviewed by Spiro, 2002).

1.2.1. N-linked oligosaccharides

In *N*-linked glycosylation, a preformed oligosaccharyl moiety ($Glc_3Man_9GlcNAc_2$) is transferred from a dolichol-linked pyrophosphate donor to an Asn residue from a nascent polypeptide within the consensus sequence Asn-X-Ser/Thr, where *X* can be any amino acid residue except Pro. This initial step in the *N*-glycosylation pathway is catalyzed by the oligosaccharyltransferase (reviewed by Yan and Lennarz, 2005) and is the most ubiquitous co-translational protein modification occurring in the lumen of the ER. Initial processing of the oligosaccharide occurs in the ER, including removal of the three glucose (Glc) and one mannose (Man) units by glucosidases I and II, and α-mannosidase, respectively. Correct folding of the nascent glycoprotein is accompanied by the removal of the third Glc residue by glucosidase II, and subsequent trimming of a Man residue by α2-mannosidase marks the exit from the ER (reviewed by Herscovics, 1999).

Processing continues in the GA with further trimming and addition of monosaccharides at the non-reducing end of the oligosaccharide by several GTs. Three different categories of *N*-linked oligosaccharides may be formed (Figure 2): high-mannose type, when the oligosaccharides remain unaltered after the initial trimming reactions, maintaining five to nine Man residues; complex-type, when there is further processing in the GA and the final structure presents a core of $Man_3GlcNAc_2$ and branches defined by *N*-acetylglucosamine (GlcNAc) residues and elongated by galactose (Gal), fucose (Fuc) and *N*-acetylneuraminic acid (NeuAc) residues; and the hybrid type when mannosidases of the GA do not act

after the addition of the first GlcNAc residue, resulting in complex structures on one arm and Man residues on the other (reviewed by Dennis *et al.*, 2001).

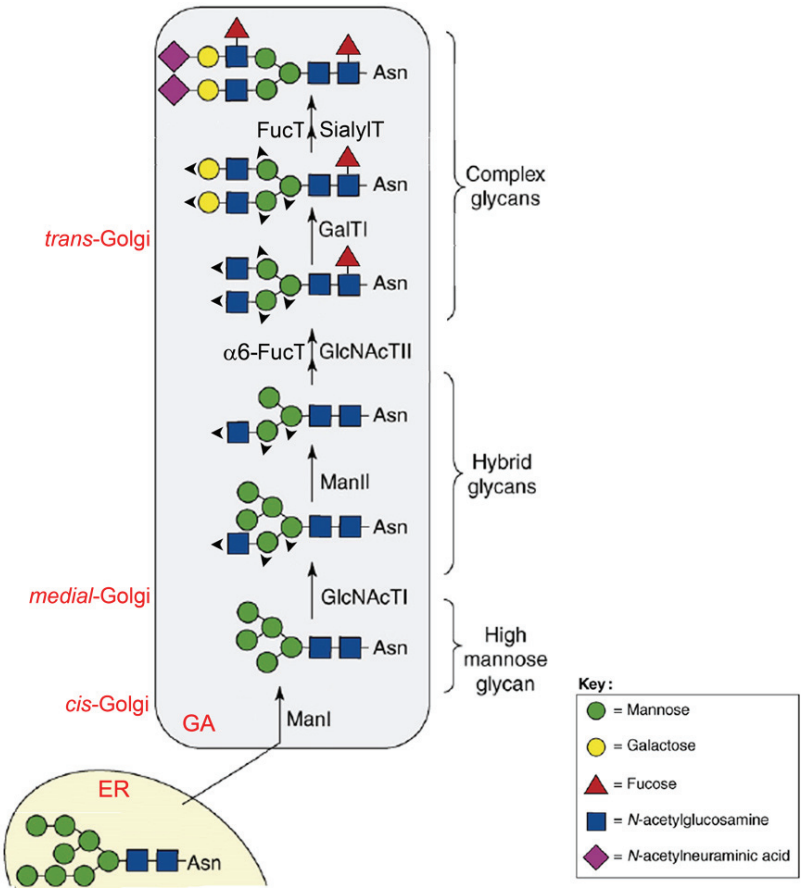

Figure 2: Schematic representation of *N*-linked oligosaccharide biosynthetic pathways in the Golgi apparatus. The high-mannose $Man_8GlcNAc_2$ core structure exits the ER to the Golgi apparatus (GA) where hybrid and complex *N*-glycans are formed by the sequential action of glycosidases and glycosyltransferases: mannosidase I (ManI); *N*-acetylglucosaminyltransferase I (GlcNAcTI); mannosidase II (ManII); *N*-acetylglucosaminyltransferase II (GlcNAcTII); α6-fucosyltransferase (α6-FucT); β4-galactosyltransferase I (GalTI), α2,3-sialyltransferase (SialylT) and α3/4-fucosyltransferase (FucT). Arrowheads indicate locations of possible elongation and branch formation. Adapted from Varki, 1999; Czlapinski and Bertozzi, 2006.

N-glycosylation presents enormous variation: macroheterogeneity arises from the fact that it does not occur at every potential glycosylation site, even among different molecules of the same protein, and microheterogeneity is caused by the different structures presented by the oligosaccharide moiety occupying each glycosylation site (reviewed by Jones *et al.*, 2005). The glycosylation profile depends upon the sequential action of Golgi-resident glycosidases and especially of GTs. Factors such as differential tissue-specific expression of the enzymes, order of distribution of the enzymes along the secretory pathway, enzyme specificity and site accessibility of the substrate, donor availability, among others, affect the final structure of the oligosaccharide (reviewed by Czlapinski and Bertozzi, 2006).

1.2.2. O-linked oligosaccharides

In *O*-linked glycosylation, monosaccharide residues are sequentially added directly onto the protein, in contrast to the pre-assembled oligosaccharyl precursor that initiates *N*-linked glycosylation. There is not a consensus sequence and there are several possible *O*-glycosidic linkages, the mucin-type (GalNAc-α-Ser/Thr) being the best characterized. Mucin-type glycosylation is based on a set of 8 core *O*-linked oligosaccharide structures, which are further elongated by the addition of Gal, Fuc and NeuAc residues, with core 1 to core 4-types being the most common (Figure 3). Core 1-type structures are formed by the addition of a β3 linked Gal residue to *N*-acetylgalactosamine (GalNAc) and further substitution of GalNAc with a GlcNAc residue in a β6 linkage gives core 2-type structures. Core 3-type structures are formed by the addition of a β3 linked GlcNAc residue to the initial GalNAc, and core 4-type structures present an additional substitution with β6 linked GlcNAc. The core

structures can be further elongated with GlcNAc, Gal, Fuc and NeuAc as exemplified in Figure 4 (reviewed by Peter-Katalinic, 2005).

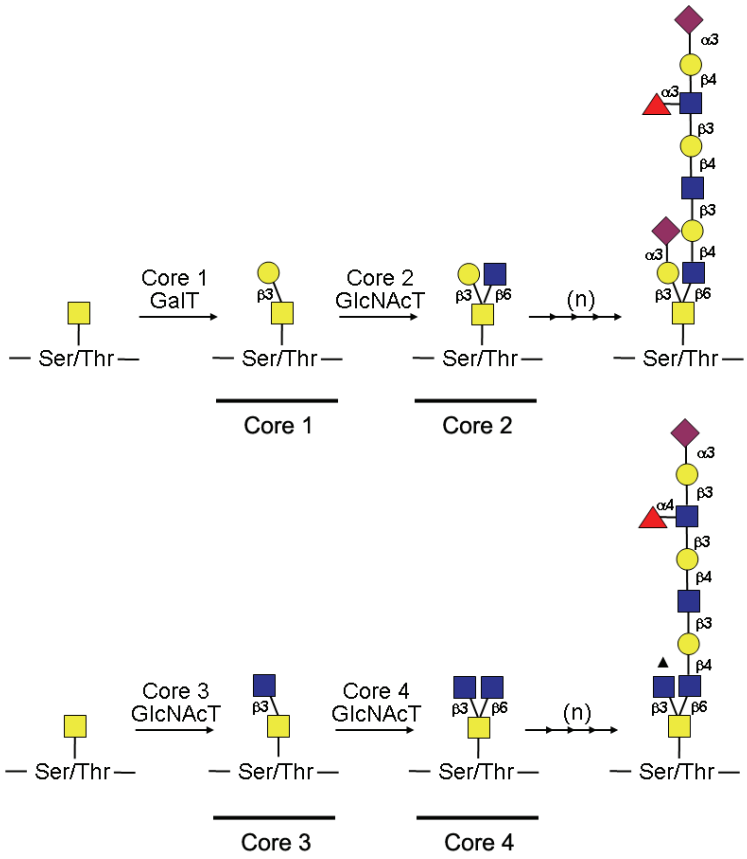

Figure 3: Schematic representation of core 1, core 2, core 3 and core 4 *O*-linked oligosaccharide subtype biosynthetic pathways. Core 1 and core 2 *O*-glycans subtype formation is regulated by β3-galactosyltransferase (Core 1 GalT) and β6-*N*-acetylglucosaminyltransferase (Core 2 GlcNAcT) activities, whereas core 3 and core 4 subtypes are controlled by β3-GlcNAcT (Core 3 GlcNAcT) and β6-GlcNAcT (Core 4 GlcNAcT). Branching by sequential action of several glycosyltransferases is represented by (n). Arrowhead indicates location of possible additional linkage. Symbols as in Figure 2 and □ for *N*-acetylgalactosamine. Adapted from Varki, 1999.

Although less investigated, *O*-GlcNAc-type glycosylation, *O*-fucosylation, *O*-mannosylation, and *O*-glucosylation are also observed (reviewed by Spiro, 2002). *O*-linked attachment of GlcNAc to Ser and Thr residues of nuclear and cytoplasmic proteins is not elongated nor further modified. It has gained considerable attention in the last years, not only because of its unusual cellular localization but also because it is rapidly reversible. Cycling of *O*-GlcNAc is controlled by soluble *N*-acetylglucosaminyltransferase (GlcNAcT) and *N*-acetylglucosaminidase in response to various cellular stimuli. This is a highly dynamic post-translational modification that plays a key role in signal transduction pathways, acting as a nutrient and stress sensor (reviewed by Hart *et al.*, 2007). Numerous proteins have been identified as targets of *O*-GlcNAc, and modulation of *O*-GlcNAc levels has been shown to modify DNA binding, enzyme activity, protein–protein interactions, protein half-life and subcellular localization (reviewed by Zachara and Hart, 2004). Deregulation of the *O*-GlcNAc glycosylation cycle has been associated with several pathologies, including diabetes, cardiomyopathy and neurological disorders (reviewed by Hart *et al.*, 2007).

1.2.3. Glycosaminoglycans

Historically, proteoglycans (PG) have been considered a distinct class of glycoproteins due to their unique structural characteristics. They are composed of a protein core that has one or more long linear glycosaminoglycan (GAG) chains, made up of repeating disaccharide units. Depending upon the composition of the GAG chains, PGs can be classified as heparin, chondroitin sulfate, dermatan sulfate, heparan sulfate or keratan sulfate PGs. GAGs are characterized by their high number of negatively charged functional groups, like carboxylate and sulfate (reviewed by Cattaruzza and Perris, 2006).

Usually PGs are heavily *O*-glycosylated, via an *O*-glycosaminoglycan linkage in which GAG chains are attached to Ser or Thr via a β-linked xylose

(reviewed by Peter-Katalinic, 2005). The sequential addition of two β-Gal residues and a β3-linked glucoronic acid (GlcA) form the common tetrasaccharide from which the polymerization reactions occur. In the case of keratan sulfates, the GAG chains can be *N*- or *O*-linked to the protein core (Bulow and Hobert, 2006).

PGs are components of the extracellular matrix (ECM) of several tissues, contributing to configuration and integrity, especially in structural tissues like cartilage, blood vessels and brain (reviewed by Cattaruzza and Perris, 2006).

1.2.4. Glycosyltransferases

Glycosyltransferases are a large family of enzymes, involved in the biosynthesis of glycoconjugates that catalyze the transfer of a monosaccharide residue from an activated nucleotide sugar donor to the acceptor glycoconjugate, forming a glycosidic bond. GTs are characterized by its exclusivity for a nucleotide-sugar donor, being named according to it, and by a very precise specificity for the acceptor substrates. The monosaccharide residues are transferred individually to the acceptor, allowing the stepwise building of the oligosaccharide chain by the sequential action of different GTs. These are distributed along the exocytic pathway, mainly in the GA. Golgi-resident GTs are type II membrane proteins with a short N-terminal cytosolic tail, a single transmembrane domain (TM), a flexible region adjacent to the TM called stem and a large C-terminal globular catalytic domain facing the lumen of the GA (Paulson and Colley, 1989).

1.2.4.1. Glycosyltransferase localization

Much of the GTs that catalyze the glycosylation of proteins and lipids in mammalian cells are localized in the GA. As referred in Section 1.2.1, relative localization of GTs is a factor of extreme importance in the determination of the oligosaccharide structures. Early-acting enzymes are concentrated in *cis* cisternae while late acting enzymes are enriched in the *medial*- and *trans*-Golgi, in an organization that has often been compared to an assembly line. Nevertheless, GTs are not strictly confined to particular cisternae but distributed in gradients along the Golgi stack, with consequent overlap of several enzymes (Nilsson *et al.*, 1993). In Figure 4, this is exemplified for GTs from the *N*-linked oligosaccharide biosynthetic pathway.

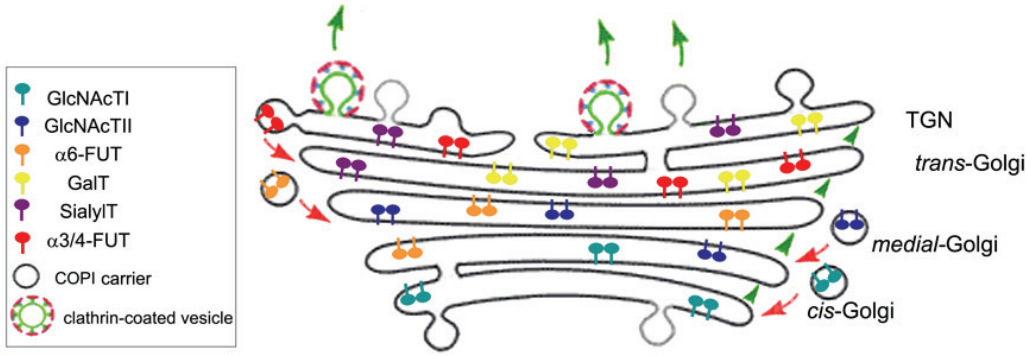

Figure 4: Schematic representation of the distribution of glycosyltransferases in the Golgi apparatus. Golgi-resident GTs are constantly recycled within the stack by retrograde transport via COPI carriers (red arrows) maintaining their distribution gradients. *N*-acetylglucosaminyltransferase I and II (GlcNAcTI and GlcNAcTII, respectively); α6-fucosyltransferase (α6-FucT); β4-galactosyltransferase (GalT); α2,3-sialyltransferase (SialylT); α3/4-fucosyltransferase (α3-FucT). Anterograde cargo is transported along the GA until the *trans*-Golgi network (TGN) (green arrowheads), where it is packed in clathrin-coated vesicles and delivered to the final destinations (green arrows). Adapted from Kornfeld and Kornfeld, 1985; Weiss and Nilsson, 2000.

Newly synthesized GTs are themselves cargo molecules of the exocytic pathway, transported from the ER to their specific destination in the GA. Thus, the mechanisms involved in their localization will be dependent on the mechanism of transport through the GA and also on the mechanisms underlying the maintenance of steady-state composition of the organelle referred in Section 1.1.1.2.

Common sorting motifs have never been found on the peptide sequences of the cytosolic tails of GTs. Studies with deletion mutants of resident GTs or fusion proteins with non-Golgi proteins have been carried out and revealed that the TM was essential for Golgi localization. Its presence was sufficient to target proteins from other subcellular compartments to the GA, as shown for β4-galactosyltransferase (GalT) (Teasdale *et al.*, 1992; Teasdale *et al.*, 1994), although the cytosolic tail of this *trans*-Golgi enzyme has also been shown to be involved in its localization (Nilsson *et al.*, 1991). It was observed for other GTs that TM flanking regions were important for Golgi localization, for example, α2,6-sialyltransferase (SialylT) cytosolic tail and stem spaced by a TM of the same length as that of SialylT were sufficient for Golgi retention (Munro, 1991). In the last years, special attention has been given to the cytosolic tail proposed to play an accessory role to TM regions, conferring the specific sub-Golgi localization. Actually, for α2-FUT and α3-GalT the cytosolic tails have been shown to be sufficient for Golgi localization (Milland *et al.*, 2001; Milland *et al.*, 2002). Furthermore, removal of the cytosolic tail of FUT3, a *trans*-Golgi/TGN resident enzyme, caused a localization shift to previous Golgi cisternae (Sousa *et al.*, 2004). For the glycolipid SialylTII and *N*-acetylgalactosaminyltransferase (GalNAcT), proximal and distal Golgi enzymes respectively, swapping of the cytosolic domains did not affect Golgi localization but was sufficient to invert sub-Golgi location of chimeric proteins (Uliana *et al.*, 2006a). These data substantiates the role of the cytosolic tail of Golgi-resident GTs on the fine regulation of intra-Golgi localization.

Several Golgi-resident enzymes, such as mannosidase II (Lanoix *et al.*, 1999; Lanoix *et al.*, 2001), GlcNAcTII, β4-GalT (Love *et al.*, 1998) and FUT3 (Sousa *et al.*, 2003), have been shown to concentrate into COPI vesicles (Figure 4). Although the direct binding of COPI coat components to the cytosolic domains of Golgi-resident proteins constitutes a direct way of ensuring the incorporation into vesicles (reviewed by Duden, 2003), this is not the case for Golgi GTs. Their cytosolic tails do not possess sorting motifs, contrary to the above-mentioned di-Lys motif present in ER-resident membrane proteins, and are probably too short to be able to interact directly with coat components. Thus, the mechanisms responsible for the correct localization of GTs in the GA are far from being understood.

1.2.4.2. Glycosyltransferase structure and mechanism

GTs have been classified into families on the basis of sequence similarities, identity of donor sugar and relative donor/product stereochemistry (Coutinho *et al.*, 2003). The CAZY (Carbohydrate-Active enzymes) database comprises almost one hundred GT families (named GT1, GT2, etc.) and is constantly being updated (http://www.cazy.org/CAZY/).

Despite the large number of families identified and the lack of significant primary structure homology among most families, the determination of the crystal structures of several GTs in recent years led to the proposal of just two major structural superfamilies: GT-A and GT-B. The classification was based on the observation of common topologies, similar or very close to the classical structural α/β/α sandwich motif called Rossmann-type fold, in the catalytic domains of the GTs for which the X-ray structure has been solved. In addition, the analysis of the uncharacterized families predicted that the majority adopt one of these two folds (Unligil and Rini, 2000; Bourne and Henrissat, 2001; Mulichak *et al.*, 2001). This

may indicate that all transferases have evolved from a small number of progenitor sequences.

All enzymes from the GT-A family share as common feature the DxD motif, shown to be involved in the interaction with the nucleotide sugar donor, via co-ordination of a divalent cation, typically Mn^{2+}, in an octahedral geometry. The cation coordinates six oxygen atoms from one or both Asp residues and the α and β phosphate groups of the donor, together with two water molecules. GTs from this family require a divalent cation as cofactor and present two conserved regions – an N-terminal nucleotide binding domain with a topology that resembles a Rossmann fold and terminates with the DxD motif and a more variable C-terminal domain involved in recognition of the acceptor (reviewed by Breton *et al.*, 2006).

On the other hand, GT-B fold is characterized by two separate domains with Rossmann topology, connected by a linker region that comprises the catalytic site. The C-terminal domain, responsible for the nucleotide binding, is highly conserved. Greater variations are observed in the N-terminal domain, in the region involved in acceptor binding. In the GT-B family no conserved residue has been observed and, although divalent cations may act as activators, they are not essential for enzymatic activity (reviewed by Breton *et al.*, 2006).

Catalytically, GTs can be classified as inverting or retaining, depending if the anomeric configuration of the added monosaccharide residue in the product is inverted or retained with respect to the starting material. The mechanism of catalysis by inverting GTs has been proposed to be analogous to the one presented by inverting glycosidases: the carboxylate anion of an acidic amino acid residue present in the catalytic site (usually an Asp) deprotonates the acceptor sugar, facilitating the nucleophilic attack at C1 of the monosaccharide donor. This favours direct SN_2 displacement of the nucleoside diphosphate with inversion of configuration (reviewed by Lairson and Withers, 2004). A metal ion (usually Mn^{2+}) plays the role of electrophilic catalyst in GT-A family GTs, as referred above. The mechanism of retaining glycosidases has not yet been

elucidated. It was proposed to be a double-displacement mechanism, involving formation of a glycosyl-enzyme intermediate but the existence of this intermediate has never been demonstrated. More recently, an alternative mechanism called SN_i-like was suggested, proposing a direct attack by the acceptor and departure of the leaving group of the donor on the same face (reviewed by Lairson and Withers, 2004).

1.3. Fucosylation

Fucose is a common component of *N*-, *O*- and lipid-linked oligosaccharides produced by mammalian cells. Usually fucosylation is a terminal modification of the glycan structure, with Fuc linked in an α2 glycosidic bond to Gal and α3, α4 or α6 to GlcNAc, although in the case of *O*-linked Fuc elongation with β-linked GlcNAc or β-linked Glc may occur (Moloney *et al.*, 1997; Moloney and Haltiwanger, 1999). This variety of possible linkages originates a multiplicity of fucosylated structures (Figure 5). A wide range of roles has been assigned to terminal Fuc-containing oligosaccharides, whose expression is often regulated during cell differentiation and development, as well as in several pathological processes. Some of these functions will be covered in the following sections but, given the diversity of Fuc containing structures, it is probable that many remain unknown.

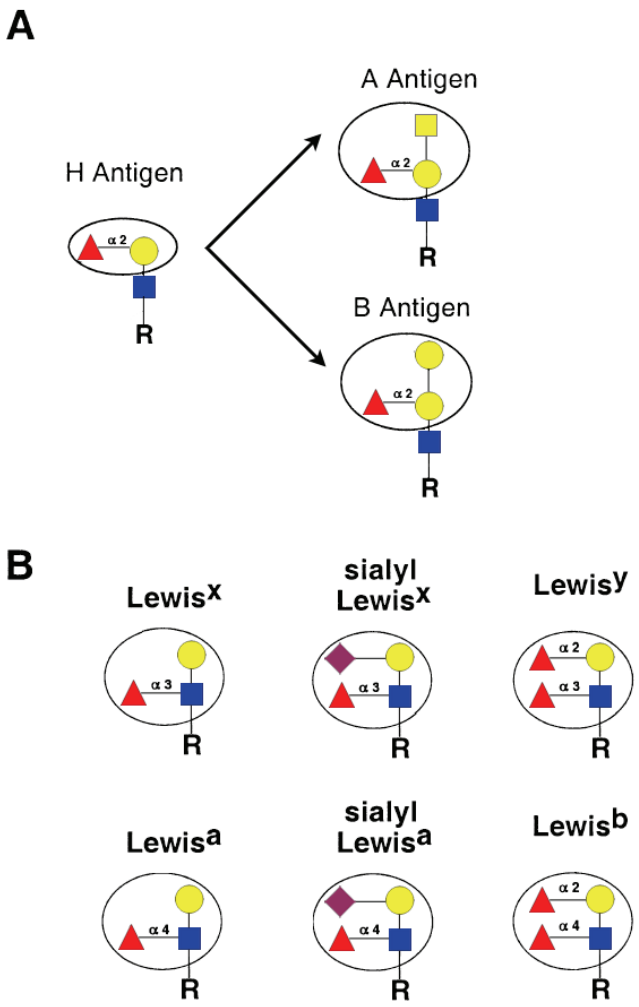

Figure 5: Structures of common fucosylated epitopes. (A) ABO blood group antigens; (B) Lewis-related antigens. R indicates *N*-, *O*- or lipid-linked precursors. Symbols as in Figure 2 and ▢ represents *N*-acetylgalactosamine. Adapted from Becker and Lowe, 2003.

The study of fucosyltransferases (FUTs), the GTs that catalyze the transfer of Fuc residues from the GDP-Fuc donor to the acceptor molecules, has been of great importance in unraveling the functions of fucosylated epitopes.

FUTs have been classified into four families - α2-FUT, α3/4-FUT, α6-FUT and O-FUT - according to the site of Fuc addition. So far, thirteen genes coding for FUTs were identified in the human genome. α2, α3/4 and α6 known FUTs are typical Golgi-resident type II membrane proteins (reviewed by Ma *et al.*, 2006) whereas O-FUTs are ER resident soluble enzymes (Luo and Haltiwanger, 2005).

Golgi-resident FUTs will be addressed in the following sections. Concerning O-FUTs, two human enzymes are known - FUT12 (POFUT1) and FUT13 (POFUT2) - which transfer Fuc directly to the hydroxyl groups of Ser and Thr residues of glycoproteins that contain the epidermal growth factor (EGF) or thrombospondin type repeat sequences, respectively (reviewed by Ma *et al.*, 2006).

1.3.1. The α2- and α6-fucosyltransferases

FUT1 and FUT2 are α2-FUTs that transfer Fuc to terminal Gal residues from glycoproteins and glycolipids, synthesizing the H blood group antigen (Figure 5A). FUT1, also known as H transferase is expressed in erythroid precursors while FUT2, or secretor transferase, is expressed in epithelial tissues and salivary glands and determines the secretory status. The H antigen can be further modified to A or B antigen, in individuals expressing the required GTs, encoded by the ABO locus. The expression of A transferase, B transferase, both or none of the enzymes are the basis of the classic ABO system of blood typing. Although the functional significance of the expression of the ABO blood group epitopes on erythrocytes is not clear, its high immunogenicity is a key issue in compatibility of blood transfusions (reviewed by Becker and Lowe, 2003).

FUT8 catalyzes the addition of Fuc in an α6 linkage to the innermost GlcNAc moiety of the core of *N*-linked glycans. Core fucosylation is frequently observed in *N*-glycans of several human glycoconjugates, including EGF, TGF-β

receptors (Wang *et al.*, 2005; Taniguchi *et al.*, 2006; Wang *et al.*, 2006) and human IgG1 (Shields *et al.*, 2002). The importance of α6-fucosylation was confirmed by the phenotype presented by the FUT8 knockout mouse: growth retardation, lung emphysema and death during postnatal development (Wang *et al.*, 2005). Recently, the X-ray structure of human FUT8 was solved (Ihara *et al.*, 2007), constituting the first known three-dimensional structure for a FUT. The enzyme appears to have a catalytic region similar to GT-B GTs rather than GT-A and, in addition, it contains an SH3 domain at the C-terminus, which is quite similar to the SH3 domains found in other proteins but unique in GTs (Ihara *et al.*, 2007). Further studies will be required to elucidate the function of this domain.

1.3.2. The α3/4-fucosyltransferase family

FUT3 to FUT7 and FUT9 constitute the α3/4-FUT family, which catalyzes the transfer of Fuc to the GlcNAc moiety of type I (Galβ3GlcNAc) or type II (Galβ4GlcNAc) *N*-acetylactosamine (LacNAc) structures, determining the synthesis of Lewis-related epitopes (Figure 5B). Sequence analysis of the α3/4-FUT family members revealed that the N-terminal regions of FUTs (variable segment) contain the highest sequence heterogeneity while the C-terminal portions (constant segment) present higher homology (Figure 6) (reviewed by de Vries *et al.*, 2001), and allowed the identification of several conserved peptide motifs in the catalytic domains.

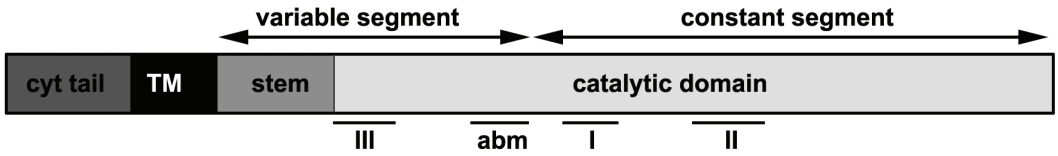

Figure 6: Schematic representation of human α3/4-fucosyltransferases. The cytosolic (cyt) tail, the transmembrane domain (TM), the stem region and the catalytic domain are represented. The conserved peptide motifs of the α3/4 family are indicated: the α3-motifs I and II; the motif III that marks the beginning of the catalytic domain and the acceptor binding motif (abm). Adapted from Dupuy *et al.*, 2004.

Motifs I and II, present in the constant segment (Figure 6), characterize the α3/4-FUTs (Oriol *et al.*, 1999). Recently, using the "Ala screening mutagenesis" approach in motif II of FUT3 and FUT6, it was determined that while some amino acid residues within this motif were essential for enzyme activity, others affected the affinity for donor and acceptor substrates (Jost *et al.*, 2005). Motif III, in the variable segment, contains the first amino acid residues required for correct folding and catalytic activity (Dupuy *et al.*, 2002). The acceptor-binding motif (abm), also in the variable segment, is involved in enzyme specificity (Dupuy *et al.*, 1999).

The specificity patterns presented by the six members of the family are different. All possess α3-activity, although FUT3, the Lewis type enzyme, has only residual α3-FUT activity and shows predominant α4-FUT activity forming the Lewis^a (Le^a), sialyl-Lewis^a (sLe^a) and Lewis^b (Le^b) determinants (Costa *et al.*, 1997). FUT3 together with FUT5 (de Vries *et al.*, 1995) are the only enzymes that present α4-FUT activity. It has been shown by domain-swapping experiments that the region responsible for the differences in type I / type II specificity was the aforementioned abm (Xu *et al.*, 1996). A single aromatic residue within this motif was required for the ability to bind type I acceptors (Dupuy *et al.*, 1999; Dupuy *et al.*, 2004). *FUT3*, *FUT5* and *FUT6* genes share very high sequence identity and are organized in a cluster, constituting the Lewis FUT gene subfamily. FUT6,

the plasma type FUT (Mollicone *et al.*, 1994), and FUT5 synthesize Lewis^x (Le^x) and sialyl-Lewis^x (sLe^x) determinants (Weston *et al.*, 1992b; Weston *et al.*, 1992a; de Vries *et al.*, 1995). FUT7, the leukocyte type, can only transfer Fuc to sialylated type II structures, with synthesis of sLe^x (Natsuka *et al.*, 1994). FUT4, the myeloid type enzyme, synthesizes mostly the Le^x epitope (Lowe *et al.*, 1991; Sherwood *et al.*, 2002). FUT9 (Kaneko *et al.*, 1999b), that also synthesizes preferentially the Le^x epitope (Toivonen *et al.*, 2002), will be discussed in further detail in Section 1.3.2.1. FUT10 and FUT11 have been identified as α3-FUTs due to their homology with other FUTs (Roos *et al.*, 2002), however, their activity has not been validated yet (Baboval *et al.*, 2000).

Lewis-related epitopes have been implicated in several cellular processes. The sLe^x determinant is of particular importance in inflammation, as it is the functional ligand of E-, P- and L-selectins, which mediate lymphocyte homing and leukocyte-endothelial cell adhesion events. FUT7 and FUT4 are the only α3-FUTs expressed in leukocytes (reviewed by Lowe, 2003). Abrogation of FUT7, FUT4 or both in the mouse model revealed that although FUT7 plays a major role in selectin-dependent adhesive activities, FUT4 also contributes to the synthesis of sLe^x (reviewed by Lowe, 2003). Another example of the important function of fucosylated glycans is their altered expression in cancer. Upregulation of sLe^a and of sLe^x has been shown for several cancers, associated with disease progression and bad prognosis. The epitopes are believed to promote metastasis via interaction with E- and P-selectins (reviewed by Becker and Lowe, 2003). Furthermore, in the host-microbe interaction between the gastric pathogen *Helicobacter pylori* and the gastric epithelium, a role for Lewis-related epitopes has been suggested. As the gastric surface epithelia express predominantly Le^a and Le^b and the gastric deep glands Le^x and Le^y, it was proposed that *H. pylori,* which expresses the same determinants, would use molecular mimicry to evade the immune system of the host and maintain a long-term infection (reviewed by Ma *et al.*, 2006). Le^x epitopes present on *H. pylori* have been shown to bind to

DC-SIGN (dendritic cell –specific ICAM-3 grabbing nonintegrin), a C-type lectin present on dendritic cells (Appelmelk *et al.*, 2003) that binds several pathogens and is thought to play an important role in the modulation of the immune response (Cambi *et al.*, 2005). The role envisioned for the Le^x epitope in the CNS and development will be discussed in Section 1.3.3.

1.3.2.1. Fucosyltransferase IX

FUT9 is the most recently cloned member of the α3/4-FUT family (Kaneko *et al.*, 1999b). Its sequence presents the lowest homology with the other FUTs and is the only one highly conserved among species (Kudo *et al.*, 1998; Kaneko *et al.*, 1999b; Baboval *et al.*, 2000; Patnaik *et al.*, 2000). Thus, FUT9 must have been under strong selective pressure during evolution, suggesting that it is responsible for an essential biological activity. FUT9 is able to synthesize efficiently the Le^x and Le^y epitopes but presents low reactivity towards NeuAcα2,3Galβ4GlcNAc and type I-based acceptors, with poor synthesis of sLe^x, Le^a, sLe^a and Le^b (Cailleau-Thomas *et al.*, 2000; Toivonen *et al.*, 2002). FUT9 exhibits a unique site-specificity, generating terminal Le^x motifs more efficiently than all the other α3-FUTs (Nishihara *et al.*, 1999).

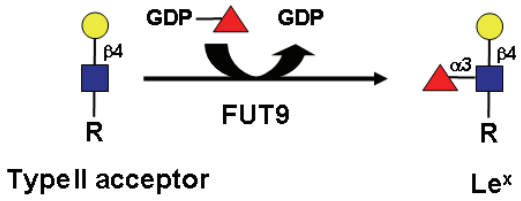

Figure 7: Schematic representation of the reaction catalized by human α3-fucosyltransferase IX (FUT9). FUT9 catalyzes the synthesis of the Lewis^x (Le^x) epitope using as substrate type II-based acceptors (Galβ4GlcNAc). R represents *N*-, *O*- and lipid-linked glycans. Symbols as in Figure 2. Adapted from de Vries *et al.*, 2001.

A detailed analysis of FUT9 specificity towards type II polylactosamine acceptors revealed that the enzyme preferentially fucosylates terminal LacNAc units of neutral chains. However, when the polylactosamine is substituted with α2,3-linked NeuAc, the site-specificity of FUT9 is shifted to the two innermost LacNAc units (Toivonen *et al.*, 2002).

The differences in the acceptor profiles together with the differences in tissue distribution of the several α3-FUTs could underlie distinct biological roles. The human *FUT9* gene is localized in chromosome 6q16 (Kaneko *et al.*, 1999a), comprises a single exon, and is transcribed in two transcripts of different sizes that present tissue specific distribution (Cailleau-Thomas *et al.*, 2000), implying that regulatory sequences may be present. The expression of the 2 kb transcript is ubiquitous in embryonic tissues and decreases in adult tissues. The 12 kb transcript presents a tissue-specific distribution, being strongly expressed in the embryonic brain and decreasing in adult brain. In adult tissues it is also detected in kidney, pancreas and placenta (Cailleau-Thomas *et al.*, 2000). FUT9 is also expressed in human granulocytes and peripheral leukocytes (Nakayama *et al.*, 2001), where it synthesizes the Le^x determinant present on a class of adhesion molecules of the immunoglobulin superfamily that binds to the DC-SIGN lectin on dendritic cells (Bogoevska *et al.*, 2006; Bogoevska *et al.*, 2007).

FUT9 is mainly expressed in the CNS, in both developing and mature brain of human, rat and mouse (Kaneko *et al.*, 1999b; Baboval *et al.*, 2000; Cailleau-Thomas *et al.*, 2000). It has also been shown to be increasingly expressed during neuronal retinoic acid-induced differentiation of PC19 murine embryonic carcinoma (EC) cells (Osanai *et al.*, 2001). FUT9 has been shown to be the α3-FUT responsible for the synthesis of Le^x in the mouse brain (Nishihara *et al.*, 2003; Kudo *et al.*, 2007), where it is controlled by *Pax6*, a transcription factor involved in brain patterning and neurogenesis (Shimoda *et al.*, 2002). Recently, the importance of FUT9 for the synthesis and role of Le^x in mouse brain was unequivocally shown with the study of $FUT9^{-/-}$ mouse (Kudo *et al.*, 2007).

This animal showed disappearance of Le^x in the brain, concomitant to increased anxiety-like behaviours. FUT9 appears to play a role in the functional regulation of interneurons from basolateral amygdala, as detected by a decreased number of calbindin-positive neurons in this region of the brain (Kudo *et al.*, 2007).

Taken together, the evidence presented points towards a spatial and temporal regulation of FUT9 expression and a specific role for this enzyme in embryonic and post-natal brain development.

1.3.3. Lewis^x in the central nervous system and development

The fucosylated carbohydrate Le^x determinant is expressed early during murine embryogenesis. Le^x, also known as stage specific embryonic antigen (SSEA)-1 (Gooi *et al.*, 1981), has been shown to be expressed at the cell surface at the morula stage and decline rapidly after compactation (Solter and Knowles, 1978). Calcium-mediated Le^x - Le^x homotypic interactions were thought to be the basis for cell recognition during this compactation stage (Bird and Kimber, 1984; Fenderson *et al.*, 1984; Eggens *et al.*, 1989; Kojima *et al.*, 1994). This interaction has recently been confirmed using Le^x bearing lipids inserted in bilayers that mimic cell membranes (Gourier *et al.*, 2004; Gourier *et al.*, 2005). Nevertheless, the analysis of the $FUT9^{-/-}$ mouse revealed that the animal was fertile and developed normally, although the expression of the Le^x, detected as SSEA-1 was absent in early embryos (Kudo *et al.*, 2004).

Le^x from glycolipids or glycoproteins is expressed in several human tissues, including the brain. Complex-type *N*-glycans with terminal Le^x on one arm are among the most abundant neutral carbohydrates detected in human brain (Albach *et al.*, 2001). In the developing CNS of diverse species, including human, rat, mouse, chicken and *Xenopus,* expression of Le^x is known to be temporally and spatially regulated (Dasgupta *et al.*, 1996; Gotz *et al.*, 1996; Mai *et al.*, 1999; Yoshida-Noro *et al.*, 1999). At the cellular level, it has been detected

in mouse neurons in the surfaces of cell bodies, processes and growth cones, as well as in cerebral primary cultures and in cerebellum sections (Nishihara *et al.*, 2003). Detection in neurons of developing *Xenopus* brain has also been reported (Yoshida-Noro *et al.*, 1999).

The hypothesis that Le^x acts as a cell-cell recognition molecule in the CNS with an important role in neurogenesis has been largely discussed in the literature but has not been clearly demonstrated. For example, selective adhesion of cells from different telencephalic regions of rat and chicken during development correlates with Le^x epitope localization and is developmentally regulated (Gotz *et al.*, 1996). Also, Le^x appears to have a role in neurite outgrowth or adhesion in *Xenopus* embryos since anti-Le^x antibodies inhibit neurite outgrowth in explant brain cultures (Yoshida-Noro *et al.*, 1999). A specific association between Le^x and mouse brain cells was also suggested by its role as a neural stem cell marker (Capela and Temple, 2002).

Until present, there has not been a clear assignment of the functional carriers of the Le^x epitope in human neurons nor of its exact biological role.

1.4. NTera2 cell line as model system for human neuronal differentiation

NTera2/cl.D1 (NT2) is a teratocarcinoma cell line derived from a human germ cell tumor, characterized by rapidly proliferating; undifferentiated, neuronally committed progenitor cells (Andrews, 1984). It preferentially differentiates into neuroectoderm, although its ability to give rise to cells belonging to all three germ layers *in vitro* has been recently reported (Pal and Ravindran, 2006). The NT2 progenitor cells can differentiate into all three neural lineages, depending on the experimental strategy (Pleasure *et al.*, 1992; Marchal-Victorion *et al.*, 2003; Sandhu *et al.*, 2003).

Exposure to all-trans retinoic acid (RA) generates an almost pure population of postmitotic neurons (NT2N) (Pleasure *et al.*, 1992) or a mixed population of NT2N neurons and astrocytes (NT2A) (Sandhu *et al.*, 2003), depending on the cell differentiation protocol. RA is a naturally occurring derivative of vitamin A known to be synthesized in the brain (Wagner *et al.*, 1990) and to affect neuronal differentiation within the CNS (Wuarin and Sidell, 1991). During RA-induced differentiation, NT2 cells substitute their immature neuroepithelial markers, like nestin (Pleasure *et al.*, 1992), for distinctive markers of mature CNS neurons, like neurofilaments (Lee and Andrews, 1986), tau protein, synaptophysin, and microtubule associated proteins (MAP) type 1 and 2 (Pleasure *et al.*, 1992). Under specific culture conditions these neurons form functional synapses (Hartley *et al.*, 1999) and express a variety of neurotransmitter phenotypes, including GABAergic, catecholaminergic, cholinergic and serotonergic (Yoshioka *et al.*, 1997; Guillemain *et al.*, 2000). Moreover, NT2N neurons express functional NMDA and non-NMDA glutamate receptors (Younkin *et al.*, 1993; Hardy *et al.*, 1994) and the amyloid precursor protein (Wertkin *et al.*, 1993). This cell type has also been used in several transplantation studies, which have demonstrated successful engraftment in animal models of stroke (Borlongan *et al.*, 1998), Huntington's (Hartley *et al.*, 1999; Muir *et al.*, 1999), Parkinson's disease (Baker *et al.*, 2000) and Amyotrophic Lateral Sclerosis (Garbuzova-Davis *et al.*, 2002). NT2N cells transplanted in patients with basal ganglia stroke improved motor and cognitive deficits (Kondziolka *et al.*, 2000). Furthermore, the NT2 cells transfected or infected with genes of interest can deliver exogenous genetic products to the host brain following transplantation (Baselga *et al.*, 1993; Hong *et al.*, 1999; Watson *et al.*, 2003). Therefore, this cell line can be used in transplantation not only as a substitute for foetal tissue but also as a vehicle for gene delivery.

NT2 cells differentiation seems to model the *in vivo* system, as high concentrations of RA, RA-binding proteins and receptors are present in the developing nervous system (Zetterstrom *et al.*, 1999). Furthermore, NT2 cells are

human EC cells, the stem cells of teratocarcinomas that resemble the pluripotent human embryo-derived embryonic stem (ES) cells. Differentiation of NT2N neurons induced by RA follows a gene expression pattern similar to that of the neuronal precursors during neurogenesis (Przyborski *et al.*, 2000). Thus, the unique properties of NT2 cells make them a model system for studying the complex events accompanying the process of human neuronal differentiation - from the commitment of human pluripotent ES cells to the neuronal lineage, and their subsequent development into a terminally differentiated neuronal phenotype. They have been used as models of neuronal differentiation in several cDNA screening methods, like RNA fingerprinting by arbitrarily primed PCR (RAP-PCR) (Cheung *et al.*, 1997), suppression subtraction hybridization (SSH) (Leypoldt *et al.*, 2001), cDNA array (Satoh and Kuroda, 2000; Bani-Yaghoub *et al.*, 2001) and microarray technology (Farlow *et al.*, 2000; Freemantle *et al.*, 2002).

Over the years, the characterization of EC and subsequently ES cells relied on the expression of a panel of cell surface antigen markers, mostly involving carbohydrate epitopes, whose exact function is still unknown. Nevertheless, the expression of these molecules is subject to tight regulation during differentiation. A switch in glycolipid synthesis from globoseries to lactoseries and ganglioseries structures (Fenderson *et al.*, 1987) marks NT2 cells differentiation induced by RA. SSEA-1, a lactoseries carbohydrate structure corresponding to the Le^x epitope, is induced early in differentiation and then declines (Fenderson *et al.*, 1987; Fenderson *et al.*, 1993; Andrews *et al.*, 1996), being present on both glycolipids and glycoproteins (Fenderson *et al.*, 1993).

Evidence points out the comparable expression of stage specific embryonic antigens of human EC, ES cells and the inner cell mass of the human blastocyst, in contrast to mouse ES and EC cells (Henderson *et al.*, 2002). Recently, cross-species transcriptional profiles of ES cells also suggested species-specific regulation mechanisms (Sun et al. 2007b). In this context, the

characteristics of the NT2 cell line make it a valuable model system to study the role of fucosylated epitopes, namely Le^x, in human neuronal differentiation.

1.5 Aims of this thesis work

Human FUT9 was the last member of the α3-FUT family to be identified. Its low homology with the other α3-FUTs and its high conservation between species envisioned an important biological role for this GT. At the beginning of this thesis work, there was evidence pointing to the importance of FUT9 in the rodent brain and a few studies concerning enzyme specificity suggested that the Le^x epitope was its main biosynthetic product. Nevertheless, information about human FUT9 specificity and its biological role was scarce. The ultimate goal of the work described in this thesis was to contribute to the understanding of the biological role of FUT9 and its biosynthetic products in human neurons.

The first objective of this thesis work consisted of the characterization of human FUT9 activity. Cloning and efficient expression of human FUT9 were needed to determine the *in vitro* specificity of FUT9 towards biologically relevant acceptors, such as GPs. As FUT9 is a Golgi-resident GT, localization can constitute an important regulation mechanism of *in vivo* activity. Therefore, human FUT9 localization was studied, focusing on the properties of the cytoplasmic domain and how it can affect the localization of the enzyme.

Obtaining high amounts of human FUT9 would be extremely useful for the establishment of the three-dimensional structure of the enzyme, as well as for synthesis purposes. In this context, the second objective of the work was to produce a recombinant soluble secreted form of human FUT9 that exhibited the ability of the native enzyme to synthesize the Le^x epitope.

The third objective consisted of the study of FUT9 and Le^x during neuronal differentiation, having in view the elucidation of the localization and biological role of the carbohydrate adhesion determinant in neuronal cells. NT2N neurons were used as cell model of CNS human neurons.

The fourth objective was to characterize the Le^x epitope in neurons from differentiating rat hippocampal neuronal cultures.

Chapter 2

Human fucosyltransferase IX efficiently fucosylates N-linked asialoglycoproteins with the synthesis of the adhesion Lewis^x determinant

Work presented in this chapter corresponds to the following manuscript:

Brito, C.; Kandzia, S.; Graça T.; Conradt, H.; Costa, J. (2007) "Human fucosyltransferase IX efficiently fucosylates *N*-linked asialoglycoproteins with the synthesis of the adhesion Lewis^x determinant" *(submitted)*.

2. *Human fucosyltransferase IX efficiently fucosylates N-linked asialoglycoproteins with the synthesis of the adhesion Lewis^x determinant*

2.1. Summary

The α3-fucosyltransferase IX (FUT9) catalyzes the transfer of fucose in an α3 linkage onto terminal type II (Galβ4GlcNAc) acceptors, the final step in the biosynthesis of the Lewis^x (Le^x) epitope, in neurons.

In the present work, FUT9 from NT2N neurons was cloned and overexpressed in HeLa cells (FUT9wt), where it was active. *In vitro*, FUT9wt was activated by Mn^{2+} and efficiently synthesized Le^x and Le^y, whereas Le^a was produced with a low efficiency, and the corresponding sialylated determinants were not fucosylated, using small synthetic oligosaccharide acceptors linked to a hydrophobic moiety as substrates. FUT9wt was found to efficiently fucosylate the desialylated *N*-linked glycoproteins secreted human asialoerythropoietin (asialoEPO) from CHO cells and bovine asialofetuin. However, sialylated EPO was not an acceptor of FUT9wt. Analysis by HPAEC-PAD and MALDI/TOF-MS revealed predominantly mono-fucosylation by FUT9wt of type II di-, tri- and tetrantennary *N*-glycans with and without *N*-acetylactosamine repeats from recombinant asialoEPO. Minor amounts of difucosylated structures were also found.

In vivo, HeLa cells transfected with FUT9wt expressed *de novo* Le^x, as detected by immunofluorescence microscopy. FUT9 was found to be a *trans*-Golgi and *trans*-Golgi network (TGN) glycosyltransferase from confocal immunofluorescence colocalization studies with markers of the secretory pathway β4-galactosyltransferase (*trans*-Golgi and TGN) and TGN-46 (TGN), further supported by localization around the microtubule organization center after

incubation with brefeldin A. Analysis of mutants generated suggest that the information for intra-Golgi localization is contained in the cytosolic tail of FUT9.

The results suggested that FUT9 could fucosylate glycoproteins with the synthesis of the cell adhesion Lewis^x determinant in neurons.

2.2. Introduction

Glycosyltransferases (GTs) mediate the transfer of monosaccharide residues from nucleotide sugar donors to glycoconjugates along their transport in the secretory pathway. α3-Fucosyltransferases (α3-FUTs) catalyze the transfer of fucose (Fuc) in an α3 linkage, onto terminal Galβ4GlcNAc motifs in the oligosaccharide chains, the final step in the biosynthesis of the Lewis^x (Le^x) epitope. FUT3, FUT4, FUT5, FUT6, FUT7 and FUT9 constitute the human α3/4-FUT family (reviewed by Becker and Lowe, 2003), presenting the type II membrane topology characteristics of Golgi resident GTs: a short N-terminal cytosolic tail, a single transmembrane domain (TM), a flexible region adjacent to the TM called stem and a large C-terminal globular catalytic domain, facing the lumen of the Golgi (Paulson and Colley, 1989).

The α3/4-FUT family members share several conserved peptide motifs in their catalytic domains (reviewed by de Vries *et al.*, 2001). FUT9 is the most recently cloned member of the α3/4-FUT family (Kaneko *et al.*, 1999b). Its sequence presents the lowest homology with the other FUTs and is the only one highly conserved among species (Kudo *et al.*, 1998; Kaneko *et al.*, 1999b; Baboval *et al.*, 2000) which indicates that it has been under strong selective pressure during evolution, suggesting that it is responsible for an essential biological activity. FUT9 exhibits a unique site-specificity, generating Le^x determinants more efficiently than all the other α3-FUTs (Nishihara *et al.*, 1999). It is also able to synthesize the Lewis^y (Le^y) epitope but not sialyl-Lewis^x (sLe^x) and type I-based acceptors are poor substrates (Cailleau-Thomas *et al.*, 2000; Toivonen *et al.*, 2002).

FUT9 is mainly expressed in the central nervous system (CNS), in both developing and mature brain of human, rat and mouse (Kaneko *et al.*, 1999b; Baboval *et al.*, 2000; Cailleau-Thomas *et al.*, 2000). The $FUT9^{-/-}$ mouse showed disappearance of Le^x in the brain, concomitantly to increased anxiety-like

behaviors (Kudo *et al.*, 2007). In human neurons in culture FUT9 is the α3-FUT responsible for the synthesis of Le^x (Brito *et al.*, 2007). Thus, it is probable that FUT9 also synthesize Le^x in human CNS similarly to that found in the mouse. Furthermore, the abundant neutral complex-type *N*-glycans with terminal Le^x on one arm detected in human brain (Albach *et al.*, 2001) may be products of FUT9 action.

The structure of the oligosaccharides present on glycoconjugates depends on the sequential action of Golgi resident glycosidases and GTs. The ordered, although overlapping, localization of GTs in the Golgi apparatus (GA) (Nilsson *et al.*, 1993) is a key factor in the *in vivo* regulation of the glycosylation profile of the nascent glycoconjugate. Several studies have implicated the TM and flanking regions of GTs in GA localization (Grabenhorst and Conradt, 1999; Fenteany and Colley, 2005; Czlapinski and Bertozzi, 2006). The TM of GTs, e.g., β4-galactosyltransferase (β4-GalT) (Teasdale *et al.*, 1992; Teasdale *et al.*, 1994) or FUT3 (Sousa *et al.*, 2003), has been shown to be required for localization in the Golgi apparatus. On the other hand, the cytosolic domain has been shown to be sufficient for GA localization for α2-FUT and α3-GalT (Milland *et al.*, 2001; Milland *et al.*, 2002), or to play a role in GT finer localization inside the GA (Sousa *et al.*, 2004).

In the present work, FUT9 cloned from NT2N neurons was efficiently expressed in HeLa cells, presenting *in vivo* activity with synthesis of Le^x. *In vitro,* recombinant FUT9wt was found to efficiently fucosylate di-, tri- and tetrantennary *N*-glycans with and without *N*-acetylactosamine (LacNAc) repeats from an asialo form of human recombinant erythropoietin (EPO), as revealed by HPAEC-PAD and MALDI/TOF-MS analysis. Furthermore, FUT9wt localized in the Golgi/TGN of HeLa cells and the cytosolic tail played an important role in the regulation of sub-Golgi localization of the enzyme.

2.3. Materials and methods

2.3.1. Cell culture

NTERA-2/cl.D1 cells were cultured and differentiated into NT2N neurons essentially as described previously (Pleasure *et al.*, 1992). Briefly, undifferentiated $NT2^-$ cells were grown in Opti-MEM I (Gibco) with 5% fetal bovine serum (FBS) (HyClone), 100 U/ml penicillin (P) and 100 μg/ml streptomycin (S) (Gibco). For differentiation, cells were cultured in Dulbecco's modified Eagle's medium (DMEM)-High Glucose (HG) (Gibco) with 10% FBS, P, S, and 10 μM retinoic acid (Sigma, St. Louis, MO) for 5 weeks. For neuron enrichment cell culture was in DMEM-HG with 5% FBS, P, S, supplemented with the mitosis inhibitors 1 μM cytosine arabinoside (Sigma), 10 μM fluorodeoxyuridine (Sigma), and 10 μM uridine (Sigma) for further 10 days. NT2N neurons were recovered after selective hydrolysis with trypsin (Gibco) and cultured on surfaces coated with 10 μg/ml poly-D-lysine (Sigma) and 0.26 mg/ml Matrigel (BD Biosciences). HeLa cells (ECCAC) were grown in DMEM-HG with 10% FBS (Gibco) and P/S. All cells were grown in a 5% CO_2 incubator, at 37°C.

2.3.2. Cloning of human FUT9 from NT2N neurons

Total RNA was extracted from $5x10^6$ NT2N neurons using the RNeasy extraction kit (Qiagen), according to the manufacturer's protocol. Two μg of total RNA were used in reverse transcription with the primer 5'-TTAATTCCAAAACCATTTCTCTA-3' (FUT9-rev): after 5 minutes at 65°C, the reaction was performed at 37°C, for 50 minutes, using 1 unit of moloney murine leukemia virus reverse transcriptase (Invitrogen), and terminated by heating at 70°C, for 15 minutes. The resulting cDNA was used to amplify two fragments of

human FUT9 by polymerase chain reaction (PCR). The 25 μl reaction mixtures contained 1 μl of cDNA, 1.5 mM $MgCl_2$, 0.2 mM dNTPs, 0.4 μM primers and 2.5 U of Taq DNA Polymerase (Invitrogen). As primer pairs 5'-ATGACATCAACATCCAAAGGAATTC-3' (FUT9-fwd) with 5'-GCTTTTCCGTGATGTAATCCTTGTG-3' (FUT9α3-rev) and 5'-GATTCAGATATCCAAGTGCCTTATG-3' (FUT9α3-fwd) with FUT9-rev were used. PCR reactions were carried out in the following conditions: initial denaturation at 94°C for 5 minutes; 25 cycles of denaturation at 94°C for 45 seconds, annealing at 55°C for 30 seconds and elongation at 68°C for 1 minute; final elongation at 68°C for 7 minutes. The PCR products were cloned into the mammalian expression vector pcDNA3.1/V5-HisTOPO (Invitrogen). A mixture of the two plasmids was used as template in a second PCR reaction where the complete human FUT9 coding sequence was amplified. The primers used were FUT9-fwd and FUT9-rev with a mixture of Taq DNA polymerase (Invitrogen) and Pfu Turbo DNA polymerase (Stratagene) as described above. The amplified fragment (FUT9wt) was cloned in the pcDNA3.1/V5-HisTOPO vector (Invitrogen) and in the PCRScriptCam vector (Stratagene). Automatic DNA sequencing confirmed FUT9 sequence (Kaneko *et al.*, 1999b).

2.3.3. Plasmid construction

The mutants FUT9dcyt, FUT9d6, FUT9S/A and FUT9wt with a V5 and His-tag were produced by PCR-based site directed mutagenesis using the PCRScriptCam-FUT9 vector as template. The V5 epitope was added at the C-terminus of FUT9 for detection purposes.

All V5-tagged mutants were constructed using the reverse primer FUT9V5-rev (5'-ATTCCAAAACCATTTCTCTA-3'). The forward primers were FUT9dcyt-fwd (5'-ATGCGCCCATTTTT-3'), FUT9d6-fwd

(5'-ATGAAAGGAATTCTT-3') and FUT9S/A-fwd (5'-ATGACAgcaACAgccAAAGGAA-3').

PCR was carried out under the following conditions: 94°C for 5 minutes; 25 cycles of 94°C for 45 seconds, 55°C for 30 seconds and 68°C for 1 minute; 68°C for 7 minutes. The 25 μl reaction mixtures contained 0.2 mM deoxynucleotides, 0.3 μM primers, 1 μg/ml of template DNA and a mixture of Taq DNA polymerase (Invitrogen) and Pfu Turbo DNA polymerase (Stratagene). All amplified fragments were cloned into the pcDNA3.1/V5-HisTOPO vector (Invitrogen). All sequences were confirmed by DNA sequencing. Clone analysis and maintenance were performed by standard techniques.

2.3.4. Western blot analysis of FUT9wt and mutants overexpressed in HeLa cells

HeLa cells, at approximately 70% confluency, were transiently transfected with FUT9 constructs using the Lipofectamine Plus (Invitrogen) reagent, according to the manufacturer's protocol.

Cells ($2.5x10^5$) were solubilized with 50 mM Tris-HCl pH 7.4 containing 5 mM EDTA, 1% Triton X-100 (TX-100) and protease inhibitors (Complete Cocktail; Roche), at 4°C, for 1 hour and cleared by centrifugation at 10000x *g*, for 5 minutes. Protein from cell extracts and corresponding supernatants were precipitated in 80% ethanol, and further deglycosylated with 100 U Endoglycosidase H (Endo H) or 1000 U of polypeptide *N*-glycosidase F (PNGase F) (New England BioLabs) under denaturing conditions, following the supplier's protocol.

Total protein was separated by SDS-PAGE and transferred to polyvinyledene difluoride membranes. Membranes were blocked in 5% nonfat dry milk (Nestle) in PBS with 0.1% Tween-20. Primary antibodies were mouse monoclonal anti-V5 antibody (Invitrogen) (1:5000) and rabbit polyclonal

anti-calnexin antibody (Chen *et al.*, 1995) (1:15000). HRP-conjugated polyclonal secondary antibodies anti-mouse IgG and anti-rabbit IgG (GE Healthcare) were used. All dilutions were in blocking solution. Chemiluminescent detection was by the ECL Plus system (GE Healthcare).

2.3.5. Fucosyltransferase activity assays

HeLa cells transiently transfected with vector pcDNA3.1/V5-HisTOPO coding for FUT9wt were assayed for fucosyltransferase activity. Twenty hours after transfection cells were solubilized with 100 mM MOPS/NaOH buffer pH 7.0, containing 1% TX-100, at 4°C, for 1 hour (Costa *et al.*, 1997; Sousa *et al.*, 2001). Activity was determined by the incorporation of radioactive Fuc from the GDP-[^{14}C]-Fuc donor onto several acceptors at 37°C. The assay mixtures (25 μl) contained: 100 mM MOPS/NaOH buffer, pH 7.0, 100 mM NaCl, 50 mM $MnCl_2$, 0.1475 mM GDP-Fuc, 0.0025 mM GDP-[^{14}C]-Fuc (1:60 molar ratio) and the acceptor. The synthetic acceptors, used at 0.35 mM concentration, were the type I - Galβ3GlcNAc-R, NeuAcα2,3Galβ3GlcNAc-R and Fucα2Galβ3GlcNAc-R (H type I); and the type II - Galβ4GlcNAc-R (LacNAc), NeuAcα2,3Galβ4GlcNAc-R (sLacNAc) and Fucα2Galβ4GlcNAc-R (H type II) (Lectinity Holding); R = O-$(CH_2)_3NHCO(CH_2)_5$NH-biotin.

The glycoprotein acceptors used were: 2 mg/ml of bovine asialofetuin (AF) (52μM, considering the molecular mass 38.4 kDa corresponding to the polypeptide chain), 0.5 mg/ml of recombinant human EPO and an asialo form of EPO (asialoEPO) (17μM, considering the molecular mass 30 kDa determined by SDS-PAGE). For detailed characterization of the fucosylated *N*-glycans from EPO, the reaction mixtures were upscaled to 500 μl and extracts of HeLa cells mock transfected with human nicastrin (Morais *et al.*, 2006) were used as negative control.

One unit of enzyme activity was defined as the amount of enzyme catalyzing the transfer of 1 μmol Fuc/min to the acceptor. Linearity of product formation was observed up to 180 minutes with the LacNAc-R acceptor.

2.3.6. Native and desialylated (asialoEPO) EPO

The EPO used in this study was expressed from a CHO cell line and was purified from cell culture supernatants by ion-exchange chromatography, gel filtration and RP-HPLC. Thorough *N*-glycosylation analysis after desialylation demonstrated the presence of di- tri- and tetrantennary oligosaccharides with and without LacNAc repeats as follows: diantennary 5.2 %, triantennary 7.0 % (2, 4 branched 20%, 2,6 branched 80%), tetrantennary 21.7%, triantennary with one two and three repeats 9.1%, 5.8% and 1.0% respectively and tetrantennary chains with one, two or three repeats, 26.9, 16.8 and 5.0 respectively. All structures were fully α6-fucosylated at the proximal *N*-acetylglucosamine as revealed by MALDI/TOF-MS analysis. In the native form >95% of the galactose residues were masked with α2,3-linked *N*-acetylneuraminic acid. Ten percent of the sialic acids were *O*-acetylated. The asialoEPO was prepared from native EPO by chemical desialylation by incubating of the intact glycoprotein in the presence of 0.22% (v/v) trifluoroacetic acid (TFA) for 1 h at 82 °C. The asialoEPO was recovered by gel filtration.

2.3.7. Immunoaffinity isolation of desialylated EPO from FUT9 incubations for N-glycan analysis

Desialylated EPO from incubations with FUT9 cell extracts was isolated by immunoaffinity chromatography using a column (1 ml of resin) with a monoclonal antibody raised against the human EPO polypeptide. Each sample

was applied to the affinity column equilibrated with PBS containing 0.02% (w/v) of sodium azide. After sample application, the column was washed with PBS buffer containing 0.02% sodium azide until the baseline was stable. EPO protein was eluted with 0.1 M glycine pH 2.5. Detection of protein was carried out at A=280 nm. The EPO containing fractions were neutralized with a 12.5% solution of NH_4OH.

The flow-through of each immunoaffinity run from each sample was re-applied, washed and eluted a second time as described above.

2.3.8. Release of N-glycans from EPO protein, purification and desalting

After immunoaffinity purification, EPO samples, after cell extract incubations in the presence of GDP-Fuc, were incubated with 25 milliunits of recombinant PNGase F overnight at 37°C. Complete de-*N*-glycosylation was monitored by the specific mobility shift of the EPO protein in SDS-PAGE. The released *N*-glycans were separated from the polypeptide by addition of three volumes of cold 100 % ethanol and incubation at –20°C for at least 2 hours. The precipitated protein was removed by centrifugation at 13000 rpm for 10 minutes at 4ºC. The pellet was then subjected to two additional washes with 500 µl ice-cold 75% ethanol. The oligosaccharides in the pooled supernatants were dried in a vacuum centrifuge (SpeedVac concentrator, Savant Instruments Inc., USA). The glycan samples were desalted using Hypercarb cartridges (100 mg) as follows: prior to use: the columns were washed three times with 500 µl 80% (v/v) acetonitrile in 0.1% (v/v) TFA followed by three washes with 500 µl water. The samples were diluted with water to a final volume of 300 µl before loading onto the cartridges. The loaded cartridges were rigorously washed with water. Oligosaccharides were eluted with 1.2 ml 25% acetonitrile containing 0.1% (v/v) TFA. The eluted oligosaccharides were neutralized with 2 M NH_4OH and were dried in a SpeedVac concentrator.

2.3.9. Analysis of neutral oligosaccharides via HPAEC-PAD

The analysis of the neutral EPO oligosaccharides via HPAEC-PAD was performed using an ICS-3000 ion chromatography system of Dionex Corporation, consisting of an AS autosampler, a DC detector/chromatography module and a DP dual pump. Twenty µl samples were injected into an equilibrated CarboPac PA200 guard column (3 x 50 mm, Dionex) connected to a CarboPac PA200 column (3 x 250 mm, Dionex). The neutral oligosaccharides were eluted by using a concentration gradient of 0.15 M sodium hydroxide (solvent A) and 0.15 M sodium hydroxide/ 0.6 M sodium acetate flow rate of 0.4 ml/min (5 minutes isocratic at 100% solvent A, 30 minutes to 85% solvent A and 10 minutes to 70% A). The column temperature was maintained at 30°C. The electrochemical detection of the oligosaccharides was performed by application of the detection potentials and durations as recommended by the manufacturer.

For subsequent MALDI/TOF-MS analysis of individual fractions from the HPAEC-PAD analysis, the corresponding fractions were desalted on-line by using a carbohydrate membrane desalter device (CMD-I; Dionex) and fractions were collected and dried in a SpeedVac concentrator.

2.3.10. Analysis of N-glycans by Matrix-Assisted Laser Desorption Ionization/ Time-of-Flight Mass Spectrometry (MALDI/TOF-MS)

Glycans were analyzed with a Bruker ULTRAFLEX time-of-flight (TOF/TOF) instrument in the linear positive ion mode. Native desialylated oligosaccharides were analyzed using 2,5-dihydroxybenzoic acid as UV-absorbing material. Samples of 1 µl at an approximate concentration of 1-10 pmol/µl were mixed with equal amounts of the respective matrix. This mixture was spotted onto a stainless steel target and dried at room temperature before analysis.

2.3.11. Immunofluorescence microscopy and image quantification

HeLa cells grown on glass coverslips to 70% confluency were transiently transfected with vector pcDNA3.1/V5-HisTOPO coding for FUT9wt and mutants. Twenty hours after transfection cells were incubated with 25 μg/ml cycloheximide for 3 hours, at 37°C and, when stated, with 5 μg/ml brefeldin A (BFA) for 45 minutes, at 37°C. Cells were washed with PBS containing 0.5 mM $MgCl_2$, fixed with 4 % paraformaldehyde in PBS for 20 minutes and permeabilized with 0.1 % TX-100 in PBS for 15 minutes. Blocking was done with 1 % bovine serum albumin (BSA) in PBS for 1 hour and primary and secondary antibodies were incubated in blocking solution, at room temperature, for 2 and 1 hours respectively. Washings were performed with PBS. Coverslips were mounted in Airvol. Primary antibodies were mouse IgG anti-Le^x SH1 (Singhal *et al.*, 1990) (10-fold concentrate with 1% BSA), rabbit anti-V5 (1:500) (Fortna *et al.*, 2004) mouse IgG anti-ERGIC-53 (Alexis Biochemicals) (1:500); mouse IgG anti-GM130 (BD Biosiences) (1:200); sheep IgG anti-GRASP55 (1:500) (Shorter *et al.*, 1999); mouse IgG anti-GalT (1:25); sheep IgG anti-TGN-46 (Serotec) (1:200); mouse IgG anti–adaptor protein 1 (AP-1) (Sigma) (1:150); mouse IgG anti-γ-tubulin GTU88 (Sigma) (1:500). Secondary antibodies were goat anti-rabbit IgG AlexaFluor594, donkey anti-rabbit IgG AlexaFluor594, goat anti-mouse IgG AlexaFluor488 and donkey anti-sheep IgG AlexaFluor488. All AlexaFluor conjugates (Invitrogen) were used 1:500.

Confocal images were acquired in a confocal microscope SP2+AOBS (Leica) equipped with a 63 x objective using zoom 2. Each fluorophore was excited and detected separately to avoid channel bleed-through. For each cell, laser intensities and amplifier gains were adjusted in order to give maximum pixel intensity (225) and to avoid saturation. This was done using the GLOW LUT on the Leica Confocal Software. Each picture consisted of a z-series of 20 images of 1024 x 1024 pixel resolution with a pinhole of 1.0 Airy unit and typically, 0.6 μm

focus intervals. Quantification of immunofluorescence images was performed using the open source Image J software version 1.30 (http://rsb.info.nih.gov/ij/). Eight to twelve cells have been analyzed per condition. Quantification of FUT9 constructs colocalizing with other markers was done using the Image J macro described previously (Sousa *et al.*, 2004). Statistical analysis was performed using the GraphPad Prism 4 software.

2.4. Results

2.4.1. Overexpression of human FUT9wt in HeLa cells and Le^x biosynthesis

Human FUT9 has been cloned from NT2N neurons. The cloned sequence was registered in GenBank™ with the accession number AY800264. It corresponded to the coding sequence of human FUT9 (Kaneko *et al.*, 1999b), a 359 amino acid protein predicted to have a type II membrane topology: a cytosolic tail of 11 amino acid residues; a TM of 21 amino acid residues and a luminal catalytic domain with three potential *N*-glycosylation sites (Asn-62, Ans-101 and Asn-153) (Figure 8A). To overexpress FUT9 in heterologous cells, this sequence was cloned in the pcDNA3.1/V5-HisTOPO vector, which codes for the V5 tag at the C-terminus for detection purposes.

FUT9wt was transiently expressed in HeLa cells and monitored by Western Blot analysis with a monoclonal anti-V5 antibody (Figure 8B). A major band was detected at approximately 54 kDa (Figure 8B, arrow), which probably corresponded to the mature form of FUT9wt. Digestion with PNGaseF caused a shift to approximately 47 kDa (Figure 8B, closed arrowhead), the predicted molecular mass of the peptide sequence of FUT9wt with the tags. After Endo H treatment two bands were detected at approximately 50 and 47 kDa (Figure 8B, open and closed arrowheads, respectively). These results together showed that the three potential *N*-glycosylation sites of FUT9 were occupied.

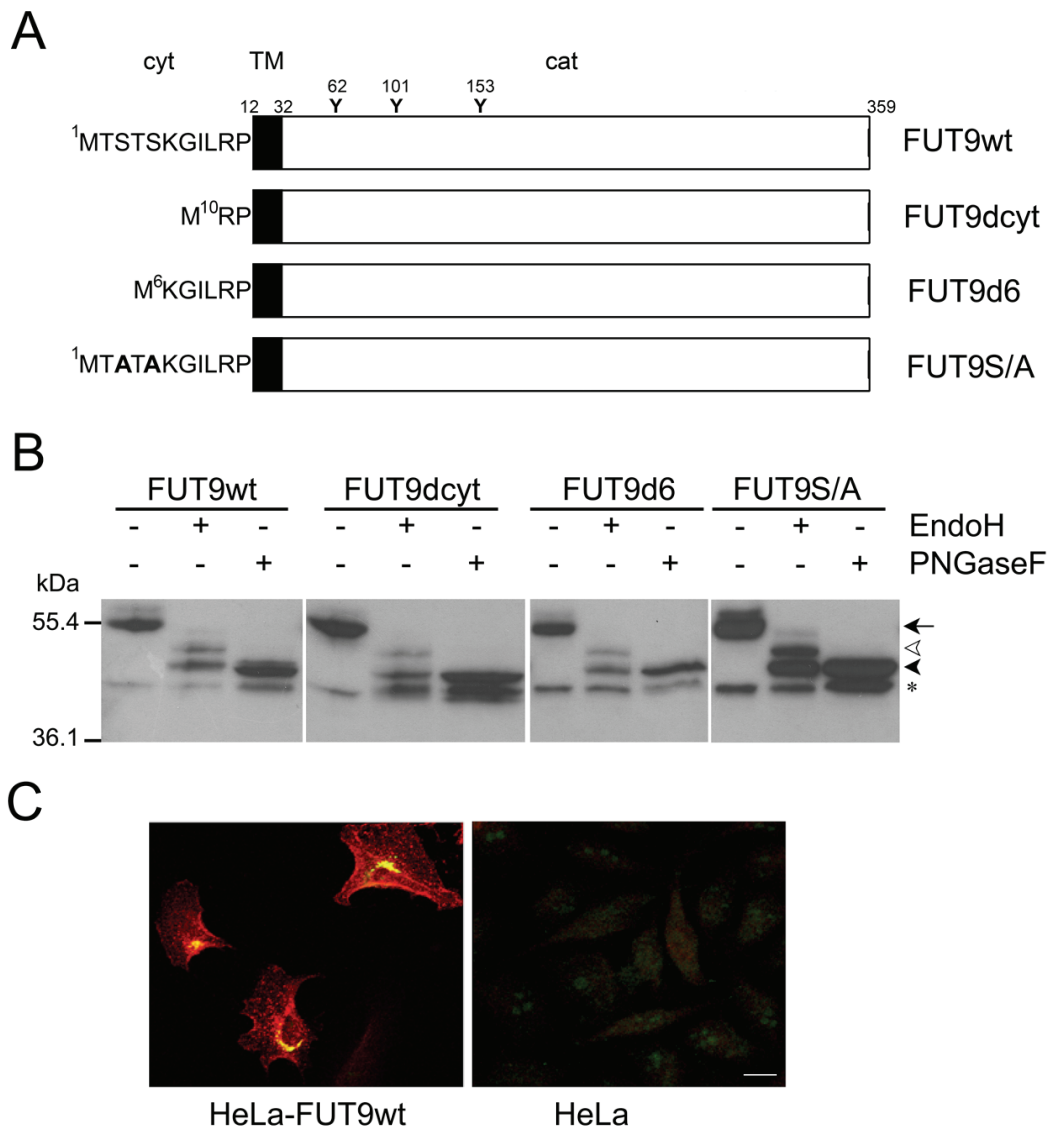

Figure 8: Overexpression of FUT9wt and mutants in HeLa cells. (A) Schematic representation of FUT9 constructs: FUT9wt is composed of a short cytosolic tail (cyt), a single transmembrane domain (TM) and a C-terminal catalytic domain (cat). The three potential *N*-glycosylation sites are indicated (Y). FUT9wt and the mutant forms were constructed with a V5 tag and His6 tail in the C-terminal region. **(B)** Western blot analysis of FUT9wt and mutants deglycosylated with EndoH and PNGaseF. Primary antibody: anti-V5 monoclonal antibody (1:500 dilution). Chemiluminescent detection was performed

by the ECL Plus system. Mature (arrow), EndoH resistant (open arrowhead) and deglycosylated (closed arrowhead) forms of FUT9wt and mutant are indicated. A degradation product is indicated with an asterisk. **(C)** Immunofluorescence confocal microscopy of FUT9wt and Lewis^x. Cells were treated with 25 μg/ml cycloheximide for 3 hours, at 37°C, fixed with 4% paraformaldehyde and permeabilized with 0.1% Triton X-100. Primary antibodies: anti-V5 polyclonal (green) and monoclonal anti-Le^x SH-1 (red) antibodies. Secondary antibodies: goat anti-rabbit AlexaFluor488-conjugated and goat anti-mouse AlexaFluor594-conjugated, respectively. Scale bar: 10 μm. Experiments were performed at least three independent times.

Probably two of the sites were occupied with high-mannose or hybrid oligosaccharides which were released with Endo H with a downward shift of 4kDa (considering the mass of a typical high mannose glycan $Man_9GlcNAc_2$ as 1.8 kDa, and the mass of a hybrid oligosaccharide substituted with proximal and peripheral Fuc and terminal neuraminic acid as 2.3 kDa). The other glycosylation site probably contained complex-type oligosaccharides that were released with PNGaseF only with a further downward shift of 3 kDa (considering that the molecular mass of a complex-type glycan can go from 2.3 kDa for a biantennary *N*-glycan with proximal Fuc and terminal neuraminic acid, up to 5.0 kDa for a tetrantennary oligosaccharide with 3 repeats, proximal Fuc, peripheral neuraminic acid in all antenna and 3 peripheral Fuc residues).

Overexpression caused *de novo* synthesis of the Le^x determinant in HeLa cells expressing FUT9wt, as detected by immunofluorescence microscopy, using the monoclonal SH1 antibody (Figure 8C). Transfected cells were also probed with monoclonal antibodies for the other Lewis determinants but no significant immunolabeling was observed (results not shown). Thus, Le^x is the major biosynthetic product of human FUT9 *in vivo*, corroborating previous *in vitro* data that described Le^x as the major product of human FUT9 (Nishihara *et al.*, 1999).

Together, these results indicated that FUT9wt was efficiently expressed in HeLa cells, correctly exported from the ER and transported to the Golgi where it

acquired complex *N*-glycans and was active in *vivo* synthesizing the Le^x determinant.

2.4.2. FUT9wt preferentially synthesizes Le^x and Le^y in vitro

The specificity of FUT9 towards small oligosaccharide acceptors was tested using cellular extracts of HeLa cells overexpressing FUT9wt without the V5 tag. For that purpose, a stop codon was introduced at the 3' end of the enzyme before cloning into the pcDNA3.1/V5-HisTOPO vector.

To establish the assay conditions for efficient Fuc transfer three issues were optimized using LacNAc-R as the substrate: Mn^{2+} concentration, pH and reaction time. The results from the literature concerning the effect of Mn^{2+} on FUT9 are contradictory, with inhibition observed for FUT9 from Namalwa cells (Kaneko *et al.*, 1999b), or activation for FUT9 from human brain homogenates (Mollicone *et al.*, 1992) or human neuroblastoma cells (Foster *et al.*, 1991). In this work, an activation effect of Mn^{2+} was observed, with an approximate 1.9-fold increase in activity at Mn^{2+} concentrations between 2.5 and 10 mM (Figure 9A). However, for higher concentrations (40 mM) there was a decrease in activity to values similar to those obtained in the absence of the cation (Figure 9A). Subsequent enzyme assays were performed in the presence of 5 mM Mn^{2+} at the optimum pH of 7.0 as determined in Figure 9B. The inhibitory effect at higher concentrations of Mn^{2+} was probably caused by the hydrolysis of the GDP-Fuc substrate by Mn^{2+} (Murray *et al.*, 1996).

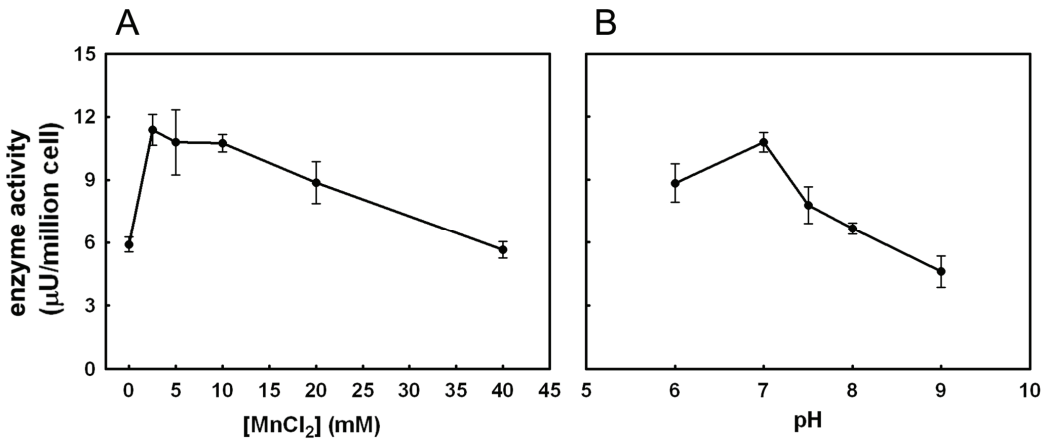

Figure 9: Effect of Mn^{2+} (A) and pH (B) on FUT9wt activity. Galβ4GlcNAc-R, where R = O-$(CH_2)_3NHCO(CH_2)_5$-NH-biotin, was used as acceptor substrate.

The activity towards the LacNAc-R acceptor was 7.9 ± 0.4 μU/10^6 cell leading to the production of the Le^x determinant (Table 1). Substitution of galactose with α2-linked Fuc (H type II-R) yielded a 1.5-fold increase in activity, with the production of the Le^y determinant. On the other hand, when galactose was substituted with α2,3-linked neuraminic acid (sLacNAc-R), radioactivity incorporation was undetectable. These results are in good agreement with the substrate specificity of human FUT9 toward low molecular mass acceptors in the absence of Mn^{2+} (Cailleau-Thomas *et al.*, 2000; Toivonen *et al.*, 2002).

Only a low FUT9 activity was observed with Galβ3GlcNAc-R (R = O-$(CH_2)_3NHCO(CH_2)_5$NH-biotin) as a substrate, corresponding to approximately 4 % of the obtained with the type II acceptor (see Table 1). Thus, we were able to demonstrate the synthesis of the Le^a determinant due to the presence of the activator Mn^{2+}, since in the absence of the cation no radioactivity incorporation was observed (data not shown).

Table 1: Substrate specificity of recombinant FUT9wt from HeLa cells.

Substrate	Activity ($\mu U/10^6$cell)	Relative Activity
Type II acceptors		
Galβ4GlcNAc-R	7.9 ± 0.4	1.00
NeuAcα2,3Galβ4GlcNAc-R	N.D.	N.D.
Fucα2Galβ4GlcNAc-R	11.8 ±0.6	1.50
Type I acceptors		
Galβ3GlcNAc-R	0.3 ± 0.0	0.04
NeuAcα2,3Galβ3GlcNAc-R	N.D.	N.D.
Fucα2Galβ3GlcNAc-R	N.D.	N.D.

R= O-$(CH_2)_3NHCO(CH_2)_5$-NH-biotin. N.D. not detectable (when the activity value was below 0.1 μU/million cell). Assays were performed in triplicate, at least twice. Values correspond to a representative experiment.

Therefore, FUT9 exhibited a clear preference for non-sialylated type II synthetic acceptors *in vitro*, with the synthesis of Le^x and Le^y.

2.4.3. FUT9wt efficiently fucosylates asialoglycoproteins

The absence of the Le^x-carrier proteins and lipids in the $FUT9^{-/-}$ mouse brain confirmed the hypothesis that FUT9 synthesizes the Le^x epitope in the mouse brain, and most probably also in the rat brain (Baboval *et al.*, 2000) as well as in human neurons (Brito *et al.*, 2007). Furthermore, human FUT9 has been shown to be responsible for the synthesis of Le^x on carcinoembryonic antigen-related cell adhesion molecule (CEACAM1) from human granulocytes (Bogoevska *et al.*, 2006). FUT9 has been found to fucosylate small oligosaccharides (Cailleau-Thomas *et al.*, 2000; Toivonen *et al.*, 2002) and

glycolipids (Baboval *et al.*, 2000; Nishihara *et al.*, 2003), resulting in the synthesis of the Le^x epitope. However, the specificity of FUT9 towards glycoproteins *N*-glycans has not yet been established.

To address this issue, we used the same FUT9wt extracts and conditions as above, with recombinant human EPO from CHO cells, the corresponding desialylated form (asialoEPO) and bovine asialofetuin (AF) as substrates.

Transfer of Fuc was detected to asialoEPO (14.1±0.1 μU/million cell) and AF (10.0±1.4 μU/million cell) but not to native sialylated EPO. Considering the high activity of FUT9wt towards type II acceptors (Table 1) it is probable that FUT9wt catalyzed the transfer of Fuc to the outermost type II structures present in all the *N*-glycans from EPO (Figure 11; Grabenhorst *et al.*, 1998) and from AF (Costa *et al.*, 1997). The failure of detection of radioactivity with native sialylated EPO (in which 98% of galactose residues are masked with α2,3 linked sialic acid) is in agreement with our findings that sialylated small oligosaccharide acceptors are not a substrate for FUT9.

To elucidate if Fuc was transferred to the *N*-glycans from EPO, native and asialoEPO were incubated with FUT9wt from HeLa cells in the presence of radiolabeled Fuc, and further analyzed by SDS-PAGE and autoradiography (Figure 10). Radiolabeled Fuc was incorporated into asialoEPO (Figure 10, lane 2), but not in EPO (Figure 10, lane 5). After de-*N*-glycosylation using PNGaseF the radioactive band was no longer detected in the autoradiography (Figure 10, lane 3). These observations unequivocally showed that FUT9 catalyzes the transfer of Fuc to the *N*-glycans of asialoEPO.

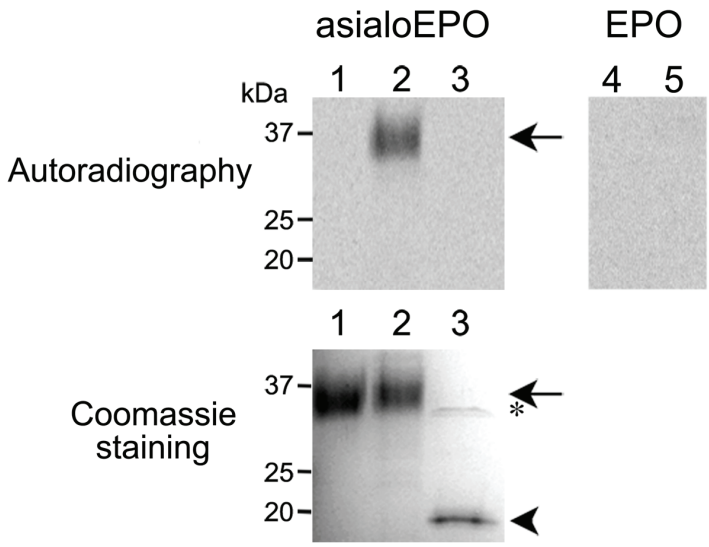

Figure 10: Analysis of asialoerythropoietin and erythropoietin after incubation with FUT9wt. Asialoerythropoietin (asialoEPO) and erythropoietin (EPO) (2.5 μg) (lanes 1 and 4) were incubated with FUT9wt in the presence of radiolabeled GDP-Fuc (lanes 2 and 5). Affinity purified radioactive asialoEPO analyzed in lane 2 was subsequently hydrolyzed with PNGaseF (lane 3). AsialoEPO (arrow), deglycosylated EPO (arrowhead) and PNGaseF (asterisk) are indicated.

2.4.4. FUT9wt efficiently fucosylates di-, tri- and tetrantennary N-glycans from asialoEPO

For a more detailed characterization of the EPO *N*-glycan fucosylation, 250 μg of asialoEPO were incubated with extracts from HeLa cells overexpressing FUT9wt or mock transfected cells in the presence of 75 nmol of GDP-Fuc, for 0, 90, 180 and 360 min, at 37°C. AsialoEPO was then purified by affinity chromatography. The *N*-glycans from the unmodified and modified asialoEPO were released by PNGaseF incubation and subjected to HPAEC-PAD (Figure 11) and MALDI/TOF-MS (Figure 12).

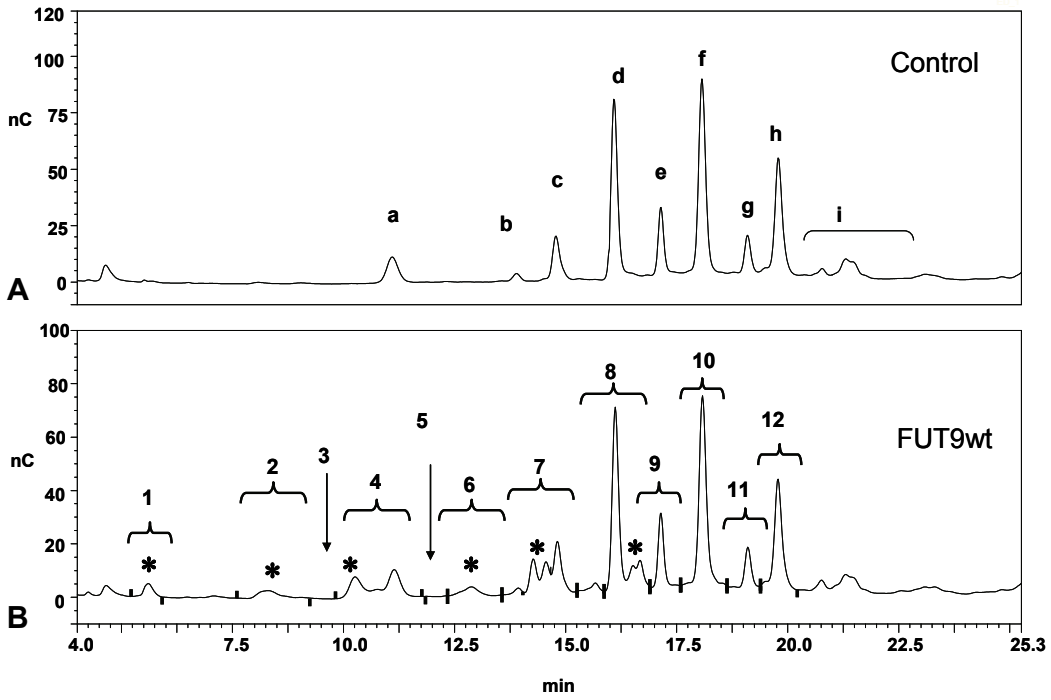

Figure 11: HPAEC-PAD analysis of the oligosaccharides released from asialoerythropoietin after incubation with FUT9wt. Oligosaccharide elution profiles from asialoerythropoietin incubated with extracts Hela cells mock-transfected (**A**; control) and HeLa cells overexpressing FUT9wt (**B**). Structures (all proximally α6 fucosylated) are as follows: a = diantennary; b = 2,4-triantennary; c = 2,6-triantennary; d = tetrantennary; e = triantennary + 1 LacNAc-repeat; f = tetrantennary + 1 LacNAc-repeat; g = triantennary + 2 LacNAc-repeats; h = tetrantennary + 2 LacNAc-repeats; i = tetrantennary + 3 LacNAc-repeats and triantennary with three repeats. Fucosylated products are indicated by asterisks. Pools indicated by numbered brackets were made following on-line desalting and subjected to MALDI/TOF-MS analysis for identification of additional fucosylation by FUT9wt.

Using a PA200 column for *N*-glycan mapping, the resulting HPAEC-PAD profile obtained from the glycan mixture of asialoEPO from mock transfected cell extracts was identical to the one of the asialoEPO starting material, co-eluted with corresponding reference standard oligosaccharides (results not shown), and

showed the peaks for di-, tri-, and tetrantennary *N*-glycans with and without LacNAc repeats and proximal Fuc, as described under Materials and Methods and in the legend to Figure 11. The profile obtained for the *N*-glycans from asialoEPO incubated in the presence of extracts from FUT9wt cells showed novel peaks in the corresponding HPAEC-PAD chromatogram (Figure 11A). Based on the peak areas a total of 22% of the HPAEC-PAD signal was attributable to the new signals as shown in Figure 11 indicating an efficient modification of asialoEPO *N*-glycans.

By MALDI/TOF-MS the pool of oligosaccharides modified by FUT9wt, showed novel mass signals at m/z 1955.6, 2321.7, 2685.7, 3051.8, 3416.8 and 3562.9 (Figure 12, indicated with asterisks).

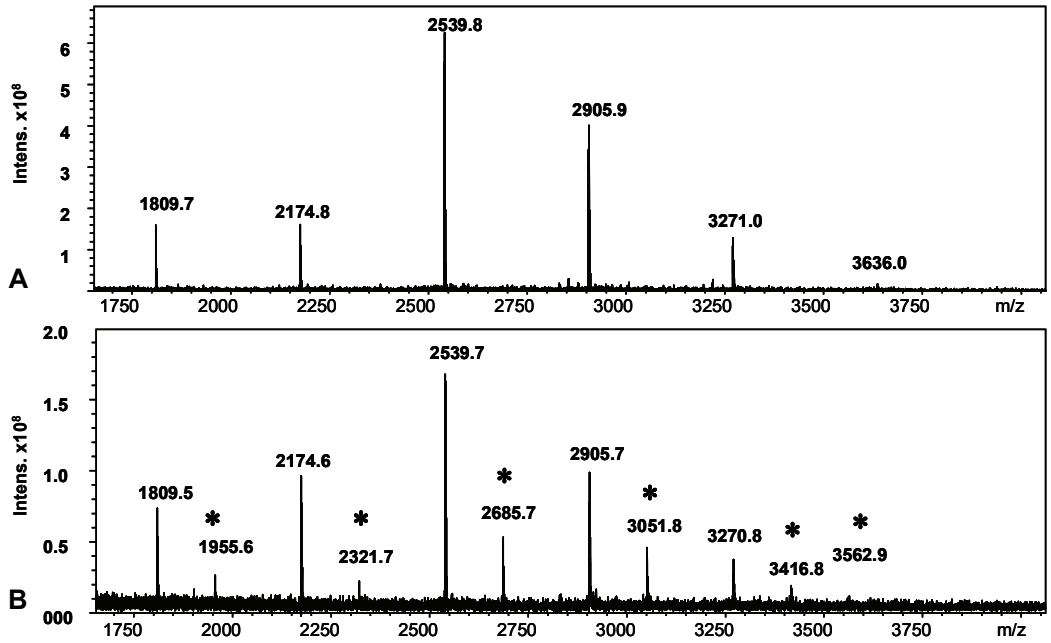

Figure 12: MALDI/TOF mass-spectrometric analysis of the oligosaccharides obtained from asialoerythropoietin after FUT9wt incubation. Oligosaccharides from asialoerythropoietin incubated with extracts of HeLa mock transfected (**A**) and HeLa overexpressing FUT9wt (**B**). Fucosylated products are indicated by asterisks.

From their masses and isotopic composition, these structures probably corresponded to monofucosylated species of diantennary, triantennary, triantennary with one LacNAc repeat or tetrantennary, triantennary with two LacNAc repeats or tetrantennary with one LacNAc repeat, and tetrantennary oligosaccharides with two LacNAc repeats, all with proximal Fuc. The novel peak at 3562.9 probably corresponded to difucosylated tetrantennary *N*-glycans with two LacNAc repeats with proximal Fuc (Table 2).

To elucidate the structures of the novel peaks detected by HPAEC-PAD, fractions indicated in Figure 11 were desalted on-line by using a carbohydrate membrane desalter device (CMD-I; Dionex) and further analyzed by MALDI/TOF-MS (results not shown). Pool 1 yielded a molecular ion signal, which is in agreement with a diantennary glycan plus an additional deoxyhexose (dHex) $[M+Na]^+$ at *m/z* 1955.7. Pool 2 contained molecular ion signals at m/z 2321.0 compatible with a triantennary glycan with an additional Fuc, and a low intensity signal at m/z 3197 indicating a tetrantennary structure with one repeating unit with two additional Fuc residues. In pool 4, a signal at m/z 1809.7 corresponding to the unmodified diantennary glycan was detected and a second signal at m/z, 2685.6, which is compatible with a tetrantennary structure with one additional Fuc. Pool 6 contained a signal m/z 2686.9, which we interpreted as a triantennary glycan with one additional Fuc as is suggested from its retention time in HPAEC-PAD. Pool 7 contained m/z 3051.2, which corresponds to a tetrantennary glycan with one repeat and one additional Fuc, and m/z 2174.7 representing the unmodified triantennary *N*-glycan. Pool 8 contained as a major signal m/z 2539.9 (unmodified tetrantennary) and a weak signal at m/z 2174.8 (corresponding to an unmodified triantennary *N*-glycan) as well as low intensity signals at m/z 3051.2 and 3416.2, which can be interpreted as a triantennary glycan with two repeats plus an additional Fuc and a tetrantennary structure with 2 repeats and with one additional Fuc. Pools 9-12 contained the unmodified *N*-glycans identical to pools e-h in Figure 11A. Pools 3 and 5 did not yield any MALDI/TOF-MS signal.

Table 2: Observed mass signals (m/z) by MALDI-TOF-MS analysis and predicted composition of the *N*-glycans from asialoerythropoietin.

Control		Incubated with FUT9wt	
m/z	Proposed structure	m/z	Modified structure
1809.7	**$HexNAc_4Hex_5dHex$** (diantennary + proximal Fuc (**a**))	1955.8	**$HexNAc_4Hex_5dHex_2$** (monofucosylated diantennary + proximal Fuc)
2174.8	**$HexNAc_5Hex_6dHex$** (triantennary + proximal Fuc (**b, c**))	2320.9	**$HexNAc_5Hex_6dHex_2$** (monofucosylated triantennary + proximal Fuc)
2539.9	**$HexNAc_6Hex_7dHex$** (triantennary + 1 LacNAc + proximal Fuc (**e**); tetrantennary + proximal Fuc (**d**))	2686.0	**$HexNAc_6Hex_7dHex_2$** (monofucosylated triantennary + 1 LacNAc + proximal Fuc; monofucosylated tetrantennary + proximal Fuc)
2905.0	**$HexNAc_7Hex_8dHex$** (triantennary + 2 LacNAc + proximal Fuc (**g**); tetrantennary + 1 LacNAc + proximal Fuc (**f**))	3051.0	**$HexNAc_7Hex_8dHex_2$** (monofucosylated triantennary + 2 LacNAc + proximal Fuc; monofucosylated tetrantennary + 1 LacNAc + proximal Fuc)
3270.2	**$HexNAc_8Hex_9dHex$** (tetrantennary + 2 LacNAc + proximal Fuc (**h**))	3416.3	**$HexNAc_8Hex_9dHex_2$** (monofucosylated tetrantennary + 2 LacNAc + proximal Fuc)
		3562.3	**$HexNAc_8Hex_9dHex_3$** (difucosylated tetrantennary + LacNAc + proximal Fuc)
3635.3	**$HexNAc_9Hex_{10}dHex$** (tetrantennary + 3 LacNAc + proximal Fuc (**i**))		

Calculated m/z of the major molecular ion $[M + Na]^+$ is shown. Abbreviations: HexNAc: *N*-acetylhexosamine (GlcNAc), dHex: deoxyhexose (Fuc); Hex: hexose (Man); LacNAc: *N*-acetylactosamine repeat. Between brackets in bold, the corresponding peaks from the HPAEC-PAD analysis (Figure 11A) are indicated.

Therefore, FUT9wt efficiently fucosylated di-, tri- and tetrantennary glycans with or without repeats, yielding significant amounts of the corresponding monofucosylated species. On the other hand, difucosylated species were only detected in low amounts for the tetrantennary glycans with two LacNAc repeats (MS analysis) or for the tetrantennary structures with one LacNAc repeat (HPAEC-PAD followed by MS analysis). These results suggested that Fuc was preferentially transferred to *N*-acetylglucosamine from the outer LacNAc motif, thus synthesizing the Le^x determinant.

2.4.5. TGN localization of FUT9 is determined by the cytosolic tail

The biosynthesis of Le^x *in vivo* will depend not only on the activity and specificity of FUT9 characterized *in vitro*, but also on the correct localization of the enzyme in the Golgi apparatus. A body of evidence has shown that information for correct localization of GTs lies within their TMs and the corresponding flanking regions (Grabenhorst and Conradt, 1999; Sousa *et al.*, 2003; Sousa *et al.*, 2004; Czlapinski and Bertozzi, 2006). Previous evidence from our laboratory showed that for FUT3 amino acids from the TM specify location in the Golgi apparatus (Sousa *et al.*, 2003), whereas the cytosolic tail is important for intra-Golgi sub-compartment localization (Sousa *et al.*, 2004). Others have shown the importance of Ser and Thr from the cytosolic tails for GTs localization (Milland *et al.*, 2002; Hathaway *et al.*, 2003). The cytosolic tail of FUT9 contains a cluster of Ser and Thr residues (Figure 8A).

In order to evaluate the importance of the cytosolic tail of FUT9 for the subcellular localization and *in vivo* activity, and more specifically the role of the Thr and Ser residues, several mutant forms were constructed (Figure 8A): FUT9dcyt, where amino acids Thr-2 to Leu-9 where deleted; FUT9d6, without the Thr and Ser residues; FUT9S/A, where Ser-3 and Ser-5 were substituted by Ala residues. The mutants contained the V5 epitope for detection purposes.

Deglycosylation analysis of HeLa cells transiently expressing FUT9dcyt, FUT9d10 and FUT9S/A revealed profiles similar to the one observed for the *wild type* protein (Figure 8B). On the other hand, all mutants were active *in vitro* (not shown). These results indicated that the mutants were correctly folded and transported to the Golgi where processing of complex type-glycans occurred.

The subcellular localization of FUT9wt and mutants, overexpressed in HeLa cells was determined by colocalization analysis with markers of the secretory pathway in cells incubated with cycloheximide to inhibit protein synthesis and allow proteins to reach their steady-state localizations (Figure 13A). FUT9wt and the mutants presented the perinuclear staining pattern characteristic of Golgi distribution with partial localization with GM130 (*cis*-Golgi marker), GalT (*trans*-Golgi and TGN) and TGN-46 (TGN). The percentage of FUT9 colocalizing with each marker was estimated by the quantification of signal intensity corresponding to FUT9 that was present in shared pixels with the marker. FUT9wt showed higher colocalization with GalT (60% of signal overlap) and TGN-46 (70%), and lower colocalization with GM130 (45%) (Figure 13B). On the other hand, FUT9dcyt and FUT9d6 showed higher colocalization with GM130 than FUT9wt (Figure 13A). Nearly 70% of FUT9dcyt and FUT9d6 colocalized with GM130, whereas only 50% of each mutant colocalized with TGN-46. FUT9dcyt also showed lower levels of colocalization with GalT with approximately 40% of overlap (Figure 13A, B). FUT9S/A presented a localization pattern similar to FUT9wt (results not shown).

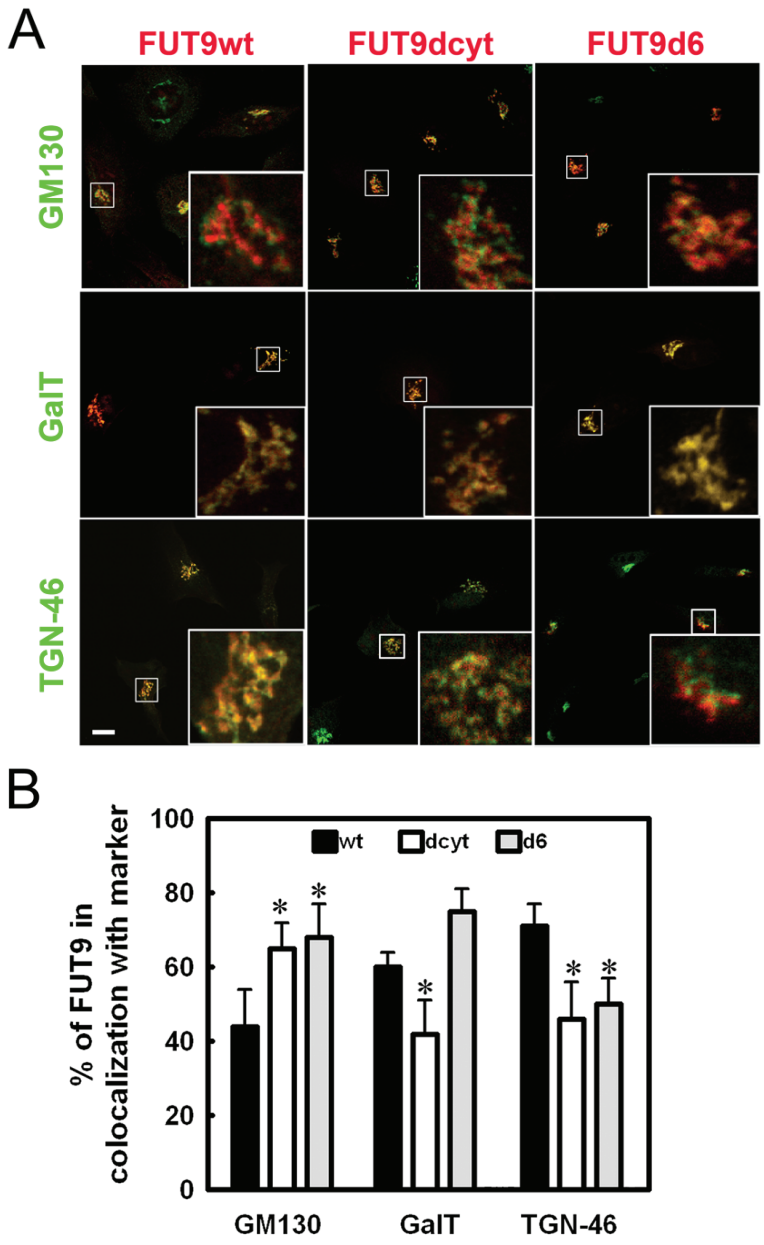

Figure 13: Subcellular localization analysis of FUT9wt and mutants. HeLa cells transiently overexpressing FUT9wt, FUT9dcyt and FUT9d6 were treated with 25 μg/ml cycloheximide for 3 hours, at 37°C, fixed with 4% paraformaldehyde and permeabilized with 0.1% Triton X-100 and processed for confocal microscopy. Cells were double-labeled with anti-V5 (secondary antibody AlexaFluor594-conjugated, shown in

red) and anti-GM130, anti-galactosyltransferase (GalT) or anti-TGN-46 (secondary antibodies AlexaFluor488-conjugated, shown in green). **(A)** Overlays of single optical sections are shown. Insets show 6-fold magnification of indicated areas. Scale bar: 10 μm. **(B)** Quantitative analysis of the distribution of FUT9 constructs relative to Golgi and TGN markers. The percentage of colocalization of FUT9 constructs with the indicated proteins was determined as described in Materials and Methods and took into account the fluorescence from 20 confocal plans along the *z*-axis of eight labeled cells. Error bars correspond to the SD of the mean value obtained from eight to twelve cells from at least two independent experiments. Asterisks indicate significant difference ($p<0.001$) from control mean by a one-way ANOVA analysis with a Tukey's *post-hoc* multiple comparison test.

Partial colocalization of FUT9wt and mutants was observed with the markers: ERGIC-53, a lectin that recycles between the ER and the Golgi (Schweizer *et al.*, 1993); GRASP55, a *medial*-Golgi matrix protein (Shorter *et al.*, 1999); adaptor protein complex–1 (AP-1) of the clathrin coat (Seaman *et al.*, 1996) in TGN exiting sites localized in the justanuclear area (results not shown).

Biotinylation of plasma membrane proteins (Sousa *et al.*, 2003) followed by Western blot analysis of FUT9wt and mutants showed that they were not localized on the plasma membrane (results not shown).

These results together suggested that FUT9wt predominantly localized in the *trans*-Golgi and TGN of HeLa cells. Deletion of the complete cytosolic tail or the cluster of Thr/ Ser caused a shift from the TGN to the *cis*-Golgi.

To confirm the shift of FUT9 mutants to earlier Golgi compartments cells were incubated with brefeldin A (BFA), and analyzed by immunofluorescence microscopy (Figure 14, shown in red). BFA inhibits the GDP/GTP exchange on ADP-ribosylation-factor-1 (ARF-1) impairing the assembly of coatomer protein complex I (COPI) and adaptor protein-1 (AP-1) onto target membranes (Elazar *et al.*, 1994). This leads to Golgi tubulation with fusion of *cis*, *medial* and *trans*-Golgi in the ER (Lippincott-Schwartz *et al.*, 1989) and redistribution of TGN in late endosomal elements near the microtubule organizing center (MTOC) (Reaves

and Banting, 1992). After 45 minutes of BFA treatment, most FUT9wt was visualized in the vicinity of the MTOC, which was stained with an anti-γ-tubulin antibody (Figure 14). On the other hand, FUT9dcyt and FUT9d6 mutants were found to redistribute into ER elements that appeared with a reticulate pattern through the cytoplasm. These results indicated that FUT9wt was predominantly found in the TGN, whereas the cytosolic tail mutants were found from *cis*- to *trans*-Golgi, thus corroborating the results presented above, where a shift to *cis*-Golgi was found.

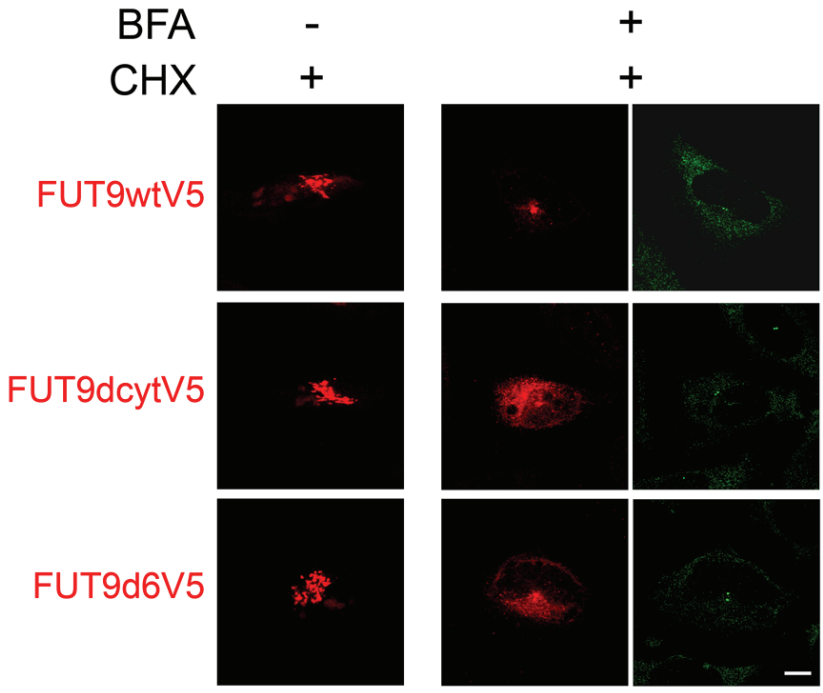

Figure 14: Effect of Brefeldin A on the localization of FUT9wt and cytosolic tail mutants. HeLa cells transiently expressing FUT9wt, FUT9dcyt and FUT9d6 were treated with 25 μg/ml cycloheximide (CHX), for 3 hours, at 37°C, or CHX followed by 5 μg/ml brefeldin A (BFA), for 45 minutes, at 37°C. Cells were fixed with 4% paraformaldehyde, permeabilized with 0.1% Triton X-100 and processed for confocal microscopy. Cells were double-labeled with anti-V5 antibody (secondary antibody AlexaFluor594-conjugated, shown in red) and anti-γ-tubulin antibody (secondary antibody AlexaFluor488-conjugated,

shown in green). Single optical sections are shown representative of the results obtained in three independent experiments. Scale bar: 10 μm.

In spite of the alterations in localization, confocal immunofluorescence microscopy analysis of HeLa cells overexpressing the mutants showed that they were all active *in vivo*, being able to synthesize Le^x. Therefore, the displacement of part of FUT9 to earlier Golgi compartments did not have a dramatic effect on its *in vivo* activity. Considering the overlapping of the different cisternae it is probable that the amount of mutant protein remaining in the *trans*-Golgi and TGN was sufficient for Le^x biosynthesis.

2.5. Discussion

In this work, human FUT9, cloned from NT2N neurons and overexpressed in HeLa cells, has been shown to efficiently fucosylate type II acceptors with the synthesis of Le^x and Le^y from small oligosaccharides linked to a hydrophobic moiety, but could not use the corresponding sialylated substrates, similarly to results described by other authors (Cailleau-Thomas *et al.*, 2000; Toivonen *et al.*, 2002). Furthermore, FUT9 was found to efficiently fucosylate non-sialylated glycoproteins. The corresponding di-, tri-, or tetrantennary *N*-glycans were fucosylated with similar efficiencies and the predominant products were found to be monofucosylated. Considering an average of ten available LacNAc units for asialoEPO (3 *N*-glycosylation sites occupied by tetra-, tri- and diantennary oligosaccharides with peripheral LacNAc in an 8:3:1 ratio) the concentrations of available LacNAc in the reaction mixtures would be of approximately 170 μM for asialoEPO. Thus, taking into account that LacNAc-R was used at 350 μM, and that FUT9 activity was approximately two-fold higher for asialoEPO, we concluded that FUT9 fucosylated asialoEPO more efficiently than the small

synthetic oligosaccharides linked to a hydrophobic moiety. The other glycoprotein tested, AF, was also a good substrate for FUT9.

FUT9wt was not capable of transferring Fuc to native sialylated EPO, which is in agreement with the results obtained with the low molecular mass acceptors. In contrast, other authors (Toivonen *et al.*, 2002) have found FUT9 activity towards LacNAc inner repeats of linear polylactosamine synthetic acceptors substituted with sialic acid. This difference could be due to the limited access of the enzyme to inner LacNAc repeats from the *N*-glycans with higher antennarity.

Our results clearly demonstrated the high specificity of FUT9 for the synthesis of the Le^x determinant in glycans *N*-linked to glycoproteins. The activity of FUT9 towards low molecular mass oligosaccharides (Nishihara *et al.*, 1999; Cailleau-Thomas *et al.*, 2000; Ikeda *et al.*, 2001; Toivonen *et al.*, 2002) and glycolipid acceptors (Baboval *et al.*, 2000; Nishihara *et al.*, 2003) *in vitro* has been shown in the literature. However, its capability of fucosylating glycoproteins was suggested *in vivo* for the rodent brain (Kudo *et al.*, 2007) and for human neurons (Brito *et al.*, 2007). Thus, our results *in vitro* strongly support FUT9 as the most likely candidate to play the key role in the CNS, regulating Le^x-mediated cellular events, by regulating the levels of expression of the determinant in the glycoprotein carriers.

Contrary to a previous report (Nishihara *et al.*, 1999) FUT9 was found to be activated by the divalent cation Mn^{2+}. This allowed the finding of low α4-FUT of FUT9wt towards the type I Galβ3GlcNAc-R acceptor, with synthesis of Le^a. FUT9 activation by metal ions is consistent with the presence of the DxD sequence in the conserved α3-Motif I ($D^{161}SD$), also found in the other α3-FUTs (Breton *et al.*, 1998; Palma *et al.*, 2004), and shown to be important for FUT activity (Pang *et al.*, 1998). The acidic motif DxD is present in many GTs and is known to be involved in the interaction with the nucleotide sugar donor, via co-ordination of a divalent cation in an octahedral geometry (reviewed by Breton

et al., 2006). The presence of the DxD motif usually indicates that a metal ion is needed as a cofactor (reviewed by Breton *et al.*, 2006) but for other members of the α3-FUT family, e.g., FUT3, the activation by metal ions without their absolute requirement has also been described (Murray *et al.*, 1996; Palma *et al.*, 2004). The inhibitory effect at higher concentrations of Mn^{2+} was probably caused by the hydrolysis of the GDP-Fuc substrate by Mn^{2+} (Murray *et al.*, 1996)

FUT9 overexpressed in HeLa cells was found in the Golgi and TGN, where it was active synthesizing the Le^x determinant *in vivo*. Since FUT9 uses as substrates peripheral LacNAc structures that require β4-GalT for Gal transfer, and considering that β4-GalT is localized in the *trans*-Golgi and TGN (Nilsson *et al.*, 1993), it would be expectable that both enzymes are in the same sub-Golgi compartments.

Human brain-type *N*-glycans have as characteristic features peripheral α3-fucosylation (Le^x), low terminal α2,3-sialylation, bisecting GlcNAc, core α6-Fuc, and many of the structures are incompletely processed (asialo- or asialo-agalactostructures) (Hoffmann *et al.*, 1994; Hoffmann *et al.*, 1995; Albach *et al.*, 2001). Since FUT9 is not capable of fucosylating sialylated type II acceptors and α2,3-sialyltransferase (α2,3-SialylT) does not sialylate fucosylated acceptors (Wlasichuk *et al.*, 1993), and considering that α2,3- SialylT is also localized in the *trans*-Golgi/TGN since it acts after β4-GalT, competition between FUT9 and α2,3- SialylT must occur in the late compartments of the Golgi. The high amount of Le^x in human as well as in mouse brain (Albach *et al.*, 2001; Ishii *et al.*, 2007), contrary to sLe^x, which is low in human brain *N*-glycans (Hoffmann *et al.*, 1994; Hoffmann *et al.*, 1995; Albach *et al.*, 2001) and non-detectable in mouse brain (Ishii *et al.*, 2007), suggests competition between the two enzymes favorable to FUT9. Other possibilities such as low expression levels of α2,3- SialylT in the brain could also be admitted and need to be further explored.

Deletion of the cytosolic tail and the cluster of Ser/Thr residues from FUT9 led to a localization shift to early Golgi sub-compartments, which is in agreement

with previous observations from our group for FUT3 (Sousa *et al.*, 2003). Furthermore, recent work by Uliana *et al.*, 2006a showed by domain swapping experiments with glycolipid GTs fluorescent chimeras that the cytosolic tails of SialylTII and *N*-acetylgalactosaminyltransferase contained information for proximal or distal Golgi concentration, respectively. The underlying mechanisms may involve retention by direct interaction of the cytosolic tail with other Golgi resident proteins of the same sub-compartment, including other GTs, and/or retrieval via interaction of the unique cytosolic tail sequences with specific components of the intra-Golgi transport machinery. Contrary to that found for FUT3, deletion of the cytosolic tail did not cause any detectable effect on the biosynthesis of Le^x. GTs are distributed through various sub-compartments of the GA with a peak of localization into a certain compartment. Even if FUT9dcyt was shifted to the *cis*-Golgi there was still a considerable amount in the late Golgi that could synthesize the Le^x.

In summary, evidence proving the efficient synthesis of the Le^x determinant from *N*-linked glycoproteins catalyzed by FUT9 has been shown *in vitro*. These findings indicate a similar biological function for FUT9 in the CNS, thus underlying neuronal adhesion and differentiation processes mediated by the Le^x determinant in this tissue.

2.6 Acknowledgments

We gratefully acknowledge: T. Graça and S. Kandzia (Glyco*T*hera, Braunschweig, Gemany), who performed the HPAEC-PAD and the MALDI/TOF-MS; Dr. H. Conradt (Glyco*T*hera, Braunschweig, Gemany) for the precious advise, fruitful discussion and the invaluable contribution in the work; Dr. V. Sousa for the image quantification method and the helpful suggestions; Dr. T. Galli and Dr. T. Piolot (Institut Jacques Monod, France) for critical opinion of the image quantification method; Dr. F. Barr (Max Planck Institute of

Biochemistry, Germany) for the anti-GRASP55 antibody, Dr. T. Nilsson (Göteborgs University, Sweden) for the anti-GalT antibody, Dr R. Doms (University of Pennsylvania, USA) for the anti-V5 polyclonal antibody and Prof. S. Hakomori (Pacific Northwest Research Institute, USA) for the SH1 antibody.

Chapter 3

Stable expression of an active soluble recombinant form of human fucosyltransferase IX in Spodoptera frugiperda Sf9 cells

Work presented in this chapter corresponds to the following manuscript:

Brito, C.; Gouveia, R.; Costa, J. (2007) Stable expression of an active soluble recombinant form of human fucosyltransferase IX in *Spodoptera frugiperda* Sf9 cells, *Biotechnology Letters*, Jul 17; [Epub ahead of print].

3. Stable expression of an active soluble recombinant form of human fucosyltransferase IX in *Spodoptera frugiperda* Sf9 cells

3.1. Summary

A secretory form of human α3-fucosyltransferase IX (sFUT9) was overexpressed in *Spodoptera frugiperda* (Sf9) insect cells, using the stable expression vector pIB/V5-His-TOPO, and the signal sequence of human interleukin 2 for efficient secretion. sFUT9 was active and its three potential *N*-glycosylation sites were occupied. sFUT9 efficiently fucosylated the type II acceptors Galβ4GlcNAc-R and Fucα2Galβ4GlcNAc-R (R = O-$(CH_2)_3$NHCO$(CH_2)_5$-NH-biotin) but not the corresponding sialylated acceptor, and only very poorly the type I (Galβ3GlcNAc-R) related acceptors. sFUT9 showed a clear preference for glycoproteins containing type II acceptors, with values of 121, 113 and 110 μU/million cell for asialofetuin, erythropoietin and asialoerythropoietin, respectively, values approximately 11-fold higher than those obtained for the small acceptors.

3.2. Introduction

The fucosylated carbohydrate Lewis^x (Le^x) determinant (Galβ4(Fucα3) GlcNAc) is expressed in several human tissues including the brain, where it has been shown Le^x on one harm is one of the most common features of neutral complex-type *N*-glycans (Albach *et al.*, 2001). Furthermore, we have recently shown that an anti-Le^x antibody impaired cell adhesion and neurite formation of human NT2N neurons (Brito *et al.*, 2007).

Human α3-fucosyltransferases (FUTs) transfer fucose (Fuc) residues to type II-based oligosaccharide chains, determining the expression of the Le^x determinant and related carbohydrate structures of cells. FUT9 synthesizes Le^x in the mouse brain and its knockout caused increased anxiety-like behaviors concomitantly to the disappearance of Le^x (Kudo *et al.*, 2007). In human neurons in culture, FUT9 has also been shown to be the α3-FUT responsible for the synthesis of Le^x (Brito *et al.*, 2007).

The evidence supporting an essential role for FUT9 in normal human brain development bring forward the importance of unraveling its specificity and catalytic properties. Moreover, the high specificity of FUT9 for the synthesis of terminal Le^x determinant makes it a good candidate enzyme for synthetic purposes.

Endogenous FUT9 from mammalian tissues is expressed in very low levels, thus it is necessary to express this enzyme in heterologous systems with high production yields. Post-translation modifications, namely *N*-linked oligosaccharides, have been shown to be essential for efficient folding and enzymatic activity of FUTs (Morais *et al.*, 2003). The *Spodoptera frugiperda* Sf9 insect cell line, capable of producing large amounts of recombinant proteins (McCarroll and King, 1997) and performing rudimentary *N*-glycosylation required for correct folding (reviewed by Altmann *et al.*, 1999), presents a potential host

system for the expression of human FUT9 that presents three potential *N*-glycosylation sites in its sequence.

In this study, we have expressed an active soluble recombinant form of human FUT9 in transformed Sf9 insect cells, using the stable pIB/V5-His-TOPO vector and the signal sequence of human interleukin-2 (IL-2). The enzyme was active, fully glycosylated and efficiently secreted with a production of 14.7 mU/l in the second day of culture. Finally, it was found that sFUT9 presented activity towards glycoproteins.

3.3. Materials and methods

3.3.1. Plasmid construction

The stable expression vector pIB-FUT9wt encoding the full-length membrane bound form of human FUT9 (Figure 15) was produced using the PCRScriptCam-FUT9 vector, which contained the complete coding sequence of FUT9, as template and the primers: 5'-ATGACATCAACATCCAAAGGAATTC-3' (FUT9-fwd) and 5'-TTAATTCCAAAACCATTTCTCTA-3' (FUT9-rev). PCR was carried out under the following conditions: initial denaturation at 94ºC for 5 minutes, 25 cycles denaturation at 94ºC for 45 seconds, annealing at 55ºC for 30 s, elongation at 68ºC for 1 minute, and a final elongation step at 68ºC for 7 minutes. The 25 μl reaction mixtures contained 0.2 mM deoxynucleotides, 0.3 μM primers, 1μg template DNA/ml and a mixture of 2.5 U of Taq DNA polymerase (Invitrogen) and 0.6 U of Pfu Turbo DNA polymerase (Stratagene). The resulting fragment (1080 bp) was cloned into the pIB/V5-His-TOPO vector (Invitrogen), at room temperature, for 30 minutes.

The pIB-sFUT9 vector encoded a soluble form of human FUT9 where amino acids Ala-1 to Ser-39 were replaced by the 20-amino acid long signal

peptide of human IL-2 plus an Ala, the first amino acid of the mature IL-2 protein (Figure 15). sFUT9 was constructed in a two-step PCR procedure. The first PCR was performed using the pCRS2FT3T2 vector (Costa *et al.*, 1997) as template and the primers 5'-ATGTACAGGATGCAAC-3' (IL2-fwd) and 5'-GGCTGATTCCATTGGAGCACTGTTTGTGACAAG-3' (IL2FUT9d40-rev), at the concentrations described above. The PCR conditions were: initial denaturation at 95ºC for 5 minutes, 25 cycles: denaturation at 95ºC for 30 seconds, annealing at 60ºC for 10 s, and a final elongation step at 68ºC for 7 minutes.

One-tenth (5 μl) of the first reaction mixture was used as forward primer in a second PCR with the PCRScriptCam-FUT9 vector as template and FUT9-rev as reverse primer. The PCR conditions were the same as for FUT9wt and the amplified fragment was also cloned into the pIB/V5-Hi-TOPO vector.

All sequences were confirmed by DNA sequencing. Clone analysis and maintenance were performed by standard molecular biology techniques.

3.3.2. Cell culture

Sf9 cells were grown in suspension at 27ºC and 90 rpm in 250 ml shake flasks containing 25 ml serum-free Sf900II medium (Gibco). Cells were subcultured at $4x10^5$ cell/ml when a cell density of $3\text{-}4x10^6$ cell/ml was reached. Cell density was determined by hemacytometer counts (Brand) and cell viability was evaluated by trypan blue exclusion dye at 0.1% (w/v) in phosphate buffer saline (PBS). Three independent growth curves were performed over a time period of 7 days and cell density determination was done in triplicate. Sf9-mock transfected cell line expressed a truncated soluble form of human L1 cell adhesion glycoprotein (L1-Ig5/6) (Gouveia *et al.*, 2007).

3.3.3. Stable expression of human FUT9 in Sf9 cells

Adherent Sf9 cells monolayers in six-well plates ($5x10^5$ cell/cm^2) were transfected with 5 μg of pIB-FUT9wt or pIB-sFUT9 using the Cellfectin (Invitrogen) transfection reagent, according to the manufacturer's protocol. In brief, 5 μg of DNA diluted in 250 μl of SF900II medium were added to 10 μl of Cellfectin diluted in 250 μl of medium. The solution was incubated for 15 minutes at room temperature, added to the cell monolayers. After 4 hours at room temperature with agitation, the transfection mixture was supplemented with 2 ml of Sf900II medium. The medium was changed 24 hours later and after another 24 hours, transfectants were selected with 50 μg/ml blasticidin-HCl (Gibco). After five weeks selection and stepwise amplifications into larger monolayer cultures, Sf9-FUT9wt and Sf9-sFUT9 blasticidin-resistant cells were cultured in suspension flasks and maintained in 10 μg/ml blasticidin-HCl supplemented medium. Expression of FUT9 was monitored by fucosyltransferase activity assay two and five weeks after transfection.

3.3.4. Fucosyltransferase activity

The FUT9 activity along the culture was monitored in the supernatants and corresponding cell extracts solubilized in 100 mM Mops/NaOH buffer pH 7.0 with 1% Triton X-100 (TX-100) for 1 hour.

Enzymatic activity was determined from the incorporation of radioactive Fuc from the GDP-[^{14}C]-Fuc (GE HealthCare) donor to the Galβ4GlcNAc-R type II acceptor (Lectinity Holding), where R = O-$(CH_2)_3NHCO(CH_2)_5$NH-biotin. The fucosyltransferase activity was assayed at 37°C for two hours, in 25 μl of the following reaction mixture: 100 mM Mops/NaOH buffer, pH 7.0, 100 mM NaCl, 50 mM $MnCl_2$, 0.15 mM GDP-Fuc (containing GDP-[^{14}C]-Fuc in a 1:60 molar

ratio) and 0.35 mM of oligosaccharide acceptor. One unit of enzyme activity was defined as the amount of enzyme catalyzing the transfer of 1 μmol Fuc/min to the acceptor.

In specificity studies Sf9-sFUT9 supernatants recovered from the second day of culture were monitored in the assay conditions described above using the following synthetic acceptor substrates: NeuAcα2,3Galβ4GlcNAc-R, Fucα2Galβ4GlcNAc-R, Galβ3GlcNAc-R, NeuAcα2,3Galβ3GlcNAc-R and Fucα2Galβ3GlcNAc-R, where R=O-$(CH_2)_3$NHCO$(CH_2)_5$-NH-biotin (Lectinity Holding). The following glycoproteins were also tested: bovine asialofetuin (Sigma) (2 mg/ml, which corresponds to 52 μM, assuming fetuin molecular mass 38.4 kDa, from Swiss-Prot) and native or asialo human erythropoietin (EPO) (*G*lyco*T*hera) (0.5 mg/ml, which corresponds to 17μM assuming EPO molecular mass 30 kDa as determined by SDS-PAGE). For type I acceptors the radioactive to non-radioactive Fuc molar ratio was 1:30. Activity determinations were done in triplicates or duplicates from two independent cultures.

3.3.5. Protein analysis

Secreted and intracellular protein corresponding to 30 μl of cell suspension was analyzed. Cell supernatants were cleared from cells and cell debris by a 500× *g* centrifugation, for 5 minutes, followed by a 10000× *g* centrifugation, for 10 minutes Cells were solubilized for 1 hour in 100 mM Mops/NaOH buffer pH 7.0 with 1% TX-100 and the extracts centrifuged at 10000× *g*, for 10 minutes. Supernatants were precipitated in 80% ethanol, at –20ºC, for 3 hours. The pellet was collected after a centrifugation at 10000× *g*, for 10 minutes, at 4°C.

Deglycosylations of sFUT9 with endoglycosidase H (EndoH) (New England Biolabs) and peptide-*N*-glycosidase F (PNGaseF) (Roche) were

performed according to the supplier's instructions. In brief, precipitated protein was solubilized in the denaturation buffer provided by the EndoH supplier. After 10 minutes of denaturation at 100ºC, samples were allowed to cool down and 100 U of EndoH or 1 U of PNGaseF and the corresponding buffers were added. For EndoH, the supplier's buffer was used and for PNGaseF the buffer was 10 mM NaH_2PO_4, 5 mM EDTA, 1% NP-40, pH 7.5. Incubations were done in 30 μl, at 37ºC for 18 hours and the reaction was stopped by precipitation in 80% ethanol at -20ºC.

Proteins were separated by SDS-PAGE and transferred to polyvinyledene difluoride membrane (Millipore). Membranes were blocked in 5% nonfat dry milk (Nestle) in PBS with 0.1% Tween-20. The anti-FUT9 polyclonal antibody C-17 (Santa Cruz Biotechnology) was used at 1:500 dilution in blocking solution. HRP-labeled polyclonal secondary antibody anti-goat IgG (Sigma) was diluted 1:20000 in blocking solution. Chemiluminescent detection was performed by the ECL Plus system (GE Healthcare). Protein from three independent growth curves was analyzed.

3.4. Results and discussion

3.4.1. Expression of soluble human FUT9 (sFUT9) in Sf9 cells

Stable expression in insect cells has been shown to yield higher productivities for FUTs than the baculovirus infection system (Morais and Costa, 2003; Munster *et al.*, 2006). Furthermore, stable expression in Sf9 insect cells has been used previously in our laboratory with successful results for a soluble form of human FUT3 using the pIB/V5-His-TOPO vector and the signal sequence of beta-trace protein (Morais and Costa, 2003), as well as for several truncated forms of the human membrane glycoprotein L1 adhesion molecule with the expression vector pMIB/V5-His-TOPO that contains the signal sequence of

honeybee melittin (Gouveia *et al.*, 2007). Thus, to obtain a stable source of human FUT9 that would allow a continuous production of active enzyme we chose the Sf9 insect cell line and generated vectors for stable expression of recombinant protein in insect cells. We used the signal sequence of human IL-2, known to be recognized and correctly cleaved in *S. frugiperda* lytic expression system (Smith *et al.*, 1985).

We cloned the full-length form of human FUT9 (FUT9wt) and a truncated form containing the catalytic domain of the enzyme (sFUT9) into the pIB/V5-His-TOPO vector, obtaining the expression vectors pIB-FUT9wt and pIB-sFUT9, respectively. sFUT9 was constructed by replacement of the cytoplasmic tail, the transmembrane domain and part of the stem region of human FUT9 (Ala-1 to Ser-39) by the signal sequence of the secreted human protein IL-2 (Figure 15).

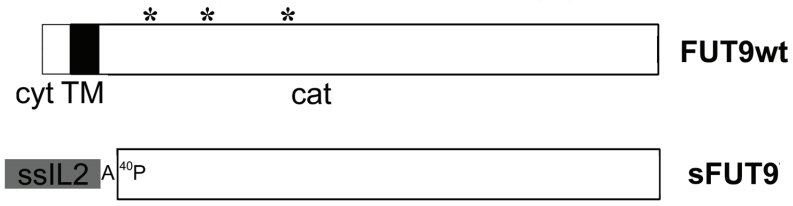

Figure 15: Schematic representation of human FUT9 constructs. Human FUT9 (FUT9wt) is composed of a short cytoplasmic tail (cyt), a single transmembrane domain (TM) and a C-terminal catalytic domain (cat). The three potential *N*-glycosylation sites are indicated (*). The truncated soluble form (sFUT9) comprises the catalytic domain of the enzyme: it contains the sequence of IL2 signal peptide (ssIL2) plus the first amino acid residue (Ala) of mature IL2, linked to Pro-40 of the FUT9 sequence.

Adherent insect Sf9 cells were transfected with the described expression vectors and selected with 50 µg/ml basticidin-HCl for five weeks. Sf9-FUT9wt and Sf9-sFUT9 cells were grown in Sf900II medium at 27ºC, in shake flasks at 90

rpm, from an initial concentration of $4x10^5$ cell/ml and reached a maximum cell density of approximately $7x10^6$ cell/ml on the fifth day of culture with a cell viability of approximately 90% (Figure 16). The growth and viability of Sf9 cells were not affected by the expression of recombinant human FUT9, when compared to Sf9 cells transfected with a vector encoding a non-related protein (Sf9-mock), under the same culture conditions (Figure 16).

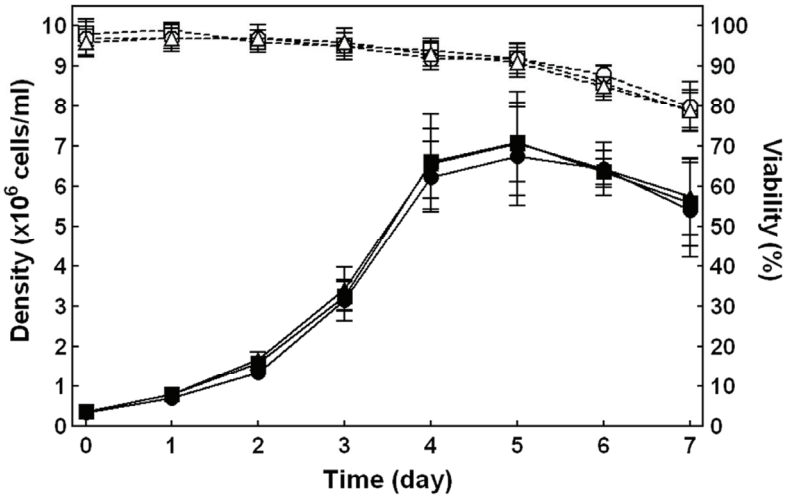

Figure 16: Production of FUT9wt and sFUT9 from Sf9 cells grown in shake flasks. Cell growth curve (closed symbols, continuous line) and viability (open symbols, broken line) of Sf9-FUT9wt (■, □), Sf9-sFUT9 (●, ○) and Sf9-mock cells (▲, △). Twenty five ml suspension cultures at initial cell densities of $4x10^5$ cell/ml were grown in Sf900II medium for 7 days. Results are presented as means ± S.D. (n=3).

In order to determine the amount of active enzyme produced, α3-FUT activity was monitored along the days in culture. The transfer of radiolabelled Fuc from GDP-[^{14}C]-Fuc to a type II acceptor coupled to a hydrophobic moiety was measured. For the soluble sFUT9 form, we observed that the secreted activity increased until the second day, when it reached the value of 14.7 mU/l in the supernatant (Figure 17). By the same time, approximately 51% of the activity was

retained inside the cells. For FUT9wt, there was also an increase in the activity recovered from the cell extracts until the second day of culture (Figure 17), although the maximum value obtained (1.8 mU/l cellular suspension) corresponded to only 12% of the activity recovered from sFUT9 under identical conditions. Subsequent production and characterization was performed with the soluble sFUT9, which contained the catalytic domain of human FUT9 and presented the α3-FUT activity, indicating that it acquired the correct fold.

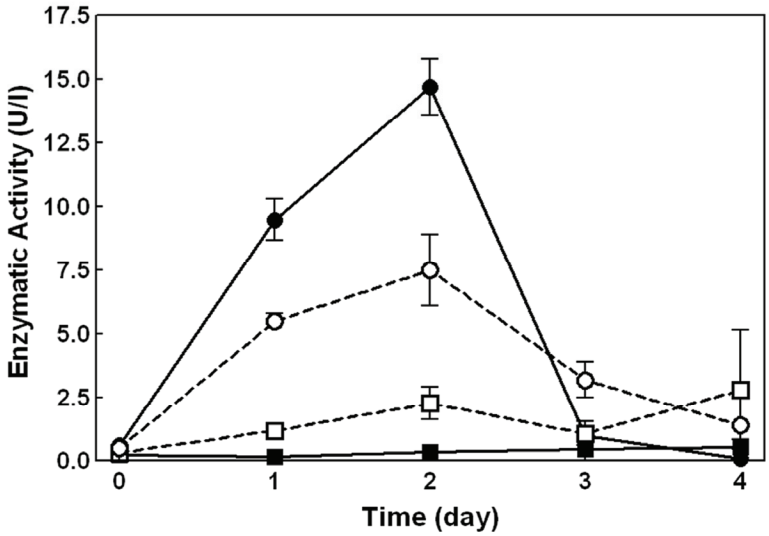

Figure 17: α3-Fucosyltransferase activity of Sf9-FUT9wt and Sf9-sFUT9 cells. α3-Fucosyltransferase activity was monitored in supernatants (closed symbols, continuous line) and cell extracts (open symbols, broken line) of Sf9-FUT9wt (■, □) and Sf9-sFUT9 cells(●, ○) corresponding to 30 μl cell suspension. The transfer of radiolabelled Fuc from GDP-[^{14}C]-Fuc to a type II acceptor coupled to a hydrophobic moiety (Galβ4GlcNAc-O-$(CH_2)_3$NHCO$(CH_2)_5$-biotin) was measured. One unit of enzyme activity was defined as the amount of enzyme catalyzing the transfer of 1 μmol Fuc/min to the acceptor.

Supernatants and cell lysates of Sf9-sFUT9 along the culture days were analyzed by SDS-PAGE and Western Blot with a polyclonal anti-human FUT9 antibody that recognizes a C-terminal peptide of the protein. In supernatants an immunoreactive band was detected with an apparent molecular mass of approximately 41.3 kDa, in the range predicted for sFUT9 (Figure 18A, arrow). A peak of protein detection at the second day of production was observed. Analysis of the corresponding cell extracts revealed that there was also an increase until the second day of culture in the sFUT9 detected intracellularly (Figure 18B, arrow). After that, the intracellular detection decreased concomitantly with the decrease of the amount of protein detected in the supernatant. Thus, we did not observe an increased intracellular accumulation of protein, which corroborated the conclusion that the active sFUT9 construct was being efficiently secreted. These results showed that the human IL-2 signal sequence was adequate for the expression in non-lytic insect cell systems.

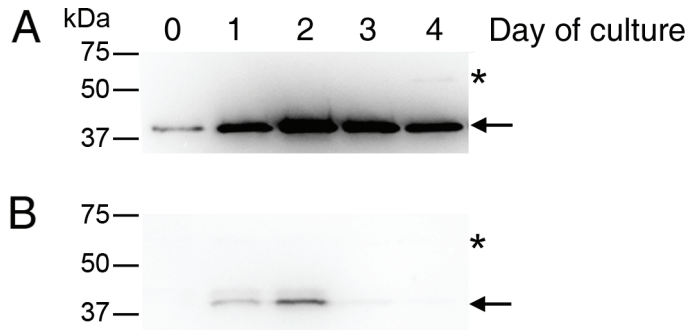

Figure 18: Western blot analysis of secreted (A) and intracellular (B) sFUT9. Protein from 15 μl of cell supernatants (A) and corresponding cell extracts (B) was analyzed. As primary antibody, the C-17 anti-FUT9 polyclonal antibody at 1:500 dilution was used. Chemiluminescent detection was performed by the ECL Plus system. sFUT9 is indicated with arrows (←) and a non-specific band (also detected in Sf9-mock cells) with asterisks (*).

The protein profiles (Figure 18) correlated with the α3-FUT activities obtained (Figure 17): after the second day of culture there was an almost total loss of the enzymatic activity recovered from the supernatant, concomitantly with a decrease in the detection of secreted sFUT9. The action of secreted proteolytic enzymes could explain the decrease of both activity and total product yield after the second day of culture. The proteolytic action may affect amino acid residues essential for enzymatic activity and later degrade the C-terminal portion of FUT9, the region recognized by the anti-FUT9 antibody. Sf9 cells express several classes of proteases, namely Cys, that are secreted into the extracellular medium (Lindskog *et al.*, 2006) and whose activity was shown to increase from the third day of culture onwards (Gotoh *et al.*, 2001). The decrease of sFUT9 activity and detection in the supernatant was not due to protein denaturation since we did not observe protein precipitation in the culture medium.

In the cell extracts, we detected several bands with lower apparent molecular masses after the second day of culture, when using higher exposure times (results not shown). These may correspond to proteolytic processing of sFUT9 by endogenous intracellular proteases, different from those secreted to the medium. Nevertheless, there was a decrease in the total amount of sFUT9 detected. sFUT9 expression may be regulated not only post-translationally, but also at the level of transcription or translation. For example, it has been described that expression of FUT9 in LEC29 CHO cells, was under a translational regulation mechanism mediated by 5'-untranslated mRNA regions (Patnaik *et al.*, 2004). Furthermore, we have previously experienced difficulties in creating stable cell lines expressing human FUT9wt or a truncated soluble form. We have performed transfection assays with the pcDNA3.1/V5-HisTOPO expression vector in several mammalian cell lines (BHK-21B hamster cell line, Neuro2A murine neuroblastoma cell line, HeLa and HEK293T human cell lines). Although significant α3-FUT activity levels and corresponding protein were detected soon after the transfection in all cell lines tested, selection of stable transfectants was not efficient, even under very stringent antibiotic conditions (Figure 19). A

single-clone selection strategy by limiting dilution and antibiotic selection methods was assayed in BHK-21B and HeLa cell lines, but the resistant cells presented no expression (Figure 19). These high expression levels obtained transiently after transfection and subsequent rapid decrease also suggested that human FUT9 is under tight regulation control.

These results together showed the advantage of using Sf9 insect cells to produce soluble and active sFUT9.

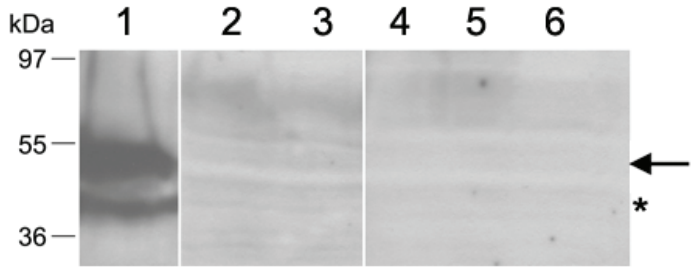

Figure 19: Western blot analysis of FUT9 transfection assays in HeLa cells. Protein from approximately $5x10^5$ cells transfected with pcDNA-FUT9wtV5 were analyzed after one day (lane 1), after two weeks of selection with 1.5 mg/ml of G418 sulphate (lane 3) or after 4 weeks of single-clone selection by limiting dilution and selection with 1.5 mg/ml of G418 sulphate (lanes 4, 5 and 6). Non-transfected HeLa cells were used as negative control (lane 2). As primary antibody, an anti-V5 monoclonal antibody at 1:5000 dilution was used. Chemiluminescent detection was performed by the ECL Plus system. FUT9wtV5 is indicated with an arrow (←) and a degradation product also recognized by the antibody with an asterisk (*).

3.4.2. Characterization of sFUT9

3.4.2.1. N-glycosylation of sFUT9

Human FUT9 has three potential *N*-glycosylation sites (Asn-62, Asn-101 and Asn-153), all present in the sFUT9 mutant. The apparent molecular mass of

sFUT9 detected in the supernatants (41.3 kDa) (Figure 18) was higher than the molecular mass predicted from the amino acid sequence of sFUT9 (37.8 kDa), suggesting that *N*-glycosylation sites of the protein were occupied. To elucidate the type of sFUT9 *N*-glycosylation, protein collected from the supernatant at the second day of culture was digested with the glycosidases PNGaseF or EndoH and analyzed by Western Blot. PNGaseF treatment yielded two bands that presented a shift to lower molecular masses (Figure 20).

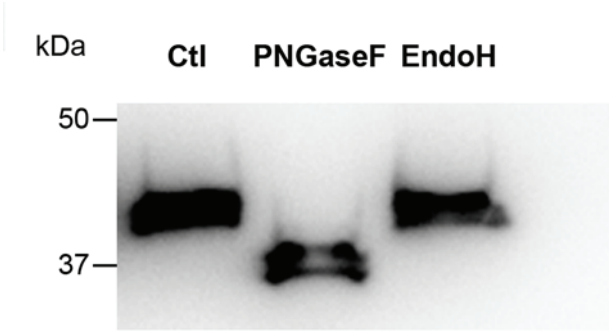

Figure 20: Deglycosylation and Western blot analysis of secreted sFUT9. Protein from 30 μl of cell supernatant was incubated with PNGaseF, EndoH, or buffer alone (Ctl) and analyzed by Western Blot. As primary antibody, the C-17 anti-FUT9 polyclonal antibody at 1:500 dilution was used. Chemiluminescent detection was performed by the ECL Plus system.

The higher band presented an apparent molecular mass of approximately 37.8 kDa, which corresponds to the predicted molecular mass for the peptide sequence of secreted sFUT9. This result suggested that the three potential *N*-glycosylation sites of FUT9 were occupied, as the most common *N*-linked oligosaccharides present in recombinant proteins expressed in Sf9 cells ($Man_3GlcNAc_2Fuc$), have a molecular mass of 1039 Da (Hollister *et al.*, 2002). The lowest band observed presented an apparent molecular mass lower than 37 kDa, and probably corresponded to a proteolytic product of sFUT9. This may have been produced due to higher sensibility to degradation of the

deglycosylated form. EndoH had no effect on secreted sFUT9 (Figure 20), indicating that the three *N*-glycans of sFUT9 sensitive to PNGaseF were of the paucimannosidic-type oligosaccharides with proximal Fuc.

3.4.2.2. Acceptor specificity of sFUT9

The maintenance of FUT9 specificity of is one of the major issues to consider when developing a production strategy of the protein. We detected activity of sFUT9 expressed in Sf9 cells towards the type II acceptor (Figure 17), which indicated that the soluble form of the enzyme retained the FUT9 biological activity, the synthesis of the Le^x epitope (Nishihara *et al.*, 2003). In order to further characterize sFUT9 specificity, fucosyltransferase activity assays were performed with cell supernatants collected in the second day of production, using a panel of oligosaccharides coupled to a hydrophobic moiety as acceptor substrates.

We observed that sFUT9 expressed in Sf9 cells had a clear preference for type II acceptors. The activity towards Galβ4GlcNAc-R was 10 ± 0.59 μU/million cell (Table 3), leading to the production of Le^x determinant. A substitution of Gal with α2-linked Fuc (Fucα2Galβ4GlcNAc-R) yielded an increase in activity of 1.6 fold, with the production of Lewis y (Le^y) determinant. Nevertheless, a substitution of Gal with α2,3-linked *N*-acetylneuraminic acid (NeuAcα2,3Galβ4GlcNAc-R) yielded undetectable radioactivity incorporation. These results are in good agreement with the substrate specificity of human FUT9 expressed in Namalwa cells (Toivonen *et al.*, 2002) and COS7 cells (Cailleau-Thomas *et al.*, 2000). Activity towards type I acceptors was also detected but at lower levels (Table 3). Of the type I acceptors tested, Galβ3GlcNAc-R presented the highest activity value (0.19 ± 0.01 μU/million cell), although activity was also detected when Gal was substituted with α2,3-linked *N*-acetylneuraminic acid (Fucα2Galβ4GlcNAc-R) or α2-linked Fuc (Fucα2Galβ3GlcNAc-R). The detection of FUT9 activity

towards type I acceptors has been found for Galβ3GlcNAc (Toivonen *et al.*, 2002), but not for Galβ3GlcNAcβ-O-$(CH_2)_8COOCH_3$ (Cailleau-Thomas *et al.*, 2000) or pyridylaminated lacto-*N*-tetraose (Galβ3GlcNAcβ3Galβ4Glc-PA) (Kaneko *et al.*, 1999b; Baboval *et al.*, 2000). In this work, we have shown that sFUT9 also synthesizes the Le^a determinant when the disaccharide acceptor is linked to a hydrophobic moiety.

Table 3: Substrate specificity of sFUT9 from Sf9 cells.

Substrate	Activity ($\mu U/10^6$cell)	Relative Activity
Type II acceptors [(a)]		
Galβ4GlcNAc-R	10.00 ± 0.59	1.00
NeuAcα2,3Galβ4GlcNAc-R	N.D.	N.D.
Fucα2Galβ4GlcNAc-R	16.02 ±1.24	1.60
Type I acceptors [(b)]		
Galβ3GlcNAc-R	0.19 ± 0.01	0.02
NeuAcα2,3Galβ3GlcNAc-R	0.13 ± 0.05	0.01
Fucα2Galβ3GlcNAc-R	0.07 ± 0.01	0.01

One unit of enzyme activity defined as the amount of enzyme catalyzing the transfer of 1 μmol Fuc/min to the acceptor. Activity relative to Galβ4GlcNAc-R at 0.35 mM in the presence of 0.15 mM GDP-Fuc, containing GDP-[^{14}C]-Fuc in a 1:60 (a) or 1:30 (b) molar ratio, and 5 mM $MnCl_2$; R= O-$(CH_2)_3NHCO(CH_2)_5$-NH-biotin. N.D.: not detected.

FUT9 activity towards glycolipid acceptors *in vitro* has been described by others (Nishihara *et al.*, 2003). During this Thesis work, we found that full-length FUT9 expressed in HeLa cells efficiently transferred Fuc to *N*-linked oligosaccharides of glycoproteins (Chapter 2).

In order to determine if sFUT9 was also able to transfer Fuc to glycoproteins, activity towards bovine asialofetuin (AF) and recombinant human

erythropoietin (EPO) expressed in CHO cells was also tested (Table 4). We detected efficient transfer of Fuc to all three glycoproteins tested, with activities of 120.6±0.7, 113.0±10.3 and 110.2±3.9 μU/million cell towards AF, EPO and asialoEPO, respectively (Table 4). Probably, sFUT9 added Fuc to the peripheral type II determinants present in AF and in asialoEPO, forming terminal Le^x determinants, as FUT9 has been described to fucosylate preferentially outermost type II structures (Toivonen *et al.*, 2002).

Table 4: Activity of sFUT9 from Sf9 cells towards glycoproteins

Glycoprotein	Activity ($\mu U/10^6$cell)	Relative Activity
Asialofetuin	120.6 ± 0. 7	12.1
Erythropoietin	113.0 ± 10.3	11.3
Asialoerythropoietin	110.2 ± 3.9	11.0

One unit of enzyme activity defined as the amount of enzyme catalyzing the transfer of 1 μmol Fuc/min to the acceptor. Activity relative to Galβ4GlcNAc-R at 0.35 mM in the presence of 0.15 mM GDP-Fuc and 5 mM $MnCl_2$; R= O-$(CH_2)_3NHCO(CH_2)_5$-NH-biotin.

Assuming that the three potential *N*-glycosylation sites of AF are occupied, and since *N*-glycans from AF are predominantly of the triantennary type with mainly peripheral type II structures (Costa *et al.*, 1997), there would be approximately 468 μM of Galβ4GlcNAc-R' acceptor in the reaction mixture, considering 9 terminal branches in average. This is 1.3 fold higher than that used for the small acceptor Galβ4GlcNAc-R. On the other hand, recombinant human EPO from CHO cells has three occupied *N*-glycosylation sites and presents peripheral type II determinants substituted with sialic acid on tetrantennary, triantennary and biantennary oligosaccharides in an 8:3:1 ratio (Chapter 2). Therefore, there would be 10 terminal branches Galβ4GlcNAc-R' in average, with the corresponding final concentration of 170μM. This value is 2.3 times lower

than that used for the small acceptor Galβ4GlcNAc-R. These results revealed a higher efficiency of sFUT9 for fucosylating glycoproteins with terminal type II structures relatively to small oligosaccharides linked to a hydrophobic moiety.

sFUT9 also presented efficient transfer of Fuc to native sialylated EPO (Table 4), contrary to that found for the sialylated type II acceptor as presented above (Table 3). It has previously been shown by others using linear synthetic acceptors with repeats that substitution of terminal Gal with sialic acid caused a shift in FUT9 specificity towards Galβ4GlcNAc inner repeats (Toivonen *et al.*, 2002). We observed that 40 and 26% of the tetrantennary oligosaccharides had one or two lactosamine repeats, respectively, and that 35 and 21% of the triantennary had one and two repeats, respectively (Chapter 2). Therefore, in the case of native EPO, sFUT9 most probably catalyzed the transfer of Fuc to the innermost type II structures of the tetrantennary or triantennary oligosaccharides with repeats.

We tested the activity of the FUT9wt membrane form produced in Sf9 cells (Figure 15) towards EPO and asialoEPO and observed that the transfer was 1.4 fold more efficient for the asialo form (results not shown), contrary to sFUT9 that presented similar efficiency for both native and asialoEPO (Table 3). Thus, it is probable that the ablation of the *N*-terminal region of FUT9 contributed to the accessibility of the enzyme to the inner repeats. Accordingly, we have previously shown that a soluble form of human FUT3 presented augmented activity towards glycoprotein acceptor substrates (Sousa *et al.*, 2001).

Furthermore, the FUT9wt membrane bound form expressed in HeLa cells presented only residual transfer to native EPO and good transfer to asialoEPO and AF. The activities towards the terminal Galβ4GlcNAc units of the glycoproteins were equivalent to those obtained for the oligosaccharide type II acceptor linked to a hydrophobic moiety (Chapter 2). Thus, FUT9 presented higher efficiency in fucosylating glycoproteins when expressed in Sf9 insect cells than in HeLa cells. This may be due to the different *N*-glycosylation of FUT9

itself, as insect cell-type glycosylation present differences from mammalian *N*-glycosylation (Hollister *et al.*, 2002). One hypothesis is that the paucimannosidic-type oligosaccharides that occupy the *N*-glycosylation sites of sFUT9 (Figure 20) allow a better accessibility and/or interaction to the glycoprotein substrates than the mammalian hybrid and complex-type oligosaccharides present in FUT9 from HeLa cells (Chapter 2).

In summary, sFUT9 was active and synthesized the Le^x and Le^y determinants *in vitro*. Furthermore, it efficiently fucosylated sialylated and non-sialylated glycoproteins.

3.5. Conclusions

In the present work**,** we have produced an active recombinant soluble form of human FUT9 from stably transformed Sf9 cells. Therefore, sFUT9 can be used for the *in vitro* synthesis of fucosylated glycoconjugates and is suitable for further functional and structural studies of the enzyme.

3.6 Acknowledgments

We gratefulyl acknowledge: Ricardo Gouveia who helped with the Sf9 cell culture; Dr. Harald Conradt (*G*lyco*T*hera, Braunschweig, Germany) for helpful discussion and useful comments. This work was funded by projects, CellPROM, Nº500039-2, and Signalling & Traffic, Nº LSHG-CT-2004-503228, European Commission.

Chapter 4

Increased levels of fucosyltransferase IX and carbohydrate Lewis^x adhesion determinant in human NT2N neurons

Work presented in this chapter has been included in the following manuscript:

Brito, C.; Escrevente, C.; Reis, C.; Lee, V.; Trojanowski, J.; Costa, J. (2007) "Increased levels of fucosyltransferase IX and carbohydrate Lewis^x adhesion determinant in human NT2N neurons" *J. Neurosci. Res.* 85, 1260-1270.

4. Increased levels of fucosyltransferase IX and carbohydrate Lewis^x adhesion determinant in human NT2N neurons

4.1. Summary

The expression of the fucosylated carbohydrate Lewis^x (Le^x) determinant (Galβ4(Fucα3)GlcNAc-R) has been found in glycoproteins, proteoglycans, and glycolipids from the nervous system. Evidence suggests its association with cell-cell recognition, neurite outgrowth, and neuronal migration during central nervous system development. In the present work, we detected increased levels of Le^x in differentiated human NT2N neurons cultured in vitro. To identify which fucosyltransferase (FUT) synthesized the Le^x in NT2N neurons, RT-PCR, FUT substrate specificity and Western blot analysis were carried out. Strong activity toward acceptors Galβ4GlcNAc-R and Fucα2Galβ4GlcNAc-R (R = O-$(CH_2)_3$NHCO$(CH_2)_5$NH-biotin), together with strong FUT9 detection by Western blot and presence of transcripts showed that FUT9 was the enzyme associated with Le^x biosynthesis in NT2N neurons. Le^x was detected at the plasma membrane of NT2N neurons, in lysosomes marked with lysosomal-associated membrane protein 1 (LAMP-1), and it was found for the first time to colocalize with the tetanus neurotoxin-insensitive vesicle-associated membrane protein (TI-VAMP) that defines the TI-VAMP exocytic compartment which is involved in neurite outgrowth. Furthermore, incubation with anti-Le^x monoclonal antibody L5 led to impaired adhesion of NT2N neurons to the surface matrix and inhibited neurite initiation. In conclusion, FUT9 and its product Le^x are detected specifically in human NT2N neurons and our results indicate that they underlie cell differentiation, cell adhesion, and initiation of neurite outgrowth in those neurons.

4.2. Introduction

Glycoconjugates containing fucose (Fuc) have been shown to play important roles in cell adhesion and cell-cell interactions. The fucosylated carbohydrate Lewis^x (Le^x) determinant (Galβ4(Fucα3)GlcNAc) from glycolipids, glycoproteins, or proteoglycans is expressed in several human tissues, including the brain. It is the most probable candidate to play an important role in normal brain development because its expression was found temporally and spatially regulated in the developing central nervous system (CNS) of diverse species, including human, rat, mouse, chicken, and *Xenopus* (Dasgupta *et al.*, 1996; Gotz *et al.*, 1996; Mai *et al.*, 1999; Yoshida-Noro *et al.*, 1999). Furthermore, complex-type *N*-glycans with terminal Le^x on one arm are among the most abundant neutral carbohydrates detected in human brain (Albach *et al.*, 2001). At the cellular level, it has been detected in mouse neurons at the surfaces of cell bodies, processes, and growth cones (Nishihara *et al.*, 2003). Furthermore, Le^x seems to have a role in neurite outgrowth or adhesion because anti-Le^x antibodies inhibit neurite outgrowth in explant brain cultures from *Xenopus* embryos (Yoshida-Noro *et al.*, 1999). A specific association between Le^x and mouse brain cells was also suggested by its role as a neural stem cell marker (Capela and Temple, 2002).

The final step in the biosynthesis of Le^x is catalyzed by α3-fucosyltransferases (α3-FUTs), which add a Fuc residue to type II-based oligosaccharide chains. To date, six α3-FUTs have been cloned and characterized (FUT3, FUT4, FUT5, FUT6, FUT7, and FUT9). FUT10 and FUT11 have been identified as fucosyltransferases due to their degree of homology with other fucosyltransferases (Roos *et al.*, 2002), however, their activity has not been validated (Baboval *et al.*, 2000). The enzymes show different specificity patterns: they can all synthesize the Le^x determinant, with the exception of FUT7 (Becker and Lowe, 2003). FUT4 and FUT9 are the main enzymes responsible for the

synthesis of Le^x (Grabenhorst *et al.*, 1998; Baboval *et al.*, 2000). FUT3 has only residual α3-FUT activity and exhibits predominant α4-FUT activity (Costa *et al.*, 1997). Their specificity differences together with their different tissue distributions underlie distinct biological roles. FUT9 is expressed mainly in the CNS, in both the developing and mature brain of human, rat, and mouse (Kaneko *et al.*, 1999b; Baboval *et al.*, 2000; Cailleau-Thomas *et al.*, 2000). α3-FUT has been shown to be responsible for the synthesis of Le^x in the mouse brain (Nishihara *et al.*, 2003), where it is controlled by *Pax6*, a transcription factor involved in brain patterning and neurogenesis (Shimoda *et al.*, 2002). Recently, the importance of FUT9 for the synthesis and role of Le^x in mouse brain was shown unequivocally with the study of $FUT9^{-/-}$ mouse (Kudo *et al.*, 2007). This animal showed disappearance of Le^x in the brain concomitantly to increased anxiety-like behaviors.

We have used NTERA-2/cl.D1 (NT2) cells as a model of the human CNS in this study. The NT2 cell line is derived from a human embryonic carcinoma (EC), and is characterized by undifferentiated neuronally committed progenitor cells ($NT2^-$) that after exposure to retinoic acid (RA), differentiate into post-mitotic neurons (NT2N) (Pleasure *et al.*, 1992). Differentiation of NT2N neurons in culture follows a pattern of differential gene expression similar to that of the neuronal precursors during neurogenesis (Przyborski *et al.*, 2000). NT2N neurons have been shown by several laboratories to have characteristics of primary human neurons (Sandhu *et al.*, 2003).

We have shown that differentiated NT2N neurons expressed Le^x, which was synthesized by FUT9. The Le^x was detected on the cell surface of both dendrites and axons and, intracellularly, was detected in lysosomes and found to colocalize with the exocytic TI-VAMP compartment that is associated with neurite outgrowth. Incubation with anti-Le^x antibody caused a decrease in the initiation of neurite outgrowth and cell adhesion.

4.3. Materials and methods

4.3.1. Neuronal culture

NTERA-2/cl.D1 cells were cultured and differentiated into neurons essentially as described previously (Pleasure *et al.*, 1992). Briefly, undifferentiated $NT2^-$ cells were grown in Opti-MEM I (Gibco) with 5% fetal bovine serum (FBS) (HyClone), 100 U/ml penicillin (P) and 100 μg/ml streptomycin (S) (Gibco). For differentiation, cells were cultured in Dulbecco's modified Eagle's medium (DMEM)-High Glucose (HG) (Gibco) with 10% FBS, P, S, and 10 μM RA (Sigma, St. Louis, MO) for 5 weeks. For neuron enrichment, cell culture was in DMEM-HG with 5% FBS, P, S, supplemented with the mitosis inhibitors 1 μM cytosine arabinoside (Sigma), 10 μM fluorodeoxyuridine (Sigma), and 10 μM uridine (Sigma) for further 10 days. NT2N neurons were recovered after selective hydrolysis with trypsin (Gibco) and plated on 10 μg/ml poly-D-lysine (Sigma) and 0.26 mg/ml Matrigel (BD Biosciences)-coated surfaces.

4.3.2. Fucosyltransferase assays

For FUT assays, cells were solubilized with 50 mM MOPS-NaOH buffer pH 7.5, containing 1% Triton X-100 (TX-100), 4°C, for 1 hour. The FUT activity in cell extracts was determined by the incorporation of radioactive Fuc from the GDP-[^{14}C]-Fuc donor onto several acceptors as described previously (Sousa *et al.*, 2001). One unit of enzyme activity was defined as the amount of enzyme catalyzing the transfer of 1 μmol Fuc/minute to the acceptor. The synthetic acceptors used were the type I: Galβ3GlcNAc-R, NeuAcα2,3Galβ3GlcNAc-R, and Fucα2Galβ3GlcNAc-R (H type I); and the type II: Galβ4GlcNAc-R (LacNAc),

NeuAcα2,3Galβ4GlcNAc-R (sLacNAc), and Fucα2Galβ4GlcNAc-R (H type II) (Lectinity Holding), where R = O-$(CH_2)_3$NHCO$(CH_2)_5$NH-biotin.

4.3.3. SDS-PAGE and Western blot analysis

Total cell protein was solubilized with 50 mM Tris-HCl buffer pH 7.4, containing 5 mM EDTA, 1% TX-100, and protease inhibitors (Complete Cocktail; Roche). Proteins were separated by SDS-PAGE and transferred to polyvinylidene difluoride membrane. Membranes were blocked in 5% non-fat dry milk (Nestle) in PBS with 0.1% Tween-20. Primary antibodies were: L5 anti-Le^x monoclonal antibody (Streit *et al.*, 1990; Streit *et al.*, 1996), C-20 anti-FUT4 and C-17 anti-FUT9 polyclonal antibodies (Santa Cruz Biotechnology) at 1:500 dilutions, L1-11A anti- L1 monoclonal antibody 1:4 (Stoeck *et al.*, 2006), H4A3 anti-human LAMP-1 monoclonal antibody (BD Biosciences) at 1:200, VC1.1 anti-HNK-1 monoclonal antibody (Sigma) at 1:10000 dilution and anti-calnexin (Chen *et al.*, 1995) at 1:15000 dilution. All dilutions were in blocking solution. HRP-labeled polyclonal secondary antibodies anti-mouse IgM, anti-goat IgG (Sigma), anti-mouse IgG and anti-rabbit IgG (Amersham Biosciences) were diluted in blocking solution. Chemiluminescent detection was by the ECL Plus system (Amersham Biosciences).

Mucin extract from a gastric mucosa adjacent to a gastric carcinoma was used as a control in anti-Le^x Western blot. The sample was obtained from a surgical specimen of a patient undergoing surgical resection in the Hospital S. João, Porto, Portugal. Sample was collected after informed consent. Mucin extraction was carried out as described previously (Reis *et al.*, 1997).

4.3.4. Glycosidase hydrolysis

Total cell protein from $5x10^5$ NT2N neurons after 8 days in plates coated with poly-D-lysine and Matrigel was solubilized with 50 mM Tris-HCl buffer pH 7.4, containing 5 mM EDTA, 1% TX-100, and protease inhibitors (Complete Cocktail; Roche), at 4ºC for 1 hour. After centrifugation at 10000× *g*, for 10 minutes, the cell extract was precipitated in 80% ethanol, at –20ºC, for 3 hours. The pellet was collected after a centrifugation 10000× *g*, 10 minutes, at 4ºC. Deglycosylations with peptide-*N*-glycosidase F (PNGase F) (Roche), neuraminidase (Roche) and chondroitinase ABC (ChABC) (Sigma) were performed according to the supplier's instructions. Twenty μg serum ferritin (Sigma) and 30 μg decorin (Sigma) were used as positive control for neuraminidase and ChABC activity, respectively. In brief, precipitated protein was solubilized in denaturation buffer (0.5% SDS and 1% β-mercaptoethanol) for 10 minutes at 100ºC, samples were allowed to cool down and 5 U of PNGase F, 50 μU neuraminidase or 25 mU of ChABC and the corresponding buffers were added. The buffers were: 10 mM NaH_2PO_4, 5 mM EDTA, 1% Nonidet P-40 (NP-40), pH 7.5 for PNGaseF; 50 mM $NaCH_3CO_2$, 5 mM $CaCl_2$ pH 5.5 for neuraminidase; 50 mM Tris, 60 mM $NaCH_3CO_2$ and 0.02 % (w/v) BSA pH 8 for ChABC. Incubations were done in 25 μl reaction mixtures, at 37ºC, for 18 hours (PNGaseF and neuraminidase) or 6 hours (ChABC) and the reactions were stopped by precipitation in 80% ethanol at -20ºC. Proteins were separated by SDS-PAGE in precasted NuPAGE Novex Tris-Acetate gels 3-8% (Invitrogen) and analyzed by Western blot with the L5 anti-Le^x monoclonal antibody, as described above.

4.3.5. Cell-surface biotinylation

Cell surface proteins were biotinylated as described before (Sousa *et al.*, 2003). NT2N neurons after 8 days in 6-well plates coated with poly-D-lysin and Matrigel, were cooled to 4ºC, three-fold washed with PBS and incubated with 0.5 mg/ml sulfo-NHS-SS-biotin (Pierce) in PBS containing 1 mM $CaCl_2$ and 1 mM $MgCl_2$ (PBSCM) for 30 minutes. After a two-fold wash with PBSCM containing 50 mM NH_4Cl followed by DMEM with 10% FCS, proteins were extracted with PBS containing 1% TX-100, 0.5% sodium deoxycholate, 0.1% SDS, 5 mM EDTA and a complete cocktail of protease inhibitors (Roche) and incubated with 50 µl streptavidin-agarose suspension (Sigma) for 2 hours. The agarose beads were five-fold washed with 10 mM Tris-HCl buffer pH 8.0, containing 0.5 M NaCl, 1 mM EDTA, 1% NP-40. All steps were performed at 4°C. The biotinylated proteins were eluted by boiling in SDS sample buffer, separated by SDS-PAGE in a precasted Tris-Acetate Criterion gel 3-8% (BioRad) and analyzed by Western blot with the L5 anti-Le^x monoclonal antibody and the rabbit polyclonal anti-calnexin antibody, as described above.

4.3.6. RNA extraction and reverse transcription

Total RNA was extracted from $NT2^-$ cells and NT2N neurons. The RNeasy extraction kit (Qiagen) was used according to the manufacturer's protocol. In brief, $5x10^6$ cells were lysed, homogenized and applied to an Rneasy minispin column of a silica-based membrane that selectively binds to RNA. Total RNA was eluted with 30 µl of RNase-free water.

Two µg of total RNA was subjected to reverse transcription primed with random primers (Invitrogen). The mixture was incubated at 65ºC for 5 minutes and chilled on ice. One unit of Moloney Murine Leukemia Virus Reverse

Transcriptase (Invitrogen) was added and the mixture was incubated at 37ºC for 50 minutes. The reaction was terminated by incubating the reaction mixture at 70ºC, for 15 minutes. One μl of the resulting cDNA was amplified in a final volume of 25 μl of polymerase chain reaction (PCR) reaction mixture containing 1.5 mM $MgCl_2$, 0.2 mM dNTPs, 0.4 μM of each primer, 5% DMSO (for FUT4) and 2.5 U Taq DNA Polymerase (Invitrogen). The primers for FUT4 were FUT4-fwd: 5'-GAGAGGCTCAGGCCGTGCTTTT-3' and FUT4-rev: 5'-GCAGGAGCCCAATTTCGGGCAC-3', described by Numahata *et al.*, 2002. The primers for β-actin have been described by Kudo and Narimatsu, 1995 - β-actin-fwd: 5'-GATATCGCCGCGCTCGTCGTCGAC-3' and β-actin-rev: 5'-CAGGAAGGAAGGCTGGAAGAGTGC-3'. The primers specific for FUT9 were deduced from cDNA sequences (Kaneko *et al.*, 1999b) - FUT9-fwd: 5'-GGGCAGACCTTTGACCTTACAT-3' and FUT9-rev: 5'-CTTTTCACATGATCGCAAGC-3'. PCR was carried out in a 2720 Thermalcycler (Applied Biosystems) under the following conditions: 94ºC for 5 minutes; 30 cycles of 94ºC for 45 seconds, 55-64ºC (depending on primers used) for 1 minute and 72ºC for 2 minutes; 72ºC for 7 minutes. The PCR products were analyzed by electrophoresis in 1.5 % agarose gel with 0.5 μg/ml ethidium bromide and their size estimated relatively to a gene ruler consisting of 1 kb and 100 bp DNA ladders.

4.3.7. Immunofluorescence microscopy

$NT2^-$ cells, grown on coverslips to half confluency, and NT2N neurons, after 8 days in 24-well plates with coverslips coated with poly-D-lysine and Matrigel, were washed with PBS containing 0.5 mM $MgCl_2$, fixed with 4% (w/v) paraformaldehyde (PF) and 4% sucrose (suc) in PBS for 20 minutes and, when described, permeabilized with 0.1 or 0.3% (w/v) TX-100 in PBS ($NT2^-$ cells and

NT2N neurons, respectively) for 20 minutes. Blocking was done with 1% bovine serum albumin (BSA) and 0.1% TX-100 in PBS for 1 hour and primary and secondary antibodies were incubated at room temperature for 2 and 1 hour, respectively. Antibody solutions were prepared in blocking solution and washes were carried out with PBS. Coverslips were mounted in Airvol. Primary antibodies were: rat IgM anti-Le^x L5 (1:200); mouse IgG anti-Le^x SH1 used at 10-fold concentrate containing BSA 1% (Singhal *et al.*, 1990); mouse IgM anti-SSEA-1 MC-480 (1:1) (DSHB); mouse IgM anti-Lewis^y (Le^y) AH6 (1:1) (Abe *et al.*, 1983); rabbit IgG anti-NF-L (1:2,000) (Trojanowski *et al.*, 1989); mouse IgG anti-hypophosphorylated NF-M RMdO.20 (1:1) (Pleasure *et al.*, 1992); rat IgG anti-highly phosphorylated NF-M H014 (1:1) (Pleasure *et al.*, 1992); mouse IgG anti-TI-VAMP clone 158.2 (1:200) (Alberts *et al.*, 2003); mouse IgG anti-EEA-1 (1:200) (BD Biosciences); mouse IgG anti-LAMP1 H4A3 (1:50); mouse IgG anti-GM130 (1:200) (BD Biosciences); and sheep IgG anti-TGN46 (1:200) (Serotec). Secondary antibodies were: goat anti-mouse IgG TRITC-conjugate (1:64) (Sigma); goat anti-rat IgM TRITC-conjugated (1:50) (Jackson ImmunoResearch); goat anti-mouse IgM TRITC-conjugated (1:50) (Jackson ImmunoResearch); goat anti-mouse IgG AlexaFluor488 (1:500) (Molecular Probes); donkey anti-mouse IgG AlexaFluor488 (1:500) (Molecular Probes); and donkey anti-sheep IgG AlexaFluor488 (1:500) (Molecular Probes). For double labeling with anti-LAMP-1 and anti-TI-VAMP mouse IgGs, neurons were permeabilized with 0.1% TX-100 for 10 minutes, and incubated sequentially with the two antibodies. After incubation with anti-LAMP-1 followed by goat anti-mouse IgG-AlexaFluor594 conjugated, non-labeled goat anti-mouse IgG Fab fragment (Sigma) at the saturating concentration of 0.2 mg/ml was used. Incubations with anti-TI-VAMP followed by goat anti-mouse IgG-AlexaFluor488 were carried out. As control, the experiment was carried out without anti-LAMP-1 or anti-TI-VAMP, and resulted in staining patterns similar to those obtained for each primary antibody independently.

Confocal images were acquired in a confocal microscope SP2+AOBS (Leica) equipped with a 63× objective using zoom 2. Each fluorophore used was excited and detected separately to avoid channel bleed-through. For each channel, photomultiplier gains and offsets were adjusted to use full image dynamic range. Each picture consisted of a z-series of 20 images of 1024 × 1024 pixel resolution with a pinhole of 1.0 Airy unit and typically, 0.6 μm focus intervals. Merge between channels and maximum *z*-projections were created using the open source ImageJ software version 1.35 (http://www.rsb.info.nih. gov/ij/). Image editing software (Adobe Photoshop, Adobe Systems) was used to create montages. The only modifications made during image editing were linear brightness and contrast adjustments.

4.3.8. Recycling assay

Live NT2N neurons, after 8 days in 24-well plates with coverslips coated with poly-D-lysine and Matrigel, were cooled and incubated with L5 anti-Le^x monoclonal antibody at 1:150 dilution at 4ºC for 1 hour. After washing with medium, neurons were incubated at 37ºC for 1, 2 or 3 hours, to allow endocytosis and recycling to occur, or at 4ºC for 1 hour. Cells were then washed, fixed with 4% PF containing 4% suc for 20 minutes and PM Le^x was detected with a goat anti-rat IgM-AlexaFluor488 (Invitrogen). NT2N neurons were then permeabilized and probed for NF-L as described above. Secondary antibody was a goat anti-rabbit IgG-AlexaFluor594 conjugated.

4.3.9. Anti-Le^x incubation assays

NT2N neurons were plated on 24-well plates (5 x 10^4 cells/cm^2) coated with poly-D-lysine and Matrigel. The assays were carried out in conditioned medium with mitosis inhibitors.

Anti-Le^x antibody (L5) was added to NT2N neurons at the time of plating or to neurons already in culture for 4 days. Equivalent volumes of PBS (the solvent of the stock solution of anti-Le^x) and equivalent concentrations of the non-related IgM MOPC-104E (Sigma) that recognizes α3-glucan (Klimpel and Goldman, 1988) were used as control. Cells were observed by bright-field microscopy using a Leica DM IRB inverted microscope attached to an Olympus DP11 digital camera. Neurite length was measured using the NeuronJ 1.1.0 plugin (Meijering *et al.*, 2004) of the open source ImageJ software version 1.35. A neurite was defined as a process with a length greater than one cell body diameter (approximately 15 μm). At least 60 neurites were measured. Experiments were carried out at least twice. Statistical analysis was carried out using the GraphPad Prism 4 software.

4.4. Results

4.4.1. Level of the Le^x determinant is increased during NT2N neurons differentiation

To monitor Le^x during differentiation of the teratocarcinoma NT2$^-$ cells into NT2N neurons on RA induction, we have analyzed the two cell types by immunofluorescence microscopy with several monoclonal anti-Le^x antibodies: L5 (Streit *et al.*, 1990; Streit *et al.*, 1996), SH1 (Singhal *et al.*, 1990), and

anti-SSEA-1 (Solter and Knowles, 1978). We found that both L5 and SH1 antibodies stained NT2N neurons but not $NT2^-$ cells (Figure 21A).

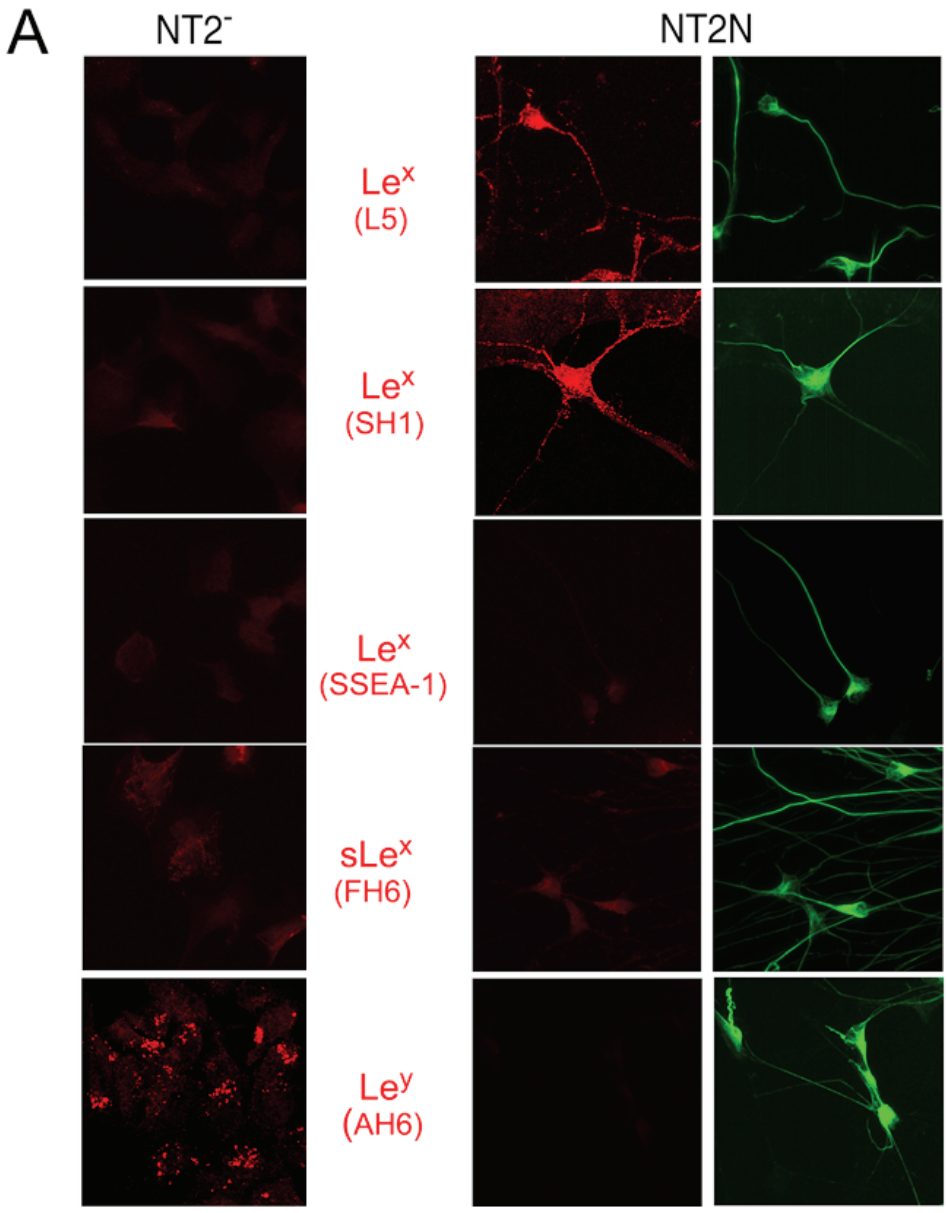

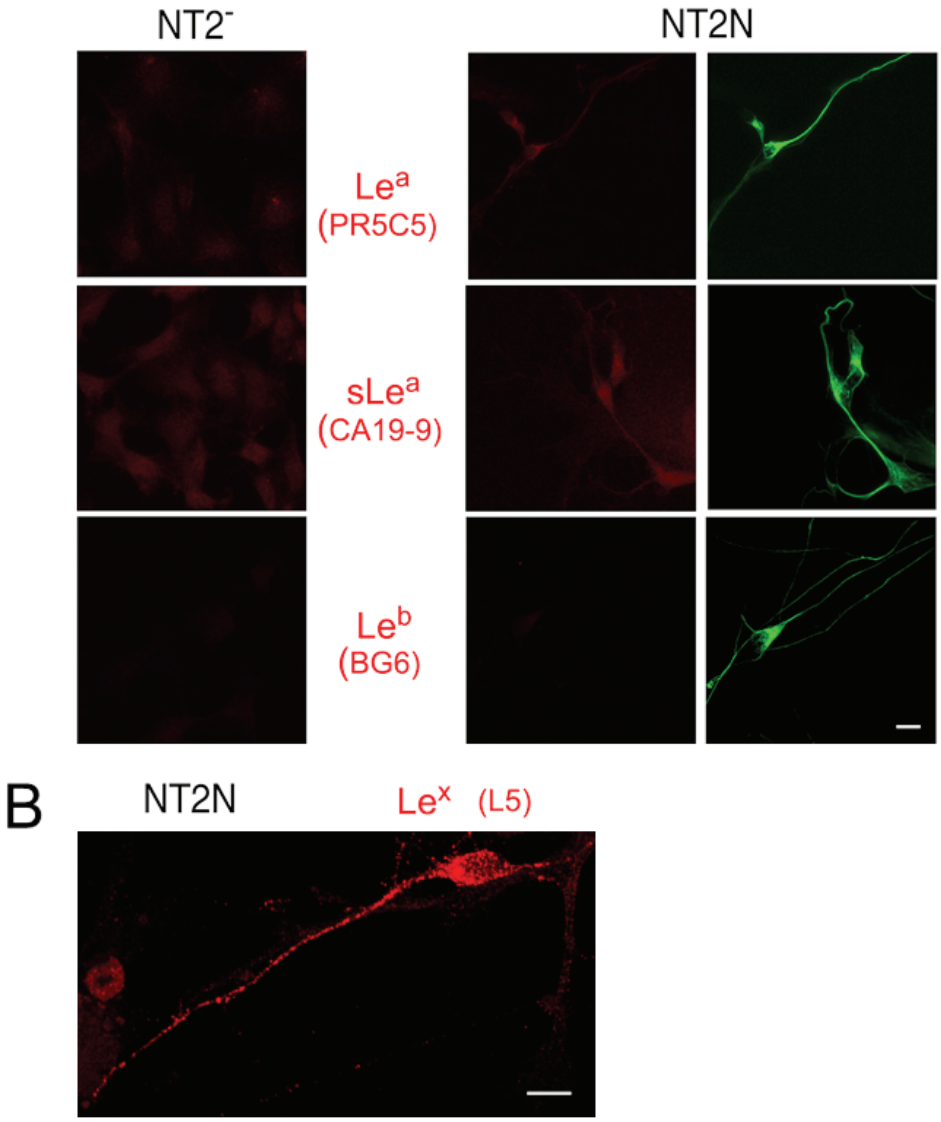

Figure 21: Immunodetection of Lewis determinants in NT2$^-$ cells and NT2N neurons by immunofluorescence confocal microscopy. **(A)** Permeabilized NT2$^-$ cells and NT2N neurons were probed with the monoclonal antibodies anti-Le^x L5, SH1 and SSEA-1; anti-sLe^x FH6; anti-Le^y AH6; anti-Le^a PR5C5; anti-sLe^a CA19-9; anti-Le^b BG6 (shown in red) and a polyclonal antibody anti-NF-L (shown in green). Secondary antibodies were: goat anti rat IgM-TRITC, goat anti-mouse IgG-AlexaFluor594, goat anti-mouse IgM-TRITC, and goat anti-rabbit IgG-AlexaFluor488. The experiment was done at least

three independent times. **(B)** Permeabilized NT2N neurons cultured on poly-D-lysine coated surfaces with serum-depleted medium were probed with the monoclonal antibody anti-Le^x L5. Secondary antibody was goat anti rat IgM-TRITC. Maximum intensity *z*-projections of 20 optical sections are shown. Scale bars = 10 μm.

The staining appeared in vesicles, which were concentrated in the cell body, with a perinuclear pattern, and extended into neurites. The anti-SSEA-1 antibody presented no reactivity in neither $NT2^-$ nor NT2N neurons (Figure 21A), as described by other authors (Fenderson *et al.*, 1987).

The labeling in NT2N neurons did not consist of material internalized from FBS nor Matrigel because it was detected by immunofluorescence microscopy in NT2N neurons cultured in serum-depleted medium and on poly-D-lysine coated surfaces (Figure 21B). As a control for neuronal differentiation, a polyclonal antibody against low molecular weight neurofilament protein (NF-L) was used as neuronal marker, which stained NT2N neurons (Figure 21A) but not $NT2^-$ cells (results not shown). Other Lewis determinants derived from type II oligosaccharides were also monitored. Le^y was detected with the AH6 antibody in $NT2^-$ cells but not in NT2N neurons (Figure 21A). This decrease was probably due to a downregulation of α2-FUT during differentiation. Alternatively, reorganization of glycosyltransferases in the Golgi during differentiation could occur in a way that α2-FUT would not have access to the type II precursor. The sLe^x epitope was not detected in $NT2^-$ cells nor in NT2N neurons (Figure 21A). Lewis determinants derived from type I precursors, Le^a, Le^b, and sLe^a, were not expressed at detectable levels in any of the cell lines (Figure 21A).

4.4.2. Le^x from NT2N neurons is synthesized by FUT9

To determine the expression pattern of FUTs during NT2N differentiation RT-PCR analysis was carried out (Figure 22).

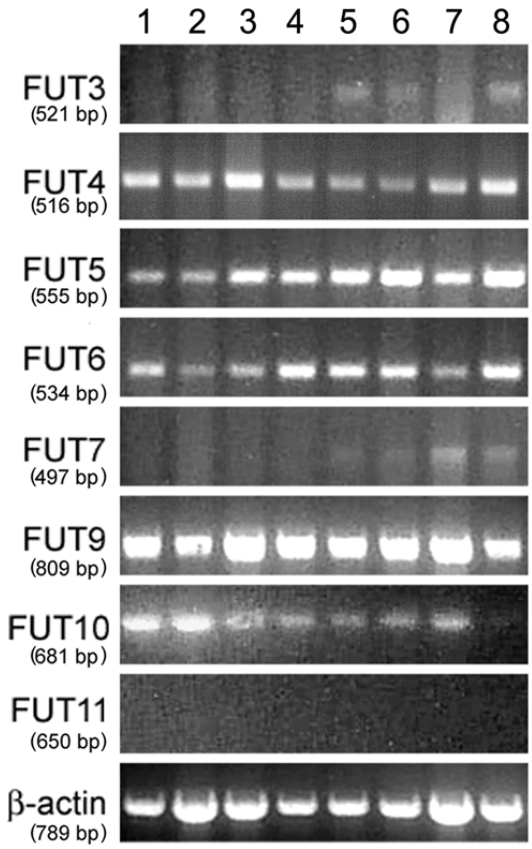

Figure 22: RT-PCR analysis of fucosyltransferases along NT2N neurons differentiation induced by retinoic acid. cDNA was obtained from undifferentiated $NT2^-$ cells (1), cells in retinoic acid for 3 (2), 10 (3), 17 (4), 24 (5), and 31 (6) days, cells in mitosis inhibitors for 10 days (7) and mature NT2N neurons plated on poly-D-lysine and Matrigel for 8 days (8). The PCR products were electrophoretically resolved on 1.5% agarose gel in the presence of 0.5 μg/ml ethidium bromide. The sizes of the amplified fragments are indicated on the left in base pairs (bp). The gels presented correspond to one representative experiment of the four experiments carried out from three independent RNA extractions.

The RT-PCR products of *FUT4* (516 bp), *FUT5* (555 bp), *FUT6* (534 bp) and *FUT9* (809 bp) were present in $NT2^-$ cells, during RA-induced differentiation, and in NT2N neurons. *FUT10* gene transcripts (681 bp) were detected in all

stages of differentiation except in NT2N neurons. *FUT3* (521 bp) and *FUT7* (497 bp) were only detected, with weak signals, in late differentiating stages, starting after 24 days in the presence of RA, and in NT2N neurons. *FUT11* transcripts (650 bp) were not detected in any of the stages analyzed. These results showed that there were transcripts of *FUT4*, *FUT5*, *FUT6*, *FUT9*, and to a minor extent *FUT3* and *FUT7*, in NT2N neurons.

To elucidate the activity profiles of FUTs during the differentiation of NT2N cells, we studied the acceptor specificities of cell homogenates during the differentiation process toward a panel of small oligosaccharides of the type I and II acceptor substrates coupled to a hydrophobic moiety (Figure 23).

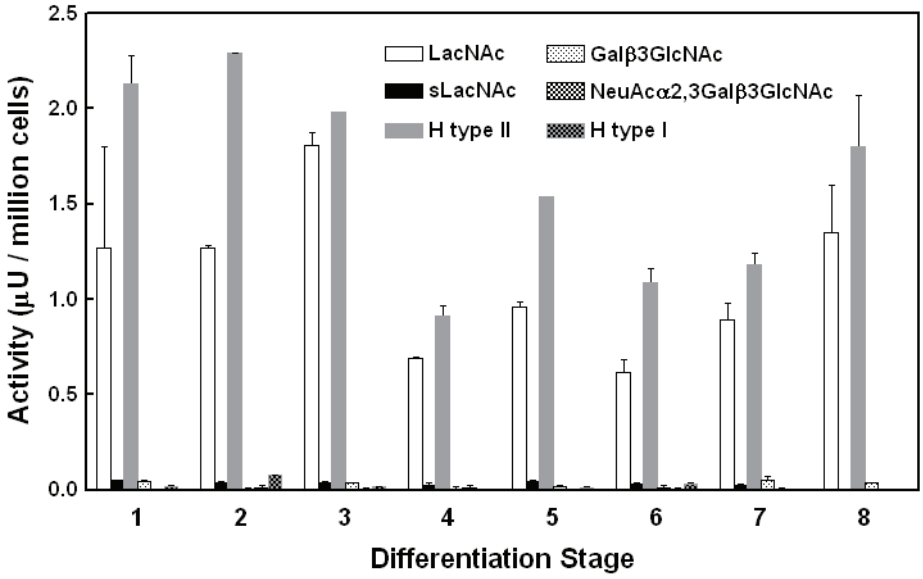

Figure 23: Fucosyltransferase activity - acceptor specificity profile along NT2N neurons differentiation induced by retinoic acid. Fucosyltransferase activity was determined using 1 × 10^6 cells of each differentiation step (1 - 8 as indicated in Figure 22 legend) per assay with the synthetic acceptors: Galβ4GlcNAc-R (LacNAc), NeuAcα2,3Galβ4GlcNAc-R (sLacNAc), Fucα2Galβ4GlcNAc-R (H type II), Galβ3GlcNAc-R, NeuAcα2,3Galβ3GlcNAc-R and Fucα2Galβ3GlcNAc-R (H type I). R = O-$(CH_2)_3$NHCO$(CH_2)_5$NH-biotin.

Activity assays showed that Galβ4GlcNAc-R (LacNAc-R) was a good substrate, leading to the production of Le^x determinant in every cell homogenate from each differentiation step analyzed. A substitution of Gal with α2-linked Fuc (H type II-R) yielded an increase in activity. Nevertheless, a substitution of the Gal with α2,3-linked *N*-acetylneuraminic acid (sLacNAc-R) yielded very low radioactivity incorporation. These results suggested that FUT4 or FUT9 would be the enzymes associated with the synthesis of Le^x in differentiating NT2N neurons, because FUT5 and FUT6 are capable of fucosylating sialylated type II acceptors (Weston *et al.*, 1992a; Weston *et al.*, 1992b), the activity of which was not observed for the cell extracts tested in this study (Figure 23).

Activity toward type I acceptors, Galβ3GlcNAc-R, NeuAcα2,3Galβ3GlcNAc-R, and H type I-R, to generate the Le^a, sLe^a, and Le^b epitopes, respectively, was very poor, from $NT2^-$ cells to NT2N neurons, representing residual or not detectable values (Figure 23). These results agreed with the absence or extremely low amounts of FUT3 transcripts detected (Figure 22).

To distinguish between FUT4 and FUT9 as the enzymes synthesizing Le^x during NT2N neuron differentiation, we have carried out Western blot analysis with polyclonal antibodies against carboxy-terminal peptides of FUT4 and FUT9. FUT4 and FUT9 proteins were detected in $NT2^-$ cells (Figure 24). FUT4 had an apparent molecular mass of 63 kDa, which probably corresponded to the long form of the enzyme, ELFT-L (Goelz *et al.*, 1990). The polypeptide chain has a predicted molecular mass of 59 kDa with two potential *N*-glycosylation sites (Goelz *et al.*, 1990). Therefore, the difference between the observed molecular mass and the theoretical prediction indicated that the glycosylation sites were occupied. FUT9 showed an apparent molecular mass of 44 kDa. The polypeptide chain has a predicted molecular mass of 42 kDa with three potential *N*-glycosylation sites (Kaneko *et al.*, 1999b). The 2 kDa molecular mass observed was probably due to *N*-glycosylation. Human FUT9 expressed transiently in HeLa

cells was used as a positive control for FUT9 detection (results not shown). After differentiation to NT2N neurons, the levels of FUT9 were increased markedly whereas FUT4 was no longer detected even after long exposure times (Figure 24). These results showed clearly that FUT9 was the α3-FUT that catalyzed the synthesis of Le^x in human NT2N neurons. Additionally, we also found transient higher levels of FUT9 in cells treated with RA for 10 and 17 days.

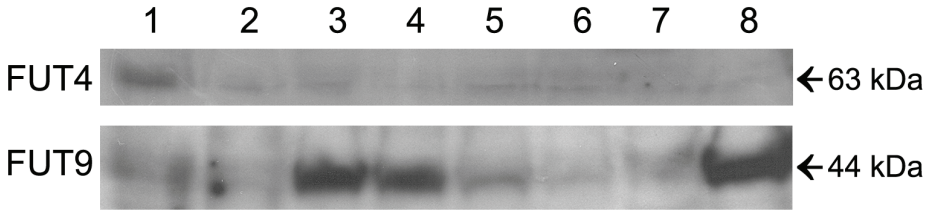

Figure 24: Immunodetection by Western blot of FUT4 and FUT9 along NT2N neurons differentiation induced by retinoic acid. Total protein from 1 × 10^6 cells of each differentiation step was applied per lane (1 - 8 as indicated in Figure 22 legend). Detection was carried out using anti-human FUT4 and FUT9 polyclonal antibodies C-17 and C-20, respectively. As secondary antibody a polyclonal antibody anti-goat IgG HRP-conjugated was used. Detection was carried out by the ECL+ method. Experiments were carried out twice from two independent protein extractions of each differentiation step. For each experiment, one blot per FUT was done and then reprobed for the other FUT to confirm that differences did not arise from different protein loads.

In conclusion, the α3-FUT activity observed in $NT2^-$ cells was the result of combined activities of FUT4 and FUT9 whereas in NT2N cells only FUT9 participated in the Le^x biosynthesis. The observation that NT2N cells contained FUT4 transcripts (Figure 22) but not the corresponding protein (Figure 24) suggested that FUT4 was post-transcriptionally downregulated in neurons.

4.4.3. Identification of a Le^x-carrier glycoprotein associated specifically with NT2N neurons

The L5 antibody has been described to react with Le^x present on neural cell adhesion molecule L1, neural chondroitin sulfate proteoglycans, and other neuronal glycosylated proteins. Furthermore, it was shown to bind a mouse astrocyte proteoglycan of approximately 500 kDa (Streit *et al.*, 1990). Therefore, to identify a possible Le^x-carrier glycoprotein from NT2N neurons, cellular extracts were analyzed by Western blot using the monoclonal anti-Le^x antibody L5 during differentiation. Most striking was the finding of a Le^x-containing glycoprotein at a molecular mass higher than 206 kDa, present in NT2N neurons but absent from NT2$^-$ cells (Figure 25, lanes 8 and 1, respectively). This protein of approximately 460 kDa was associated endogenously with NT2N neurons and was not internalized from the FBS because it was still detected by Western blot in neurons cultured in serum-depleted medium (Figure 26A, lane 1). Furthermore, it was not internalized from the Matrigel used to coat the plates because the carrier was already detected in extracts of cells differentiated with RA and in MI for 10 days (Figure 25, lane 7). Finally, it was absent from Western blot analysis of Matrigel extracts (Figure 26A, lane 5). A less abundant glycoprotein was also detected in NT2N neurons but not in NT2$^-$ cells that had an apparent molecular mass of approximately 175 kDa (Figure 25, lanes 8 and 1, respectively). Other Le^x-containing glycoproteins were detected transiently at intermediary differentiation stages at 10-17 days after RA addition (Figure 25, lanes 3 and 4). At these stages, higher levels of FUT9 were also observed, as shown above (Figure 24). It is probable that the higher FUT9 levels would underlie the higher Le^x-carrier glycoprotein detection observed by Western blot. Le^x-containing mucins extracted from a gastric mucosa adjacent to a gastric carcinoma were used as positive control (Figure 25, lane C).

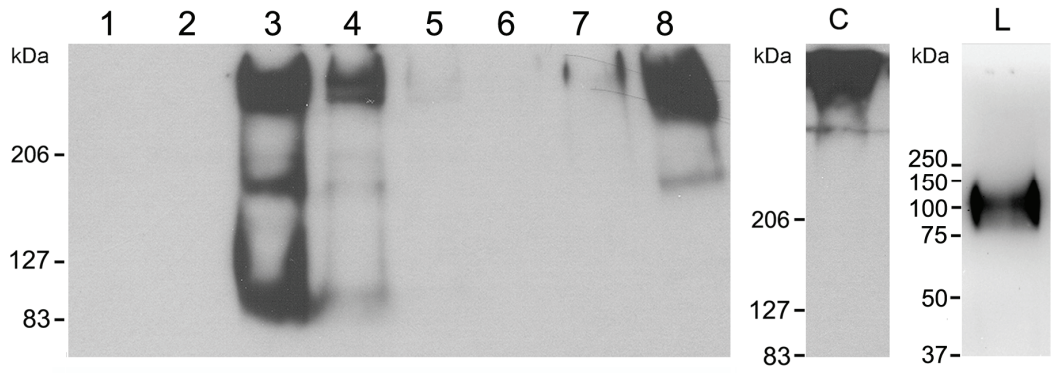

Figure 25: Immunodetection by Western blot of Le^x-carrier proteins along NT2N neurons differentiation induced by retinoic acid and of LAMP-1 in NT2N neurons. Total protein from 1 × 10^6 cells of each differentiation step was applied by lane (1 - 8 as indicated in Figure 22 legend). Detection was carried out using the anti-Le^x monoclonal antibody L5. Mucins containing Le^x extracted from a gastric mucosa adjacent to a gastric carcinoma were used as positive control (lane C). Total protein from 1 × 10^5 NT2N neurons was applied for detection with the anti-LAMP-1 monoclonal antibody H4A3 (lane L). As secondary antibodies polyclonal anti-mouse IgM and goat anti-mouse IgG HRP-conjugated were used. Detection was carried out by the ECL+ method. Experiments were carried out three times from at least two independent protein extractions of each differentiation step.

As referred above, L5 has been shown to bind astrochondrin, a chondroitin sulfate proteoglycan of approximately 500 kDa present in mouse astrocytes (Streit *et al.*, 1990; Streit *et al.*, 1993). L5 binding to astrochondrin, to other Le^x–carriers present in the mouse brain (Streit *et al.*, 1990) and also to a 500 kDa carrier present in the neural tissue of the chick embryo (Roberts *et al.*, 1991), showed sensitivity to PNGaseF digestion. According to the characterization of the L5 antibody reactivity (Streit *et al.*, 1990; Streit *et al.*, 1996), it recognizes preferentially the Le^x epitope in *N*-linked glycans from glycoproteins.

Aiming to characterize the high molecular mass Le^x-carrier glycoprotein identified in NT2N neurons, we performed digestions with PNGaseF, neuraminidase and chondroitinase ABC (ChABC) before Le^x detection with the L5 antibody (Figure 26A, lanes 2, 3 and 4, respectively). After incubation of NT2N neurons extracts with each of the enzymes, we did not observe changes in the detection pattern, neither disappearance of the detected band nor a shift in its apparent molecular mass. Use of increased amount of enzyme or extended incubation time did not increase the digestion efficiencies (results not shown).

Decorin, a chondroitin sulfate proteoglycan from bovine articular cartilage was used as a positive control for chondroitinase activity (Figure 26B). Decorin was detected in SDS-PAGE as a diffuse band above 100 kDa (Figure 26B, arrowhead) and after ChABC digestion there was a shift to approximately 40 kDa (Figure 26B, arrow), the molecular mass deduced from the polypeptide chain. The maintenance of the L5 binding after PNGase F digestion (Figure 26A, lane 2) suggested that the Le^x determinant was present in oligosaccharides attached to the polypeptide chain via a linkage other than *N*-glycosidic. Nevertheless, we cannot rule out that the enzyme was not able to exert its catalytic activity due to spatial restrictions caused, for example, by glycosaminoglycan chains.

Resistance to ChABC digestion suggested that the nature of the Le^x-carrier identified in human NT2N neurons was distinct from those previously identified in mouse astrocytes (Streit *et al.*, 1990) and embryonic rat brain (Shimoda *et al.*, 2002). It may correspond to a heparan sufate proteoglycan, a class of proteoglycans involved in several roles in the developing nervous system, such as connectivity between neurons and target cells (reviewed by Van Vactor *et al.*, 2006).

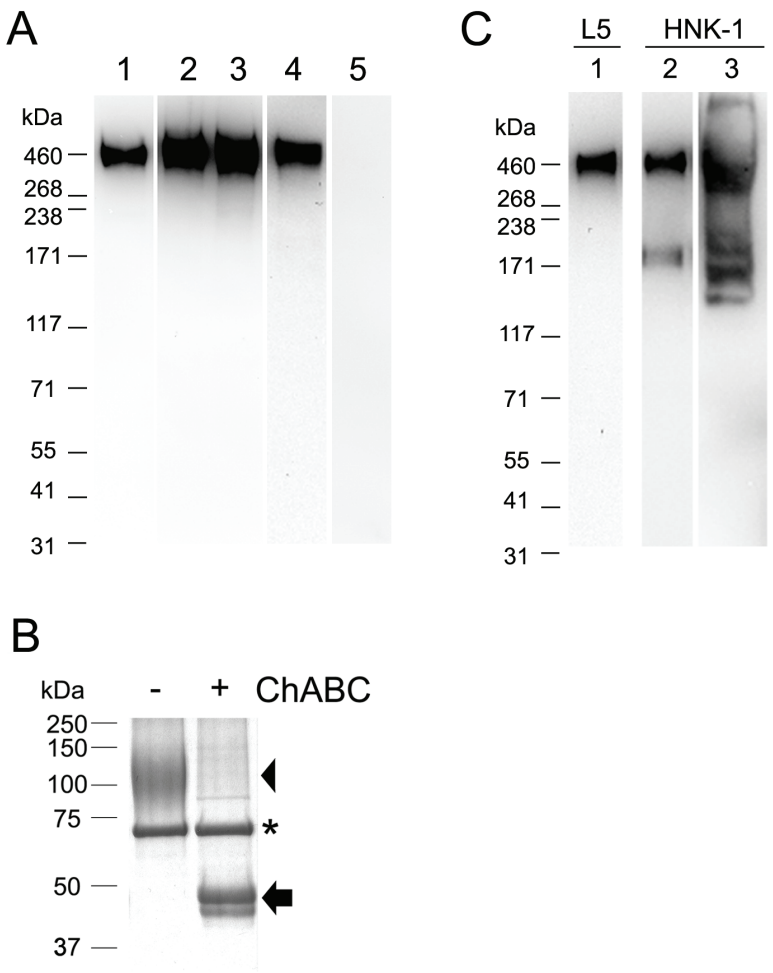

Figure 26: Characterization of Le^x-carrier protein of NT2N neurons. (A) Western blot of Le^x-carrier proteins of extracts of NT2N neurons: cultured in serum depleted medium (lane 1); after digestion with PNGaseF (lane 2), neuraminidase (lane 3) and chondroitinase ABC (lane 4). Matrigel extract (lane 5) was also probed. Detection was carried out using the anti-Le^x monoclonal antibody L5. **(B)** SDS-PAGE analysis of decorin (arrowhead) digestion (arrow) with chondroitinase ABC (ChABC). BSA from the ChABC incubation buffer is also detected (asterisk). **(C)** Western blot analysis of Le^x and HNK-1-carrier proteins of NT2N neuron extracts (lane 1 and 2, respectively) and of HNK-1-carrier proteins of rat brain extract (lane 3). Detection was carried out using the anti-Le^x monoclonal antibody L5 and the anti-HNK-1 monoclonal antibody clone VC1.1. Detection was performed by the ECL+ method.

The HNK-1 (human natural killer-1) epitope is a common carbohydrate antigen in the CNS, present in neuronal glycoproteins, glycolipids, and proteoglycans, including astrochondrin (Streit *et al.*, 1990), proposed to play important functional roles in neural development (reviewed by Yanagisawa and Yu, 2007). We probed the NT2N neurons extract with L5 and an anti-HNK-1 antibody and observed that, in addition to Le^x (Figure 26B, lane 1), the HNK-1 epitope was also present in the 460 kDa carrier (Figure 26B, lane 2). The anti-HNK-1 antibody also recognized a 170 kDa band that could correspond to neuronal cell adhesion molecule (N-CAM). In rat brain extract, used as a positive control for anti-HNK-1 binding, we detected a group of bands between 117 and 238 kDa that probably included the membrane bound forms 145 and 170 forms of N-CAM and the myelin associated membrane protein (Naegele and Barnstable, 1991). Another band between 268 and 460 kDa was also detected which could correspond to chondroitin or keratan sulfate proteoglycans carrying HNK-1 described in other species (Zaremba *et al.*, 1990). A possibility is that the HNK-1 and Le^x epitopes are present in *O*-mannosyl oligosaccharides, as this type of *O*-glycosidic linkage has been described in rat brain proteoglycans (Krusius *et al.*, 1987) which carry HNK-1 (Yuen *et al.*, 1997) and Le^x (Kogelberg *et al.*, 2001).

Additional studies will be required to clarify the nature of the Le^x-carrier glycoprotein identified.

4.4.4. Le^x determinant is localized at the plasma membrane and in the TI-VAMP compartment of NT2N neurons

We further analyzed Le^x subcellular localization in NT2N neurons by immunofluorescence microscopy using the L5 antibody. Le^x was found to be present at the PM of non-permeabilized NT2N neurons at the cell bodies as well as at the neurites (Figure 27A).

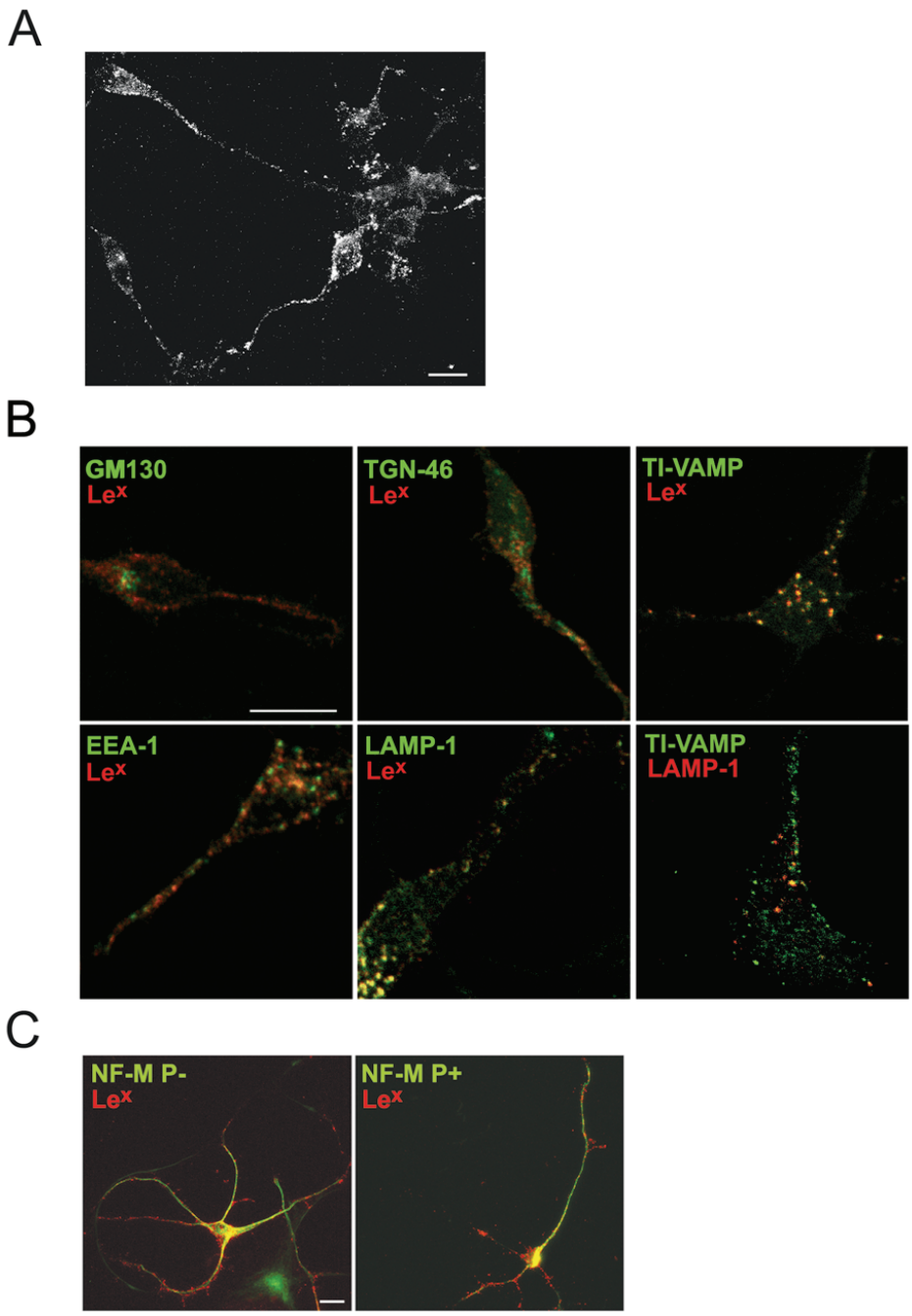

Figure 27: Localization of Le^x in NT2N neurons by immunofluorescence confocal microscopy. (**A**) NT2N neurons without permeabilization were probed with the antibody anti-Le^x L5. As secondary antibody, a goat anti-rat IgM-TRITC was used. (**B**).

Colocalization analysis of Le^x with markers of the endocytic and exocytic pathways and of LAMP-1 with TI-VAMP. (**C**) Colocalization analysis of Le^x with axon and dendrite markers. B, C: Permeabilized NT2N neurons were probed with the following antibodies: monoclonal anti-Le^x L5 and monoclonal anti-GM130, polyclonal anti-TGN-46, monoclonals anti-EEA-1, anti-LAMP-1, anti-TI-VAMP, anti-hypophosphorylated medium molecular weight neurofilament protein (NF-M P-), or anti-hyperphosphorylated medium molecular weight neurofilament protein (NF-M P+). Secondary antibodies were: goat anti-mouse IgG-AlexaFluor594, goat anti-mouse IgG-AlexaFluor488, goat anti-rat IgG-AlexaFluor488, goat anti-rat IgM-TRITC, and goat anti-sheep IgG-AlexaFluor488. Maximum intensity *z*-projections of 20 optical sections are shown in (A) and (C) and single optical sections in (B). The experiments were carried out at least three times and in each at least five neurons per marker were analyzed by confocal microscopy. Scale bar = 10 μm.

The epitope presented a discrete distribution, being accumulated in clusters at the membrane. These did not correspond to labeled intracellular vesicles because *in vivo* incubation of NT2N neurons with L5 antibody at 4°C for 1 hour yielded the same labeling pattern (Figure 29A).

To identify the intracellular vesicles containing Le^x identified above (Figure 21), we carried out colocalization analysis with markers of the exocytic and endocytic pathways by confocal immunofluorescence microscopy (Figure 27B). Most striking was the finding that Le^x colocalized with the v-SNARE tetanus neurotoxin insensitive vesicle-associated membrane protein (TI-VAMP) or VAMP7. TI-VAMP is a v-SNARE with a broad neuronal expression, proposed to mediate a specific exocytic pathway (Proux-Gillardeaux *et al.*, 2005). In neuronal cells, the TI-VAMP defines an exocytic pathway involved in neurite outgrowth via late endosome/lysosome compartment labeled by CD63, but not via early recycling endosomes containing the transferrin receptor or EEA-1 (Coco *et al.*, 1999). It has been shown recently that there was an extensive colocalization between TI-VAMP and lysosomal-associated membrane protein-1 (LAMP-1)-positive late endosomes/lysosomes in developing primary mouse

neurons from sympathetic cervical ganglia (SCGs) (Arantes and Andrews, 2006). We observed that in human NT2N neurons there was also colocalization between TI-VAMP and LAMP-1, both in cell bodies and in neurites (Figure 27B), although there was not a complete overlap, contrary to that found in SCG neurons (Arantes and Andrews, 2006). This may arise from differences between species, type of neurons, or differences in the development stage analyzed. Le^x colocalized extensively with LAMP-1, but not with the early endosomal marker early endosomal antigen-1 (EEA-1) (Figure 27B). LAMP-1 is a lysosomal highly glycosylated protein (Carlsson *et al.*, 1988), therefore, we investigated if it would be the carrier of the Le^x epitope in NT2N neurons. This was not the case, however, because LAMP-1 had an apparent molecular weight of approximately 114 kDa as detected in duplicate by SDS-PAGE and Western blot analysis (Figure 25, lane 8), which is lower than the masses of the two bands detected with the L5 antibody. Furthermore, immunoprecipitated LAMP-1 was not recognized by the L5 antibody, corroborating that in NT2N human neurons LAMP-1 was not a Le^x-carrier (results not shown). The staining observed in the lysosomes was not due to protein uptake from the serum or from the Matrigel coat because the staining with L5 was also observed in NT2N neurons cultured in serum-depleted medium for 24 hours and in poly-D-lysine coated plates.

Le^x showed only minor colocalization with the Golgi protein GM130 and the *trans*-Golgi network (TGN) marker TGN-46 (Figure 27B).

NT2N neurons possess identifiable dendrites and axons (Pleasure *et al.*, 1992). Using monoclonal antibodies that recognize specifically the hypophosphorylated (RMdO.20) and highly phosphorylated (HO14.4) forms of medium molecular weight neurofilament protein (NF-M), exclusively found on somatodendritic and axonal domains respectively, it is possible to distinguish between dendrites and axons. Le^x was found on neurites marked with both antibodies (Figure 27C). These results suggested that the Le^x participated in cell events common to dendrites and axons (e.g., neurite initiation and elongation of outgrowth).

To investigate if the Le^x-containing glycoproteins found in NT2N neurons (Figures 25 and 26) were also present at the PM we have isolated biotinylated PM proteins following a procedure described before (Sousa *et al.*, 2003), and have analyzed them by Western blot using the L5 antibody. We observed that the heavier glycoprotein was partially found at the PM (Figure 28, arrow) whereas the lighter less abundant one was predominantly found at the PM (Figure 28, arrowhead).

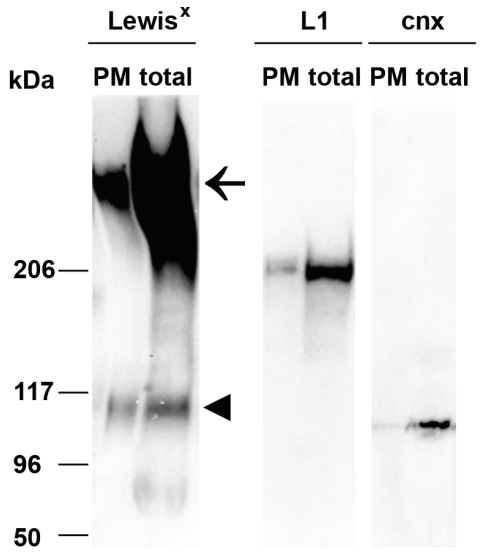

Figure 28: Western blot analysis of biotinylated plasma membrane proteins containing the Le^x determinant. PM proteins were biotinylated with sulfo-NHS-SS-biotin and isolated by affinity with streptavidin-agarose beads. The primary antibody used was L5. As secondary antibody, a polyclonal antibody anti-mouse IgM HRP-conjugated was used. An arrow and an arrowhead identify the two detected carriers. As positive control L1 detection was performed using the primary monoclonal antibody L1-11A, and secondary anti-mouse IgG HRP-conjugated. As negative control calnexin (cnx) detection was performed using a polyclonal antibody anti-cnx, and secondary anti-rabbit IgG HRP-conjugated. Detection was carried out by the ECL+ method.

As positive control, we used the L1 cell adhesion molecule, that recycles between the PM and endocytic organelles of neurons (Kamiguchi and Lemmon, 2000), and we observed that a fraction of total L1 was indeed found in the PM fraction (Figure 28). As negative control, we have analyzed the intracellular protein calnexin, an endoplasmic reticulum resident chaperone (Hammond *et al.*, 1994), and we observed that the level of calnexin found in the PM fraction was almost undetectable (Figure 28). This small fraction was probably from a low number of lysed cells. Thus, although Le^x was detected on the PM, an intracellular pool was also observed. This may corresponded to the TI-VAMP and LAMP-1-positive vesicles detected (Figure 27B).

4.4.5. Le^x is recycled to the plasma membrane of NT2N neurons

To investigate the trafficking of the Le^x-carriers detected by immunofluorescence microscopy (Figure 27B) we have labeled living NT2N neurons with the L5 antibody at 4ºC for 1 hour, followed by incubations of 1, 2 and 3 hours at 37ºC to allow adsorption, endocytosis and recycling to occur. Subsequent fixation and incubation with a fluorescently labeled secondary antibody allowed the visualization of the Le^x fraction that was present at the PM. After the initial incubation at 4°C, Le^x–labeling was accumulated in discrete clusters in cell bodies and neurites (Figure 29A), a distribution similar to that found by immunofluorescence microscopy of non-permeabilized cells (Figure 27A). Subsequent incubation at 37ºC for 1 and 2 hours caused a decrease in the Le^x detected at the PM to almost undetectable levels(Figure 29B, C), suggesting that the Le^x-carrier - L5 antibody complexes had been internalized. After 3-hour incubation, Le^x reappeared at the PM (Figure 29D).

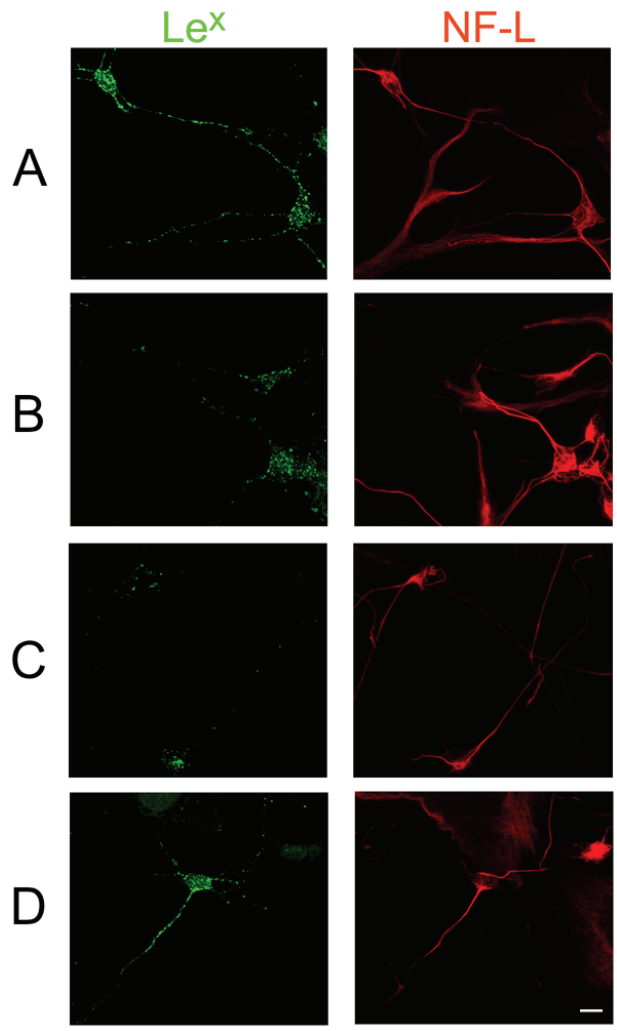

Figure 29: Plasma membrane distribution of recycled Le^x in NT2N neurons by immunofluorescence confocal microscopy. Live NT2N neurons were incubated with L5 anti-Le^x antibody at 4ºC for 1 hour **(A)** and allowed to internalize and recycle the L5–Le^x-carrier complex at 37ºC for 1 **(B)** 2 **(C)** or 3 **(D)** hours. Cells were fixed and L5–Le^x-carrier complex present at the PM detected by a goat anti-rat IgM-AlexaFluor488 antibody. After permeabilization, NT2N neurons were also probed with an anti-NF-L polyclonal antibody followed by a goat anti-rabbit IgG-AlexaFluor594. Maximum intensity *z*-projections of 20 optical sections are shown. The experiments were carried out at least two times and in each at least five neurons per marker were analyzed by confocal microscopy. Scale bar = 10 μm.

These results suggested that Le^x-carriers present at the PM of NT2N neurons were endocytosed and recycled back to the cell surface. This may occur via the membrane compartment defined by TI-VAMP which has been implicated in the trafficking of molecules that recycle between the PM and endocytic organelles of neurons, like the L1 cell adhesion molecule (Alberts *et al.*, 2003).

4.4.6. Anti-Le^x antibody impairs initiation of neurite outgrowth and adhesion of NT2N neurons

To investigate the biologic role of Le^x in NT2N neurons, we have studied the effect of anti-Le^x monoclonal antibody L5 on the neurons. We have used a non-related IgM (ctl IgM) to rule out unspecific effects caused by the IgM size. In cultures that were allowed to adhere and form neurites before the incubation with anti-Le^x antibody, we observed that attachment of neurons and their neurites to the surface was significantly impaired with 30 nM of antibody, when compared to incubation with 30 nM of control IgM (Figure 30A, arrows). At 15 nM L5, the effect was already visible but was less evident (results not shown). Furthermore, it seemed that traces of neurite remaining after detachment or retraction were observed (Figure 30A, arrowheads). When incubations were prolonged for 48 hours, neurons were detached from the surface at 10 nM L5 (results not shown). These results indicated that the L5 antibody inhibited NT2N cell adhesion to the plates.

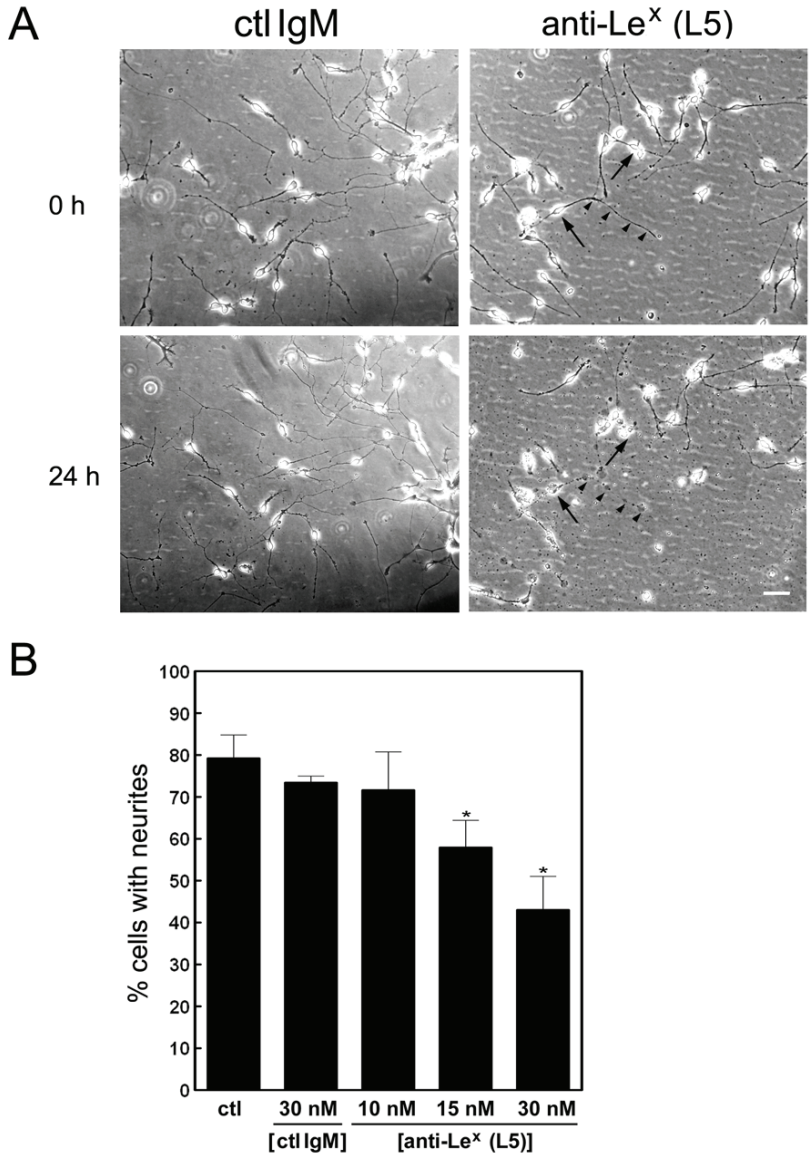

Figure 30: Effect of anti-Le^x antibody L5 on the adhesion and initiation of neurite outgrowth from NT2N neurons. (A) NT2N neurons in culture for 4 days were incubated with 30 nM anti-Le^x antibody L5; 30 nM of a non-related IgM (ctl IgM) was used as control. The same areas of the cultures were monitored at the time of the antibody addition (0 hr) and 24 hours later (24 hr). The assay was carried out in one (ctl IgM) or three independent experiments in duplicate. Scale bar = 50 μm. **(B)** Quantification of NT2N neurons with neurites in the presence of increasing L5 concentrations. L5 was

added to the cultures at the time of plating and PBS was used as control. The percentage of neurons with neurites was quantified 24 hours later. Data are mean ± SD of at least 150 neurons counted in 10 equivalent optical fields from one (30 nM ctl IgM), two (10 and 30 nM L5), and three (ctl and 15 nM L5) independent experiments in duplicate. *Indicates significant difference ($P < 0.001$) from 30 nM ctl IgM mean by a one-way ANOVA analysis with a Tukey's post-hoc multiple comparison test.

To investigate the effect of L5 on neurite outgrowth incubation in the presence of the antibody at the time of plating was carried out. Twenty-four hours later we observed that a lower number of NT2N neurons developed neurites on L5 addition. The effect was dose-dependent because increasing L5 concentration from 0 to 30 nM caused a decrease of the percentage of cells with neurites, from 79 ± 6% to 43 ± 8% (Figure 30B). There were no statistically significant differences between control without antibody and incubation with 30 nM of control IgM (Figure 30B). Furthermore, differences between incubations with 30 nM of control IgM and with 15 or 30 nM L5 were statistically different ($P < 0.001$) as evaluated by a one-way ANOVA analysis with a Tukey's post-hoc multiple comparison test. In the presence of L5 the cell bodies presented a round morphology. We have also measured neurite length in both experiments. In average, 24 hours after plating, neurites were 51 μm long in the presence (51 ± 36 μm) or absence of L5 (51 ± 35 μm). These results showed that L5 prevented the initiation of neurite outgrowth in NT2N cells but not its elongation.

4.5. Discussion

We have shown that during neuronal differentiation of human NT2N neurons from teratocarcinoma $NT2^-$ cells there was an increase in the levels of the cell adhesion carbohydrate Le^x determinant, concomitantly to FUT9 detection. The results obtained from RT-PCR analysis, FUT activities toward several

acceptor substrates, and Western blot analysis indicated clearly that FUT9 was the FUT responsible for the synthesis of Le^x in NT2N neurons. FUT9 has also been shown to be required for the synthesis of Le^x in mouse brain (Nishihara *et al.*, 2003; Kudo *et al.*, 2007) and to be increasingly expressed during neuronal RA induced differentiation of PC19 murine EC cells (Osanai *et al.*, 2001). In addition, FUT9 is regulated by the transcription factor *Pax6* in murine brain (Shimoda *et al.*, 2002). Because *Pax6* was increased during RA-induced differentiation of NT2N neurons (Przyborski *et al.*, 2000), it could be assumed that it also upregulates FUT9 in NT2N neurons, thus supporting our conclusion.

We found high levels of FUT9 in cells treated with RA for 10 and 17 days. Accordingly, at this stage higher levels of Le^x-containing glycoproteins were also detected (Figure 23, lanes 3, 4). These results suggested that the expression of FUT9 was induced transiently during RA-induced differentiation and that it catalyzed the synthesis of Le^x in vivo, the glycoproteins detected constituting the endogenous acceptor substrates. Because, at that stage, NT2 cells are in a phase of differentiation where committed precursor cells began to leave the cell cycle and follow a program of neuronal cell differentiation, as monitored by the transcription of *neuroD1* gene (Przyborski *et al.*, 2000), it is conceivable that the expression of FUT9 and Le^x in the same phase would have a correlation with such initial events from neuronal differentiation.

The FUT9 sequence is highly conserved between species (Kaneko *et al.*, 1999b; Baboval *et al.*, 2000), indicating that it has been under strong selective pressure during evolution. Even if the $FUT9^{-/-}$ mouse develops well and is fertile (Kudo *et al.*, 2004), recent evidence has shown the disappearance of Le^x from its brain concomitant to increased anxiety-like behaviors. FUT9 seems to play a role in the functional regulation of interneurons from basolateral amygdala as detected by a decreased number of calbindin-positive neurons in this region of the brain (Kudo *et al.*, 2007).

Regarding cellular localization, we have shown that Le^x was predominantly localized on the PM, and intracellularly, in the TI-VAMP

compartment and in lysosomes, both LAMP-1-containing intracellular compartments (Figures 27 and 28). The TI-VAMP compartment has been proposed to define an exocytic pathway involved in neurite outgrowth, based on the observations that expression of TI-VAMP mutants (Martinez-Arca *et al.*, 2001) and TI-VAMP silencing in neuronal cells (Alberts *et al.*, 2003) impaired neurite outgrowth. The exact nature and molecular composition of this pathway is not yet clarified. In mouse sympathetic neurons it has been shown that it occurs via late endosomes/lysosomes immunoreactive for both TI-VAMP and LAMP-1 (Arantes and Andrews, 2006). We have detected in human NT2N neurons a subset of vesicular structures labeled with TI-VAMP and LAMP-1, that possibly correspond to this pathway. Until now, two proteins are known to be associated with the TI-VAMP pathway in neurons: L1, a cell-cell adhesion molecule involved in axonal growth, whose surface expression and recycling was shown to be TI-VAMP mediated (Alberts *et al.*, 2003); and synaptotagmin VII, a Ca^{2+}-sensing synaptotagmin (Arantes and Andrews, 2006). A possible candidate of another cargo molecule for this pathway could be the high molecular mass Le^x- and HNK-1-carrier glycoprotein that we have identified (Figures 25 and 26), which was distinct from L1 because it was not detected by Western blot with the monoclonal antibody L1-11A (results not shown), that recognizes the membrane bound form of L1 with 220 kDa (Stoeck *et al.*, 2006), and also distinct from synaptotagmin VII, which has a molecular mass of 45.6 kDa. The Le^x-carrier may correspond to a neuronal proteoglycan, other than a chondroitin sulfate, as it was not sensitive to ChABC (Figure 26). One possibility is a heparan sulfate, a class of proteoglycans found at cell surfaces and extracellular matrixes and known to be involved in neuronal connectivity (reviewed by Bishop *et al.*, 2007; Van Vactor *et al.*, 2006). We cannot, however, exclude the possibility that by immunofluorescence microscopy, the L5 antibody detected molecules distinct from the Le^x-carrier glycoprotein, such as glycolipids.

With respect to the possible biological role of Le^x, we have found that the anti-Le^x L5 antibody decreased the adhesion of neurons and neurites already

formed to the surface (Figure 30A), and also caused a decrease in the initiation of outgrowing neurites (Figure 30B) in human NT2N neurons. It did not, however, inhibit neurite elongation of outgrowth contrary to that reported by others for explant *Xenopus* brain cultures (Yoshida-Noro *et al.*, 1999). It is possible that incubation with the anti-Le^x antibody would block interactions between the neurons and matrix components essential for adhesion and neurite outgrowth. Alternatively, it could be internalized (Figure 29) via the TI-VAMP pathway, negatively affecting the intracellular interactions that regulate neurite outgrowth. Others also observed that anti-Le^x antibody L5 inhibited process formation of astrocytes and granule cell migration in mouse cerebellar explant cultures (Streit *et al.*, 1993). Further studies are required to clarify the function at the molecular level of Le^x in human NT2N neurons.

In summary, we found that the adhesion carbohydrate Le^x determinant was upregulated during differentiation from human $NT2^-$ cells to NT2N neurons, where it was synthesized by FUT9. Le^x was localized on the PM and in the exocytic TI-VAMP compartment and it played an important role in neuronal cell adhesion and neurite initiation of outgrowth.

4.6 Acknowledgments

We gratefully acknowledge: C. Escrevente, who designed the RT-PCR primers; Dr. C. Reis who performed the mucin extraction; Prof. A. Streit and Prof. T. Feizi for the generous gift of L5 antibody and for useful comments; Dr. T. Galli for the anti-TI-VAMP antibody and the suggestions; Prof. S. Hakomori for SH1 antibody; Prof. A. Helenius for the anti-calnexin antibody; C. Page for transmitting her expertise on NT2 cells; Dr. H. Conradt for critical reading of the manuscript.

The MC-480 antibody, developed by Dr. D. Solter and Dr. B.B. Knowles, was obtained from the Developmental Studies Hybridoma Bank developed under

the auspices of the NICHD and maintained by the University of Iowa, Department of Biological Sciences.

Chapter 5

Levels of Lewis^x during differentiation of rat primary hippocampal cultures

5. *Levels of Lewis^x during differentiation of rat primary hippocampal cultures*

5.1. Summary

The Lewis^x (Le^x) epitope has been associated with central nervous system development of diverse species including human and rodents.

In this work, we observed that Le^x expression was regulated during development of rat hippocampus neurons in culture. We found increased levels of Le^x in a subset of neurons, which were identified as GABAergic interneurons. Le^x from the cell bodies and neuritic processes was localized in the cell periphery and also intracellularly, where it colocalized with the v-SNARE tetanus neurotoxin insensitive vesicle-associated membrane protein (TI-VAMP) that defines the TI-VAMP exocytic compartment, involved in neurite outgrowth. These results were in good agreement to our previous observations of Le^x localized at the plasma membrane and in the TI-VAMP compartment of human NT2N neurons.

In conclusion, we showed that rat hippocampal neuronal cultures, which have the advantage of presenting optimized experimental tools, are a valid model to study the cross talk between Le^x-carriers and the TI-VAMP compartment.

5.2. Introduction

The Lewis^x (Le^x) determinant is temporally and spatially regulated in the developing central nervous system (CNS) of diverse species, including human, rat, mouse, chicken, and *Xenopus* (Dasgupta *et al.*, 1996; Gotz *et al.*, 1996; Mai *et al.*, 1999; Yoshida-Noro *et al.*, 1999).

As described in Chapter 4, we observed that Le^x expression was induced during human neuronal differentiation, being detected in NT2N neurons but not in undifferentiated NT2 cells (Brito *et al.*, 2007). In NT2N neurons Le^x was restricted to the membrane-trafficking pathway mediated by the v-SNARE TI-VAMP/VAMP7 (Brito *et al.*, 2007). In neurons, this exocytic pathway via late endosomes / lysosomes has been implicated in neurite outgrowth (reviewed by Proux-Gillardeaux *et al.*, 2005) and, until now, only two proteins are known to be associated with it. L1, a cell-cell adhesion molecule involved in axonal growth, whose surface expression and recycling was shown to be TI-VAMP mediated (Alberts *et al.*, 2003), and synaptotagmin VII (SYT7), a Ca^{2+}-sensing SYT (Arantes and Andrews, 2006). Another possible cargo molecule for the TI-VAMP pathway is the high molecular mass glycoprotein identified by us in human NT2N neurons which was a carrier of the Le^x and HNK-1 (human natural killer-1) epitopes (Chapter 4).

The overlapping localization of Le^x and TI-VAMP in NT2N neurons, together with the evidence suggesting the involvement of Le^x in neuronal development (Gotz *et al.*, 1996; Yoshida-Noro *et al.*, 1999; Brito *et al.*, 2007), unraveled the possibility that the Le^x-carriers may be cargo of the TI-VAMP compartment and play a role in the cell-cell or cell-matrix interactions responsible for neurite outgrowth.

The descriptions of Le^x expression in rat brain during development and in adult are numerous (reviewed by Gocht *et al.*, 1996). Le^x-carrier glycoproteins and glycolipids developmentally regulated were identified in rat embryonic, postnatal and adult brain (Chou *et al.*, 1996; Allendoerfer *et al.*, 1999). Aiming to

develop an experimental system that would allow us to study the correlation between neuronal Le^x-carriers and the membrane-trafficking pathway mediated by TI-VAMP, in the present work, we characterized Le^x expression during development of neurons from rat hippocampal cultures.

We showed that Le^x expression was regulated during development of rat hippocampal cultures. A subset of GABAergic interneurons was found to express Le^x-carriers, localized in the cell bodies and neuritic processes. The Le^x epitope was detected in lysosomal associated membrane protein-1 (LAMP-1)-positive lysosomes and found to colocalize with the exocytic TI-VAMP compartment that is associated with neurite outgrowth.

5.3. Materials and methods

5.3.1. Neuronal culture

Hippocampal cultures were prepared as described previously (Danglot *et al.*, 2003). Briefly, hippocampi were dissected from embryonic E18 Sprague–Dawley rats in Hank's balanced salt solution (HBSS) (Sigma) 1-fold concentrated and 20 mM HEPES (Gibco) (HBSS-HEPES). Cells were dissociated by treatment with 0.25% trypsin (Gibco) for 15 min at 37°C, and triturated through a fire-constricted Pasteur pipette in HBSS-HEPES with 0.1 mg/ml DNase (Sigma), at 37°C. Cells were plated at $1.65x10^4$ or $3.3x10^4$ cells/cm^2, onto 40 μg/ml poly-DL-ornithine (PO) (Sigma)-coated glass coverslips, and at $2.1x10^4$ cells/cm^2, onto 35-mm dishes. Plating was done in minimum essential medium (MEM) (Gibco) supplemented with 10% horse serum, 0.6% glucose (Sigma), 0.2% $NaHCO_3$ (Gibco), 2 mM glutamine (Gibco), and 10 U/ml penicillin–streptomycin (P/S) (Gibco) (complete MEM). After attachment of cells, neurons were maintained in NB-B27 conditioned media (see below), up to 4 weeks with replacement of 1/3 of the media weekly.

Glial cultures were also prepared from hippocampi dissected by the same procedure. Cells were plated in T75 culture flasks, at a density of $1x10^5$ cells/cm^2 in complete MEM. Medium was changed every 3 days until confluency. NB-B27 conditioned medium was prepared by incubating serum-free neurobasal medium (Gibco) supplemented with B27 (Gibco), 2 mM glutamine (Gibco) and 5 U/ml P/S (Gibco) with the glial monolayers for one week.

All cultures were maintained at 37°C in a 5% CO_2 humidified incubator.

5.3.2. Immunofluorescence microscopy

Hippocampal neurons cultured on PO-coated glass coverslips were analyzed after 4 and 18 hours; 1, 2, 3, 7 and 14 days *in vitro* (DIV). Neurons were washed with phosphate buffer saline (PBS), fixed with 4% (w/v) paraformaldehyde (PF) and 4% sucrose (suc) in PBS for 20 minutes, quenched with 50 mM NH_4Cl in PBS for 20 minutes, permeabilized with 0.1% (w/v) Triton X-100 (TX-100) for 4 minutes and then blocked in 0.25% (w/v) cold water fish gelatin in PBS for 30 minutes. Primary and secondary antibodies were incubated at room temperature for 1 hour and 45 minutes, respectively. Antibody solutions were prepared in 0.1% (w/v) gelatin in PBS and washes were carried out with PBS. Coverslips were mounted in Mowiol (Calbiochem).

Primary antibodies were: rat IgM anti-Le^x L5 (1:200) (Streit *et al.*, 1990; Streit *et al.*, 1996); rabbit IgG anti-microtubule-associated proteins (MAPs) (1:200) (Sigma); mouse IgG anti-TI-VAMP clone 158.2 (1:200) (Muzerelle *et al.*, 2003); mouse IgG anti-rat LAMP-1 LYC6 (1:5) (DSHB); rabbit IgG anti-synaptophysin MC1 (1:1000) (Chilcote *et al.*, 1995); rabbit IgG anti-glutamate decarboxylase (GAD) 65/67 (1:500) (Chemicon). Secondary antibodies were: goat anti-rat IgM AlexaFluor594 (1:400) (Molecular Probes); cross adsorbed goat anti-mouse IgG AlexaFluor488 (1:400) (Molecular Probes);

cross adsorbed goat anti-rabbit IgG AlexaFluor488 (1:400) (Molecular Probes); cross adsorbed goat anti-rabbit IgG Cy5 (1:200) (Jackson ImmunoResearch).

Fluorescence images were acquired on a Leica DMRD microscope using FITC, Cy3, Cy5 and DAPI-specific sets of filters and a high-resolution camera driven by the Metamorph Image Analysis System. Confocal images were acquired in a confocal microscope SP2+AOBS (Leica) equipped with a 63× objective. Each fluorophore used was excited and detected separately to avoid channel bleed-through. For each channel, photomultiplier gains and offsets were adjusted to use full image dynamic range. Typically, stacks of 10 to 15 sections of 1024 × 1024 pixel resolution, with a pinhole of 1.0 Airy unit and a 0.5 µm focus interval, were scanned 4 times, to optimize the signal/noise ratio.

Merge between channels and maximum *z*-projections were created using the open source ImageJ software version 1.35 (http://www.rsb.info.nih. gov/ij/). The only modifications made during image editing were linear brightness and contrast adjustments, using the Adobe Photoshop software (Adobe Systems).

5.3.3. SDS-PAGE and Western blot analysis

Hippocampal neurons cultured on PO-coated 35-mm dishes, in the presence of 1 µM of the mitosis inhibitor cytosine arabinoside (ara-C) (Sigma) when stated, were analyzed after 8 hours *in vitro*, 1, 2, 3, 7, 14 and 21 DIV.

Total protein was solubilized with 50 mM Tris-HCl buffer pH 8, containing 150 mM NaCl, 1 mM EDTA, 1% TX-100, and protease inhibitors (Complete Cocktail; Roche), at 4ºC for 30 minutes. After 20 minutes centrifugation at 16,000× *g*, at 4ºC, the protein was precipitated in 80% ethanol, at –20ºC, for 3 hours and then solubilized in sample buffer provided by the SDS-PAGE gel supplier (Invitrogen).

Proteins were separated by SDS-PAGE in precasted NuPAGE Novex Tris-Acetate gels 3-8% (Invitrogen) and transferred to polyvinylidene difluoride membranes. Blocking was with 5% non-fat dry milk (Nestle) and 0.1% Tween-20 in PBS. Primary antibodies were: L5 anti-Le^x monoclonal antibody 1:500, anti-L1 polyclonal antibody 1:2000 and anti-β-tubulin monoclonal antibody 1:50000 (DSHB). HRP-labeled polyclonal secondary antibodies anti-mouse IgM, (Sigma), anti-rabbit IgG (Jackson ImmunoResearch) and anti-mouse IgG (Jackson ImmunoResearch) were used. All dilutions were in blocking solution. Chemiluminescent detection was by the ECL system (GE Healthcare).

5.4. Results

5.4.1. Le^x expression is induced during development of rat hippocampal cultures

In order to characterize Le^x expression during development of rat hippocampus neurons at a cellular level, we monitored Le^x by immunofluorescence microscopy during rat hippocampal cultures. We used the L5 monoclonal antibody, specific for the Le^x epitope, and a polyclonal antibody anti-microtubule-associated proteins (MAPs), to distinguish neurons from glia cells, also present in the hippocampal cultures. To screen the cultures after 4 and 18 hours *in vitro*, 1, 2, 3, 7, and 14 DIV.

In the first hours after plating many of the adherent cells, neurons and glia, were labeled with L5 at the surface (Figure 31a). As differentiation proceeded, from 18 hours *in vitro* to 3 DIV, the Le^x staining was restricted to cells that were not labeled by anti- MAPs, used as a neuronal marker (Figure 31b). At 7 DIV, Le^x was detected in a minoritary population of neurons that presented highly branched neurites as common feature. The immunoreactivity was observed on neuronal cell bodies and neurites in discrete puncta (Figure 31c). From 7 to 14 DIV cultures Le^x staining remained confined to a neuronal

subpopulation, generally with high degree of neuritic arborisation (Figure 31d). Moreover, many of the cells labeled with L5 were MAP-negative (Figure 31d).

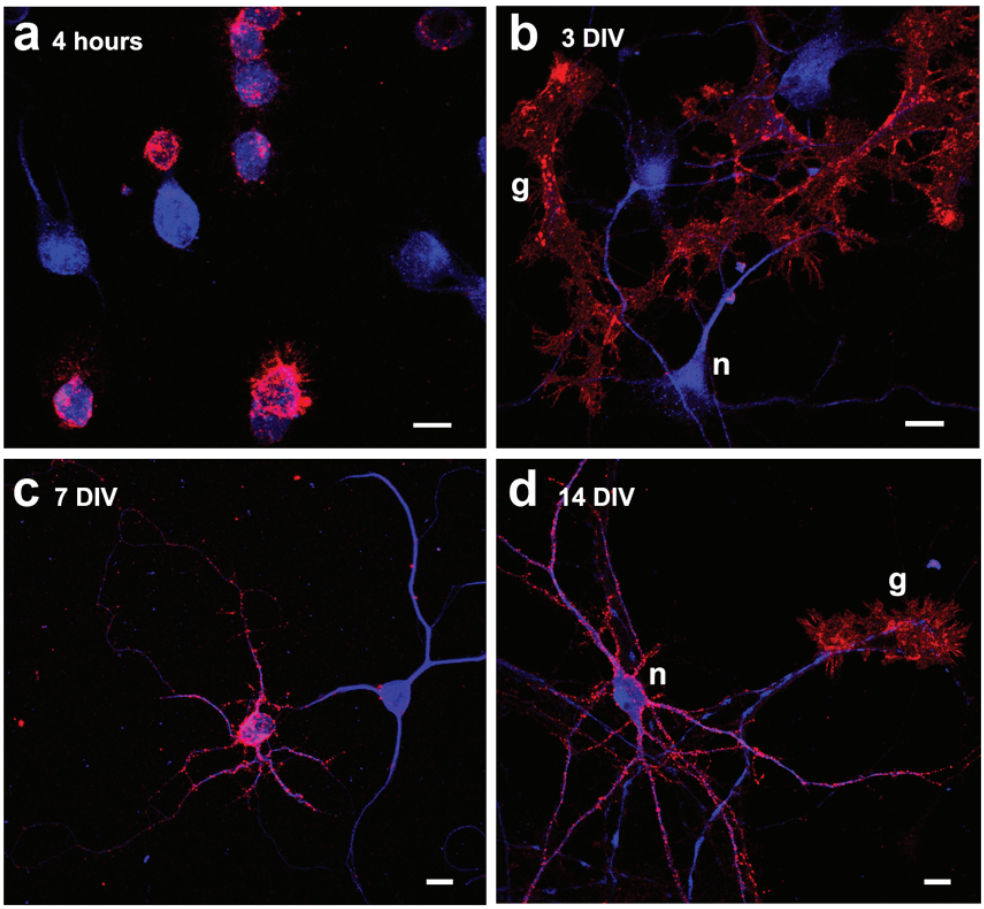

Figure 31: Detection of the Le^x determinant along rat hippocampal cultures development by immunofluorescence confocal microscopy. Primary cultures from rat hippocampus plated on poly-DL-ornithine coated coverslips were fixed at different times: 4 hours **(a)**; 3 DIV **(b)**; 7 DIV **(c)**; 14 DIV. Permeabilized cells were probed with the anti-Le^x L5 antibody (shown in red) and an anti-MAPs antibody (shown in blue) to distinguish neurons (n) from glia cells (g). Secondary antibodies were: goat anti-rat IgM-AlexaFluor594 and goat anti-rabbit IgG-Cy5. Maximum intensity *z*-projections of 10 to 15 optical sections of 0.5 μm are shown. Scale bars = 10 μm. The experiment was performed with at least two independent cultures. .

5.4.2. GABAergic neurons from rat hippocampus express Le^x-carriers

The observation that only a small population of highly branched hippocampal neurons expressed the Le^x epitope (Figure 31) led us to hypothesize that those could correspond to a subtype of hippocampal interneurons. Interneurons in the CNS are usually inhibitory neurons and γ-aminobutyric acid (GABA) is the principal inhibitory neurotransmitter in the brain (Maccaferri and Lacaille, 2003). Thus, aiming to identify the population of neurons that expressed the Le^x determinant, we probed 14 DIV hippocampal cultures with L5 and an antibody for glutamate decarboxylase (GAD), the enzyme that catalyzes the conversion of L-glutamate to GABA (reviewed by Varju *et al.*, 2001). All neurons positive for GAD detected in the cultures also presented Le^x labeling (Figure 32a, b), indicating that at 14 DIV hippocampal interneurons express Le^x-carriers.

Le^x staining at 14 DIV presented a punctate pattern in the cell bodies and in neuritic processes (Figures 31d and 32). As shown at higher magnification (Figure 32c), the two stainings were interspersed and did not overlap. Le^x puncta accumulated in spine-like protrusions or phillopodia (arrows in Figure 32e and 32f, the higher magnifications insets of 32d). Nevertheless, Le^x-containing glycoconjugates were not exclusive of interneurons as some MAP-positive cells not labeled by GAD also presented Le^x staining (Figure 32a), suggesting that distinct Le^x-carriers may be present in a different subpopulation of neurons, in addition to glial cells (Figure 31).

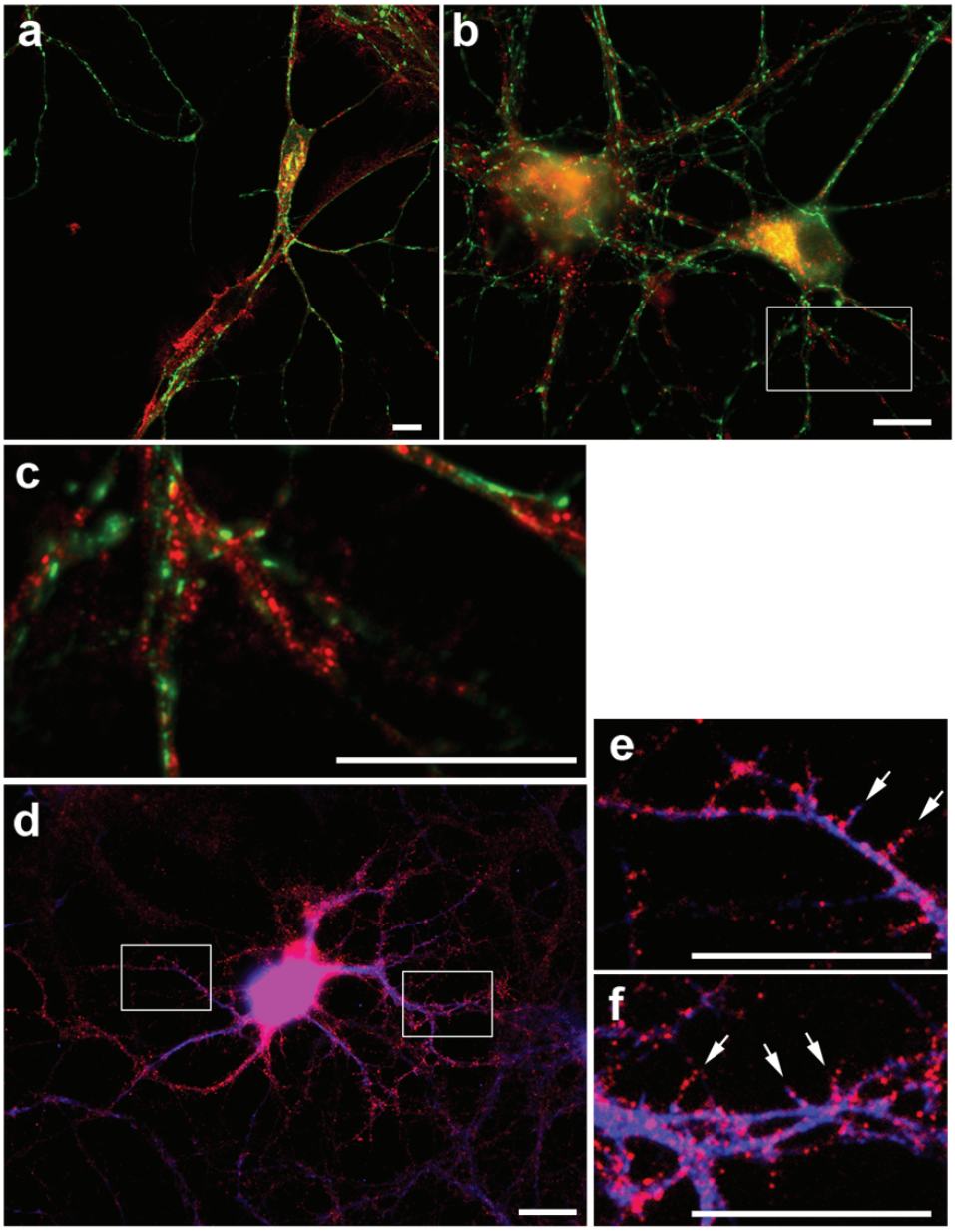

Figure 32: Detection of the Le^x determinant in 14 DIV rat hippocampus neurons by immunofluorescence microscopy. Primary cultures from rat hippocampus plated on poly-DL-ornithine coated coverslips were fixed at 14 DIV. Permeabilized cells were probed with the following antibodies: anti-Le^x L5 (shown in red) and anti-GAD (shown in green) **(a, b, c)** or anti-Le^x L5 (shown in red) and anti-MAPs (shown in blue) **(d, e, f)**.

Secondary antibodies were: goat anti-rat IgM-AlexaFluor594, goat anti-rabbit IgG-A488 and goat anti-rabbit IgG-Cy5. The insets indicated in **(b)** and **(d)** are presented at higher magnification in **(c)**, **(e)** and **(f)**, respectively. Arrows indicate Le^x labeling in spine-like protrusions or phillopodia. Scale bars = 10 μm. The experiment was performed with two independent cultures.

5.4.3. The Le^x determinant is localized at the plasma membrane and in the TI-VAMP compartment of rat hippocampus neurons

To check if the Le^x-carriers detected by the L5 antibody in rat hippocampal neurons were contained in the TI-VAMP compartment, as in human NT2N neurons (Chapter 4), we performed colocalization analysis with TI-VAMP and LAMP-1 by confocal immunofluorescence microscopy in 7 DIV cultures. Neurons were identified by staining with polyclonal anti-MAPs antibody.

In neurons, Le^x colocalized with TI-VAMP in the cell body and most extensively in the puncta stained along the neurites (Figure 33a, inset magnified in 33b). Le^x and TI-VAMP positive puncta were also detected in growth cones, presenting a lower level of colocalization (Figure 33c, inset magnified in 33d). In MAP-negative cells labeled with Le^x there was also TI-VAMP staining, although no colocalization was observed (results not shown). These results indicate that Le^x-carriers may be cargo of the TI-VAMP compartment in GABAergic neurons but not in glia cells.

Le^x and LAMP-1-positive puncta were observed mainly in the cell body, where LAMP-1 labeling was more intense and colocalization was almost total (Figure 33e, inset magnified in 33f). There was also some colocalization in the neuritic processes (Figure 33e, inset magnified in 33f).

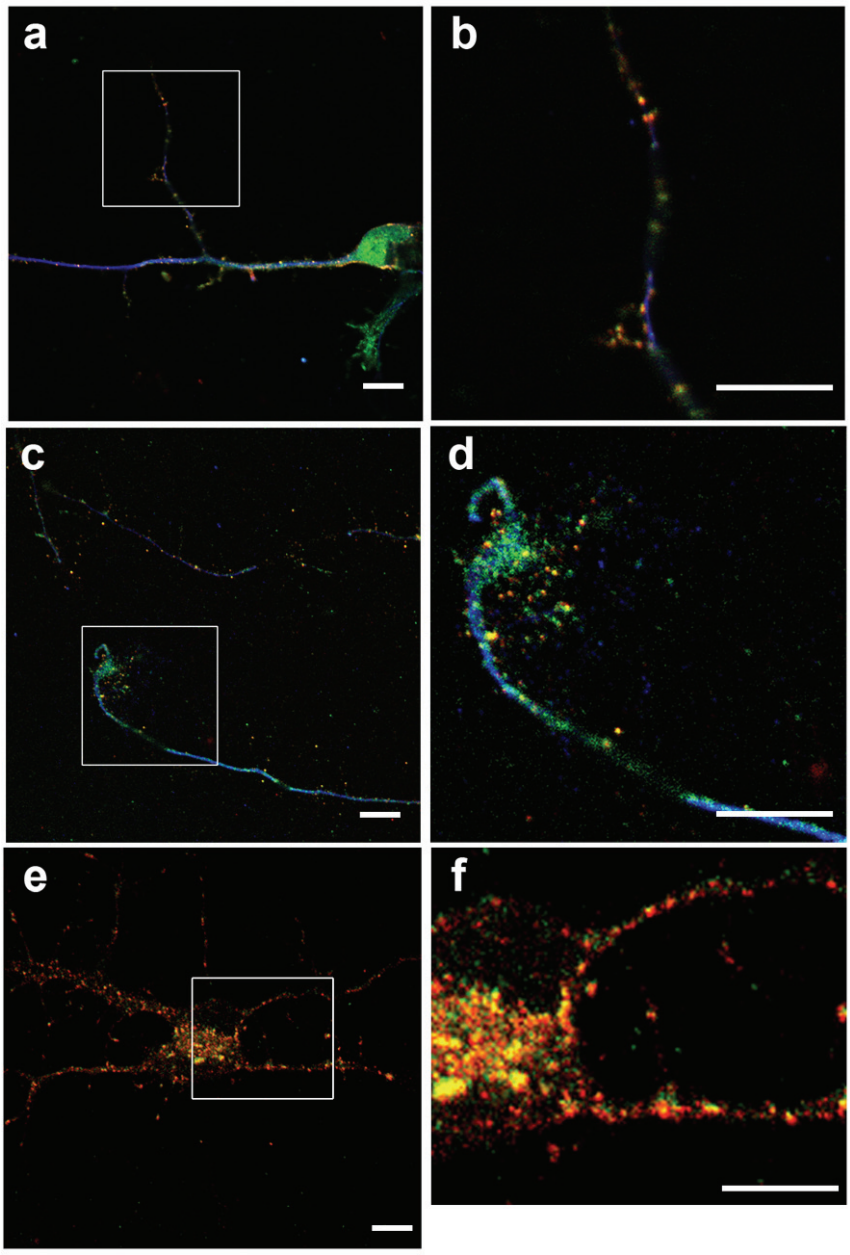

Figure 33: Colocalization analysis of Le^x in hippocampus neurons by immunofluorescence confocal microscopy. Primary cultures from rat hippocampus plated on poly-DL-ornithine coated coverslips were fixed at 7 DIV. Permeabilized cells were probed with the following antibodies: anti-Le^x L5 (shown in red), anti-TI-VAMP (shown in green) and anti-MAPs (shown in blue) **(a, b, c, d)** or anti-Le^x L5 (shown in red)

and anti-LAMP-1 (shown in green) **(e, f)**. Secondary antibodies were: goat anti-rat IgM-AlexaFluor594, goat anti-mouse IgG-AlexaFluor488 and goat anti-rabbit IgG-Cy5. Single optical sections of 500 nm are shown. Scale bars = 10 μm. The insets indicated in **(a)**, **(c)** and **(e)** are presented at higher magnification in **(b)**, **(d)** and **(f)**, respectively. The experiments were carried out with at least two independent cultures and for each condition at least five neurons per marker were analyzed by confocal microscopy.

The possibility of LAMP-1, a lysosomal highly glycosylated protein (Carlsson *et al.*, 1988), being a carrier of the Le^x epitope in rat hippocampal primary cultures, was ruled out by SDS-PAGE and Western Blot analysis (see below, Figure 34). LAMP-1 has an apparent molecular mass of approximately 120 kDa (Carlsson *et al.*, 1988) and no Le^x-reactive bands were detected in hippocampus primary cultures homogenates in that molecular mass range (Figure 34a). Thus, the Le^x-carriers detected in GABAergic neurons are localized in the lysosomal or TI-VAMP compartments, different from LAMP-1, and probably neuron-specific proteins.

5.4.4. Le^x-carrier glycoproteins are expressed by neurons in rat hippocampal cultures

Le^x-carriers have been described in glycoproteins and glycolipids of the developing rat brain (Allendoerfer *et al.*, 1999). Aiming to identify Le^x-carrier glycoproteins from rat hippocampal neurons, cellular extracts from primary cultures were analyzed along differentiation *in vitro*, in the presence of the mitosis inhibitor ara-C in order to obtain a culture enriched in post-mitotic neurons. Extracts from cells for 8 hours *in vitro*; 1, 2, 3, 7, 14 and 21 DIV were screened by Western blot with the monoclonal anti-Le^x antibody L5 (Figure 34).

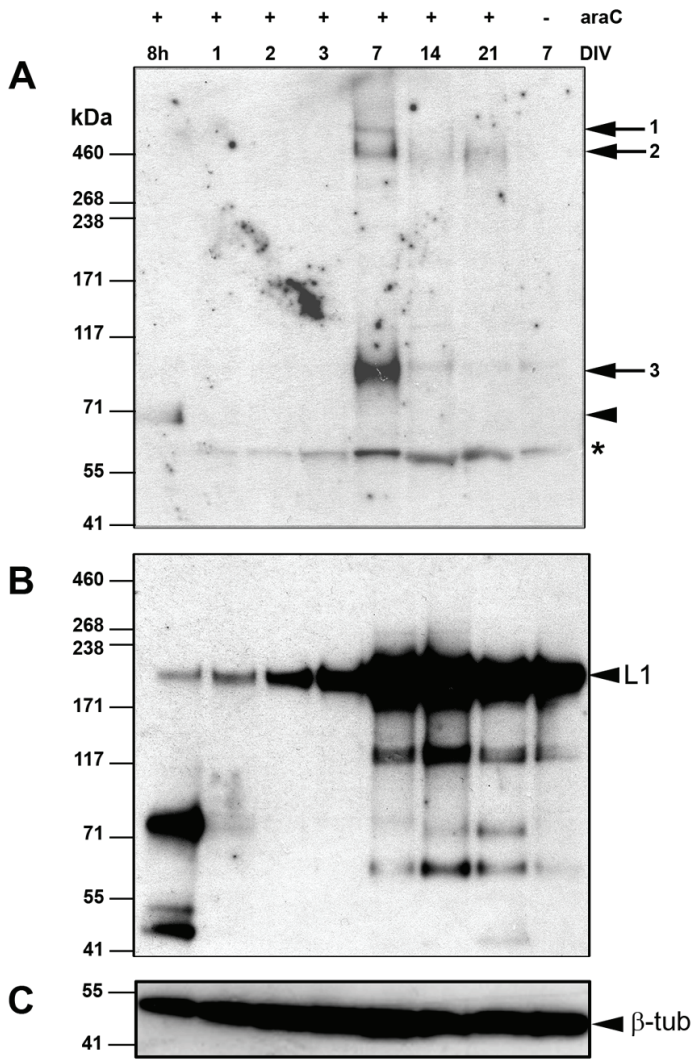

Figure 34: Immunodetection by Western blot of Le^x-carrier proteins from hippocampal cultures. SDS-PAGE and Western Blot analysis of cultures with 8 hours, 1, 2, 3, 7, 14, and 21 days *in vitro* (DIV), in the presence of cytosine arabinoside (ara-C), when stated. Equivalent amounts of protein were applied by lane. **(A)** Anti-Le^x L5 antibody detected a Le^x-carrier at 8 hours of culture (arrowhead) and three Le^x-carriers at 7 DIV (arrows 1, 2 and 3). The heavy chains of rat IgMs present in the cell extracts were detected by the secondary anti-rat IgM antibody (asterisk). **(B)** Reprobe with an anti-L1 antibody detected the full-length form of L1 (arrowhead) and several proteolytic products. **(C)** Reprobe with an anti-β-tubulin (β-tub) antibody was used as a loading control

(arrowhead). Secondary antibodies were HRP-conjugated anti-mouse IgM, anti-rabbit IgG and anti-mouse IgG. Detection was carried out by the ECL method.

Eight hours after plating, a single band was detected that migrated near the 71 kDa marker (Figure 34A, arrowhead). This band did not correspond to a cleaved form of L1, a cargo molecule of the TI-VAMP compartment (Alberts *et al.*, 2003), as confirmed by re-probing of the membrane with an anti-L1 antibody (Figure 34B), nor to LAMP-1 as the latest migrates at approximately 120 kDa (Carlsson *et al.*, 1988). No L5 immunoreactive bands were observed from 1 to 3 DIV (Figure 34a). At 7 DIV three Le^x-carriers were detected: one that migrated above the 460 kDa marker (Figure 34A, arrow 1), a second that co-migrated with the 460 kDa marker (Figure 34A, arrow 2) and a third carrier of lower apparent molecular mass between the 71 and the 117 kDa markers (Figure 34A, arrow 3). In 7 DIV cultures that were not incubated with ara-C, presenting mainly glial cells, the three carriers were not detected (Figure 34A). Thus, the glycoproteins detected with the L5 antibody in rat hippocampal primary cultures were most probably expressed by neurons. The three bands peaked at 7 DIV and from that day on, along the maturation of the culture, the detection levels of the carriers decreased markedly (Figure 34A).

The variations observed during the *in vitro* culture were not due to differences in total protein content, as shown by the detection of equivalent levels of β-tubulin (Figure 34C, arrowhead). From 1 to 21 DIV a band was observed between the 71 and 55 kDa markers (Figure 34A, asterisk), also detected only with secondary anti-rat IgM antibody (results not shown), that most probably corresponded to the heavy chain of rat IgM.

5.5. Discussion

In this study, we detected the cell adhesion carbohydrate Le^x determinant in different phases of differentiation of rat hippocampal primary cultures and in distinct cell types (Figure 31). Our results suggested that during the culture time the Le^x epitope was present in different carriers, expressed by distinct cell types, in a developmentally regulated manner. In agreement, data obtained from immunolabeling experiments in rat brain indicated that the Le^x epitope was carried by distinct glycoproteins and glycolipids during embryonic and post-natal development (Allendoerfer *et al.*, 1999). Furthermore, Le^x was also detected in rat telencephalic regions during development, presenting a correlation with selective adhesion of cell subpopulations (Gotz *et al.*, 1996).

We detected Le^x soon after plating (Figure 31a), consistent with the presence of Le^x in rat neural stem cells (Ko *et al.*, 2005). Furthermore, Le^x has also been described as a marker of murine neuronal progenitor cells, particularly strong in regions with prolonged neurogenesis, such as the hippocampus (Capela and Temple, 2006).

During the first days of differentiation of the *in vitro* culture (18 hours to 3 DIV), the Le^x-positive cells detected were essentially MAP-negative non-neuronal cells (Figure 31b). Although we did not investigate further the lineage of MAP-negative cells, morphologically they resembled the GFAP and vimentin-positive population of immature astrocytes, also labeled by anti-Le^x in primary cultures of brain from mouse (Streit *et al.*, 1990) and rat embryos (Sajdel-Sulkowska, 1998).

At 7 DIV there was the increase in the detection of Le^x in a subset of neurons (Figure 31c). The Le^x-positive neurons were mostly highly branched GABAergic interneurons, as shown by labeling with both L5 and an anti-GAD antibody in 14 DIV hippocampal cultures (Figure 32).

The Le^x epitope was detected in the hippocampal neurons in punctate structures localized in the cell bodies and in the neuritic processes (Figure 31, 32 and 33). These puncta did not colocalize with GAD, that labels inhibitory synaptic

regions (Figure 32c). In the neurites, Le^x-positive structures were detected in spine-like protrusions or phillopodia (arrows in figure 32e and 32f, the higher magnifications insets of 32d). These are highly dynamic post-synaptic structures characteristic of sites of excitatory synaptic contact on dendrites (Dailey and Smith, 1996). Furthermore, preliminary results indicated that Le^x-labeling was in apposition with structures labeled with an anti-synaptophysin antibody (results not shown), a presynaptic protein that, as synaptogenesis occurs, forms high density of puncta in the cell bodies and in the neurites (de Lima *et al.*, 1997). Moreover, Le^x staining was often peripherally localized or even detected in extracellular locations, adjacent to MAP labeling. These results suggested that the Le^x-carriers of GABAergic interneurons were probably on the plasma membrane and on the extracellular matrix, in post-synaptic domains closely related to the sites of establishment of synapses.

Also regarding cellular localization, we showed that intracellularly Le^x was localized in the TI-VAMP compartment and in LAMP-1-containing endosomal compartments (Figure 33). Previously, we have shown that the Le^x epitope was present on the plasma membrane and in the TI-VAMP compartment of human NT2N neurons, playing a role in neuronal adhesion and neurite regeneration (Chapter 4). Furthermore, many of the TI-VAMP-labeled vesicles detected in the cell bodies and neurites of NT2N neurons were LAMP-1-positive late endosomes/lysosomes (Brito *et al.*, 2007). Moreover, in developing primary mouse sympathetic neurons, the TI-VAMP exocytic pathway has been shown to occur via late endosomes/lysosomes immunoreactive for both TI-VAMP and LAMP-1 (Arantes and Andrews, 2006). Although there was some discrepancy in the degree of overlapping between TI-VAMP and LAMP-1, which may reflect differences in the types of neurons or in the development stage analyzed, our results strengthened the hypothesis that the neuronal TI-VAMP exocytic pathway share common cross-species features.

Concerning the identification of Le^x-carriers, we have detected three proteins by Western Blot at 7 DIV (Figure 34A), a stage coincident with the

detection of Le^x-carriers in the TI-VAMP compartment (Figure 33). One of the detected high molecular mass carriers observed (Figure 34A) may correspond to a form of phosphocan. This high molecular mass chondroitin sulfate proteoglycan (CSPG) contains Le^x in mannose-linked *O*-oligosaccharides when expressed in the early postnatal rat brain (Krusius *et al.*, 1986; Allendoerfer *et al.*, 1995). Furthermore, phosphocan is a soluble alternative splicing product of a transmembrane receptor-type protein-tyrosine phosphatase (RPTPβ) which binds neural cell adhesion molecules (Maurel *et al.*, 1994). Mannose-linked *O*-oligosaccharides have been described in rat brain proteoglycans that carry Le^x and HNK-1 epitopes (Krusius *et al.*, 1987; Yuen *et al.*, 1997; Kogelberg *et al.*, 2001). In addition, in human NT2N neurons we also detected a Le^x and HNK-1-carrier of 460 kDa that, although not being a CSPG, presented Le^x labeling insensitive to PNGaseF digestion (Chapter 4), suggesting that it could be attached to mannose-linked *O*-oligosaccharides. Recently, Cat-315, an *O*-mannose linked epitope of the HNK-1 family was also found in proteoglycans related to neuritogenesis and synaptogenesis (Dino *et al.*, 2006).

Astrochondrin is another Le^x-bearing CSPG identified in rodent brain, with a molecular mass of 500 kDa, proposed to be involved in the outgrowth of astrocytes processes on the extracellular matrix (Streit *et al.*, 1990; Streit *et al.*, 1993). Despite the similar apparent molecular masses of the carriers 1 and 2 identified by us (Figure 34A), these could not correspond to astrochondrin as this proteoglycan is produced by astrocytes (Streit *et al.*, 1990; Streit *et al.*, 1993) and not by neurons. Le^x has also been described on mouse neural cell adhesion molecule L1 (Streit *et al.*, 1990), a known cargo molecule of the TI-VAMP pathway (Alberts *et al.*, 2003), nevertheless in rat hippocampal neurons we did not detect the epitope on this protein (Figure 34).

In summary, we found that the adhesion carbohydrate Le^x determinant was upregulated in a subset of GABAergic neurons during differentiation of rat hippocampal neurons. Le^x was localized in extra-synaptic sites and in the exocytic TI-VAMP compartment. The characterization performed in this work

opens the door for further studies to better understand connections between neuronal Le^x-carriers, the TI-VAMP exocytic mediated pathway and neurite outgrowth. This includes, for example, the evaluation of the effect of impaired TI-VAMP-mediated membrane trafficking, and consequent inhibition of neurite outgrowth, on Le^x distribution, using the siRNA methodology that was optimized for rat hippocampus primary cultures (Alberts *et al.*, 2003).

5.6 Acknowledgments

We gratefully acknowledge: Dr. Lydia Danglot for performing and transmitting her technical expertise on primary cultures and specially for sharing her knowledge of central nervous system development and membrane trafficking and for the challenging discussion; Dr Thierry Galli for the useful suggestions and comments; Prof. A. Streit and Prof. T. Feizi for the generous gift of the L5 antibody.

The anti-β-tubulin antibody was obtained from the Developmental Studies Hybridoma Bank developed under the auspices of the NICHD and maintained by the University of Iowa, Department of Biological Sciences.

Chapter 6

General discussion and conclusions

6. *General discussion and conclusions*

6.1. General discussion and perspectives

The Le^x determinant is expressed in glycolipids and glycoproteins of the brain of several species (Roberts *et al.*, 1991; Dasgupta *et al.*, 1996; Allendoerfer *et al.*, 1999; Mai *et al.*, 1999; Shimoda *et al.*, 2002), being one of the most abundant carbohydrate structures detected in neutral complex-type *N*-glycans in the human brain (Albach *et al.*, 2001). Furthermore, Le^x has been implicated in cell-cell recognition, neurite outgrowth and neuronal migration in the CNS of *Xenopus* (Yoshida-Noro *et al.*, 1999), rodents and chicken (Streit *et al.*, 1993; Gotz *et al.*, 1996) and loss of Le^x expression in the murine CNS led to anxiety-like behaviors (Kudo *et al.*, 2007) .

Specificity studies of FUT activity from human brain homogenates (Mollicone *et al.*, 1990; Mollicone *et al.*, 1992) and human neuroblastoma cells (Foster *et al.*, 1991) showed the synthesis of Le^x and Le^y but not of sLe^x or Le^a. These characteristics corresponded to the FUT9 and FUT4 profiles but not to the ones of any other member of the family (reviewed by Becker and Lowe, 2003). Moreover, FUT4 and FUT9 were found to be significantly expressed in the human embryonic brain (Cailleau-Thomas *et al.*, 2000) and in rodent embryonic and adult brain (Kaneko *et al.*, 1999b; Baboval *et al.*, 2000). Further evidence suggested that FUT9 catalyzed Le^x synthesis in the mouse brain (Shimoda *et al.*, 2002; Nishihara *et al.*, 2003). Demonstration by cDNA macroarray of a developmentally regulated expression pattern of FUT9 in embryonic and adult mouse cerebral cortex, correlating with Le^x detection on complex *N*-glycans (Ishii *et al.*, 2007), and observation of disappearance of the Le^x epitope from the $FUT9^{-/-}$ mouse brain (Kudo *et al.*, 2007), confirmed that FUT9 is the enzyme that synthesizes Le^x in the brain. Despite the evidence accumulated until present

supporting the importance of FUT9 and its biosynthetic product Le^x in the CNS, several issues were poorly addressed or remain to be elucidated.

The glycosylation profile of a newly synthesized glycoconjugate depends on several factors (reviewed by Czlapinski and Bertozzi, 2006). These include the levels of expression and the specificity of glycan modifying enzymes, the availability of donor substrates for GTs and the sequential action of glycosidases and GTs, organized throughout the Golgi in an ordered, although overlapping, way. As FUT9 is the last GT involved in the biosynthesis of the Le^x epitope, it plays a key role in the regulation of Le^x expression. In this context, we studied human FUT9 specificity towards biologically relevant acceptors, such as GP, and the localization of the enzyme in the secretory pathway. Concerning Le^x function, we focused on its *in vivo* expression in the CNS and on the assignment of the Le^x-carriers and their biological role during neuronal differentiation.

6.1.1. Characterization of recombinant full-length and soluble forms of human FUT9

The role of human FUT9 in the CNS was not known at the beginning of this thesis work. A detailed characterization of FUT9 catalytic properties has been performed, in particular its specificity towards acceptor substrates of biological relevance, in order to assess the enzyme function *in vivo*.

As endogenous FUT9 from neuronal sources is expressed in low levels, it was necessary to use heterologous systems in order to obtain higher amounts of the enzyme. The FUT9 sequence was cloned from human NT2N neurons and transiently transfected into the HeLa human cell line (Chapter 2). *In vitro* specificity studies, using a panel of small oligosaccharides coupled to a hydrophobic moiety as acceptor substrates, confirmed that the recombinant full-length FUT9 (FUT9wt) expressed in HeLa cells was essentially an α3-FUT, as it showed a clear preference for type II acceptor structures (Chapter 2).

Substitution of the hydroxyl group at the C-2 of Gal from LacNAc with Fuc resulted in enhanced transfer rates, whereas substitution at C-3 with NeuAc reduced the transfer to undetectable levels, in agreement with the specificity described for human FUT9 (Cailleau-Thomas *et al.*, 2000; Toivonen *et al.*, 2002).

Most interestingly, we showed that human FUT9 presented activity towards GP acceptor substrates with high specificity for the synthesis of the Le^x determinant in *N*-linked glycans. The detailed analysis of the resulting *N*-linked oligosaccharide chains revealed that human FUT9 was an *N*-glycan fucosylating enzyme with the ability of transferring Fuc residues to asialo *N*-glycans, irrespective of the number of branches or of LacNAc repeats in each branch. The results suggested that FUT9 could fucosylate GPs with the synthesis of the cell adhesion Le^x determinant *in vivo*, including in human neurons. This was the first study of FUT9 activity towards GPs *in vitro*. *In vivo*, several studies have indicated that FUT9 would use *N*-glycans on GPs as acceptor substrates. Examples include: the adhesion molecule CEACAM-1, co-expressed with human FUT9 in HEK cells (Bogoevska *et al.*, 2006); GPs from CHO Lec8 cells co-transfected with human FUT9 and β4-GalNAcT (Kawar *et al.*, 2005); a CSPG from rat embryonic brain (Shimoda *et al.*, 2002); GPs from mouse brain (Ishii *et al.*, 2007; Kudo *et al.*, 2007). On the other hand, FUT9 has also been shown to fucosylate synthetic analogues *of N*- and *O*-glycans *in vitro* (Toivonen *et al.*, 2002).

Stable transfection of FUT9 was achieved using the Sf9 insect cell line (Chapter 3), characterized by high producing levels of recombinant proteins that acquire post-translational modifications required for correct folding (reviewed by Altmann *et al.*, 1999). Two cell lines were constructed expressing the membrane-bound form, FUT9wt, and a soluble form, sFUT9, of the enzyme. FUT9wt produced in Sf9 insect cell line maintained the *in vitro* specificity profile towards small oligosaccharide acceptors already observed (Chapter 2). Most striking, the enzyme was able to catalyze the transfer of Fuc to the native sialylated form of EPO, although less efficiently than to the asialo form of the GP.

This result differed from the one obtained for FUT9wt expressed in HeLa cells but correlated with the specificity profile of human FUT9 detected by other authors towards polylactosamine chains. It has been reported that the transfer of Fuc was shifted to the internal LacNAc units when terminal Gal was substituted with neuraminic acid, in levels lower than the observed for terminal LacNAc units of asialo polylactosamine chains (Nakayama *et al.*, 2001; Toivonen *et al.*, 2002). Thus, FUT9wt expressed in Sf9 cells most probably transferred Fuc to the inner LacNAc units of the terminally sialylated, triantennary and tetrantennary structures with LacNAc repeats present on native EPO.

Analysis of the specificity of the efficiently secreted sFUT9 form revealed that removal of the cytoplasmic tail, transmembrane domain and stem region of the enzyme did not alter the *in vitro* specificity profile towards small oligosaccharide acceptors (Chapter 3). However, when activity towards GPs was assayed, differences were observed when compared to FUT9wt: 1) sFUT9 transferred Fuc to LacNAc units from GP with higher efficiency than from oligosaccharide acceptors; 2) sFUT9 did not distinguish between sialylated and asialo *N*-glycans of EPO, being able to fucosylate both types of structures with equivalent efficiency. Those data suggested that, although the *N*-terminal regions of FUT9 were not essential for enzyme activity, they might play an important role in enzyme specificity, in particular in the recognition of the protein environment of the acceptor substrate. Previous results obtained by us for human FUT3 also support this hypothesis - we have shown that truncation of the *N*-terminal region of FUT3 produced a soluble form of the enzyme, which presented activity towards GP, contrary to the full-length enzyme (Sousa *et al.*, 2001).

During the optimization of the FUT9 activity assay, we found an approximately 2-fold activating effect of Mn^{2+}, in the 2.5-10 mM concentration range, despite not being essential for the α3-activity (Chapter 2). The dependence of divalent cations by GTs has been associated with the motif Asp-X-Asp (DxD), Glu-X-Asp (ExD), or equivalent, known to be involved in the co-ordination of the nucleotide sugar donor. The DxD/ExD motif is present in the

catalytic domain of enzymes of the GT-A structural superfamily that require a divalent cation as cofactor, but typically absent from members of the GT-B that may be activated by divalent cations although not strictly needing them for activity (reviewed by Qasba *et al.*, 2005). Human α3-FUTs have been proposed to belong to the GT-B superfamily of GTs (Breton *et al.*, 1996; Breton *et al.*, 2006), however, they have the DxD motif (Breton *et al.*, 1998; Palma *et al.*, 2004). In these enzymes Mn^{2+} acts as an activator, probably through the coordination of the phosphate groups of GDP-Fuc (Palma *et al.*, 2004) and binding to the DxD motif ($D^{161}SD$ for FUT9). In the absence of Mn^{2+} they are active, possibly due to the interaction of conserved amino acid residues with the donor substrate, via hydrogen bounds, similarly to that found from the X-ray structure of an *H. Pylori* α3-FUT (Sun *et al.*, 2007a) that possesses the DxE motif (Ma *et al.*, 2003).

The presence of Mn^{2+} allowed the detection of low levels of α4-FUT activity towards the Galβ4GlcNAc-R acceptor (where R = O-$(CH_2)_3$NHCO$(CH_2)_5$NH-biotin) for both FUT9wt and sFUT9 (Chapters 2 and 3). The absence in the FUT9 sequence of the Trp residue of the acceptor binding motif, shown to be responsible for the recognition of type I acceptors in human FUT3 and FUT5 (Dupuy *et al.*, 1999; Sherwood *et al.*, 2002; Dupuy *et al.*, 2004) and *H. Pylori* α3/4-FUT (Ma *et al.*, 2005), could justify the low α4-activity of FUT9.

The full understanding of the catalytic properties and mechanism of FUT9 will necessarily require the determination of the three-dimensional structure of the protein. Additionally, co-crystallization with Mn^{2+} and GDP-Fuc will allow the clear assignment of the role of the divalent cation in the catalytic activity of the enzyme. The sFUT9 form produced by us in the Sf9 insect cell line may be utilized as a source of enzyme for this purpose.

In summary, we found that FUT9 presented high α3-activity towards asialoGPs, irrespective of the degree of branching or LacNAc repeats of the *N*-glycans, synthesizing the Le^x epitope with great specificity. Moreover, we were

able to produce a secreted recombinant form of FUT9 in Sf9 insect cells (sFUT9) with enhanced ability to fucosylate sialylated GPs with LacNAc repeated units in their *N*-glycans. The described characteristics make sFUT9 a good candidate enzyme for *in vitro* synthesis of glycoconjugates containing fucosylated determinants, specially the Le^x epitope.

6.1.2. Localization of human FUT9

Besides the *in vitro* specificity of each particular GT, other factors contribute to the regulation of glycosylation *in vivo* including the sequential action of glycosidases and GTs, organized throughout the Golgi in an ordered way (Rabouille *et al.*, 1995). The full-length FUT9wt was found to localize in the *trans*-Golgi and the TGN of transfected HeLa cells (Chapter 2). The late localization of FUT9wt in the glycan biosynthetic pathway is in accordance with the functional role of the enzyme, which is involved in the last step of the biosynthesis of the terminal glycan epitope Le^x. Thus, FUT9wt acted after the production of LacNAc catalyzed by β4-GalT, an enzyme assigned to the *trans*-Golgi/TGN of HeLa cells (Nilsson *et al.*, 1993).

Deletion of the cytosolic tail of FUT9 (FUT9dcyt) caused a redistribution of the protein in the GA, as revealed by colocalization analysis with markers of the secretory pathway and BFA treatment (Chapter 2). FUT9dcyt localization was shifted to earlier Golgi sub-compartments, when compared to FUT9wt, and there was no accumulation in later compartments of the secretory pathway, namely the plasma membrane. As addressed in Chapter 1, the localization of GTs in the Golgi has been the subject of numerous studies in the last decades and the N-terminal portions (cytosolic tail, transmembrane domain and stem region) of several Golgi-resident GTs have been implicated (reviewed by Kartberg *et al.*, 2005). Our data pointed to the importance of the cytosolic tail of FUT9 in the regulation of its sub-compartment localization, in accordance to our previous

observations for another late-Golgi localized GT, human FUT3 (Sousa *et al.*, 2003). Studies from different laboratories with other GTs (Milland *et al.*, 2002; Fenteany and Colley, 2005; Uliana *et al.*, 2006a) also substantiate the hypothesis that the cytosolic tails of GTs play an essential role in the fine-tuning of Golgi localization. In this work, detailed analysis of the cytosolic tail of FUT9, by deletions and point mutations, suggested that amino acid residues containing hydroxyl groups could be important for the sub-compartment localization of the enzyme (Chapter 2). Accordingly, others have shown that a hydroxylated amino acid residue of the cytosolic tail of α2-FUT mediated its intra-Golgi localization (Milland *et al.*, 2002).

According to the cisternal maturation model, which is widely accepted to explain the steady-state maintenance of the GA contents, sorting into retrograde COPI transporters would be responsible for the correct localization of the Golgi-resident proteins. Therefore, FUT9 should be incorporated into COPI vesicles in order to be maintained in the correct Golgi cisternae. The 11 amino acid residues of the cytosolic tail of human FUT9 do not encode any known sorting motif and, most probably, this domain is too short to interact directly with COPI coat components. Nevertheless, the cytoplasmic tail could mediate interactions with other GTs in the formation of multienzyme complexes, as observed for GTs involved in the synthesis of gangliosides (Giraudo *et al.*, 2001; Giraudo and Maccioni, 2003) and yeast GTs (reviewed by de Graffenried and Bertozzi, 2004; Young, 2004). Considering the importance of the Ser and Thr residues of the cytosolic tail of FUT9 for the sub-compartment localization of the enzyme, the referred interactions could occur via hydrogen bonds. The incorporation of FUT9 in multienzyme complexes has never been addressed, thus further studies are required to explore this hypothesis.

The unique sequences of the cytoplasmic tails of GTs may also be involved in interactions with other types of Golgi-resident proteins, such as members of the intra-Golgi transport machinery. Tethering factors have been shown to interact with components of the COPI coat, other tethering factors and

SNARE proteins (reviewed by Ungar *et al.*, 2006), defining subpopulations of COPI vesicles enriched in distinct cargo molecules (Malsam *et al.*, 2005). In this context hypothetical interaction partners of FUT9 would be, for example, subunits of the COG tethering complex, essential for GT recycling and normal protein glycosylation, as shown by accumulation of intra-Golgi COG complex-dependent (CCD) vesicles in knock-down cells for the Cog3 and Cog7 subunits (Zolov and Lupashin, 2005). These vesicles were enriched in the *medial*-Golgi enzymes GlcNAcTI and mannosidase II and in the *trans*-Golgi enzyme GalT (Shestakova *et al.*, 2006) thus, it is feasible that FUT9 may also be accumulated in those vesicles.

Additional levels of complexity in the regulation of sorting of Golgi-resident proteins seem to be played by lipid environment (Bretscher and Munro, 1993; Mitra *et al.*, 2004) and the pH gradient present in the GA. It has been shown that the pH influenced oligomerization and stable retention of the late-Golgi enzyme α2,6-SialylT (Chen *et al.*, 2000; Fenteany and Colley, 2005) and that the neutralization of the pH gradient of the GA caused alterations in the localization of GlcNAcTI, GlcNAcTII and GalT (Axelsson *et al.*, 2001). Lumenal pH may induce protein-protein interactions or structural/conformational changes in Golgi-resident proteins (Weiss and Nilsson, 2000) that could expose the cytoplasmic tails and make them available to specific sorting interactions. Only the identification of the molecular partners of the cytoplasmic tails of GTs, in particular of FUT9, and the determination of the nature of the interaction will allow the clarification of the role of this domain in the *trans*-Golgi/TGN localization of the enzyme.

In vivo, the LacNAc acceptor substrate can originate several glycan structures besides Le^x, some of which were found in the brain. Generally, brain-type glycosylation is characterized by predominance of neutral *N*-glycans and low levels of peripheral sialylation (reviewed by Albach *et al.*, 2001). However, NeuAc is known to play important functions in the CNS, and the

α2,3-linked NeuAc acid in the reducing end of LacNAc of *N*-glycans can be the starting point for the formation of polysialic acid (Finne, 1982; Muhlenhoff *et al.*, 1996; Nakayama and Fukuda, 1996). As endogenous FUT9 is not capable of fucosylating sialylated type II acceptors (Chapters 2 and 4) and α2,3-SialylT is not capable of sialylating fucosylated acceptors (Wlasichuk *et al.*, 1993), the enzymes catalyze mutually exclusive reactions. Another possible product formed from LacNAc in the brain is the HNK-1 epitope (SO_3^--GlcAβ3Galβ4GlcNAc) (Schachner and Martini, 1995). In several regions of the murine brain it was observed that HNK-1 and Le^x presented complementary locations (Mai *et al.*, 1995). Moreover, both epitopes can decorate the same glycoconjugate in a developmentally-regulated manner, like it has been observed for the CSPG phosphocan (Maeda *et al.*, 1994; Allendoerfer *et al.*, 1995). Thus, the synthesis of Le^x, polysialic acid or HNK-1 will be determined by the competition between FUT9, α2,3-SialylT and β3-glucoronyltransferase. The predominance of one structure over the others may depend on the affinities of the different GTs for the terminal LacNAc acceptor substrate, the levels of expression of each GT and the relative localization of the competing enzymes in the GA. Recently, it was shown that the sub-Golgi localization of glycolipid GTs integrated in multienzyme complexes was influenced by the relative contribution of each element of the complex (Uliana *et al.*, 2006b). This study suggested that sub-compartment localization of GTs may change according to the levels of expression, reinforcing the concept that interference in the correct localization of FUT9 may have a great impact on the definition of the predominant biosynthetic route and, consequently, on the biological events to which these carbohydrate epitopes are associated, such as neural cell-adhesion, cell migration and neurite outgrowth (Fujimoto *et al.*, 2001; Chou *et al.*, 2004; Johnson *et al.*, 2005).

6.1.3. Expression of FUT9 and Le^x during neuronal development

In this thesis work, FUT9 was identified as the enzyme responsible for Le^x biosynthesis in NT2N neurons, a model of human CNS neurons (Pleasure *et al.*, 1992). This conclusion was based on the detection of both FUT9 transcripts and protein, which correlated with Le^x expression levels, and on the presence of an α3-FUT activity with an acceptor specificity profile typical of FUT9 (Chapter 4). As referred above, FUT9 had already been assigned as the α3-FUT that catalyzes the synthesis of Le^x in the rodent brain. Our data associating FUT9 and Le^x in human CNS generalize the definition of FUT9 as the *brain-type* FUT cross-species.

An important role for FUT9 has been hypothesized since its first cloning from a cDNA library of human gastric mucosa (Kaneko *et al.*, 1999b). The divergence of the FUT9 from the other α3-FUT family members and the high conservation of the *FUT9* gene between species (Kudo *et al.*, 1998; Kaneko *et al.*, 1999b; Baboval *et al.*, 2000; Patnaik *et al.*, 2000) at the level of genes such as histone and α-actin (Kaneko *et al.*, 1999b), suggested a strong selective pressure during evolution.

The biosynthetic product of FUT9, the Le^x epitope, was upregulated during human NT2N neurons differentiation *in vitro,* being detected in the majority of the NT2N neurons (Chapter 4). Moreover, analysis of the levels of the Le^x epitope in rat hippocampal cultures showed detection of Le^x confined to a small sub-population of neurons (Chapter 5). The Le^x could play a similar functional role in the CNS of the two species.

We have identified a subset of rat hippocampus neurons that expressed the Le^x determinant as GABAergic interneurons (Chapter 5). In the brain of the FUT9$^{-/-}$ mouse, concomitantly to Le^x disappearance, a reduction in the number of amygdalar calbindin (CB)-positive GABAergic neurons was observed (Kudo *et al.*, 2007). The NT2 cell line is a model system of human neuronal

differentiation and NT2N neurons present features of CNS human immature neurons (Pleasure *et al.*, 1992; Przyborski *et al.*, 2000), such as the ability to express several neurotransmitter phenotypes, including GABA (Yoshioka *et al.*, 1997; Guillemain *et al.*, 2000). Thus, it is feasible to hypothesize that the NT2 cell line, under the used culture conditions, differentiated preferentially into GABAergic neurons, the neuronal subtype that presented high detection of the Le^x epitope in rat hippocampus. Favoring this hypothesis, results obtained using differentiation conditions similar to ours, indicated that 62 to 66% of the total NT2N neurons in culture were GABAergic (Guillemain *et al.*, 2000). Co-detection of Le^x and a marker of GABAergic neurons, such as GABA or GAD, in NT2N neurons will be needed to clarify this issue.

Concerning the cellular localization of Le^x, both in human NT2N neurons and rat hippocampus GABAergic neurons, the epitope was present in the cell bodies and in the neuritic processes, localized at the plasma membrane and in TI-VAMP and LAMP-1 positive intracellular structures (Chapters 4 and 5). These most probably corresponded to the TI-VAMP exocytic compartment, which is associated with LAMP-1 positive late endosomes/lysosomes (Arantes and Andrews, 2006), and known to be involved in neurite outgrowth in rodent (reviewed by Proux-Gillardeaux *et al.*, 2005). Our results suggested that the neuronal TI-VAMP exocytic pathway might share common cross-species features, including Le^x-carriers as cargo, and, consequently, common functions.

Several Le^x-carrier proteins of high apparent molecular masses (above 400 kDa) were identified in human NT2N neurons and rat hippocampus neurons and might correspond to the cargo of the TI-VAMP pathway detected by immunofluorescence microscopy (Chapters 4 and 5). So far, besides the already mentioned LAMP-1, only the L1 adhesion molecule (Alberts *et al.*, 2003) and the SYT7 Ca^{2+}-sensor (Arantes and Andrews, 2006) have been identified as components of the TI-VAMP neuronal pathway. In spite of being glycosylated (Carlsson *et al.*, 1988; Streit *et al.*, 1990) none of these proteins where identified

by us as Le^x-carriers. The 460 kDa carrier detected in NT2N neurons was also decorated with the HNK-1 epitope in addition to Le^x. Both epitopes were insensitive to PNGaseF digestion and the apparent molecular mass of the carrier remained unaltered after chondroitinase ABC incubation, suggesting that the Le^x and HNK-1 epitopes could be attached to *O*-mannosyl oligosaccharides on a neuronal PG, which was not of the chondroitin sulfate type (Chapter 4). Supporting this hypothesis, there were previous reports of mannose-linked *O*-oligosaccharides in rat brain proteoglycans that carried Le^x and HNK-1 epitopes (Krusius *et al.*, 1987; Yuen *et al.*, 1997; Kogelberg *et al.*, 2001). Furthermore, Cat-315, a neuron specific epitope of the HNK-1 family, probably *O*-mannose linked, was recently detected in proteoglycans and related to neuritogenesis and synaptogenesis (Dino *et al.*, 2006). Changes in the carbohydrate epitopes presented by the same glycoconjugate have been reported (Rauch *et al.*, 1991; Maeda *et al.*, 1994; Allendoerfer *et al.*, 1995) and are thought to regulate its function. Additional studies will be required to clarify the nature of the Le^x-carriers identified in human and rat neurons and to understand if the expression of the determinant occurs in the same glycoconjugates.

An important role for Le^x in neuronal adhesion and neurite initiation of outgrowth was revealed by anti-Le^x antibody incubation assays. In human NT2N neurons, an anti-Le^x antibody impaired adhesion of neurons and neurites already formed to the surface and caused a decrease in the initiation of outgrowing neurites (Chapter 5). The antibody could block interactions between the neurons and matrix components or it could be internalized via the TI-VAMP pathway, affecting intracellular interactions important for the above-mentioned functions. On the other hand, a role for the Le^x-carriers in synaptogenesis was suggested by analysis of mature rat hippocampal co-cultures, 3 weeks after plating. It was observed that at the plasma membrane of GABAergic neurons, the Le^x-carriers were in post-synaptic domains, including spine-like protrusions or phillopodia. The labelling was closely related to the sites of establishment of synapses, as

determined by the detection of Le^x epitope in punctate structures that were not in colocalization with GAD and were in apposition with synaptophysin labeling (Chapter 5).

In order to relate the results obtained in both cell systems it will be useful to perform additional studies. NT2N neurons become mature and functional, forming excitatory and inhibitory synapses, when in co-culture with astrocytes (Hartley *et al.*, 1999). The detection of Le^x, neuronal subtype markers and synaptic markers in these cultures would help not only to relate the pattern of expression of Le^x-carriers with the neurotransmitter phenotype but also to investigate if, accordingly to our hypothesis, in human NT2N neurons there is also an association of Le^x with synaptogenesis. Furthermore, studies performed in human and rat cultures that would allow the evaluation of the effect of impaired TI-VAMP mediated membrane trafficking, and consequent inhibition of neurite outgrowth on Le^x distribution, would be of great importance for the enlightenment of the relation between Le^x-carriers and the TI-VAMP exocytic mediated pathway in neurite outgrowth and synaptogenesis. Finally, the identification of the Le^x-carriers would allow the undoubtedly assignment of the conserved function of the Le^x epitope in the CNS.

6.2. General conclusions

The work described in this thesis allowed a better understanding of the properties and functions of FUT9 and its biosynthetic product, Le^x, in the CNS.

In vitro, human FUT9 was shown to efficiently catalyze the synthesis of the Le^x determinant in *N*-glycans from glycoproteins. In human NT2N neurons, Le^x synthesis was assigned to FUT9, defining the enzyme as the brain-type α3-FUT.

Le^x was shown to be upregulated during neuronal differentiation both on human NT2N neurons and on a subpopulation of GABAergic rat hippocampus interneurons. In both cellular systems, Le^x was localized on the PM and in the exocytic TI-VAMP compartment, suggesting a common function for the TI-VAMP pathway in human and rat CNS.

Le^x played an important role in neuronal cell adhesion and neurite initiation of outgrowth from human NT2N neurons. Furthermore, it was present in synaptic adjacent regions from rat hippocampus GABAergic interneurons.

In summary, this work indicates that FUT9 synthesizes the Le^x epitope in the human CNS, specifically on *N*-linked oligosaccharides of glycoproteins, underlying the biological functions of Le^x in neuronal adhesion and differentiation processes, such as initiation of neurite outgrowth and possibly synaptogenesis.

References

Abe K., McKibbin J. M. and Hakomori S. (1983) The monoclonal antibody directed to difucosylated type 2 chain (Fuc alpha 1 leads to 2Gal beta 1 leads to 4[Fuc alpha 1 leads to 3]GlcNAc; Y Determinant). *J Biol Chem* 258**,** 11793-11797.

Aguirre A. A., Chittajallu R., Belachew S. and Gallo V. (2004) NG2-expressing cells in the subventricular zone are type C-like cells and contribute to interneuron generation in the postnatal hippocampus. *J Cell Biol* 165**,** 575-589.

Albach C., Klein R. A. and Schmitz B. (2001) Do rodent and human brains have different N-glycosylation patterns? *Biol Chem* 382**,** 187-194.

Alberts P., Rudge R., Hinners I., Muzerelle A., Martinez-Arca S., Irinopoulou T., Marthiens V., Tooze S., Rathjen F., Gaspar P. and Galli T. (2003) Cross talk between tetanus neurotoxin-insensitive vesicle-associated membrane protein-mediated transport and L1-mediated adhesion. *Mol Biol Cell* 14**,** 4207-4220.

Allan B. B., Moyer B. D. and Balch W. E. (2000) Rab1 recruitment of p115 into a cis-SNARE complex: programming budding COPII vesicles for fusion. *Science* 289**,** 444-448.

Allendoerfer K. L., Magnani J. L. and Patterson P. H. (1995) FORSE-1, an antibody that labels regionally restricted subpopulations of progenitor cells in the embryonic central nervous system, recognizes the Le(x) carbohydrate on a proteoglycan and two glycolipid antigens. *Mol Cell Neurosci* 6**,** 381-395.

Allendoerfer K. L., Durairaj A., Matthews G. A. and Patterson P. H. (1999) Morphological domains of Lewis-X/FORSE-1 immunolabeling in the embryonic neural tube are due to developmental regulation of cell surface carbohydrate expression. *Dev Biol* 211**,** 208-219.

Altmann F., Staudacher E., Wilson I. B. and Marz L. (1999) Insect cells as hosts for the expression of recombinant glycoproteins. *Glycoconj J* 16**,** 109-123.

Andrews N. W. (2002) Lysosomes and the plasma membrane: trypanosomes reveal a secret relationship. *J Cell Biol* 158**,** 389-394.

Andrews P. W. (1984) Retinoic acid induces neuronal differentiation of a cloned human embryonal carcinoma cell line in vitro. *Dev Biol* 103**,** 285-293.

Andrews P. W., Casper J., Damjanov I., Duggan-Keen M., Giwercman A., Hata J., von Keitz A., Looijenga L. H., Millan J. L., Oosterhuis J. W., Pera M., Sawada M., Schmoll H. J., Skakkebaek N. E., van Putten W. and Stern P. (1996) Comparative analysis of cell

surface antigens expressed by cell lines derived from human germ cell tumours. *Int J Cancer* 66**,** 806-816.

Appelmelk B. J., van Die I., van Vliet S. J., Vandenbroucke-Grauls C. M., Geijtenbeek T. B. and van Kooyk Y. (2003) Cutting edge: carbohydrate profiling identifies new pathogens that interact with dendritic cell-specific ICAM-3-grabbing nonintegrin on dendritic cells. *J Immunol* 170**,** 1635-1639.

Arantes R. M. and Andrews N. W. (2006) A role for synaptotagmin VII-regulated exocytosis of lysosomes in neurite outgrowth from primary sympathetic neurons. *J Neurosci* 26**,** 4630-4637.

Axelsson M. A., Karlsson N. G., Steel D. M., Ouwendijk J., Nilsson T. and Hansson G. C. (2001) Neutralization of pH in the Golgi apparatus causes redistribution of glycosyltransferases and changes in the O-glycosylation of mucins. *Glycobiology* 11**,** 633-644.

Baboval T., Henion T., Kinnally E. and Smith F. I. (2000) Molecular cloning of rat alpha1,3-fucosyltransferase IX (Fuc-TIX) and comparison of the expression of Fuc-TIV and Fuc-TIX genes during rat postnatal cerebellum development. *J Neurosci Res* 62**,** 206-215.

Baker K. A., Hong M., Sadi D. and Mendez I. (2000) Intrastriatal and intranigral grafting of hNT neurons in the 6-OHDA rat model of Parkinson's disease. *Exp Neurol* 162**,** 350-360.

Bani-Yaghoub M., Felker J. M., Ozog M. A., Bechberger J. F. and Naus C. C. (2001) Array analysis of the genes regulated during neuronal differentiation of human embryonal cells. *Biochem Cell Biol* 79**,** 387-398.

Baselga J., Maerz W. J., Moy D., Miller W. H., Jr., Castro L., Reuter V. E., Yao T. J., Masui H. and Dmitrovsky E. (1993) Over-expression of transforming growth factor alpha antagonizes the anti-tumorigenic but not the differentiation actions of retinoic acid in a human teratocarcinoma cell. *Oncogene* 8**,** 3257-3263.

Becker D. J. and Lowe J. B. (2003) Fucose: biosynthesis and biological function in mammals. *Glycobiology* 13**,** 41R-53R.

Bird J. M. and Kimber S. J. (1984) Oligosaccharides containing fucose linked alpha(1-3) and alpha(1-4) to N-acetylglucosamine cause decompaction of mouse morulae. *Dev Biol* 104**,** 449-460.

Bishop J. R., Schuksz M. and Esko J. D. (2007) Heparan sulphate proteoglycans fine-tune mammalian physiology. *Nature* 446**,** 1030-1037.

Bogoevska V., Horst A., Klampe B., Lucka L., Wagener C. and Nollau P. (2006) CEACAM1, an adhesion molecule of human granulocytes, is fucosylated by fucosyltransferase IX and interacts with DC-SIGN of dendritic cells via Lewis x residues. *Glycobiology* 16**,** 197-209.

Bogoevska V., Nollau P., Lucka L., Grunow D., Klampe B., Uotila L. M., Samsen A., Gahmberg C. G. and Wagener C. (2007) DC-SIGN binds ICAM-3 isolated from peripheral human leukocytes through Lewis x residues. *Glycobiology* 17**,** 324-333.

Bonfanti L., Mironov A. A., Jr., Martinez-Menarguez J. A., Martella O., Fusella A., Baldassarre M., Buccione R., Geuze H. J., Mironov A. A. and Luini A. (1998) Procollagen traverses the Golgi stack without leaving the lumen of cisternae: evidence for cisternal maturation. *Cell* 95**,** 993-1003.

Bonifacino J. S. and Lippincott-Schwartz J. (2003) Coat proteins: shaping membrane transport. *Nat Rev Mol Cell Biol* 4**,** 409-414.

Borlongan C. V., Tajima Y., Trojanowski J. Q., Lee V. M. and Sanberg P. R. (1998) Transplantation of cryopreserved human embryonal carcinoma-derived neurons (NT2N cells) promotes functional recovery in ischemic rats. *Exp Neurol* 149**,** 310-321.

Bourne Y. and Henrissat B. (2001) Glycoside hydrolases and glycosyltransferases: families and functional modules. *Curr Opin Struct Biol* 11**,** 593-600.

Breton C., Oriol R. and Imberty A. (1996) Sequence alignment and fold recognition of fucosyltransferases. *Glycobiology* 6**,** vii-xii.

Breton C., Oriol R. and Imberty A. (1998) Conserved structural features in eukaryotic and prokaryotic fucosyltransferases. *Glycobiology* 8**,** 87-94.

Breton C., Snajdrova L., Jeanneau C., Koca J. and Imberty A. (2006) Structures and mechanisms of glycosyltransferases. *Glycobiology* 16**,** 29R-37R.

Bretscher M. S. and Munro S. (1993) Cholesterol and the Golgi apparatus. *Science* 261**,** 1280-1281.

Brito C., Escrevente C., Reis C. A., Lee V. M., Trojanowski J. Q. and Costa J. (2007) Increased levels of fucosyltransferase IX and carbohydrate Lewis(x) adhesion determinant in human NT2N neurons. *J Neurosci Res* 85**,** 1260-1270.

Bulow H. E. and Hobert O. (2006) The molecular diversity of glycosaminoglycans shapes animal development. *Annu Rev Cell Dev Biol* 22**,** 375-407.

Cailleau-Thomas A., Coullin P., Candelier J. J., Balanzino L., Mennesson B., Oriol R. and Mollicone R. (2000) FUT4 and FUT9 genes are expressed early in human embryogenesis. *Glycobiology* 10**,** 789-802.

Cambi A., Koopman M. and Figdor C. G. (2005) How C-type lectins detect pathogens. *Cell Microbiol* 7**,** 481-488.

Capela A. and Temple S. (2002) LeX/ssea-1 is expressed by adult mouse CNS stem cells, identifying them as nonependymal. *Neuron* 35**,** 865-875.

Capela A. and Temple S. (2006) LeX is expressed by principle progenitor cells in the embryonic nervous system, is secreted into their environment and binds Wnt-1. *Dev Biol* 291**,** 300-313.

Carlsson S. R., Roth J., Piller F. and Fukuda M. (1988) Isolation and characterization of human lysosomal membrane glycoproteins, h-lamp-1 and h-lamp-2. Major sialoglycoproteins carrying polylactosaminoglycan. *J Biol Chem* 263**,** 18911-18919.

Cattaruzza S. and Perris R. (2006) Approaching the proteoglycome: molecular interactions of proteoglycans and their functional output. *Macromol Biosci* 6**,** 667-680.

Chen C., Ma J., Lazic A., Backovic M. and Colley K. J. (2000) Formation of insoluble oligomers correlates with ST6Gal I stable localization in the golgi. *J Biol Chem* 275**,** 13819-13826.

Chen W., Helenius J., Braakman I. and Helenius A. (1995) Cotranslational folding and calnexin binding during glycoprotein synthesis. *Proc Natl Acad Sci U S A* 92**,** 6229-6233.

Chen Y. J., Wing D. R., Guile G. R., Dwek R. A., Harvey D. J. and Zamze S. (1998) Neutral N-glycans in adult rat brain tissue--complete characterisation reveals fucosylated hybrid and complex structures. *Eur J Biochem* 251**,** 691-703.

Cheung W. M., Chu A. H. and Ip N. Y. (1997) Identification of candidate genes induced by retinoic acid in embryonal carcinoma cells. *J Neurochem* 68**,** 1882-1888.

Chilcote T. J., Galli T., Mundigl O., Edelmann L., McPherson P. S., Takei K. and De Camilli P. (1995) Cellubrevin and synaptobrevins: similar subcellular localization and biochemical properties in PC12 cells. *J Cell Biol* 129**,** 219-231.

Chou D. K., Suzuki Y. and Jungalwala F. B. (1996) Expression of neolactoglycolipids: sialosyl-, disialosyl-, O-acetyldisialosyl- and fucosyl- derivatives of neolactotetraosyl ceramide and neolactohexaosyl ceramide in the developing cerebral cortex and cerebellum. *Glycoconj J* 13**,** 295-305.

Chou D. K., Zhang J., Smith F. I., McCaffery P. and Jungalwala F. B. (2004) Developmental expression of receptor for advanced glycation end products (RAGE), amphoterin and sulfoglucuronyl (HNK-1) carbohydrate in mouse cerebellum and their role in neurite outgrowth and cell migration. *J Neurochem* 90**,** 1389-1401.

Coco S., Raposo G., Martinez S., Fontaine J. J., Takamori S., Zahraoui A., Jahn R., Matteoli M., Louvard D. and Galli T. (1999) Subcellular localization of tetanus neurotoxin-insensitive vesicle-associated membrane protein (VAMP)/VAMP7 in neuronal cells: evidence for a novel membrane compartment. *J Neurosci* 19**,** 9803-9812.

Cosson P. and Letourneur F. (1994) Coatomer interaction with di-lysine endoplasmic reticulum retention motifs. *Science* 263**,** 1629-1631.

Cosson P., Amherdt M., Rothman J. E. and Orci L. (2002) A resident Golgi protein is excluded from peri-Golgi vesicles in NRK cells. *Proc Natl Acad Sci U S A* 99**,** 12831-12834.

Costa J., Grabenhorst E., Nimtz M. and Conradt H. S. (1997) Stable expression of the Golgi form and secretory variants of human fucosyltransferase III from BHK-21 cells. Purification and characterization of an engineered truncated form from the culture medium. *J Biol Chem* 272**,** 11613-11621.

Coutinho P. M., Deleury E., Davies G. J. and Henrissat B. (2003) An evolving hierarchical family classification for glycosyltransferases. *J Mol Biol* 328**,** 307-317.

Czlapinski J. L. and Bertozzi C. R. (2006) Synthetic glycobiology: Exploits in the Golgi compartment. *Curr Opin Chem Biol* 10**,** 645-651.

Dailey M. E. and Smith S. J. (1996) The dynamics of dendritic structure in developing hippocampal slices. *J Neurosci* 16**,** 2983-2994.

Danglot L., Triller A. and Bessis A. (2003) Association of gephyrin with synaptic and extrasynaptic GABAA receptors varies during development in cultured hippocampal neurons. *Mol Cell Neurosci* 23**,** 264-278.

Danglot L., Triller A. and Marty S. (2006) The development of hippocampal interneurons in rodents. *Hippocampus* 16**,** 1032-1060.

Dasgupta S., Hogan E. L. and Spicer S. S. (1996) Stage-specific expression of fuco-neolacto- (Lewis X) and ganglio-series neutral glycosphingolipids during brain development: characterization of Lewis X and related glycosphingolipids in bovine, human and rat brain. *Glycoconj J* 13**,** 367-375.

de Graffenried C. L. and Bertozzi C. R. (2004) The roles of enzyme localisation and complex formation in glycan assembly within the Golgi apparatus. *Curr Opin Cell Biol* 16**,** 356-363.

de Lima A. D., Merten M. D. and Voigt T. (1997) Neuritic differentiation and synaptogenesis in serum-free neuronal cultures of the rat cerebral cortex. *J Comp Neurol* 382**,** 230-246.

de Vries T., Srnka C. A., Palcic M. M., Swiedler S. J., van den Eijnden D. H. and Macher B. A. (1995) Acceptor specificity of different length constructs of human recombinant alpha 1,3/4-fucosyltransferases. Replacement of the stem region and the transmembrane domain of fucosyltransferase V by protein A results in an enzyme with GDP-fucose hydrolyzing activity. *J Biol Chem* 270**,** 8712-8722.

de Vries T., Knegtel R. M., Holmes E. H. and Macher B. A. (2001) Fucosyltransferases: structure/function studies. *Glycobiology* 11**,** 119R-128R.

Dennis J. W., Warren C. E., Granovsky M. and Demetriou M. (2001) Genetic defects in N-glycosylation and cellular diversity in mammals. *Curr Opin Struct Biol* 11**,** 601-607.

Dino M. R., Harroch S., Hockfield S. and Matthews R. T. (2006) Monoclonal antibody Cat-315 detects a glycoform of receptor protein tyrosine phosphatase beta/phosphacan early in CNS development that localizes to extrasynaptic sites prior to synapse formation. *Neuroscience* 142**,** 1055-1069.

Duden R. (2003) ER-to-Golgi transport: COP I and COP II function (Review). *Mol Membr Biol* 20**,** 197-207.

Dupuy F., Petit J. M., Mollicone R., Oriol R., Julien R. and Maftah A. (1999) A single amino acid in the hypervariable stem domain of vertebrate alpha1,3/1,4-fucosyltransferases determines the type 1/type 2 transfer. Characterization of acceptor substrate specificity of the lewis enzyme by site-directed mutagenesis. *J Biol Chem* 274**,** 12257-12262.

Dupuy F., Germot A., Marenda M., Oriol R., Blancher A., Julien R. and Maftah A. (2002) Alpha1,4-fucosyltransferase activity: a significant function in the primate lineage has appeared twice independently. *Mol Biol Evol* 19**,** 815-824.

Dupuy F., Germot A., Julien R. and Maftah A. (2004) Structure/function study of Lewis alpha3- and alpha3/4-fucosyltransferases: the alpha1,4 fucosylation requires an aromatic residue in the acceptor-binding domain. *Glycobiology* 14**,** 347-356.

Eggens I., Fenderson B., Toyokuni T., Dean B., Stroud M. and Hakomori S. (1989) Specific interaction between Lex and Lex determinants. A possible basis for cell recognition in preimplantation embryos and in embryonal carcinoma cells. *J Biol Chem* 264**,** 9476-9484.

Elazar Z., Orci L., Ostermann J., Amherdt M., Tanigawa G. and Rothman J. E. (1994) ADP-ribosylation factor and coatomer couple fusion to vesicle budding. *J Cell Biol* 124**,** 415-424.

Farlow D. N., Vansant G., Cameron A. A., Chang J., Khoh-Reiter S., Pham N. L., Wu W., Sagara Y., Nicholls J. G., Carlo D. J. and Ill C. R. (2000) Gene expression monitoring for gene discovery in models of peripheral and central nervous system differentiation, regeneration, and trauma. *J Cell Biochem* 80**,** 171-180.

Fenderson B. A., Zehavi U. and Hakomori S. (1984) A multivalent lacto-N-fucopentaose III-lysyllysine conjugate decompacts preimplantation mouse embryos, while the free oligosaccharide is ineffective. *J Exp Med* 160**,** 1591-1596.

Fenderson B. A., Andrews P. W., Nudelman E., Clausen H. and Hakomori S. (1987) Glycolipid core structure switching from globo- to lacto- and ganglio-series during retinoic acid-induced differentiation of TERA-2-derived human embryonal carcinoma cells. *Dev Biol* 122**,** 21-34.

Fenderson B. A., Radin N. and Andrews P. W. (1993) Differentiation antigens of human germ cell tumours: distribution of carbohydrate epitopes on glycolipids and glycoproteins analyzed using PDMP, an inhibitor of glycolipid synthesis. *Eur Urol* 23**,** 30-36; discussion 36-37.

Fenteany F. H. and Colley K. J. (2005) Multiple signals are required for alpha2,6-sialyltransferase (ST6Gal I) oligomerization and Golgi localization. *J Biol Chem* 280**,** 5423-5429.

Finne J. (1982) Occurrence of unique polysialosyl carbohydrate units in glycoproteins of developing brain. *J Biol Chem* 257**,** 11966-11970.

Fortna R. R., Crystal A. S., Morais V. A., Pijak D. S., Lee V. M. and Doms R. W. (2004) Membrane topology and nicastrin-enhanced endoproteolysis of APH-1, a component of the gamma-secretase complex. *J Biol Chem* 279**,** 3685-3693.

Foster C. S., Gillies D. R. and Glick M. C. (1991) Purification and characterization of GDP-L-Fuc-N-acetyl-beta-D-glucosaminide alpha 1----3fucosyltransferase from human

neuroblastoma cells. Unusual substrate specificities of the tumor enzyme. *J Biol Chem* 266**,** 3526-3531.

Freemantle S. J., Kerley J. S., Olsen S. L., Gross R. H. and Spinella M. J. (2002) Developmentally-related candidate retinoic acid target genes regulated early during neuronal differentiation of human embryonal carcinoma. *Oncogene* 21**,** 2880-2889.

Fujimoto I., Bruses J. L. and Rutishauser U. (2001) Regulation of cell adhesion by polysialic acid. Effects on cadherin, immunoglobulin cell adhesion molecule, and integrin function and independence from neural cell adhesion molecule binding or signaling activity. *J Biol Chem* 276**,** 31745-31751.

Garbuzova-Davis S., Willing A. E., Milliken M., Saporta S., Zigova T., Cahill D. W. and Sanberg P. R. (2002) Positive effect of transplantation of hNT neurons (NTera 2/D1 cell-line) in a model of familial amyotrophic lateral sclerosis. *Exp Neurol* 174**,** 169-180.

Giraudo C. G., Daniotti J. L. and Maccioni H. J. (2001) Physical and functional association of glycolipid N-acetyl-galactosaminyl and galactosyl transferases in the Golgi apparatus. *Proc Natl Acad Sci U S A* 98**,** 1625-1630.

Giraudo C. G. and Maccioni H. J. (2003) Ganglioside glycosyltransferases organize in distinct multienzyme complexes in CHO-K1 cells. *J Biol Chem* 278**,** 40262-40271.

Gleeson P. A., Lock J. G., Luke M. R. and Stow J. L. (2004) Domains of the TGN: coats, tethers and G proteins. *Traffic* 5**,** 315-326.

Gocht A., Struckhoff G. and Lhler J. (1996) CD15-containing glycoconjugates in the central nervous system. *Histol Histopathol* 11**,** 1007-1028.

Goelz S. E., Hession C., Goff D., Griffiths B., Tizard R., Newman B., Chi-Rosso G. and Lobb R. (1990) ELFT: a gene that directs the expression of an ELAM-1 ligand. *Cell* 63**,** 1349-1356.

Gooi H. C., Feizi T., Kapadia A., Knowles B. B., Solter D. and Evans M. J. (1981) Stage-specific embryonic antigen involves alpha 1 goes to 3 fucosylated type 2 blood group chains. *Nature* 292**,** 156-158.

Gotoh T., Miyazaki Y., Kikuchi K. and Bentley W. E. (2001) Investigation of sequential behavior of carboxyl protease and cysteine protease activities in virus-infected Sf-9 insect cell culture by inhibition assay. *Appl Microbiol Biotechnol* 56**,** 742-749.

Gotz M., Wizenmann A., Reinhardt S., Lumsden A. and Price J. (1996) Selective adhesion of cells from different telencephalic regions. *Neuron* 16**,** 551-564.

Gourier C., Pincet F., Perez E., Zhang Y., Mallet J. M. and Sinay P. (2004) Specific and non specific interactions involving Le(X) determinant quantified by lipid vesicle micromanipulation. *Glycoconj J* 21**,** 165-174.

Gourier C., Pincet F., Perez E., Zhang Y., Zhu Z., Mallet J. M. and Sinay P. (2005) The natural LewisX-bearing lipids promote membrane adhesion: influence of ceramide on carbohydrate-carbohydrate recognition. *Angew Chem Int Ed Engl* 44**,** 1683-1687.

Gouveia R. M., Morais V. A., Peixoto C., Sousa M., Regalla M., Alves P. M. and Costa J. (2007) Production and purification of functional truncated soluble forms of human recombinant L1 cell adhesion glycoprotein from Spodoptera frugiperda Sf9 cells. *Protein Expr Purif* 52**,** 182-193.

Grabenhorst E., Nimtz M., Costa J. and Conradt H. S. (1998) In vivo specificity of human alpha1,3/4-fucosyltransferases III-VII in the biosynthesis of LewisX and Sialyl LewisX motifs on complex-type N-glycans. Coexpression studies from bhk-21 cells together with human beta-trace protein. *J Biol Chem* 273**,** 30985-30994.

Grabenhorst E. and Conradt H. S. (1999) The cytoplasmic, transmembrane, and stem regions of glycosyltransferases specify their in vivo functional sublocalization and stability in the Golgi. *J Biol Chem* 274**,** 36107-36116.

Gu F., Crump C. M. and Thomas G. (2001) Trans-Golgi network sorting. *Cell Mol Life Sci* 58**,** 1067-1084.

Guillemain I., Alonso G., Patey G., Privat A. and Chaudieu I. (2000) Human NT2 neurons express a large variety of neurotransmission phenotypes in vitro. *J Comp Neurol* 422**,** 380-395.

Hammond C., Braakman I. and Helenius A. (1994) Role of N-linked oligosaccharide recognition, glucose trimming, and calnexin in glycoprotein folding and quality control. *Proc Natl Acad Sci U S A* 91**,** 913-917.

Hardy M., Younkin D., Tang C. M., Pleasure J., Shi Q. Y., Williams M. and Pleasure D. (1994) Expression of non-NMDA glutamate receptor channel genes by clonal human neurons. *J Neurochem* 63**,** 482-489.

Harris S. L. and Waters M. G. (1996) Localization of a yeast early Golgi mannosyltransferase, Och1p, involves retrograde transport. *J Cell Biol* 132**,** 985-998.

Hart G. W., Housley M. P. and Slawson C. (2007) Cycling of O-linked beta-N-acetylglucosamine on nucleocytoplasmic proteins. *Nature* 446**,** 1017-1022.

Hartley R. S., Margulis M., Fishman P. S., Lee V. M. and Tang C. M. (1999) Functional synapses are formed between human NTera2 (NT2N, hNT) neurons grown on astrocytes. *J Comp Neurol* 407**,** 1-10.

Hathaway H. J., Evans S. C., Dubois D. H., Foote C. I., Elder B. H. and Shur B. D. (2003) Mutational analysis of the cytoplasmic domain of beta1,4-galactosyltransferase I: influence of phosphorylation on cell surface expression. *J Cell Sci* 116**,** 4319-4330.

Henderson J. K., Draper J. S., Baillie H. S., Fishel S., Thomson J. A., Moore H. and Andrews P. W. (2002) Preimplantation human embryos and embryonic stem cells show comparable expression of stage-specific embryonic antigens. *Stem Cells* 20**,** 329-337.

Herscovics A. (1999) Importance of glycosidases in mammalian glycoprotein biosynthesis. *Biochim Biophys Acta* 1473**,** 96-107.

Hoe M. H., Slusarewicz P., Misteli T., Watson R. and Warren G. (1995) Evidence for recycling of the resident medial/trans Golgi enzyme, N-acetylglucosaminyltransferase I, in ldlD cells. *J Biol Chem* 270**,** 25057-25063.

Hoffmann A., Nimtz M., Wurster U. and Conradt H. S. (1994) Carbohydrate structures of beta-trace protein from human cerebrospinal fluid: evidence for "brain-type" N-glycosylation. *J Neurochem* 63**,** 2185-2196.

Hoffmann A., Nimtz M., Getzlaff R. and Conradt H. S. (1995) 'Brain-type' N-glycosylation of asialo-transferrin from human cerebrospinal fluid. *FEBS Lett* 359**,** 164-168.

Hollister J., Grabenhorst E., Nimtz M., Conradt H. and Jarvis D. L. (2002) Engineering the protein N-glycosylation pathway in insect cells for production of biantennary, complex N-glycans. *Biochemistry* 41**,** 15093-15104.

Hong C. S., Caromile L., Nomata Y., Mori H., Bredesen D. E. and Koo E. H. (1999) Contrasting role of presenilin-1 and presenilin-2 in neuronal differentiation in vitro. *J Neurosci* 19**,** 637-643.

Hong W. (2005) SNAREs and traffic. *Biochim Biophys Acta* 1744**,** 120-144.

Ihara H., Ikeda Y., Toma S., Wang X., Suzuki T., Gu J., Miyoshi E., Tsukihara T., Honke K., Matsumoto A., Nakagawa A. and Taniguchi N. (2007) Crystal structure of mammalian alpha1,6-fucosyltransferase, FUT8. *Glycobiology* 17**,** 455-466.

Ikeda N., Eguchi H., Nishihara S., Narimatsu H., Kannagi R., Irimura T., Ohta M., Matsuda H., Taniguchi N. and Honke K. (2001) A remodeling system of the 3'-sulfo-Lewis a and 3'-sulfo-Lewis x epitopes. *J Biol Chem* 276**,** 38588-38594.

Ishii A., Ikeda T., Hitoshi S., Fujimoto I., Torii T., Sakuma K., Nakakita S., Hase S. and Ikenaka K. (2007) Developmental changes in the expression of glycogenes and the content of N-glycans in the mouse cerebral cortex. *Glycobiology* 17**,** 261-276.

Jinno S. and Kosaka T. (2002) Immunocytochemical characterization of hippocamposeptal projecting GABAergic nonprincipal neurons in the mouse brain: a retrograde labeling study. *Brain Res* 945**,** 219-231.

Johnson C. P., Fujimoto I., Rutishauser U. and Leckband D. E. (2005) Direct evidence that neural cell adhesion molecule (NCAM) polysialylation increases intermembrane repulsion and abrogates adhesion. *J Biol Chem* 280**,** 137-145.

Jones J., Krag S. S. and Betenbaugh M. J. (2005) Controlling N-linked glycan site occupancy. *Biochim Biophys Acta* 1726**,** 121-137.

Jost F., de Vries T., Knegtel R. M. and Macher B. A. (2005) Mutation of amino acids in the alpha 1,3-fucosyltransferase motif affects enzyme activity and Km for donor and acceptor substrates. *Glycobiology* 15**,** 165-175.

Kamiguchi H. and Lemmon V. (2000) Recycling of the cell adhesion molecule L1 in axonal growth cones. *J Neurosci* 20**,** 3676-3686.

Kaneko M., Kudo T., Iwasaki H., Shiina T., Inoko H., Kozaki T., Saitou N. and Narimatsu H. (1999a) Assignment of the human alpha 1,3-fucosyltransferase IX gene (FUT9) to chromosome band 6q16 by in situ hybridization. *Cytogenet Cell Genet* 86**,** 329-330.

Kaneko M., Kudo T., Iwasaki H., Ikehara Y., Nishihara S., Nakagawa S., Sasaki K., Shiina T., Inoko H., Saitou N. and Narimatsu H. (1999b) Alpha1,3-fucosyltransferase IX (Fuc-TIX) is very highly conserved between human and mouse; molecular cloning, characterization and tissue distribution of human Fuc-TIX. *FEBS Lett* 452**,** 237-242.

Kartberg F., Elsner M., Froderberg L., Asp L. and Nilsson T. (2005) Commuting between Golgi cisternae--mind the GAP! *Biochim Biophys Acta* 1744**,** 351-363.

Kawar Z. S., Haslam S. M., Morris H. R., Dell A. and Cummings R. D. (2005) Novel poly-GalNAcbeta1-4GlcNAc (LacdiNAc) and fucosylated poly-LacdiNAc N-glycans from mammalian cells expressing beta1,4-N-acetylgalactosaminyltransferase and alpha1,3-fucosyltransferase. *J Biol Chem* 280**,** 12810-12819.

Keller S., Sanderson M. P., Stoeck A. and Altevogt P. (2006) Exosomes: from biogenesis and secretion to biological function. *Immunol Lett* 107**,** 102-108.

Kirkham M. and Parton R. G. (2005) Clathrin-independent endocytosis: new insights into caveolae and non-caveolar lipid raft carriers. *Biochim Biophys Acta* 1745**,** 273-286.

Klimpel K. R. and Goldman W. E. (1988) Cell walls from avirulent variants of Histoplasma capsulatum lack alpha-(1,3)-glucan. *Infect Immun* 56**,** 2997-3000.

Ko I. K., Kato K. and Iwata H. (2005) Parallel analysis of multiple surface markers expressed on rat neural stem cells using antibody microarrays. *Biomaterials* 26**,** 4882-4891.

Kogelberg H., Chai W., Feizi T. and Lawson A. M. (2001) NMR studies of mannitol-terminating oligosaccharides derived by reductive alkaline hydrolysis from brain glycoproteins. *Carbohydr Res* 331**,** 393-401.

Kojima N., Fenderson B. A., Stroud M. R., Goldberg R. I., Habermann R., Toyokuni T. and Hakomori S. (1994) Further studies on cell adhesion based on Le(x)-Le(x) interaction, with new approaches: embryoglycan aggregation of F9 teratocarcinoma cells, and adhesion of various tumour cells based on Le(x) expression. *Glycoconj J* 11**,** 238-248.

Kondziolka D., Wechsler L., Goldstein S., Meltzer C., Thulborn K. R., Gebel J., Jannetta P., DeCesare S., Elder E. M., McGrogan M., Reitman M. A. and Bynum L. (2000) Transplantation of cultured human neuronal cells for patients with stroke. *Neurology* 55**,** 565-569.

Kornfeld R. and Kornfeld S. (1985) Assembly of asparagine-linked oligosaccharides. *Annu Rev Biochem* 54**,** 631-664.

Krusius T., Finne J., Margolis R. K. and Margolis R. U. (1986) Identification of an O-glycosidic mannose-linked sialylated tetrasaccharide and keratan sulfate oligosaccharides in the chondroitin sulfate proteoglycan of brain. *J Biol Chem* 261**,** 8237-8242.

Krusius T., Reinhold V. N., Margolis R. K. and Margolis R. U. (1987) Structural studies on sialylated and sulphated O-glycosidic mannose-linked oligosaccharides in the chondroitin sulphate proteoglycan of brain. *Biochem J* 245**,** 229-234.

Kudo T. and Narimatsu H. (1995) The beta 1,4-galactosyltransferase gene is post-transcriptionally regulated during differentiation of mouse F9 teratocarcinoma cells. *Glycobiology* 5**,** 397-403.

Kudo T., Ikehara Y., Togayachi A., Kaneko M., Hiraga T., Sasaki K. and Narimatsu H. (1998) Expression cloning and characterization of a novel murine alpha1, 3-fucosyltransferase, mFuc-TIX, that synthesizes the Lewis x (CD15) epitope in brain and kidney. *J Biol Chem* 273**,** 26729-26738.

Kudo T., Kaneko M., Iwasaki H., Togayachi A., Nishihara S., Abe K. and Narimatsu H. (2004) Normal embryonic and germ cell development in mice lacking alpha 1,3-fucosyltransferase IX (Fut9) which show disappearance of stage-specific embryonic antigen 1. *Mol Cell Biol* 24**,** 4221-4228.

Kudo T., Fujii T., Ikegami S., Inokuchi K., Takayama Y., Ikehara Y., Nishihara S., Togayachi A., Takahashi S., Tachibana K., Yuasa S. and Narimatsu H. (2007) Mice lacking alpha1,3-fucosyltransferase IX demonstrate disappearance of Lewis x structure in brain and increased anxiety-like behaviors. *Glycobiology* 17**,** 1-9.

Kweon H. S., Beznoussenko G. V., Micaroni M., Polishchuk R. S., Trucco A., Martella O., Di Giandomenico D., Marra P., Fusella A., Di Pentima A., Berger E. G., Geerts W. J., Koster A. J., Burger K. N., Luini A. and Mironov A. A. (2004) Golgi enzymes are enriched in perforated zones of golgi cisternae but are depleted in COPI vesicles. *Mol Biol Cell* 15**,** 4710-4724.

Lairson L. L. and Withers S. G. (2004) Mechanistic analogies amongst carbohydrate modifying enzymes. *Chem Commun (Camb)***,** 2243-2248.

Lanoix J., Ouwendijk J., Lin C. C., Stark A., Love H. D., Ostermann J. and Nilsson T. (1999) GTP hydrolysis by arf-1 mediates sorting and concentration of Golgi resident enzymes into functional COP I vesicles. *Embo J* 18**,** 4935-4948.

Lanoix J., Ouwendijk J., Stark A., Szafer E., Cassel D., Dejgaard K., Weiss M. and Nilsson T. (2001) Sorting of Golgi resident proteins into different subpopulations of COPI vesicles: a role for ArfGAP1. *J Cell Biol* 155**,** 1199-1212.

Lee V. M. and Andrews P. W. (1986) Differentiation of NTERA-2 clonal human embryonal carcinoma cells into neurons involves the induction of all three neurofilament proteins. *J Neurosci* 6**,** 514-521.

Letourneur F., Gaynor E. C., Hennecke S., Demolliere C., Duden R., Emr S. D., Riezman H. and Cosson P. (1994) Coatomer is essential for retrieval of dilysine-tagged proteins to the endoplasmic reticulum. *Cell* 79**,** 1199-1207.

Leypoldt F., Lewerenz J. and Methner A. (2001) Identification of genes up-regulated by retinoic-acid-induced differentiation of the human neuronal precursor cell line NTERA-2 cl.D1. *J Neurochem* 76**,** 806-814.

Lindskog E., Svensson I. and Haggstrom L. (2006) A homologue of cathepsin L identified in conditioned medium from Sf9 insect cells. *Appl Microbiol Biotechnol* 71**,** 444-449.

Lippincott-Schwartz J., Yuan L. C., Bonifacino J. S. and Klausner R. D. (1989) Rapid redistribution of Golgi proteins into the ER in cells treated with brefeldin A: evidence for membrane cycling from Golgi to ER. *Cell* 56**,** 801-813.

Lippincott-Schwartz J. and Liu W. (2006) Insights into COPI coat assembly and function in living cells. *Trends Cell Biol* 16**,** e1-4.

Losev E., Reinke C. A., Jellen J., Strongin D. E., Bevis B. J. and Glick B. S. (2006) Golgi maturation visualized in living yeast. *Nature* 441**,** 1002-1006.

Love H. D., Lin C. C., Short C. S. and Ostermann J. (1998) Isolation of functional Golgi-derived vesicles with a possible role in retrograde transport. *J Cell Biol* 140**,** 541-551.

Lowe J. B., Kukowska-Latallo J. F., Nair R. P., Larsen R. D., Marks R. M., Macher B. A., Kelly R. J. and Ernst L. K. (1991) Molecular cloning of a human fucosyltransferase gene that determines expression of the Lewis x and VIM-2 epitopes but not ELAM-1-dependent cell adhesion. *J Biol Chem* 266**,** 17467-17477.

Lowe J. B. (2003) Glycan-dependent leukocyte adhesion and recruitment in inflammation. *Curr Opin Cell Biol* 15**,** 531-538.

Luo Y. and Haltiwanger R. S. (2005) O-fucosylation of notch occurs in the endoplasmic reticulum. *J Biol Chem* 280**,** 11289-11294.

Lupashin V. and Sztul E. (2005) Golgi tethering factors. *Biochim Biophys Acta* 1744**,** 325-339.

Ma B., Wang G., Palcic M. M., Hazes B. and Taylor D. E. (2003) C-terminal amino acids of Helicobacter pylori alpha1,3/4 fucosyltransferases determine type I and type II transfer. *J Biol Chem* 278**,** 21893-21900.

Ma B., Lau L. H., Palcic M. M., Hazes B. and Taylor D. E. (2005) A single aromatic amino acid at the carboxyl terminus of Helicobacter pylori {alpha}1,3/4 fucosyltransferase determines substrate specificity. *J Biol Chem* 280**,** 36848-36856.

Ma B., Simala-Grant J. L. and Taylor D. E. (2006) Fucosylation in prokaryotes and eukaryotes. *Glycobiology* 16**,** 158R-184R.

Maccaferri G. and Lacaille J. C. (2003) Interneuron Diversity series: Hippocampal interneuron classifications--making things as simple as possible, not simpler. *Trends Neurosci* 26**,** 564-571.

Maeda N., Hamanaka H., Shintani T., Nishiwaki T. and Noda M. (1994) Multiple receptor-like protein tyrosine phosphatases in the form of chondroitin sulfate proteoglycan. *FEBS Lett* 354**,** 67-70.

Mai J. K., Bartsch D. and Marani E. (1995) CD15 and HKN-1 reveal cerebellar compartments with a complex overlap. *Eur J Morphol* 33**,** 101-107.

Mai J. K., Krajewski S., Reifenberger G., Genderski B., Lensing-Hohn S. and Ashwell K. W. (1999) Spatiotemporal expression gradients of the carbohydrate antigen (CD15) (Lewis X) during development of the human basal ganglia. *Neuroscience* 88**,** 847-858.

Malhotra V., Serafini T., Orci L., Shepherd J. C. and Rothman J. E. (1989) Purification of a novel class of coated vesicles mediating biosynthetic protein transport through the Golgi stack. *Cell* 58**,** 329-336.

Malsam J., Satoh A., Pelletier L. and Warren G. (2005) Golgin tethers define subpopulations of COPI vesicles. *Science* 307**,** 1095-1098.

Marchal-Victorion S., Deleyrolle L., De Weille J., Saunier M., Dromard C., Sandillon F., Privat A. and Hugnot J. P. (2003) The human NTERA2 neural cell line generates neurons on growth under neural stem cell conditions and exhibits characteristics of radial glial cells. *Mol Cell Neurosci* 24**,** 198-213.

Martinez-Arca S., Alberts P. and Galli T. (2000) Clostridial neurotoxin-insensitive vesicular SNAREs in exocytosis and endocytosis. *Biol Cell* 92**,** 449-453.

Martinez-Arca S., Coco S., Mainguy G., Schenk U., Alberts P., Bouille P., Mezzina M., Prochiantz A., Matteoli M., Louvard D. and Galli T. (2001) A common exocytotic mechanism mediates axonal and dendritic outgrowth. *J Neurosci* 21**,** 3830-3838.

Martinez-Menarguez J. A., Prekeris R., Oorschot V. M., Scheller R., Slot J. W., Geuze H. J. and Klumperman J. (2001) Peri-Golgi vesicles contain retrograde but not anterograde proteins consistent with the cisternal progression model of intra-Golgi transport. *J Cell Biol* 155**,** 1213-1224.

Martinez I., Chakrabarti S., Hellevik T., Morehead J., Fowler K. and Andrews N. W. (2000) Synaptotagmin VII regulates Ca(2+)-dependent exocytosis of lysosomes in fibroblasts. *J Cell Biol* 148**,** 1141-1149.

Matsuura-Tokita K., Takeuchi M., Ichihara A., Mikuriya K. and Nakano A. (2006) Live imaging of yeast Golgi cisternal maturation. *Nature* 441**,** 1007-1010.

Maurel P., Rauch U., Flad M., Margolis R. K. and Margolis R. U. (1994) Phosphacan, a chondroitin sulfate proteoglycan of brain that interacts with neurons and neural cell-adhesion molecules, is an extracellular variant of a receptor-type protein tyrosine phosphatase. *Proc Natl Acad Sci U S A* 91**,** 2512-2516.

McCarroll L. and King L. A. (1997) Stable insect cell cultures for recombinant protein production. *Curr Opin Biotechnol* 8**,** 590-594.

McDonald A. J. and Mascagni F. (2001) Colocalization of calcium-binding proteins and GABA in neurons of the rat basolateral amygdala. *Neuroscience* 105**,** 681-693.

Meijering E., Jacob M., Sarria J. C., Steiner P., Hirling H. and Unser M. (2004) Design and validation of a tool for neurite tracing and analysis in fluorescence microscopy images. *Cytometry A* 58**,** 167-176.

Milland J., Taylor S. G., Dodson H. C., McKenzie I. F. and Sandrin M. S. (2001) The cytoplasmic tail of alpha 1,2-fucosyltransferase contains a sequence for golgi localization. *J Biol Chem* 276**,** 12012-12018.

Milland J., Russell S. M., Dodson H. C., McKenzie I. F. and Sandrin M. S. (2002) The cytoplasmic tail of alpha 1,3-galactosyltransferase inhibits Golgi localization of the full-length enzyme. *J Biol Chem* 277**,** 10374-10378.

Mironov A. A., Beznoussenko G. V., Nicoziani P., Martella O., Trucco A., Kweon H. S., Di Giandomenico D., Polishchuk R. S., Fusella A., Lupetti P., Berger E. G., Geerts W. J., Koster A. J., Burger K. N. and Luini A. (2001) Small cargo proteins and large aggregates can traverse the Golgi by a common mechanism without leaving the lumen of cisternae. *J Cell Biol* 155**,** 1225-1238.

Mironov A. A., Beznoussenko G. V., Polishchuk R. S. and Trucco A. (2005) Intra-Golgi transport: a way to a new paradigm? *Biochim Biophys Acta* 1744**,** 340-350.

Mitra K., Ubarretxena-Belandia I., Taguchi T., Warren G. and Engelman D. M. (2004) Modulation of the bilayer thickness of exocytic pathway membranes by membrane proteins rather than cholesterol. *Proc Natl Acad Sci U S A* 101**,** 4083-4088.

Mollicone R., Gibaud A., Francois A., Ratcliffe M. and Oriol R. (1990) Acceptor specificity and tissue distribution of three human alpha-3-fucosyltransferases. *Eur J Biochem* 191**,** 169-176.

Mollicone R., Candelier J. J., Mennesson B., Couillin P., Venot A. P. and Oriol R. (1992) Five specificity patterns of (1----3)-alpha-L-fucosyltransferase activity defined by use of synthetic oligosaccharide acceptors. Differential expression of the enzymes during human embryonic development and in adult tissues. *Carbohydr Res* 228**,** 265-276.

Mollicone R., Reguigne I., Fletcher A., Aziz A., Rustam M., Weston B. W., Kelly R. J., Lowe J. B. and Oriol R. (1994) Molecular basis for plasma alpha(1,3)-fucosyltransferase gene deficiency (FUT6). *J Biol Chem* 269**,** 12662-12671.

Moloney D. J., Lin A. I. and Haltiwanger R. S. (1997) The O-linked fucose glycosylation pathway. Evidence for protein-specific elongation of o-linked fucose in Chinese hamster ovary cells. *J Biol Chem* 272**,** 19046-19050.

Moloney D. J. and Haltiwanger R. S. (1999) The O-linked fucose glycosylation pathway: identification and characterization of a uridine diphosphoglucose: fucose-beta1,3-glucosyltransferase activity from Chinese hamster ovary cells. *Glycobiology* 9**,** 679-687.

Morais V. A. and Costa J. (2003) Stable expression of recombinant human alpha3/4 fucosyltransferase III in Spodoptera frugiperda Sf9 cells. *J Biotechnol* 106**,** 69-75.

Morais V. A., Costa M. T. and Costa J. (2003) N-glycosylation of recombinant human fucosyltransferase III is required for its in vivo folding in mammalian and insect cells. *Biochim Biophys Acta* 1619**,** 133-138.

Morais V. A., Brito C., Pijak D. S., Crystal A. S., Fortna R. R., Li T., Wong P. C., Doms R. W. and Costa J. (2006) N-glycosylation of human nicastrin is required for interaction with the lectins from the secretory pathway calnexin and ERGIC-53. *Biochim Biophys Acta* 1762**,** 802-810.

Muhlenhoff M., Eckhardt M., Bethe A., Frosch M. and Gerardy-Schahn R. (1996) Polysialylation of NCAM by a single enzyme. *Curr Biol* 6**,** 1188-1191.

Muir J. K., Raghupathi R., Saatman K. E., Wilson C. A., Lee V. M., Trojanowski J. Q., Philips M. F. and McIntosh T. K. (1999) Terminally differentiated human neurons survive and integrate following transplantation into the traumatically injured rat brain. *J Neurotrauma* 16**,** 403-414.

Mulichak A. M., Losey H. C., Walsh C. T. and Garavito R. M. (2001) Structure of the UDP-glucosyltransferase GtfB that modifies the heptapeptide aglycone in the biosynthesis of vancomycin group antibiotics. *Structure* 9**,** 547-557.

Munro S. (1991) Sequences within and adjacent to the transmembrane segment of alpha-2,6-sialyltransferase specify Golgi retention. *Embo J* 10**,** 3577-3588.

Munro S. (2005) The Golgi apparatus: defining the identity of Golgi membranes. *Curr Opin Cell Biol* 17**,** 395-401.

Munster J., Ziegelmuller P., Spillner E. and Bredehorst R. (2006) High level expression of monomeric and dimeric human alpha1,3-fucosyltransferase V. *J Biotechnol* 121**,** 448-457.

Murray B. W., Takayama S., Schultz J. and Wong C. H. (1996) Mechanism and specificity of human alpha-1,3-fucosyltransferase V. *Biochemistry* 35**,** 11183-11195.

Muzerelle A., Alberts P., Martinez-Arca S., Jeannequin O., Lafaye P., Mazie J. C., Galli T. and Gaspar P. (2003) Tetanus neurotoxin-insensitive vesicle-associated membrane protein localizes to a presynaptic membrane compartment in selected terminal subsets of the rat brain. *Neuroscience* 122**,** 59-75.

Naegele J. R. and Barnstable C. J. (1991) A carbohydrate epitope defined by monoclonal antibody VC1.1 is found on N-CAM and other cell adhesion molecules. *Brain Res* 559**,** 118-129.

Nakayama F., Nishihara S., Iwasaki H., Kudo T., Okubo R., Kaneko M., Nakamura M., Karube M., Sasaki K. and Narimatsu H. (2001) CD15 expression in mature granulocytes is determined by alpha 1,3-fucosyltransferase IX, but in promyelocytes and monocytes by alpha 1,3-fucosyltransferase IV. *J Biol Chem* 276**,** 16100-16106.

Nakayama J. and Fukuda M. (1996) A human polysialyltransferase directs in vitro synthesis of polysialic acid. *J Biol Chem* 271**,** 1829-1832.

Natsuka S., Gersten K. M., Zenita K., Kannagi R. and Lowe J. B. (1994) Molecular cloning of a cDNA encoding a novel human leukocyte alpha-1,3-fucosyltransferase capable of synthesizing the sialyl Lewis x determinant. *J Biol Chem* 269**,** 16789-16794.

Nilsson T., Lucocq J. M., Mackay D. and Warren G. (1991) The membrane spanning domain of beta-1,4-galactosyltransferase specifies trans Golgi localization. *Embo J* 10**,** 3567-3575.

Nilsson T., Pypaert M., Hoe M. H., Slusarewicz P., Berger E. G. and Warren G. (1993) Overlapping distribution of two glycosyltransferases in the Golgi apparatus of HeLa cells. *J Cell Biol* 120**,** 5-13.

Nishihara S., Iwasaki H., Kaneko M., Tawada A., Ito M. and Narimatsu H. (1999) Alpha1,3-fucosyltransferase 9 (FUT9; Fuc-TIX) preferentially fucosylates the distal GlcNAc residue of polylactosamine chain while the other four alpha1,3FUT members preferentially fucosylate the inner GlcNAc residue. *FEBS Lett* 462**,** 289-294.

Nishihara S., Iwasaki H., Nakajima K., Togayachi A., Ikehara Y., Kudo T., Kushi Y., Furuya A., Shitara K. and Narimatsu H. (2003) Alpha1,3-fucosyltransferase IX (Fut9) determines Lewis X expression in brain. *Glycobiology* 13**,** 445-455.

Numahata K., Satoh M., Handa K., Saito S., Ohyama C., Ito A., Takahashi T., Hoshi S., Orikasa S. and Hakomori S. I. (2002) Sialosyl-Le(x) expression defines invasive and metastatic properties of bladder carcinoma. *Cancer* 94**,** 673-685.

Opat A. S., van Vliet C. and Gleeson P. A. (2001) Trafficking and localisation of resident Golgi glycosylation enzymes. *Biochimie* 83**,** 763-773.

Orci L., Glick B. S. and Rothman J. E. (1986) A new type of coated vesicular carrier that appears not to contain clathrin: its possible role in protein transport within the Golgi stack. *Cell* 46**,** 171-184.

Orci L., Tagaya M., Amherdt M., Perrelet A., Donaldson J. G., Lippincott-Schwartz J., Klausner R. D. and Rothman J. E. (1991) Brefeldin A, a drug that blocks secretion, prevents the assembly of non-clathrin-coated buds on Golgi cisternae. *Cell* 64**,** 1183-1195.

Orci L., Amherdt M., Ravazzola M., Perrelet A. and Rothman J. E. (2000) Exclusion of golgi residents from transport vesicles budding from Golgi cisternae in intact cells. *J Cell Biol* 150**,** 1263-1270.

Oriol R., Mollicone R., Cailleau A., Balanzino L. and Breton C. (1999) Divergent evolution of fucosyltransferase genes from vertebrates, invertebrates, and bacteria. *Glycobiology* 9**,** 323-334.

Osanai T., Chai W., Tajima Y., Shimoda Y., Sanai Y. and Yuen C. T. (2001) Expression of glycoconjugates bearing the Lewis X epitope during neural differentiation of P19 EC cells. *FEBS Lett* 488**,** 23-28.

Owen D. J., Collins B. M. and Evans P. R. (2004) Adaptors for clathrin coats: structure and function. *Annu Rev Cell Dev Biol* 20**,** 153-191.

Pal R. and Ravindran G. (2006) Assessment of pluripotency and multilineage differentiation potential of NTERA-2 cells as a model for studying human embryonic stem cells. *Cell Prolif* 39**,** 585-598.

Palma A. S., Morais V. A., Coelho A. V. and Costa J. (2004) Effect of the manganese ion on human alpha3/4 fucosyltransferase III activity. *Biometals* 17**,** 35-43.

Pang H., Koda Y., Soejima M. and Kimura H. (1998) Significance of each of three missense mutations, G484A, G667A, and G808A, present in an inactive allele of the human Lewis gene (FUT3) for alpha(1,3/1,4)fucosyltransferase inactivation. *Glycoconj J* 15**,** 961-967.

Patnaik S. K., Zhang A., Shi S. and Stanley P. (2000) alpha(1,3)fucosyltransferases expressed by the gain-of-function Chinese hamster ovary glycosylation mutants LEC12, LEC29, and LEC30. *Arch Biochem Biophys* 375**,** 322-332.

Patnaik S. K., Potvin B. and Stanley P. (2004) LEC12 and LEC29 gain-of-function Chinese hamster ovary mutants reveal mechanisms for regulating VIM-2 antigen synthesis and E-selectin binding. *J Biol Chem* 279**,** 49716-49726.

Paulson J. C. and Colley K. J. (1989) Glycosyltransferases. Structure, localization, and control of cell type-specific glycosylation. *J Biol Chem* 264**,** 17615-17618.

Perret E., Lakkaraju A., Deborde S., Schreiner R. and Rodriguez-Boulan E. (2005) Evolving endosomes: how many varieties and why? *Curr Opin Cell Biol* 17**,** 423-434.

Peter-Katalinic J. (2005) Methods in enzymology: O-glycosylation of proteins. *Methods Enzymol* 405**,** 139-171.

Pleasure S. J., Page C. and Lee V. M. (1992) Pure, postmitotic, polarized human neurons derived from NTera 2 cells provide a system for expressing exogenous proteins in terminally differentiated neurons. *J Neurosci* 12**,** 1802-1815.

Proux-Gillardeaux V., Rudge R. and Galli T. (2005) The tetanus neurotoxin-sensitive and insensitive routes to and from the plasma membrane: fast and slow pathways? *Traffic* 6**,** 366-373.

Przyborski S. A., Morton I. E., Wood A. and Andrews P. W. (2000) Developmental regulation of neurogenesis in the pluripotent human embryonal carcinoma cell line NTERA-2. *Eur J Neurosci* 12**,** 3521-3528.

Puthenveedu M. A. and Linstedt A. D. (2004) Gene replacement reveals that p115/SNARE interactions are essential for Golgi biogenesis. *Proc Natl Acad Sci U S A* 101**,** 1253-1256.

Qasba P. K., Ramakrishnan B. and Boeggeman E. (2005) Substrate-induced conformational changes in glycosyltransferases. *Trends Biochem Sci* 30**,** 53-62.

Rabouille C., Hui N., Hunte F., Kieckbusch R., Berger E. G., Warren G. and Nilsson T. (1995) Mapping the distribution of Golgi enzymes involved in the construction of complex oligosaccharides. *J Cell Sci* 108 (Pt 4)**,** 1617-1627.

Rao S. K., Huynh C., Proux-Gillardeaux V., Galli T. and Andrews N. W. (2004) Identification of SNAREs involved in synaptotagmin VII-regulated lysosomal exocytosis. *J Biol Chem* 279**,** 20471-20479.

Rauch U., Gao P., Janetzko A., Flaccus A., Hilgenberg L., Tekotte H., Margolis R. K. and Margolis R. U. (1991) Isolation and characterization of developmentally regulated chondroitin sulfate and chondroitin/keratan sulfate proteoglycans of brain identified with monoclonal antibodies. *J Biol Chem* 266**,** 14785-14801.

Reaves B. and Banting G. (1992) Perturbation of the morphology of the trans-Golgi network following Brefeldin A treatment: redistribution of a TGN-specific integral membrane protein, TGN38. *J Cell Biol* 116**,** 85-94.

Reddy A., Caler E. V. and Andrews N. W. (2001) Plasma membrane repair is mediated by Ca(2+)-regulated exocytosis of lysosomes. *Cell* 106**,** 157-169.

Rein U., Andag U., Duden R., Schmitt H. D. and Spang A. (2002) ARF-GAP-mediated interaction between the ER-Golgi v-SNAREs and the COPI coat. *J Cell Biol* 157**,** 395-404.

Reis C. A., David L., Nielsen P. A., Clausen H., Mirgorodskaya K., Roepstorff P. and Sobrinho-Simoes M. (1997) Immunohistochemical study of MUC5AC expression in human gastric carcinomas using a novel monoclonal antibody. *Int J Cancer* 74**,** 112-121.

Roberts C., Platt N., Streit A., Schachner M. and Stern C. D. (1991) The L5 epitope: an early marker for neural induction in the chick embryo and its involvement in inductive interactions. *Development* 112**,** 959-970.

Rodriguez-Boulan E. and Musch A. (2005) Protein sorting in the Golgi complex: shifting paradigms. *Biochim Biophys Acta* 1744**,** 455-464.

Rodriguez A., Webster P., Ortego J. and Andrews N. W. (1997) Lysosomes behave as Ca2+-regulated exocytic vesicles in fibroblasts and epithelial cells. *J Cell Biol* 137**,** 93-104.

Roos C., Kolmer M., Mattila P. and Renkonen R. (2002) Composition of Drosophila melanogaster proteome involved in fucosylated glycan metabolism. *J Biol Chem* 277**,** 3168-3175.

Rothman J. E. and Wieland F. T. (1996) Protein sorting by transport vesicles. *Science* 272**,** 227-234.

Ruddock L. W. and Molinari M. (2006) N-glycan processing in ER quality control. *J Cell Sci* 119**,** 4373-4380.

Sajdel-Sulkowska E. M. (1998) Immunofluorescent detection of CD15-fucosylated glycoconjugates in primary cerebellar cultures and their function in glial-neuronal adhesion in the central nervous system. *Acta Biochim Pol* 45**,** 781-790.

Sandhu J. K., Pandey S., Ribecco-Lutkiewicz M., Monette R., Borowy-Borowski H., Walker P. R. and Sikorska M. (2003) Molecular mechanisms of glutamate neurotoxicity in mixed cultures of NT2-derived neurons and astrocytes: protective effects of coenzyme Q10. *J Neurosci Res* 72**,** 691-703.

Satoh J. and Kuroda Y. (2000) Differential gene expression between human neurons and neuronal progenitor cells in culture: an analysis of arrayed cDNA clones in NTera2 human embryonal carcinoma cell line as a model system. *J Neurosci Methods* 94**,** 155-164.

Schachner M. and Martini R. (1995) Glycans and the modulation of neural-recognition molecule function. *Trends Neurosci* 18**,** 183-191.

Schweizer A., Ericsson M., Bachi T., Griffiths G. and Hauri H. P. (1993) Characterization of a novel 63 kDa membrane protein. Implications for the organization of the ER-to-Golgi pathway. *J Cell Sci* 104 (Pt 3)**,** 671-683.

Seaman M. N., Sowerby P. J. and Robinson M. S. (1996) Cytosolic and membrane-associated proteins involved in the recruitment of AP-1 adaptors onto the trans-Golgi network. *J Biol Chem* 271**,** 25446-25451.

Sherwood A. L., Upchurch D. A., Stroud M. R., Davis W. C. and Holmes E. H. (2002) A highly conserved His-His motif present in alpha1-->3/4fucosyltransferases is required for optimal activity and functions in acceptor binding. *Glycobiology* 12**,** 599-606.

Shestakova A., Zolov S. and Lupashin V. (2006) COG complex-mediated recycling of Golgi glycosyltransferases is essential for normal protein glycosylation. *Traffic* 7**,** 191-204.

Shields R. L., Lai J., Keck R., O'Connell L. Y., Hong K., Meng Y. G., Weikert S. H. and Presta L. G. (2002) Lack of fucose on human IgG1 N-linked oligosaccharide improves binding to human Fcgamma RIII and antibody-dependent cellular toxicity. *J Biol Chem* 277**,** 26733-26740.

Shimoda Y., Tajima Y., Osanai T., Katsume A., Kohara M., Kudo T., Narimatsu H., Takashima N., Ishii Y., Nakamura S., Osumi N. and Sanai Y. (2002) Pax6 controls the expression of Lewis x epitope in the embryonic forebrain by regulating alpha 1,3-fucosyltransferase IX expression. *J Biol Chem* 277**,** 2033-2039.

Shorter J., Watson R., Giannakou M. E., Clarke M., Warren G. and Barr F. A. (1999) GRASP55, a second mammalian GRASP protein involved in the stacking of Golgi cisternae in a cell-free system. *Embo J* 18**,** 4949-4960.

Shorter J., Beard M. B., Seemann J., Dirac-Svejstrup A. B. and Warren G. (2002) Sequential tethering of Golgins and catalysis of SNAREpin assembly by the vesicle-tethering protein p115. *J Cell Biol* 157**,** 45-62.

Singhal A. K., Orntoft T. F., Nudelman E., Nance S., Schibig L., Stroud M. R., Clausen H. and Hakomori S. (1990) Profiles of Lewisx-containing glycoproteins and glycolipids in sera of patients with adenocarcinoma. *Cancer Res* 50**,** 1375-1380.

Smith G. E., Ju G., Ericson B. L., Moschera J., Lahm H. W., Chizzonite R. and Summers M. D. (1985) Modification and secretion of human interleukin 2 produced in insect cells by a baculovirus expression vector. *Proc Natl Acad Sci U S A* 82**,** 8404-8408.

Sohda M., Misumi Y., Yoshimura S., Nakamura N., Fusano T., Ogata S., Sakisaka S. and Ikehara Y. (2007) The interaction of two tethering factors, p115 and COG complex, is required for Golgi integrity. *Traffic* 8**,** 270-284.

Solter D. and Knowles B. B. (1978) Monoclonal antibody defining a stage-specific mouse embryonic antigen (SSEA-1). *Proc Natl Acad Sci U S A* 75**,** 5565-5569.

Sousa V. L., Costa M. T., Palma A. S., Enguita F. and Costa J. (2001) Localization, purification and specificity of the full-length membrane-bound form of human recombinant alpha 1,3/4-fucosyltransferase from BHK-21B cells. *Biochem J* 357**,** 803-810.

Sousa V. L., Brito C., Costa T., Lanoix J., Nilsson T. and Costa J. (2003) Importance of Cys, Gln, and Tyr from the transmembrane domain of human alpha 3/4

fucosyltransferase III for its localization and sorting in the Golgi of baby hamster kidney cells. *J Biol Chem* 278**,** 7624-7629.

Sousa V. L., Brito C. and Costa J. (2004) Deletion of the cytoplasmic domain of human alpha3/4 fucosyltransferase III causes the shift of the enzyme to early Golgi compartments. *Biochim Biophys Acta* 1675**,** 95-104.

Spiro R. G. (2002) Protein glycosylation: nature, distribution, enzymatic formation, and disease implications of glycopeptide bonds. *Glycobiology* 12**,** 43R-56R.

Stinchcombe J., Bossi G. and Griffiths G. M. (2004) Linking albinism and immunity: the secrets of secretory lysosomes. *Science* 305**,** 55-59.

Stoeck A., Keller S., Riedle S., Sanderson M. P., Runz S., Le Naour F., Gutwein P., Ludwig A., Rubinstein E. and Altevogt P. (2006) A role for exosomes in the constitutive and stimulus-induced ectodomain cleavage of L1 and CD44. *Biochem J* 393**,** 609-618.

Streit A., Faissner A., Gehrig B. and Schachner M. (1990) Isolation and biochemical characterization of a neural proteoglycan expressing the L5 carbohydrate epitope. *J Neurochem* 55**,** 1494-1506.

Streit A., Nolte C., Rasony T. and Schachner M. (1993) Interaction of astrochondrin with extracellular matrix components and its involvement in astrocyte process formation and cerebellar granule cell migration. *J Cell Biol* 120**,** 799-814.

Streit A., Yuen C. T., Loveless R. W., Lawson A. M., Finne J., Schmitz B., Feizi T. and Stern C. D. (1996) The Le(x) carbohydrate sequence is recognized by antibody to L5, a functional antigen in early neural development. *J Neurochem* 66**,** 834-844.

Sun H. Y., Lin S. W., Ko T. P., Pan J. F., Liu C. L., Lin C. N., Wang A. H. and Lin C. H. (2007a) Structure and mechanism of Helicobacter pylori fucosyltransferase. A basis for lipopolysaccharide variation and inhibitor design. *J Biol Chem* 282**,** 9973-9982.

Sun Y., Li H., Liu Y., Shin S., Mattson M. P., Rao M. S. and Zhan M. (2007b) Cross-species transcriptional profiles establish a functional portrait of embryonic stem cells. *Genomics* 89**,** 22-35.

Suvorova E. S., Duden R. and Lupashin V. V. (2002) The Sec34/Sec35p complex, a Ypt1p effector required for retrograde intra-Golgi trafficking, interacts with Golgi SNAREs and COPI vesicle coat proteins. *J Cell Biol* 157**,** 631-643.

Tang B. L., Wang Y., Ong Y. S. and Hong W. (2005) COPII and exit from the endoplasmic reticulum. *Biochim Biophys Acta* 1744**,** 293-303.

Taniguchi N., Miyoshi E., Gu J., Honke K. and Matsumoto A. (2006) Decoding sugar functions by identifying target glycoproteins. *Curr Opin Struct Biol* 16**,** 561-566.

Teasdale R. D., D'Agostaro G. and Gleeson P. A. (1992) The signal for Golgi retention of bovine beta 1,4-galactosyltransferase is in the transmembrane domain. *J Biol Chem* 267**,** 4084-4096.

Teasdale R. D., Matheson F. and Gleeson P. A. (1994) Post-translational modifications distinguish cell surface from Golgi-retained beta 1,4 galactosyltransferase molecules. Golgi localization involves active retention. *Glycobiology* 4**,** 917-928.

Toivonen S., Nishihara S., Narimatsu H., Renkonen O. and Renkonen R. (2002) Fuc-TIX: a versatile alpha1,3-fucosyltransferase with a distinct acceptor- and site-specificity profile. *Glycobiology* 12**,** 361-368.

Traub L. M. (2005) Common principles in clathrin-mediated sorting at the Golgi and the plasma membrane. *Biochim Biophys Acta* 1744**,** 415-437.

Trojanowski J. Q., Kelsten M. L. and Lee V. M. (1989) Phosphate-dependent and independent neurofilament protein epitopes are expressed throughout the cell cycle in human medulloblastoma (D283 MED) cells. *Am J Pathol* 135**,** 747-758.

Uliana A. S., Giraudo C. G. and Maccioni H. J. (2006a) Cytoplasmic tails of SialT2 and GalNAcT impose their respective proximal and distal Golgi localization. *Traffic* 7**,** 604-612.

Uliana A. S., Crespo P. M., Martina J. A., Daniotti J. L. and Maccioni H. J. (2006b) Modulation of GalT1 and SialT1 sub-Golgi localization by SialT2 expression reveals an organellar level of glycolipid synthesis control. *J Biol Chem* 281**,** 32852-32860.

Ungar D., Oka T., Krieger M. and Hughson F. M. (2006) Retrograde transport on the COG railway. *Trends Cell Biol* 16**,** 113-120.

Unligil U. M. and Rini J. M. (2000) Glycosyltransferase structure and mechanism. *Curr Opin Struct Biol* 10**,** 510-517.

van der Goot F. G. and Gruenberg J. (2006) Intra-endosomal membrane traffic. *Trends Cell Biol* 16**,** 514-521.

van Niel G., Porto-Carreiro I., Simoes S. and Raposo G. (2006) Exosomes: a common pathway for a specialized function. *J Biochem (Tokyo)* 140**,** 13-21.

Van Vactor D., Wall D. P. and Johnson K. G. (2006) Heparan sulfate proteoglycans and the emergence of neuronal connectivity. *Curr Opin Neurobiol* 16**,** 40-51.

Varju P., Katarova Z., Madarasz E. and Szabo G. (2001) GABA signalling during development: new data and old questions. *Cell Tissue Res* 305**,** 239-246.

Varki A. (1999) *Essentials of glycobiology*. Cold Spring Harbor Laboratory Press, Cold Spring Harbor, NY.

Wagner M., Thaller C., Jessell T. and Eichele G. (1990) Polarizing activity and retinoid synthesis in the floor plate of the neural tube. *Nature* 345**,** 819-822.

Wang X., Inoue S., Gu J., Miyoshi E., Noda K., Li W., Mizuno-Horikawa Y., Nakano M., Asahi M., Takahashi M., Uozumi N., Ihara S., Lee S. H., Ikeda Y., Yamaguchi Y., Aze Y., Tomiyama Y., Fujii J., Suzuki K., Kondo A., Shapiro S. D., Lopez-Otin C., Kuwaki T., Okabe M., Honke K. and Taniguchi N. (2005) Dysregulation of TGF-beta1 receptor activation leads to abnormal lung development and emphysema-like phenotype in core fucose-deficient mice. *Proc Natl Acad Sci U S A* 102**,** 15791-15796.

Wang X., Gu J., Ihara H., Miyoshi E., Honke K. and Taniguchi N. (2006) Core fucosylation regulates epidermal growth factor receptor-mediated intracellular signaling. *J Biol Chem* 281**,** 2572-2577.

Watson D. J., Longhi L., Lee E. B., Fulp C. T., Fujimoto S., Royo N. C., Passini M. A., Trojanowski J. Q., Lee V. M., McIntosh T. K. and Wolfe J. H. (2003) Genetically modified NT2N human neuronal cells mediate long-term gene expression as CNS grafts in vivo and improve functional cognitive outcome following experimental traumatic brain injury. *J Neuropathol Exp Neurol* 62**,** 368-380.

Watson P. and Stephens D. J. (2005) ER-to-Golgi transport: form and formation of vesicular and tubular carriers. *Biochim Biophys Acta* 1744**,** 304-315.

Weiss M. and Nilsson T. (2000) Protein sorting in the Golgi apparatus: a consequence of maturation and triggered sorting. *FEBS Lett* 486**,** 2-9.

Wertkin A. M., Turner R. S., Pleasure S. J., Golde T. E., Younkin S. G., Trojanowski J. Q. and Lee V. M. (1993) Human neurons derived from a teratocarcinoma cell line express solely the 695-amino acid amyloid precursor protein and produce intracellular beta-amyloid or A4 peptides. *Proc Natl Acad Sci U S A* 90**,** 9513-9517.

Weston B. W., Nair R. P., Larsen R. D. and Lowe J. B. (1992a) Isolation of a novel human alpha (1,3)fucosyltransferase gene and molecular comparison to the human Lewis blood group alpha (1,3/1,4)fucosyltransferase gene. Syntenic, homologous, nonallelic genes encoding enzymes with distinct acceptor substrate specificities. *J Biol Chem* 267**,** 4152-4160.

Weston B. W., Smith P. L., Kelly R. J. and Lowe J. B. (1992b) Molecular cloning of a fourth member of a human alpha (1,3)fucosyltransferase gene family. Multiple homologous sequences that determine expression of the Lewis x, sialyl Lewis x, and difucosyl sialyl Lewis x epitopes. *J Biol Chem* 267**,** 24575-24584.

Wiggins C. A. and Munro S. (1998) Activity of the yeast MNN1 alpha-1,3-mannosyltransferase requires a motif conserved in many other families of glycosyltransferases. *Proc Natl Acad Sci U S A* 95**,** 7945-7950.

Wlasichuk K. B., Kashem M. A., Nikrad P. V., Bird P., Jiang C. and Venot A. P. (1993) Determination of the specificities of rat liver Gal(beta 1-4)GlcNAc alpha 2,6-sialyltransferase and Gal(beta 1-3/4)GlcNAc alpha 2,3-sialyltransferase using synthetic modified acceptors. *J Biol Chem* 268**,** 13971-13977.

Wuarin L. and Sidell N. (1991) Differential susceptibilities of spinal cord neurons to retinoic acid-induced survival and differentiation. *Dev Biol* 144**,** 429-435.

Xu Z., Vo L. and Macher B. A. (1996) Structure-function analysis of human alpha1,3-fucosyltransferase. Amino acids involved in acceptor substrate specificity. *J Biol Chem* 271**,** 8818-8823.

Yan A. and Lennarz W. J. (2005) Unraveling the mechanism of protein N-glycosylation. *J Biol Chem* 280**,** 3121-3124.

Yanagisawa M. and Yu R. K. (2007) The expression and functions of glycoconjugates in neural stem cells. *Glycobiology* 17**,** 57R-74R.

Yoshida-Noro C., Heasman J., Goldstone K., Vickers L. and Wylie C. (1999) Expression of the Lewis group carbohydrate antigens during Xenopus development. *Glycobiology* 9**,** 1323-1330.

Yoshioka A., Yudkoff M. and Pleasure D. (1997) Expression of glutamic acid decarboxylase during human neuronal differentiation: studies using the NTera-2 culture system. *Brain Res* 767**,** 333-339.

Young W. W., Jr. (2004) Organization of Golgi glycosyltransferases in membranes: complexity via complexes. *J Membr Biol* 198**,** 1-13.

Younkin D. P., Tang C. M., Hardy M., Reddy U. R., Shi Q. Y., Pleasure S. J., Lee V. M. and Pleasure D. (1993) Inducible expression of neuronal glutamate receptor channels in the NT2 human cell line. *Proc Natl Acad Sci U S A* 90**,** 2174-2178.

Yuen C. T., Chai W., Loveless R. W., Lawson A. M., Margolis R. U. and Feizi T. (1997) Brain contains HNK-1 immunoreactive O-glycans of the sulfoglucuronyl

lactosamine series that terminate in 2-linked or 2,6-linked hexose (mannose). *J Biol Chem* 272**,** 8924-8931.

Zachara N. E. and Hart G. W. (2004) O-GlcNAc a sensor of cellular state: the role of nucleocytoplasmic glycosylation in modulating cellular function in response to nutrition and stress. *Biochim Biophys Acta* 1673**,** 13-28.

Zaremba S., Naegele J. R., Barnstable C. J. and Hockfield S. (1990) Neuronal subsets express multiple high-molecular-weight cell-surface glycoconjugates defined by monoclonal antibodies Cat-301 and VC1.1. *J Neurosci* 10**,** 2985-2995.

Zetterstrom R. H., Lindqvist E., Mata de Urquiza A., Tomac A., Eriksson U., Perlmann T. and Olson L. (1999) Role of retinoids in the CNS: differential expression of retinoid binding proteins and receptors and evidence for presence of retinoic acid. *Eur J Neurosci* 11**,** 407-416.

Zolov S. N. and Lupashin V. V. (2005) Cog3p depletion blocks vesicle-mediated Golgi retrograde trafficking in HeLa cells. *J Cell Biol* 168**,** 747-759.


UNIVERSIDADE NOVA DE LISBOA
ITQB
INSTITUTO DE TECNOLOGIA QUÍMICA E BIOLÓGICA
OMNIS CAUSA CONTRA SE DIVISA NON STABIT